

Northumbria Research Link

Citation: Wright, Jennifer Anne (2020) The study of the activation of Bacillus subtilis urease in vivo. Doctoral thesis, Northumbria University.

This version was downloaded from Northumbria Research Link:
<http://nrl.northumbria.ac.uk/id/eprint/48184/>

Northumbria University has developed Northumbria Research Link (NRL) to enable users to access the University's research output. Copyright © and moral rights for items on NRL are retained by the individual author(s) and/or other copyright owners. Single copies of full items can be reproduced, displayed or performed, and given to third parties in any format or medium for personal research or study, educational, or not-for-profit purposes without prior permission or charge, provided the authors, title and full bibliographic details are given, as well as a hyperlink and/or URL to the original metadata page. The content must not be changed in any way. Full items must not be sold commercially in any format or medium without formal permission of the copyright holder. The full policy is available online: <http://nrl.northumbria.ac.uk/policies.html>

The study of the activation of *Bacillus subtilis* urease *in vivo*.

J A Wright

PhD

2020

The study of the activation of *Bacillus subtilis* urease *in vivo*.

JENNIFER ANNE WRIGHT

A thesis submitted in partial fulfilment
of the requirements of the
University of Northumbria at Newcastle
for the degree of
Doctor of Philosophy

Research undertaken in the
Faculty of Health and Life Sciences

December 2020

Abstract

In the natural environment, calcium carbonate (CaCO_3) precipitation often coincides with biological processes. It is well documented that microbes in soil can induce the precipitation of CaCO_3 in both the laboratory and the natural setting through microbial induced calcium carbonate precipitation (MICP). MICP utilises microorganisms as a result of their active metabolism, to precipitate CaCO_3 . The most studied MICP mechanism is urea hydrolysis. This process is catalysed by urease, a metalloenzyme that hydrolyses urea producing ammonium. The accumulation of ammonium causes the increase in surrounding pH that leads to CaCO_3 precipitation when sufficient calcium is present. Many soil microbes participate in MICP, including *Bacillus subtilis*; a model, Gram positive, spore-forming, soil bacterium that produces urease. However, little is known about MICP by *B. subtilis*. Increased understanding of the urease of non-pathogenic *B. subtilis* could enable the development of a bacterial system where urease expression is increased under mechanical pressure leading to the production of CaCO_3 for soil improvement.

This process has been explored in engineering terms, however, to fully harness MICP we must first increase our understanding of the genetics responsible for urease regulation and activation.

Bacterial ureases are composed of three highly conserved structural subunits (encoded by *ureABC*) and four accessory proteins (encoded *ureDEFG*) essential for urease activation. Unlike other urease-producing bacteria, *B. subtilis* only contains urease structural genes (*ureABC*) and within its genome lacks any homologues to genes coding for accessory proteins. The research carried out in this thesis aims to understand the activation of urease in *B. subtilis*.

The work in this thesis utilises molecular biology and bioinformatic analysis in order to characterise urease activation in *B. subtilis* 168; two main approaches were explored including altering growth conditions such as pH, nitrogen availability and metal ion concentrations; utilising a comparative proteomics approach to investigate the differentially-expressed proteins and assessing their role in the activation of urease *in vivo*.

Urease assays highlighted specific genes of interest as being involved in urease activity, particularly peptide transporters, however the proteomic and bioinformatic analysis identified an

increase in or similar level of urease structural unit expression. Any decrease in urease activity in specific knockouts was associated with poor urease activation, via enzyme assays and proteomic analysis. This confirmed the requirement for the combination of the enzyme assays and proteomic evaluations in understanding urease activity. Recombinant urease expression of structural proteins was then investigated utilising *E. coli* which identified the recombinant protein conformation was not optimum (trimer of trimers) as mostly the dimer of trimers was evident. This highlights the necessity for the recombinant expression method to be optimised in order to achieve a full understanding of urease activation in *B. subtilis*.

Table of Contents

ABSTRACT	ii
ACCOMPANYING MATERIAL.....	xiv
ACKNOWLEDGEMENTS.....	xvi
CHAPTER 1 <i>B. SUBTILIS</i> UREASE AND ITS FUTURE ROLE IN MICROBIAL INDUCED CALCIUM CARBONATE PRECIPITATION (MICP).....	1
1.1 INTRODUCTION	2
1.1.1 <i>Biom mineralisation</i>	2
1.2 MICROBIAL INDUCED CARBONATE PRECIPITATION (MICP).....	3
1.2.1 <i>MICP – Metabolic Processes</i>	3
1.2.2 <i>Ureolysis Process</i>	4
1.2.3 <i>Factors affecting ureolytic MICP</i>	6
1.2.4 <i>Applications of MICP</i>	7
1.3 UREASE	10
1.3.1 <i>History of Urease Discovery</i>	10
1.3.2 <i>Ureolytic Microorganisms</i>	11
1.3.3 <i>Urease Proteins and Activation</i>	13
1.3.4 <i>Urease Gene Clusters</i>	17
1.4 <i>BACILLUS SUBTILIS</i> AND ITS UREASE.....	19
1.4.1 <i>B. subtilis Urease</i>	20
1.4.1 <i>The Function of Urease in B. subtilis</i>	20
1.4.2 <i>The Use of B. subtilis in MICP</i>	22
1.5 AIMS AND OBJECTIVES.....	23
CHAPTER 2 MATERIALS AND METHODS	25
2.1 MATERIALS AND METHODS	26
2.1.1 <i>Bacterial strains and growth conditions</i>	26
2.1.2 <i>Media Preparation</i>	26
2.1.3 <i>Growth Conditions</i>	28
2.1.4 <i>Buffers used in Cell harvest and enzyme assay</i>	29
2.1.5 <i>Whole Cell assay of urease activity using Nessler reagent</i>	29
2.1.6 <i>Optimization of Buffers for Whole Cell assay of urease activity using Nessler reagent</i>	30
2.1.7 <i>Cell Free Extract (CFE) Assay of Urease using Nessler Reagent</i>	30
2.1.8 <i>Impact of Metal ion Additions in the growth medium on the urease activity</i>	33
2.1.9 <i>Effect of pH in growth medium on the urease activity</i>	33
2.1.10 <i>Enzyme Assay Controls</i>	33
2.1.11 <i>Enzyme Activity definition</i>	34

2.1.12	<i>Culture for Proteomics Study</i>	34
2.1.13	<i>Buffer optimisation of method in Protein extraction for proteomics study</i>	34
2.1.14	<i>Sodium Dodecyl Sulphate–Polyacrylamide Gel electrophoresis (SDS-PAGE)</i>	36
2.1.15	<i>In gel digestion</i>	38
2.1.16	<i>Liquid Chromatography and Mass Spectrometer analysis of Peptide Samples (LC-MS)</i> ..	39
2.1.1	<i>MASCOT MS/MS search for individual protein identification</i>	40
2.1.2	<i>Bioinformatic analysis for comparative proteomics</i>	41
2.1.3	<i>Bioinformatic analysis to determine specific of genes of interest</i>	42
2.1.4	<i>Addgene knockouts</i>	44
2.1.5	<i>Proteomic and bioinformatics analysis</i>	44
2.1.6	<i>Plasmids and Bacterial Cells</i>	45
2.1.7	<i>Maintenance of pURE91 plasmid</i>	45
2.1.8	<i>Transformation into E.coli BL21 (DE3) cells - Control</i>	46
2.1.9	<i>Recombinant Protein Expression and Extraction</i>	46
2.1.10	<i>Western Blot Analysis to Detect B. subtilis UreC</i>	46
2.1.11	<i>Analysis of Urease Conformation using Native Tris Glycine Gels</i>	49
2.1.12	<i>Analysis of Urease Conformation using Size Exclusion Chromatography (SEC)</i>	50
2.1.13	<i>Visualization and Protein ID Analysis of Peak Fractions from SEC</i>	52

CHAPTER 3 UREASE ACTIVITY OF BACILLUS SUBTILIS CULTURED IN A DEFINED MINIMAL MEDIA .53

3.1	INTRODUCTION	54
3.1.1	<i>Regulation of Urease Synthesis in Microorganisms</i>	54
3.1.2	<i>Nitrogen Regulation of Urease</i>	58
3.1.1	<i>Regulation by Metal Ions</i>	59
3.1.2	<i>Regulation by pH</i>	60
3.1.3	<i>Complex regulation of urease</i>	61
3.1.4	<i>Urease regulation in B. subtilis</i>	62
3.2	UREASE ENZYME ASSAYS	70
3.2.2	<i>Factors which influence Urease Assays</i>	71
3.2.3	<i>Ammonium transportation</i>	73
3.3	NICKEL AND METALLOENZYMES.....	74
3.3.1	<i>Metal ion interactions with urease</i>	74
3.3.1	<i>Metal binding proteins that could affect urease activity</i>	75
3.4	AIMS AND OBJECTIVES.....	75
3.5	RESULTS AND DISCUSSION	77
3.5.1	<i>Media optimisation and growth curves</i>	77
3.5.2	<i>Determination of Urease Activity in Various Conditions</i>	83
3.5.1	<i>Urease Activity in Different Growth Phases</i>	84
3.5.2	<i>Effect of Nitrogen upon urease activity in B. subtilis</i>	85
3.5.1	<i>Effect of Ammonium Sulphate in the Growth Medium on Urease Activity</i>	88

3.5.1	<i>Effect of metal ion additions on urease activity</i>	89
3.5.2	<i>Cell free extract (CFE) and urease activity</i>	92
3.6	DIFFERENCE BETWEEN UREASE ASSAYS USING WHOLE CELL AND CFE.....	94
3.6.1	<i>Effect of pH on urease activity in B. subtilis</i>	96
3.6.2	<i>Summary</i>	98
CHAPTER 4 A PROTEOMICS APPROACH TO UNDERSTANDING THE ACTIVATION AND REGULATION OF B. SUBTILIS UREASE IN NITROGEN LIMITING CONDITIONS.		101
4.1	INTRODUCTION	102
4.1.1	<i>Nickel and urease activation</i>	102
4.1.2	<i>Proteomics</i>	110
4.1.3	<i>Proteomic studies of B. subtilis</i>	112
4.1.4	<i>Aims and Objectives</i>	112
4.2	RESULTS AND DISCUSSION	114
4.2.1	<i>Buffer Optimisation</i>	115
4.2.2	<i>Comparative Proteomic analysis of B. subtilis 168 cultured under Nitrogen limited conditions (NLC).</i> 120	
4.2.3	<i>Functional Analysis of Proteins Upregulated in Nitrogen Limited Media (NLM)</i>	132
4.2.4	<i>Significant Proteins for further analysis</i>	146
4.3	SUMMARY	149
CHAPTER 5 INVESTIGATION OF THE ROLES OF SPECIFIC GENES OF B. SUBTILIS IN UREASE ACTIVATION. 153		
5.1	INTRODUCTION	154
5.1.1	<i>ABC Transporter genes of interest</i>	154
5.1.2	<i>Zn²⁺ binding proteins</i>	155
5.1.3	<i>Aims and Objectives</i>	156
5.2	RESULTS	157
5.2.1	<i>Ammonium Producing proteins</i>	157
5.2.2	<i>Analysis of Urease Activity of ΔureC</i>	157
5.2.3	<i>Analysis of urease activity of the opp operon knockout strains</i>	160
5.2.4	<i>Analysis of urease activity of dpp operon knockout strains</i>	190
5.2.5	<i>Analysis of urease activity of the High Affinity Zinc Transport System knockout strains</i> ...	193
5.2.6	<i>Bioinformatic analysis of Ycic and analysis of urease activity in ΔyciC.</i>	198
5.2.1	<i>Further Y genes of interest</i>	204
5.3	SUMMARY	205
CHAPTER 6 RECOMBINANT UREASE EXPRESSION AND ACTIVITY.....		210
6.1	INTRODUCTION	211
6.1.1	<i>B. subtilis Recombinant Urease Activity in Literature</i>	212

6.1.2	<i>Aims of this Chapter</i>	214
6.2	RESULTS AND DISCUSSION	215
6.2.1	<i>Urease expression in recombinant strain</i>	215
6.2.1	<i>Western blot analysis to confirm the expression of UreC</i>	217
6.2.2	<i>Urease activity comparison between B. subtilis 168 and recombinant E.coli</i>	219
6.2.3	<i>Protein Conformation Analysis Using Native Tris-Glycine Gels</i>	223
6.2.4	<i>Size Exclusion Chromatography (SEC) for Protein Conformation Analysis of Recombinant Urease.</i> 225	
6.3	SUMMARY	238
CHAPTER 7	CONCLUSIONS AND FUTURE WORK	241
7.1	SUMMARY AND CONCLUSION	242
7.2	FUTURE WORK	246
CHAPTER 8	REFERENCES	249
CHAPTER 9	APPENDICES	276
9.1	<i>B. SUBTILIS UREABC</i> GENETIC SEQUENCE	277
9.2	CHAPTER 2	278
9.3	CHAPTER 3	280
9.4	PROTEOMIC EVALUATION OF NLM AND NPM	280
9.5	<i>ST. AUREUS OPP</i> (Ni ²⁺ TRANSPORTER) AND <i>B. SUBTILIS OPP</i> ANALYSIS	283
9.6	YcIC (ZAGA) AND UREG SEQUENCE AND STRUCTURAL COMPARISON	286
9.7	PROTEOMIC DATA ANALYSIS	288
9.8	NZY MINIPREP METHOD	299
9.9	VECTOR MAP PET22B	300

List of figures

Figure 1-1. Urea Hydrolysis for MICP	5
Figure 1-2. Depiction of the events occurring during the ureolytic induced carbonate precipitation (De Muynck, De Belie and Verstraete, 2010).....	6
Figure 1-3 Urease active site containing two nickel ions in <i>K. aerogenes</i> . (Carter <i>et al.</i> , 2009).	11
Figure 1-4 The trimeric urease structure adapted from Nim <i>et al.</i> (2019) (Nim and Wong, 2019).	14
Figure 1-5. The activation of <i>Klebsiella aerogenes</i> urease with accessory genes.....	16
Figure 1-6. Organization of representative urease gene clusters adapted from (Yang <i>et al.</i> , 2015; Chen and Burne, 2003; Carter <i>et al.</i> , 2009).	18
Figure 3-1. Regulatory mechanisms of urease in various bacteria.	56
Figure 3-2. The ureA promoter region of <i>H. pylori</i>	60
Figure 3-3. <i>B. subtilis ureABC</i> promoter region (Cruz-Ramos <i>et al.</i> , 1997).	63
Figure-3-4. Nucleotide sequences of <i>ureABC</i> P2 and P3 promoters in <i>B. subtilis</i> , and <i>GlnR/TnrA</i> and <i>PucR</i> binding sites of P3.	64
Figure 3-5. Nucleotide sequence in <i>pucH</i> and <i>pucR</i> regulatory region.	68
Figure 3-6. <i>B. subtilis ureABC</i> operon.....	69
Figure 3-7. Growth curve of <i>B. subtilis</i> 168 in SMM.	79
Figure 3-8. Growth analysis of <i>B. subtilis</i> 168 cultured in small scale BSS (JW).	81
Figure 3-9. Growth analysis of <i>B. subtilis</i> 168 cultured in large scale BSS (JW).	82
Figure 3-10. Ammonium Chloride standard curve (0-20mg/L) for Nessler Assay.	83
Figure 3-11. Urease activity of <i>B. subtilis</i> 168 at mid and end exponential growth phases in whole cells	84
Figure 3-12. Urease activity of <i>B. subtilis</i> when cells are cultured in LB and BSS (JW).	86
Figure 3-13. Growth comparison of <i>B. subtilis</i> 168 cultured in large scale BSS (JW) (500 ml) with varying concentrations of glutamic acid.	87
Figure 3-14. Urease activity of <i>B. subtilis</i> 168 cultured in various concentrations of glutamic acid (low 2.5 g/L, high 10 g/L and normal 2.5 g/L) in BSS (JW).	88
Figure 3-15. The effect of Ammonium Sulphate (nitrogen excess) on urease activity of <i>B. subtilis</i> 168.....	89
Figure 3-16. Addition of Zn^{2+} (2 mg/L), Mn^{2+} (2 mg/L) and Fe^{2+} (2 mg/L) to BSS (JW) to determine the effect on urease activity in <i>B. subtilis</i> 168.	92
Figure 3-17. Urease activity of <i>B. subtilis</i> 168 using CFE prepared under various sonication frequencies.	94
Figure 3-18. Urease activity of <i>B. subtilis</i> 168 in CFE from sample also analysed for activity in whole cells.....	96

Figure 3-19. Urease activity of <i>B. subtilis</i> 168 in whole cells from sample also analysed for activity in CFE.	96
Figure 3-20. Growth of <i>B. subtilis</i> 168 in BSS (JW) media over approximately 20-45 hours under different pH conditions.	97
Figure 3-21. Urease activity of <i>B. subtilis</i> 168 in whole cells at pH 5 and pH 7.	98
Figure 4-1. Conformational changes in UreF recruit UreG to the UreGFD complex in <i>H. pylori</i>	104
Figure 4-2. UreG protein sequences of various bacteria.	105
Figure 4-3. Venn diagram indicating all proteins extracted using the three buffers compared to the blank; TE, TBS and HEPES all with the addition of 1 mM PMSF.	117
Figure 4-4. Urease activity of <i>B. subtilis</i> urease using different buffers for cell harvest.	118
Figure 4-5. Urease activity in CFE of <i>B. subtilis</i> 168 at various pH.	119
Figure 4-6. Venn diagram detailing number of proteins identified in NLM (BSS (JW)) and NPM (BSS (JW) + (NH ₄) ₂ SO ₄).	121
Figure 4-7. COG analysis of proteins upregulated in nitrogen limited media.	128
Figure 4-8. COG analysis of proteins downregulated in the NLM BSS (JW).	132
Figure 4-9. Purine-degradative pathway in <i>B. subtilis</i> (Brandenburg <i>et al.</i> , 2002a)	135
Figure 4-10 ABC transport system operons in <i>B. subtilis</i> 168.	139
Figure 4-11. MUSCLE alignment comparison of the <i>B. subtilis</i> OppD and NikD of <i>S. aureus</i> which detailed 42.22%.	140
Figure 4-12. Sequence comparison of <i>ureE</i> <i>S. pasteurii</i> and <i>B. subtilis</i> 168 <i>oppF</i>	141
Figure 4-13. Comparison of AppF and YkfD in <i>B. subtilis</i> and AppF in <i>Bacillus amyloliquefaciens</i>	143
Figure 5-1. Small scale growth curve of $\Delta ureC$ in BSS (JW).	158
Figure 5-2. Large scale growth curve of $\Delta ureC$ in BSS (JW).	158
Figure 5-3. Urease activity of <i>B. subtilis</i> 168 and $\Delta ureC$ urease in whole cells.	159
Figure 5-4. Preliminary growth analysis of 5 <i>B. subtilis opp</i> knockout strains cultured in 50 ml of BSS (JW) at 30°C and 150 rpm.	161
Figure 5-5. Growth curves of <i>B. subtilis opp</i> knockout strains in 500 ml of BSS (JW) at 30°C and 150 rpm.	162
Figure 5-6. Urease activity of <i>B. subtilis</i> 168 and $\Delta oppA$ urease in whole cells.	163
Figure 5-7. Urease activity of <i>B. subtilis</i> 168 and $\Delta oppA$ urease in CFE.	164
Figure 5-8. Sequence comparisons of DppE and OppA of <i>B. subtilis</i> 168.	165
Figure 5-9. COG analysis of proteins upregulated in $\Delta oppA$	175
Figure 5-10. COG analysis of proteins downregulated in $\Delta oppA$ cultured in NLM BSS (JW).	180
Figure 5-11. Proteins upregulated in $\Delta oppA$ compared to wild-type 168 both cultured in NLM.	180
Figure 5-12. Activity of <i>B. subtilis</i> 168 and $\Delta oppB-F$ urease in whole cells.	189

Figure 5-13. Activity of <i>B. subtilis</i> 168, $\Delta oppB$, $\Delta oppC$, $\Delta oppD$ and $\Delta oppF$ urease in CFE...	190
Figure 5-14. Growth analysis of <i>B. subtilis</i> 168 and $\Delta dppA$ cultured in BSS (JW) at 30°C 150 rpm.	191
Figure 5-15. Activity of <i>B. subtilis</i> 168 and $\Delta dppA$ urease in whole cells.	192
Figure 5-16 Urease activity of <i>B. subtilis</i> 168 and $\Delta dppA$ in CFE (0.756mg/ml protein).	192
Figure 5-17. Growth of $\Delta znuA$ in BSS (JW) carried out in Biotek Synergy Plate Reader at 30°C and medium shaking.	194
Figure 5-18. Growth analysis of $\Delta znuA$ and $\Delta znuB$ from 35 – 60 hours cultured in BSS (JW) at 30°C 150 rpm.	195
Figure 5-19. Urease activity of <i>B. subtilis</i> 168, $\Delta znuA$ and $\Delta znuB$ in whole cells.	196
Figure 5-20. Urease activity of <i>B. subtilis</i> 168, $\Delta znuA$, $\Delta znuB$ urease in CFE.	196
Figure 5-21. COG analysis of proteins upregulated in $\Delta znuA$ and $\Delta znuB$	198
Figure 5-22. Amino acid sequence alignments.	200
Figure 5-23. Structural and folding analysis of <i>B. subtilis</i> YciC using PHYRE2.	201
Figure 5-24. Growth analysis of <i>B. subtilis</i> 168 and $\Delta yciC$ in BSS (JW).	202
Figure 5-25. Urease activity of <i>B. subtilis</i> 168 and $\Delta yciC$ urease in whole cell.	203
Figure 5-26. Urease activity of <i>B. subtilis</i> 168 and $\Delta yciC$ in CFE.	203
Figure 6-1. <i>B. subtilis</i> ureABC operon including promoters and binding sites (CodY, PucR and GlnR) (Karp <i>et al.</i> , 2019).	211
Figure 6-2. Urease expression in <i>B. subtilis</i> 168 and the recombinant strain <i>E. coli</i> BL21 (DE3) at 20°C and 30°C with additions of 1 mM IPTG.	216
Figure 6-3. Recombinant urease expression visualised using 14% (w/v) SDS-PAGE.	216
Figure 6-4. Sequence comparison of <i>B. subtilis</i> UreC and <i>H. pylori</i> UreB.	218
Figure 6-5. Western blot overlay of recombinant <i>E. coli</i> BL21+pURE91 total protein (TP), CFE and <i>B. subtilis</i> 168 CFE.	219
Figure 6-6. Urease activity of <i>B. subtilis</i> 168, the recombinant strain <i>E. coli</i> BL21 (DE3) + pURE91 and BL21 (DE3) control in whole cells.	220
Figure 6-7. Urease activity of <i>B. subtilis</i> 168, <i>E. coli</i> BL21 (DE3) + pURE91 and BL21(DE3) (control) in CFE.	221
Figure 6-8. Native gel 6% analysis of urease in CFE from recombinant <i>E. coli</i> and 168 strain.	225
Figure 6-9. The SEC chromatogram of recombinant urease CFE utilising S-300 column and 100 μ l loop	229
Figure 6-10. SEC Chromatogram of recombinant urease CFE separated using S-300 column with 2 ml loop. Chromatogram of recombinant CFE 2 ml detailing 5 peaks	232
Figure 6-11. SEC Chromatogram of <i>B. subtilis</i> 168 urease CFE separated using S-300 column with 2 ml loop. <i>B. subtilis</i> 168 CFE chromatogram using S-300 2 ml loop identifying 6 prominent peaks.	233
Figure 6-12. Recombinant CFE Peak fractions from AKTA S-300 2 ml loop.	236

Figure 6-13. SDS-PAGE gel of each pooled peak from S-300 column with 2 ml loop of recombinant urease CFE.....	238
Appendix Figure 9-1 <i>Bacillus subtilis</i> 168 <i>ureABC</i> gene sequence (Region: 3766714 - 3769108 (reverse complement))	277
Appendix Figure 9-2. SOP for Progenesis/MASCOT use.....	279
Appendix Figure 9-1. Sequence alignment of <i>St. aureus opp</i> (Ni ²⁺ transporter) and <i>B. subtilis opp</i> transport systems.....	285
Appendix Figure 9-2. PHYRE2 analysis of <i>B. subtilis</i> YciC sequence comparison.....	286
Appendix Figure 9-3 Sequence alignment comparisons of <i>B. subtilis</i> YciC and UreG of <i>K. pneumonia</i> , HypB of <i>H. pylori</i> and UreG of <i>H. pylori</i>	287
Appendix Figure 9-4. pET23 Vector Map and sequence landmarks (Robert, 1988)	300
Appendix Figure 9-5. pET-22b Vector map	301
Appendix Figure 9-6. Recombinant urease expression at different temperatures with 1 mM IPTG. Lane 1 ladder, lane 2 CFE at 16°C, lane 3 TP at 16°C, lane 4 CFE at 30°C, lane 5 TP at 30°C, lane 6 CFE at 37°C and lane 7 TP at 37°C.	301
Appendix Figure 9-7. Urease expression in <i>B. subtilis</i> 168, <i>E. coli</i> BL21 (DE3) +pURE91 and <i>E. coli</i> BL21 (DE3) as a control. Lanes 1&2 <i>B. subtilis</i> 168 CFE, Lanes 3&4 Recombinant <i>E. coli</i> BL21 (DE3) +pURE91 and lanes 5&6 <i>E. coli</i> BL21 (DE3) control. Lane 7 Molecular marker. Highlighted in red is the active site of urease, UreC which is evident in the recombinant and not the control (<i>E.coli</i> cultured in different media).....	302
Appendix Figure 9-8. Native gel 14% including CFE from <i>B. subtilis</i> 168, Recombinant urease and the standards from size exclusion gel electrophoresis	302
Appendix Figure 9-9. S-200 Chromatogram of HR Standards (5) using S-200 column with 100 µl loop	304
Appendix Figure 9-10. S-200 Chromatogram of Recombinant CFE using S-200 with 100 µl loop	305
Appendix Figure 9-11. S-300 Chromatogram of HR Standards (5) with 100 µl loop	306
Appendix Figure 9-12. S-300 2 ml loop BSA Chromatogram. BSA chromatogram detailing two peaks. Peak 1 Dimer 132 kDa Peak 2 Monomer 66 kDa (Trimer EV 50).....	307
Appendix Figure 9-13. Recombinant SEC Chromatogram of recombinant urease CFE separated using S-300 column with 2 ml loop. Repeated recombinant urease expression detailing 5 peaks.	308
Figure 9-14 A. S-300 column fractions 168 CFE (peak 1). B. S-300 column fractions 168 CFE plus pooled P1, Peak 2. C. Gel 3 S-300 column fractions 168 CFE peaks 2 D. S-300 column fractions 168 CFE peak 3.....	310

List of Tables

Table 1-1. Metabolic pathways leading to MICP.	4
Table 1-2. Challenges of MICP	10
Table 2-1. Buffers used in urease assay	29
Table 2-2. Optimised methods for whole cell and Cell Free Extractions (CFE).....	32
Table 2-3. Reaction mixture standard for Nessler assay.....	32
Table 2-4. Metal ion additions to growth media investigating urease activity.	33
Table 2-5. Buffers used in determining protein extraction method	35
Table 2-6. Solutions SDS-PAGE.....	36
Table 2-7. Components for 15% SDS-PAGE gel.....	37
Table 2-8. Components for 4% stacking gel.....	37
Table 2-9. Binary buffer system components.	39
Table 2-10. Buffers required for specific time points to generate LC elution	40
Table 2-11. Bioinformatic tools and their function used in this study.....	42
Table 2-12. COG list and specific functional description.....	43
Table 2-13. Bacterial strains and knockouts used within the research and utilised in proteomics experiments.	44
Table 6-1. Plasmids and host cells used in this research	45
Table 6-2. Recipes for Western Blot solutions	47
Table 6-3. Solutions required for Native gel preparation	49
Table 6-4. Separating Gel Mixture preparation	50
Table 6-5. Stacking gel solution preparation (4ml)	50
Table 6-6. Sephacryl columns and fraction ranges used in the study	51
Table 6-7 Gel filtration standards (Sigma 1511901) for S-200 and S-300.....	52
Table 3-1. Gene expression in nitrogen limited conditions of TnrA and GlnR in <i>B. subtilis</i>	66
Table 3-2. Genes involved in urease regulation in <i>B. subtilis</i> during nitrogen limiting conditions (Wray, Ferson and Fisher, 1997b; Brandenburg <i>et al.</i> , 2002a; Fisher, 1999).....	70
Table 3-3. Known ammonium producers in <i>B. subtilis</i> and their corresponding reaction (Uniprot).	73
Table 3-4. Preliminary data identifying media suitable for growth of both <i>Bacillus</i> strains in use.	78
Table 3-5. Growth of <i>B. subtilis</i> 168 in BSS MM with varying supplements identified as necessary for <i>B. subtilis</i> growth. (Dawes and Mandelstam, 1970; Vasantha and FREESE, 1979).	80
Table 4-1 Molecular functions and biological processes associated with urease accessory proteins including Gene Ontology (GO) terms associated with each function and process.....	107

Table 4-2. Comparison of different buffers with the addition of 1 mM PMSF for proteomics evaluation.....	116
Table 4-3. Proteins upregulated in the nitrogen limited condition of BSS (JW) compared to BSS (JW) + Ammonium Sulphate.....	122
Table 4-4. Proteins downregulated in the nitrogen limited condition of BSS (JW) compared to BSS (JW) + Ammonium Sulphate.....	129
Table 4-5. Known Urease accessory proteins and their associated COG's.....	133
Table 4-6. <i>B. subtilis</i> genes of interest for further study identified from comparative analysis of upregulated proteins in NLM.....	148
Table 5-1. Proteins upregulated in $\Delta oppA$ cultured in BSS (JW). Proteins were filtered by fold change >3, peptide score >2 and annova p <0.05.....	167
Table 5-2. Proteins downregulated in $\Delta oppA$ with fold change >3.....	176
Table 5-3. Proteins upregulated in both wild-type 168 and $\Delta oppA$	181
Table 5-4. Proteins of interest identified from $\Delta oppA$ proteomic and bioinformatic analysis proposed to be involved in urease activation in <i>B. subtilis</i>	188
Table 5-5. Y genes chosen for knockout analysis identified via nitrogen limitation media.....	205
Table 5-6. A simplistic reference to urease activity and expression in <i>B. subtilis</i> 168 knockouts used in this study compared to the wild-type 168 cultured in NLM.....	209
Table 6-8. Approximate molecular weights (kDa) of the urease structural subunits and their corresponding folding protein structures. Molecular weights (Consortium, 2018).....	224
Table 6-9. Approximate protein sizes identified from SEC standards on S-300 column using 100 μ l loop.....	228
Table 6-10. Approximate protein sizes identified from SEC standards on S-300-column using 100 μ l and BSA on 2 ml loop.....	230
Table 6-11. SEC Combined chromatogram results S-300 2ml loop.....	234
Appendix Table 9-1. Upregulated proteins of NLM BSS 9JW) fold change <3.....	280
Appendix Table 9-1 Genes activated by the PucR Regulon.....	287
Appendix Table 9-2. Proteins upregulated < 3 fold in oppA.....	288
Appendix Table 9-3. Proteins downregulated in oppA with fold change >3.....	291
Appendix Table 9-4. <i>B. subtilis</i> 168 knockouts and expression of urease upregulated or downregulated.....	298
Appendix Table 9-5.....	311

Accompanying Material

Abbreviations	Full Names
Ab	Antibody
ABC	ATP-binding cassette transporters
ACN	Acetonitrile
ATP	Adenosine Triphosphate
<i>B. subtilis</i>	<i>Bacillus subtilis</i>
BSA	Bovine Serum Albumin
BSS	Basal Salts Solution
CFE	Cell Free Extract
°C	Degrees Celsius
DNA	Deoxyribonucleic acid
DTT	Dithiothreitol
EC	Enzyme Comission Number
ECF	Energy - coupling factor transporters
FBI-GS	Feedback Inhibited Glutamine Synthetase
GS	Glutamine Synthetase
g	gram
x g	gravity
GGGS	Glucose Glutamate Glycine Salts
GTP	Guanosine-5'-triphosphate
HEPES	4-(2-hydroxyethyl)-1-piperazineethanesulfonic acid
IAA	2-Iodoacetamide
IPTG	isopropyl- β -D-thiogalactoside
kB	kilo bases
kDa	kilo daltons
Km	Michaelis constant; amount of substrate needed for the enzyme to obtain half of its maximum rate of reaction
KHz	KiloHertz
LB	Luria Bertani Broth
L	Litre
LC-MS	Liquid chromatography–mass spectrometry
MICP	Microbial Induced Carbonate Precipitation
min	Minute
mg	milligram
ml	millilitres
MM	Minimal Media
mM	Millimolar
MSU	Michigan State University
NL	Nitrogen Limited
NLC	Nitrogen Limited Condition
NLM	Nitrogen Limited Media (BSS (JW))
NPM	Nitrogen Plus Media (BSS (JW) + Ammonium Sulphate)
nm	nano metre
OD	Optical Density

%	percent
PMSF	Phenylmethane Sulfonyl Fluoride
rpm	revolutions per minute
SDS	Sodium Dodecyl Sulphate
SDS-PAGE	Sodium Dodecyl Sulphate Poly Acrylamide Gel Electrophoresis
SMM	Spiziens Minimal Media
μl	microlitre
v/v %	concentration in volume/volume percent

Acknowledgements

Throughout my PhD journey I received a great deal of support, advice and encouragement. I would first like to thank my wonderful principal supervisor Dr. Meng Zhang for giving me the opportunity to carry out this research. Her expertise, knowledge, guidance, patience and encouragement was invaluable throughout my PhD. Her supervision has developed my confidence and provided me with the skills to become an independent researcher. I would also like to acknowledge my co-supervisors Prof. Gary Black, Prof. Martyn Dade-Robertson and Prof. Anil Wipat for their expertise of the subject, sound advice and feedback.

I would like to thank my family and friends for their unconditional love and support. In particular my parents for all they have done for me, my Father for all he still does and my Mother who is dearly missed. I would like to dedicate this work to my amazing Mother who was not able to see me start and then complete this journey. Huge thanks to my Husband and two children. Their encouragement, questioning and curiosity of the subject allowed me to continue the conversations at home and their support was invaluable throughout this process. I'm thankful of their understanding of my aspiration to complete this work, which often meant I missed valuable time with them.

I must also acknowledge my colleagues, in particular Dr. Nicola Brown for being a great friend, always being so helpful and knowledgeable in the lab and always making time to answer any questions. Dr. Jose Munoz for his guidance in using the AKTA, Dr. William Cheung for his assistance in using the GeLC-MS and Dr. Jonathan Thompson for his invaluable help, friendship and knowledge not only in the lab but with Microsoft word too.

Acknowledgements also must go to the project students involved in the initial study of candidate y genes in urease activity. Working with them in the lab was great fun and also helped confirm my methodologies.

I would also like to thank all past and present PhD students of D216. Without their friendship and encouragement the whole PhD journey would have been a great deal harder.

Finally, I would like to acknowledge the ESPRC and Northumbria University for the funding of this project.

Chapter 1 *B. subtilis* urease
and its future role in
microbial induced calcium
carbonate precipitation
(MICP)

1.1 Introduction

As the global population increases there is a compelling need for increased, yet sustainable civil infrastructure. The ability to utilise biological processes in order to improve ground stability; as well as creating construction materials without adding to climate damage is necessary. In almost every environment on earth, microorganisms and microbial-mediated mineralisation (biomineralisation) processes are active (Achal *et al.*, 2009). In the natural environment, chemical calcium carbonate precipitation often coincides with biological processes. It is well documented that microbes present in soil can induce the precipitation of calcium carbonate in both the laboratory and the natural setting.

1.1.1 Biomineralisation

Bio-geochemical processes that induce mineral precipitation have been used in many applications including, improving soil and sand stiffness (Mortensen and DeJong, 2011; Montoya, DeJong and Boulanger, 2013; Mujah, Shahin and Cheng, 2017; Cheng, Cord-Ruwisch and Shahin, 2013). Biomineralisation is a naturally occurring process in living organisms controlled by specific cellular processes that leads to the creation of well-organized inorganic biominerals. These minerals often play a vital role in protecting living organisms, like in mollusc shells and brachiopod shells. They also help to support certain organisms structurally by forming bones, coral skeletons and producing functionally hardened surfaces e.g. teeth (Chen *et al.*, 2019c).

Biomineralisation is divided into three categories: a) biologically controlled mineralisation (BCM) – the metabolic activity of the microbe completely controls composition, localisation, nucleation and morphology of the minerals (examples include mollusc shells); b) biologically induced mineralisation (BIM) – an active process where indirect precipitation of biominerals occurs, due to interactions of metabolic by-products of microorganisms and ions present in the localised environment these biominerals are often of poor crystallinity and morphology and have a range of sizes (Frankel and Bazylinski, 2003) and this active process is commonly named microbial induced carbonate precipitation (MICP); and c) biologically mediated mineralisation (BMM) – a passive process where minerals are formed without the need of extracellular or intracellular biological activities (Castro Alonso *et al.*, 2019); passive biomineralisation is a BMM

process which can take place via the interactions of the organic matrix. Microorganisms also produce extracellular polymeric substances (EPS) which are an organic matrix, the natural polymers are of high molecular weight and are secreted by micro-organisms such as bacteria, cyanobacteria and microalgae (Costa, Raaijmakers and Kuramae, 2018). EPSs establish the functional and structural integrity of biofilms, and consist of polysaccharides, proteins, and DNA. EPS and calcium ions can bind without the need of contemporary biological activity as functional groups such as carboxylic acids and hydroxyl groups deprotonate due to in the increase in pH, facilitating the binding properties (Castro Alonso *et al.*, 2019).

1.2 Microbial Induced Carbonate Precipitation (MICP)

MICP processes involve a number of biochemical reactions that are affected by many factors, including bacterial species, concentration of bacteria, temperature, pH, composition and concentration of cementation solution and soil properties (Tang *et al.*, 2020). The benefit of microorganisms as a supplement in soil biocementation was first suggested by Whiffin (2004) and then Mitchell and Santamarina (2005). Research in this field has dramatically increased. MICP is now commercially utilised in the construction industry (bioMASON[®], BioCement[™]) as the biomineral deposits enable a natural, stronger construction material, capable of binding, protecting, consolidating and remediating building materials.

1.2.1 MICP – Metabolic Processes

MICP utilises the metabolic pathways of bacteria to form CaCO₃ which binds the soil particles together, leading to increased soil strength and stiffness. MICP occurs via various processes including: urea hydrolysis by ureolytic bacteria, ammonification of amino acids by myxobacteria, denitrification by nitrate-reducing bacteria, dissimilatory sulphate-reduction by sulphate reducing bacteria and photosynthesis *via* cyanobacteria (Table 1-1).

Table 1-1. Metabolic pathways leading to MICP.

Adapted from (Achal and Pan, 2014b; Zhu and Dittrich, 2016; Seifan and Berenjian, 2019).

Metabolism	Reaction	By-product
Urea Hydrolysis (Catalysed by urease)	$\text{CO}(\text{NH}_2)_2 + 2\text{H}_2\text{O} + \text{Ca}^{2+} + \text{Cell} \rightarrow 2\text{NH}_4^+ + \text{Cell}\cdot\text{CaCO}_3$	NH_4^+
Ammonification (amino acid deamination)	$\text{R-NH}_3^+ \rightarrow \text{R} + \text{NH}_4^+$ $\text{NH}_4^+ + \text{OH}^- \rightarrow \text{HCO}_3^- \rightarrow \text{CO}_3^{2-} + \text{H}^+$	NH_4^+
Denitrification	$\text{CH}_2\text{COO}^- + 2.6\text{H}^+ + 1.6\text{NO}_3^- \rightarrow 2\text{CO}_2 + 0.8\text{N}_2 + 2.8\text{H}_2\text{O}$ $\text{Ca}^{2+} + \text{CO}_2 (\text{aq}) + 2\text{OH}^- \rightarrow \text{CaCO}_3 (\text{s}) + \text{H}_2\text{O}$	Complete reaction: $\text{CO}_2 + \text{N}_2$ Incomplete Reaction $\text{NO} + \text{N}_2\text{O}$
Sulphate reduction	$\text{SO}_4^{2-} + 2[\text{CH}_2\text{O}] + \text{OH}^- + \text{Ca}^{2+} \rightarrow \text{CaCO}_3 + \text{CO}_2 + 2\text{H}_2\text{O} + \text{HS}^-$	CO_2 HS^-
Photosynthesis	$2\text{HCO}_3^- + \text{Ca}^{2+} \rightarrow \text{CH}_2\text{O} + \text{CaCO}_3 + \text{O}_2$	O_2

Of the metabolic processes involved in MICP, urea hydrolysis is considered the least complex and produces more CaCO_3 precipitation when compared to the others, which is why it is the most studied process (Achal *et al.*, 2009).

1.2.2 Ureolysis Process

MICP by urea hydrolysis involves a series of reactions driven by urease, detailed in Figure 1-1. Urea is transported into cells, depending on the organism this may be via passive transport or utilising specific urea transport systems. The hydrolysis of urea produces 2 molecules of ammonia (Figure 1-1 step 1) and 1 molecule of carbamate, which upon further hydrolysis leads to an accumulation of ammonium and carbonic acid which equilibrate in water forming bicarbonate (Figure 1-1 step 2) and 2 molecules of NH_4^+ which increases the pH (Figure 1-1 step 3). This creates a shift in the bicarbonate equilibrium which creates a favourable environment for the microbial deposition of CaCO_3 in calcium rich surroundings (Figure 1-1 step 4). The negatively-charged functional groups of the cell envelope bind the Ca^{2+} ions, then CaCO_3 formation occurs when calcium ion activity is sufficient and saturation conditions for CaCO_3 precipitation are favourable (Figure 1-2 A and B). In this process, bacterial cells act as nucleation sites which encourage MICP. Fisher *et al.* (1999) observed that chemical precipitation of calcium (adding carbonate) was roughly 34-54% efficient, however when MICP bacteria were utilised this value

increased to 98% (Torres-Aravena *et al.*, 2018). These figures portray the beneficial effect bacteria have as simple nucleation sites. Successive stratification then occurs whereby layers of CaCO₃ develop on the cell surface Figure 1-2 (C). Nutrient transfer within the cell is abolished and so predictably cell death occurs. The cells become embedded by the CaCO₃ crystals.

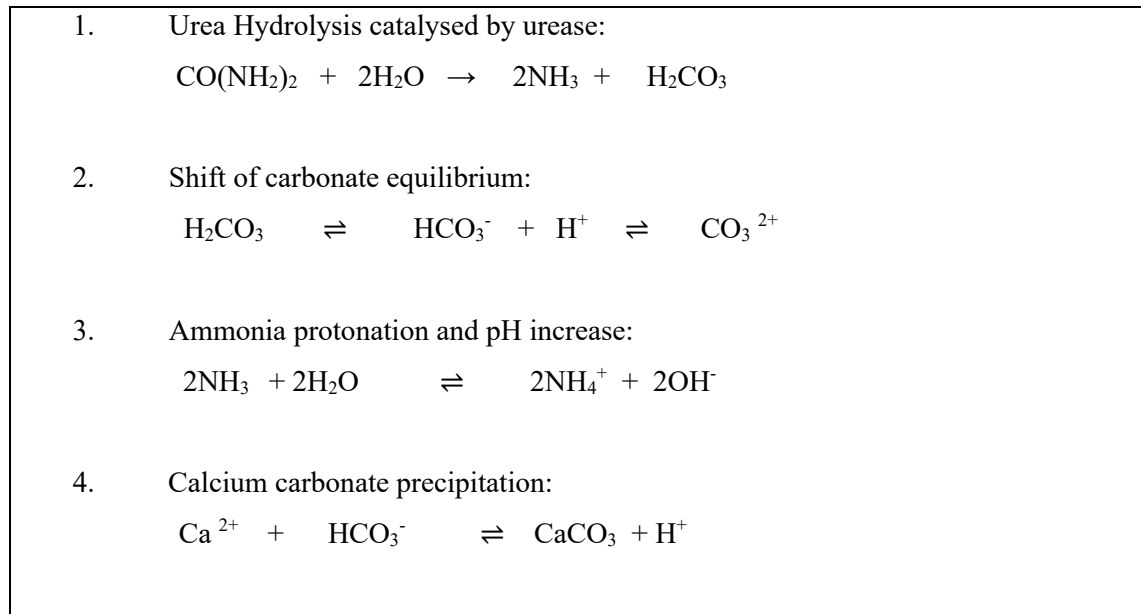


Figure 1-1. Urea Hydrolysis for MICP

As mentioned, cell surfaces and EPS have been demonstrated as competent nucleation sites for carbonate precipitation and in particular the cell wall of Gram-positive bacteria such as *B. subtilis*. The negatively-charged functional groups such as carboxyl, phosphate and amine etc. are adept at binding metal ions. They can bind a considerable amount of Mg²⁺, Fe³⁺, Cu²⁺, Na⁺, K⁺, Mn²⁺, Zn²⁺, Ca²⁺, Au³⁺, and Ni²⁺ (Zhu and Dittrich, 2016). The increase in metal ion concentration in the environment along with the presence of bicarbonate or carbonate produces an oversaturation of crystals.

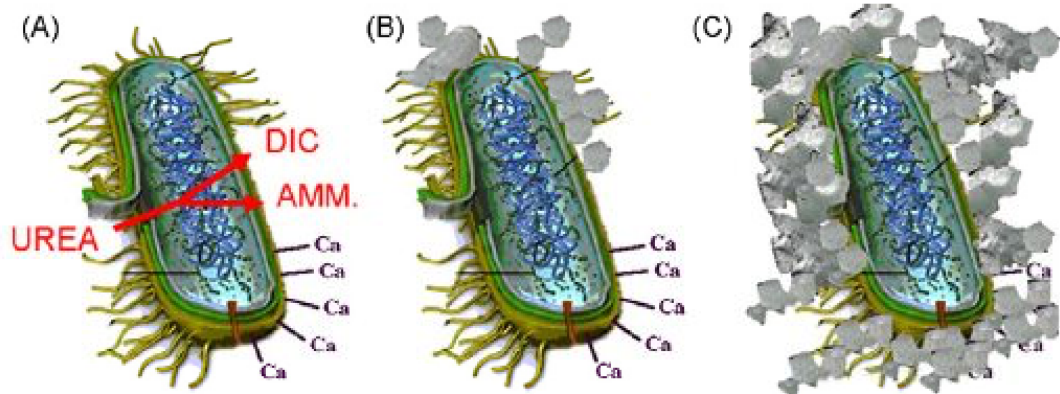


Figure 1-2. Depiction of the events occurring during the ureolytic induced carbonate precipitation (De Muynck, De Belie and Verstraete, 2010).

Bacteria include a negative charge on the cell wall which attracts calcium ions, the degradation of urea and dissolved inorganic carbon (DIC) and ammonium (AMM) are released into the microenvironment.

1.2.3 Factors affecting ureolytic MICP

There are many factors that control and influence the ureolytic MICP process. These include the type of microbe, as different microbial species and strains can alter the characteristics of CaCO_3 crystals e.g. crystal morphology (EPS can differ in biochemical properties), rate of precipitation, structure of crystals and urease activity (discussed later in this work) can affect cementation. Bacterial concentration is a factor, more nucleation sites influence the concentration and saturation of H^+ , Ca^{2+} and CO_3^{2-} . It is also imperative to create an environment in which the bacteria remain viable or the spores are able to germinate. The ability of bacteria to resist alkaline conditions by producing spores is essential to MICP. If sporulation occurs, they are then able to germinate, or ‘reactivate’ their metabolic activity when in the presence of CO_2 , SO_4 and NO_3 which can be seeded in the soil or via nutrient infusion. Other factors affecting ureolytic MICP include Ca^{2+} concentrations, urea concentration, different chemical elements within the surroundings (for example Mg^{2+}). Temperature and pH are obviously factors, with regard to any reaction catalysed by an enzyme as the stability or activity of the catalyst is critically important. There are numerous microorganisms that produce high levels of urease activity including *Sporosarcina pasteurii*, *Bacillus thuringiensis*, *Halomonas spp* and *Lysinibacillus sphaericus* CH5. *S. pasteurii* is the most studied and tested bacterium involved in MICP with regard to geo-materials (Achal *et al.*, 2009; Sarda *et al.*, 2009; Mortensen and DeJong, 2011; Raut, Sarode and

Lele, 2014). It is non-pathogenic, able to tolerate extreme conditions and although its urease has been well studied, the enzyme is still not fully understood with regards to its activation and catalysis.

1.2.3.1 pH range

An important factor in MICP is pH, which describes the acid-base chemical equilibrium, ultimately defining the precipitation of carbonate. The effect of pH is multifactorial, as it affects the enzyme itself, affecting the affinity to the substrate (Robinson, 2015). The optimum pH range for urease is pH 6-10, but this drastically decreases as the pH exceeds 10 (Gorospe *et al.*, 2013). The use of whole cells in MICP increases the tolerance to pH change, compared to the purified enzyme. The pH of the environment can also affect urease expression. There are specific ureolytic bacteria which under conditions of acidic pH will express urease for instance *Helicobacter pylori* where acidic conditions trigger cytoplasmic urease (Weeks *et al.*, 2000) and *Streptococcus salivarius* 57.1 where urease gene expression is induced (Huang, Burne and Chen, 2014).

1.2.3.2 Temperature

Temperature is vital to the growth and metabolism of bacteria and as with all enzymes, temperature is vital to the catalysis involved. The optimal temperature range for urease activity is 20 - 37°C. Temperature will affect the chemical equilibrium and therefore the solubility of CaCO₃ produced. Previous research identified the temperature for urease activity varies from 30 to 70°C for *S. pasteurii* and the optimum temperature for calcite precipitation is 50 °C (Okwadha and Li, 2010).

1.2.4 Applications of MICP

The production of materials via MICP has various applications. These include solid phase capture of contaminants (Fujita *et al.*, 2008), building restoration; where there is great evidence that microbial mineral technologies can be applied to the repair of limestone monuments and sand columns (De Muynck, De Belie and Verstraete, 2010), also part of building restoration is concrete remediation which utilises bio-concrete to fill concrete cracks. This is characterised as a self-healing concrete (Wiktor and Jonkers, 2011). Bio-concrete is gaining huge attention due to its

self-healing properties, the improvement of the concrete durability and its environmentally friendly and economic properties (Santosh *et al.*, 2001).

MICP is also a process now being applied to soil stability. The CaCO₃ crystals are metabolically precipitated in soil pores. This cements the soil particles, binding the particles together increasing stability and strength of the soil. The life expectancy of MICP treated soil is 50 years, which is comparable to the service life of geotechnical structures such as oil platforms and artificial islands (DeJong *et al.*, 2014). Many researchers (Harkes *et al.*, 2010; Whiffin, Van Paassen and Harkes, 2007) have investigated the use of MICP in soil stability where an improved strength, increased stiffness and resistance to liquefaction is observed. These properties are much sought after particularly in the built environment.

Other applications include bioremediation via co-precipitation of heavy metals (Fujita *et al.*, 2008; Achal, Kumari and Pan, 2011), CO₂ sequestration (Bose and Satyanarayana, 2017) and aspects of ground engineering as mentioned; soil stabilisation and erosion resistance, rock fracture and well sealing (Whiffin, 2004; Mortensen and DeJong, 2011; Santosh *et al.*, 2001; Gomez *et al.*, 2015).

1.2.4.1 Advantages of MICP

The use of MICP is an eco-friendly alternative concept to the current traditional construction and remediation technologies. The major advantage of MICP include its cost effectiveness. Whiffin *et al.* (2007) identified MICP to be cost-saving as the bacterial enzyme could be reused in subsequent applications, which meant MICP offers a cheaper treatment in the long term compared to other solutions (Whiffin, Van Paassen and Harkes, 2007). The MICP system regarding soil treatment is reliable, as stated by Mujah *et al.* (2017). MICP can be adjusted, mechanically and biologically which produces an optimal treatment depending on the soil (Mujah, Shahin and Cheng, 2017). The main advantage of MICP is sustainability. The use of MICP promotes the idea of sustainability via the use of natural materials to create a cementing bond. The process is able to be utilised not just in current construction sites but also in the remediation of old buildings and statues.

1.2.4.2 Challenges of MICP

There are also challenges of MICP listed in Table 1-2. The economic challenges of MICP are often the most investigated, as nutrients (especially laboratory grade) for large scale development of the process would be expensive. Previous examples to combat the expense have seen the introduction of inexpensive materials such as corn steep liquor (Achal and Pan, 2014b), as well as pig urine as a urea source, which lowers cost and is better for the environment (Chen *et al.*, 2019a). For some MICP processes, undesired by-products could be problematic. Particularly, in the case of urea hydrolysis, ammonia gas could be produced when the $\text{pH} > 9$, which is an environmental concern and has been found to lead to the discolouration of stone (Dhami, Reddy and Mukherjee, 2014).

Current processes for MICP include the repeated application of nutrients to a system which creates a nutritious environment, however this may nurture unwanted microbes. This may not necessarily incur a negative impact, as additional nucleation sites may aid the precipitation. However, the problem may occur if unwanted bacteria compete with bacteria being utilised in ureolytic MICP.

The microbial process as a whole could be classed as a challenge as the microbial activity depends on a variety of environmental factors such as temperature, pH and metabolites (Zhang *et al.*, 2017). The production of specific precipitation is also a factor concerning challenges of MICP but could be overcome via further investigations and optimisation of the process. There have been investigations into the optimal bacterial concentration for compressive strength, along with research into the morphology of microbial CaCO_3 which can be affected by the genera of bacteria (due to their cell surface properties), the viscosity of the media and the type of electron acceptors (Ca^{2+}) (Mondal and Ghosh, 2018; Seifan, Samani and Berenjian, 2016). Understanding the microbiological and molecular components involved in MICP will improve the process and performance.

Table 1-2. Challenges of MICP

Challenge of MICP	References
Economic	(Lee and Park, 2018; Achal and Pan, 2014a; Mitchell and Santamarina, 2005; Chen <i>et al.</i> , 2019a; Rajasekar, Loo Chin Moy and Wilkinson, 2017)
Microbial Process	(Lee and Park, 2018; Mondal and Ghosh, 2018; Pham <i>et al.</i> , 2018; Seifan and Berenjian, 2019)
Development of Unwanted Microbes	(Lee and Park, 2018; Mujah, Shahin and Cheng, 2017; Amidi and Wang, 2015)
Undesired by-product	(Lee and Park, 2018; Dhami, Reddy and Mukherjee, 2014; Ashraf, Azahar and Yusof, 2017)
Microbial study	(Lee and Park, 2018; Mujah, Shahin and Cheng, 2017; Dhami <i>et al.</i> , 2017; Castro Alonso <i>et al.</i> , 2019)
Inconvenient Application Procedures	(Lee and Park, 2018; Mujah, Shahin and Cheng, 2017; Wang <i>et al.</i> , 2017)

1.3 Urease

Urease, also called urea amidohydrolase was discovered approximately 150 years ago (Sumner, 1937). The biological function of urease is the hydrolysis of urea to yield ammonia and carbamate, these are unstable, and upon further hydrolysis spontaneously forms carbonic acid and ammonium, as shown in Fig 1-1 step 1 and step 2. The protein is a high molecular weight multi-subunit nickel containing metalloenzyme which includes an active site housing two Ni²⁺ ions (Zambelli *et al.*, 2011), although some exceptions to the co-factor (described in 3.1.3) have been identified (Carter *et al.*, 2011; Follmer *et al.*, 2002).

1.3.1 History of Urease Discovery

In 1874 von Musculus identified the first ureolytic protein from putrid urine, and later as proposed by Miquel in 1890, it was named urease (Sumner, 1937). It was then in 1926 that James B. Sumner identified urease as a protein by detailing the crystalline structure of Jack Bean Urease (JBU) (*Canavalia ensiformis*), in turn, demonstrating that a protein can function as an enzyme. This led

to the knowledge that most enzymes are proteins. In 1946 Sumner was awarded the Nobel Prize in Chemistry for his work. Continuing Sumner's legacy, Blakeley and Zerner in 1975 discovered the active site of urease includes the divalent metal nickel. Karplus *et al.* (1995) then successfully used X-ray crystal technology to describe the structure of *Klebsiella aerogenes* urease. It was the first enzyme shown to contain nickel as a co-factor, and so has historical biochemistry importance. Figure 1-3, shows nickel as the co-factor of *K. aerogenes* urease.

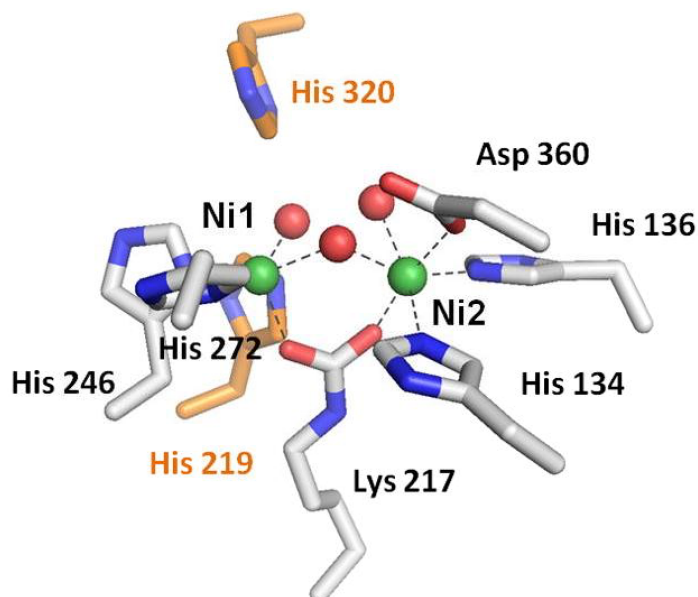


Figure 1-3 Urease active site containing two nickel ions in *K. aerogenes*. (Carter *et al.*, 2009).

The urease active site contains two nickel ions (green) which are bridged by a carboxylated lysine and hydroxyl group. Two histidines and a solvent molecule coordinate Ni 1 whereas Ni 2 is again coordinated by two histidines with an aspartic acid residue and a water molecule. Water molecules are identified in red, the metal binding side chains are identified with white carbon atoms and in orange are the two histidines which function in the catalysis.

1.3.2 Ureolytic Microorganisms

Urease activity is extensively found amongst prokaryotes, as well as in eukaryotes including fungi and plants (Li, Csetenyi and Gadd, 2014). However, most urease work has focused on microorganisms, many of which are soil microorganisms, but some are human pathogens.

1.3.2.1 Ureolysis in Pathogenic Microorganisms

Urease has been identified as a virulence factor for many microbial pathogens (Moraes *et al.*, 2014). Originally the enzyme was thought only to be a virulence factor in strains such as *H.*

pylori, which colonises the stomach, *Staphylococcus saprophyticus* which causes gastritis, and *Proteus mirabilis*, which causes urinary tract infections, and in *Klebsiella* species which cause pneumonia, bloodstream infections, wound infections, urinary tract infections and meningitis (Konieczna *et al.*, 2012; Jones, Li and Zamble, 2018). It is also a major virulence factor of the invasive fungus *Cryptococcus neoformans* (Fu *et al.*, 2018).

Ureases are responsible for certain human diseases such as peptic ulceration, pyelonephritis, and kidney stones. Ureolysis provides an alkaline urinary environment. Urease is not present in sterile human urine, and so infection with an ureolytic microbe is an essential prerequisite for the formation of kidney stones (containing calcium oxalate or struvite). Ureolytic activity also enhances microbial survival in the host. The production of ammonium ions and bicarbonate creates a buffering system, maintaining a neutral cytosolic pH, enabling the bacteria to withstand acidic environments. This is highly important in pathogenic bacteria, where colonization of the digestive and urinary tract is made possible by the production of urease.

1.3.2.2 Ureolysis in Non-pathogenic Microorganisms

Urease has been identified in numerous non-pathogenic bacteria from terrestrial and aquatic habitats (Dunn, Campbell, Perez-Perez, & Blaser, 1990; Gatermann & Marre, 1989; Graham *et al.*, 1987; Jones & Mobley, 1988), and plays an essential role in the nitrogen cycle of the microorganisms that inhabit these terrains where urea hydrolysis generates accessible nitrogen for plant growth. Urea can enter the soil via excretions of animals and through the degrading of animal and plant material. It is also globally the most commonly used nitrogen fertiliser and as the substrate for urease is subject to hydrolysis generating ammonia which increases soil fertility.

Combining the skills of geotechnical engineering, microbiology and now synthetic biology will facilitate the advancement of biocementation. That is, harnessing microbiological activity to improve the engineering properties of construction materials and the soil itself. MICP is now commonplace in order to achieve soil biocementation through inducement. The enzyme urease (EC 3.5.1.5) therefore has a major role in the MICP process.

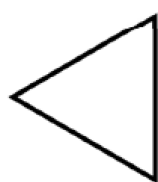
1.3.3 Urease Proteins and Activation

Urease is a metalloenzyme. Metalloenzymes usually require complex metallocentre assembly systems to generate functional active sites (Farrugia, Macomber and Hausinger, 2013).

1.3.3.1 Urease Structural Proteins

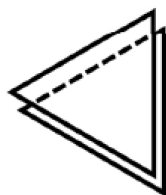
Bacterial urease structures can vary but are based on a trimeric structure identified from x-ray crystallography studies (Krajewska, 2009). The amino acid sequence of bacterial ureases and JBU are closely related which suggests a common evolutionary origin (Follmer, 2008). Plant and fungi ureases consist of a single polypeptide chain as their functional unit (α), whereas bacterial urease can consist of either 2 polypeptide chains (α and β) currently only found in *Helicobacter* species (where β and γ are incorporated as β) or 3 polypeptide chains (α , β and γ) in most bacterial ureases creating the structural unit. The quaternary structure of most bacterial ureases are referred to as a trimer of trimers $[(\alpha\beta\gamma)_3]$. As detailed in Figure 1-4, the trimeric urease is schematically represented as triangles, forming the basic repeating unit of urease to form the more complex quaternary structures as seen in *Klebsiella aerogenes* and *S. pasteurii*.

The urease structural subunits consist of 3 polypeptide chains, they are; UreA (subunit γ), UreB (subunit β) and UreC (subunit α).



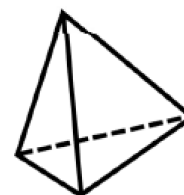
Trimer (ABC)₃

K. aerogenes



Hexamer (A₃)₂

C. ensiformis (JBU)



Dodecamer [(AB)₃]₄

H. pylori

Figure 1-4 The trimeric urease structure adapted from Nim *et al.* (2019) (Nim and Wong, 2019).

Trimeric urease is schematically represented as triangles which form the basic repeating unit of urease to form more complex quaternary structures. Plant urease such as *C. ensiformis* consist of two urease trimers stacked in symmetry to form a hexameric quaternary structure. A dodecameric urease is formed by *H. pylori* which assembles a tetrahedral symmetry.

1.3.3.2 Urease Active site

The cytosolic enzyme was first found to contain Ni²⁺ in its active site (1975) and this was the first indication of a biological role for the metal. There has been much research carried out on *K. aerogenes* and *S. pasteurii* urease and their crystal structures, their active sites are so similar they could be superimposed (Balasubramanian and Ponnuraj, 2010). This indicates that the active site architecture is typical of most bacterial ureases. In general, the active site is on UreC. The active site consists of two nickel ions (Ni²⁺), a carbmylated lysine, four histidines and an aspartate residue.

In *K. aerogenes* the active site as detailed in Figure 1-3, is found in UreC (α subunit) and contains 2 nickel ions bridged by a carboxylated lysine (LYS217) and solvent molecule (Carter *et al.*, 2009). The first Ni²⁺ (Ni1) is coordinated by 2 His residues (246 and 272) and a terminal water molecule. However, the second Ni²⁺ (Ni2) is coordinated by 2 His (134 and 136), Asp (360) and a terminal solvent. The active site also consists of 2 His residues which are believed to participate in the substrate binding and possibly catalysis. The binding of Ni²⁺ (and zinc) ions in proteins is dominated by His residues. Therefore, His rich sequences by sequential annotation should bind Ni²⁺ also important is the ability to adopt a suitable configuration.

A 'mobile flap' forms in the active site from a conserved cysteine. This acts as a gate for the substrate, urea. The mobile flap is accountable for the influx and efflux of substrate via motion control of a conserved histidine (Kappaun *et al.*, 2018).

1.3.3.3 Urease Accessory Proteins

To make those sites active, the co-factor Ni^{2+} has to be inserted into the metal binding sites with the aid of accessory proteins. The general understanding of accessory proteins functions are to act as Ni^{2+} transporters, incorporating the ions into the cell and directing the ions into the metallocentre of the apoenzyme (Konieczna *et al.*, 2012). Regarding the activation of the urease, the most well studied, but yet, still not fully understood bacterial urease systems include those of *K.aerogenes*, *H. pylori* and *S. pasteurii*. Figure 1-6 shows the activation mechanisms based on *K. aerogenes* urease which were proposed by Carter (2009). In order to facilitate urease activation, *K. aerogenes* also expresses accessory proteins which are UreD, UreE, UreF, and UreG. These proteins are necessary for active site metalation and urease maturation as visualised in Figure 1-5. Briefly, UreD provides the scaffold function in order to recruit the other accessory units. Sequentially, UreF then binds to the apoprotein and UreD and confirms metallocentre fidelity. The GTPase, UreG, does not interact with the apoprotein itself, but binds to UreD and UreF. Finally, UreE is considered to be the metallochaperone, binding and delivering the nickel ions to the apoprotein via the chaperone complex UreD-UreF-UreG. The whole process is GTP-dependent. There is an alternative theory as detailed in Figure 1-5 whereby UreDFG preexists and binds to the apoprotein. The roles of these proteins in the urease activation will be discussed in next section.

Other accessory proteins have been reported in different microorganisms and plants. For example, UreH, HypA and HypB were found to work as accessory and essential proteins for activation of the *H. pylori* urease (Benoit *et al.*, 2007).

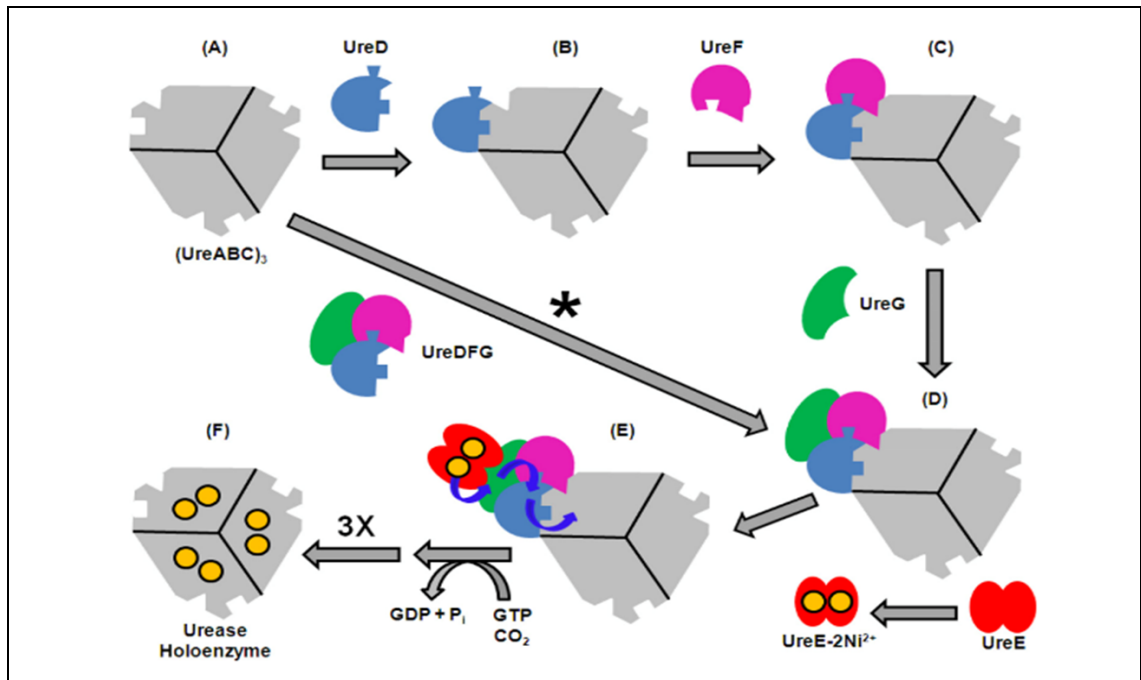


Figure 1-5. The activation of *Klebsiella aerogenes* urease with accessory genes.

The urease apoprotein (A) binds UreD, UreF, and UreG to form UreABC-UreD (B), UreABC-UreDF (C), and UreABC-UreDFG (D). The urease apoprotein binds to UreD and to UreF; UreD and UreF bind each other; and UreG binds to these proteins with no direct interactions to urease. A metallochaperone UreE incorporates the nickel ion into the enzyme (Carter *et al.*, 2009).

1.3.3.4 Urease Activation

Urease is a dinuclear Ni²⁺ enzyme whereby Ni²⁺ is inserted into the active site via a GTP dependent process with the facilitation of the accessory proteins. The most studied mechanisms for urease activation are based on *K. aerogenes* (Figure 1-5). In this bacterium, the accessory proteins have been identified as forming specific protein-protein complexes: Apo·UreD, Apo·UreD·UreF, Apo·UreD·UreF·UreG, UreH·UreF, UreD/H·UreF·UreG (Hausinger, 2011). Therefore, it has been hypothesised that the urease apoprotein will bind 3 molecules of UreD, forming the complex Apo·UreD, UreF forming Apo·UreDF then UreG forming Apo·UreDFG or it may interact with the protein complex (UreDFG)₂ to produce the same species. UreE, the metallochaperone then donates Ni²⁺ to UreG, the Ni²⁺ bound UreG then forms the Apo·UreD·UreF·UreG·Ni structure. GTPase activity of UreG drives the Ni²⁺ transfer from UreG to Apo, a molecular tunnel in the UreF and UreD/H scaffold allows the passage of the Ni²⁺. Once assembled the metalcentre dissociates, the accessory proteins dissociate from the urease holoenzyme. With regard to *H. pylori*, HypA and HypB are assumed to provide nickel to UreE

(Hausinger, 2011). Urease accessory proteins are discussed in further detail in sections 4.1.1.1 to 4.1.1.5.

1.3.4 Urease Gene Clusters

Microorganisms that possess an active urease usually include structural subunits and accessory proteins. Subsequently, it is necessary to have genes coding for structural proteins and genes coding as accessory proteins which are usually located in a joint cluster in the same operon (Konieczna *et al.*, 2012). As shown in Figure 1-6, most of the microorganisms have 3 structural genes (*ureABC*) which are adjacent to each other, however, there are huge variations in the range of the accessory genes. The majority contain the accessory genes *ureDEFG*, which encode all the accessory proteins as in *K. aerogenes*, although the location of those genes can vary.

Urease accessory genes encode proteins of varying functions in specific bacterial strains. Although not present in all urease operons; *ureI* of *Helicobacter* (Figure 1-6) encodes UreI which functions as an acid activated urea channel, increasing the rate of urea into the cytoplasm. In *Helicobacter* species *ureD* is renamed *ureH*, with its protein function being consistent with UreD. In some *Bacillus sp* *ureD* and *ureH* are conserved (Carter *et al.*, 2009) and so the function of *ureH* still remains unclear. Again, although not present in all urease operons the *ureMQO* complex of *Streptococcus salivarius* (Figure 1-6) functions as a Ni²⁺ transporter and the operon consists of 11 genes (*ureIABCEFGDMQO*) (Chen and Burne, 2003). Any mutations involving the components of the Ni²⁺ transporter system of *S. salivarius* produced a complete abolishment of urease activity.

Urease gene cluster combinations vary greatly not only between different species of bacteria but also between different strains (Figure 1-6). As stated, ureolytic bacteria typically require UreD, UreE, UreF and UreE, as maturation proteins. Plants and fungi include homologues of UreD, UreF and UreG but are deficient in proteins comparable to the chaperone UreE. *Helicobacter* species are extraordinary as the urease gene clusters consists of only 2 subunits and 4 accessory genes (where *ureH* replaces *ureD*); the cluster typically includes a proton gated urea permease (UreI). Also, unique to this bacterium are the hydrogenase activation proteins HypA and HypB, which are also essential for urease activation (Ge *et al.*, 2013).

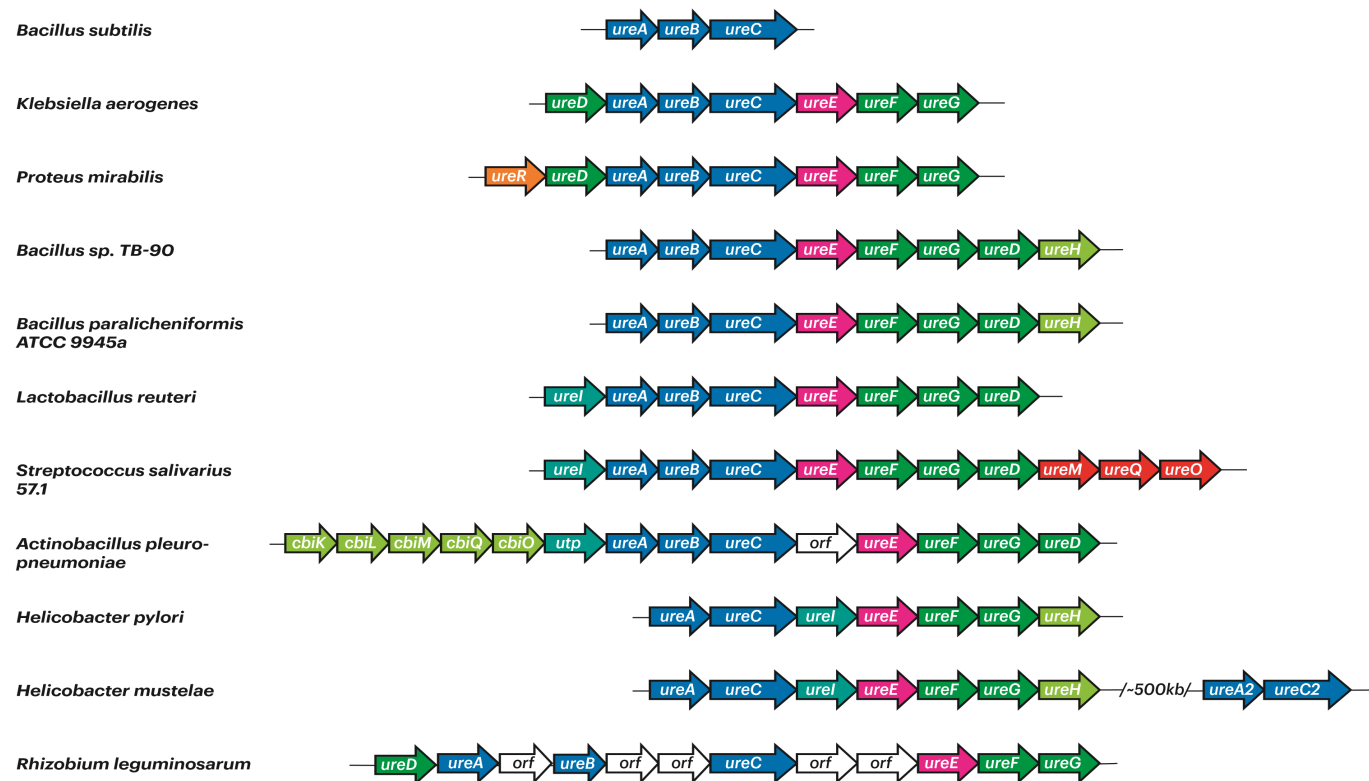


Figure 1-6. Organization of representative urease gene clusters adapted from (Yang *et al.*, 2015; Chen and Burne, 2003; Carter *et al.*, 2009).

Urease gene clusters of well-studied bacteria and the organisational differences between them. *K. aerogenes* urease is one of the most well studied urease operons (*ureDABCEFG*) and the genetic organization found in other bacteria differs greatly. *R. leguminosarum*, contains insertions dispersed within the urease genes; *Bacillus sp.* TB-90, repositions *ureD* and includes a nickel permease (*ureH*); *A. pleuropneumoniae*, aligns genes encoding a nickel transport system (*cbiKLMO*) and urea permease (*utp*); *Helicobacter* species include a proton-gated urea channel (*ureI*); and *B. subtilis* completely lacks any urease accessory genes.

Genome sequencing has revealed that, unlike other urease-producing bacteria, *B. subtilis* 168 only contains urease structural genes (*ureABC*) (Figure 1-6) and within its genome lacks any homologues to genes coding for accessory proteins (Cruz-Ramos *et al.*, 1997). *B. subtilis* defies traditional thinking, as the organism exhibits urease activity (although with poor efficiency) and can grow using urea as the sole nitrogen source (Kim, Mulrooney and Hausinger, 2005a). To understand urease activation of *B. subtilis* would be of great importance and possibly reveal another mechanism of activation.

1.4 *Bacillus subtilis* and its urease

B. subtilis was originally named *Vibrio subtilis* in 1835 by Christian Gottfried Ehrenberg and renamed *Bacillus subtilis* in 1872 by Ferdinand Cohn (Kovacs, 2019). It is a Gram-positive, rod shape soil bacterium. *B. subtilis* was commonly regarded as an obligate aerobe, however, it was later shown to be able to grow anaerobically by nitrate respiration and by fermentation (Nakano and Zuber, 1998). A distinctive property of *B. subtilis*, is the organism's ability to form endospores. The endospore in unfavourable conditions houses the cell's DNA, heavily guarded by the spore structure. The spore is able to withstand extreme tolerance for example heat, cold, radiation and pressure (Chen *et al.*, 2019).

The *B. subtilis* strains used in virtually all academic research and many industrial processes derive from a single tryptophan-requiring auxotroph, strain 168 (Zeigler *et al.*, 2008). *B. subtilis* 168 was isolated after the *B. subtilis* Marburg was mutagenized with X-rays by the Yale University botanists, Paul Burkholder and Norman Giles. This strain was subsequently circulated around the globe and researchers developed classical genetic methods utilising recombinant and genomic technologies—to understand the physiology and spore development of this strain (Zeigler *et al.*, 2008). *B. subtilis* is the most studied Gram-positive organism and as such is a model organism and was one of the first bacteria to have its genome fully sequenced, identifying a 4.2 Mbp chromosome with about 4100 genes (Errington and Aart, 2020).

This soil bacterium is highly adept to environmental changes, and this cements the basis of its success, not just in nature, but also in commercial applications.

1.4.1 *B. subtilis* Urease

The primary habitat of *B. subtilis* is the upper layer of soil. This ecosystem offers a wide variety of environmental challenges as well as nutrient limitations that generate adaptation mechanisms that allow them to survive under such conditions (Petrackova *et al.*, 2010). *B. subtilis* can produce a urease enzyme, however, genome sequencing has acknowledged that unlike other ureolytic organisms, *B. subtilis* only contains urease structural genes (*ureABC*), and within its genome there lacks any comparison to any known accessory proteins (Kim, Mulrooney and Hausinger, 2005a).

1.4.1 The Function of Urease in *B. subtilis*

Urease which is not constitutively produced can be activated for variety of reasons; such as the presence of urea, acid resistance as in *S. salivarius* and nitrogen limitation. The enzyme represents a pathway for the release and utilisation of ammonia from urea. This can be as an external source or as an intermediate of purine degradation. Those bacteria that possess urease encoding operons demonstrate the importance of urea as a nitrogen source. Urea is a nitrogenous compound that is produced from the degradation of arginine and purines and *B. subtilis* synthesises urease in order to hydrolyse urea to produce ammonium as a nitrogenous source.

Extensive research of *B. subtilis* urease was carried out by numerous groups, to name a few; Mobley and Hausinger, Fisher *et al.*, Carter *et al.* in the 1990s. As technology and genome sequencing developed Mobley *et al.* 1995 was able to review numerous urease gene clusters and explore the regulation of urease gene expression in different bacterial species.

It is understood that accessory proteins are required for urease activity. However, *B. subtilis* defies conventional thinking as it exhibits urease activity and can grow using urea as the sole nitrogen source (Konieczna *et al.*, 2012). Fisher's group described this activity, and interestingly their research demonstrated that increased levels of *B. subtilis* urease are produced when there is nitrogen limited growth conditions, where one nitrogenous source is a medium constituent (Atkinson and Fisher, 1990).

B. subtilis urease consists; 11 kDa UreA (subunit γ), 13.6 kDa UreB (subunit β) and 61 kDa UreC (subunit α) and its genetic sequence is detailed as in the Appendix Figure 9-1. Kim *et al.* (2005) discuss evidence supporting the idea that *B. subtilis* includes novel accessory genes (Kim, Mulrooney and Hausinger, 2005b). The first line of evidence is due to *B. subtilis* showing an increased efficiency of urease activation, especially in nitrogen limited media (NLM). This was identified by Atkinson and Fisher (1990) who classified medium containing a single nitrogen source as “nitrogen limiting”; a terminology that will be used here throughout. The second indication was identified when *B. subtilis* cells overexpressing recombinant *ureABC* (from *B. subtilis*) lacked increased urease activity. The recombinant *B. subtilis* cells were expected to contain nickel and bicarbonate concentrations comparable to that of the wild-type *B. subtilis* cells, however, a lower percentage of urease is shown to be activated. These results may support the idea that an unidentified accessory protein/s are involved in urease activation within *B. subtilis*. It is apparent that further studies are necessary to clarify urease activation in *B. subtilis*.

As mentioned in section 1.3.4, urease genes (structural genes and accessory genes) are often usually located in a joint cluster (Konieczna *et al.*, 2012) such as *K. aerogenes* and *L. reuteri*. However, in some microbes their urease genes are interrupted by intervening sequences, such as the bacterium *Rhizobium leguminosarum*, *Synechocystis sp.* strain PCC 6803 and *Thermosynechococcus elongatus BP-1* as detailed in Figure 1-6.

The actinobacterium, *Mycobacterium tuberculosis* Erdman strain is interesting when comparing it to the *B. subtilis* urease system. This strain consists of a gene cluster of only *ureABCFG*, yet it is still able to synthesize active urease without *ureD*, or *ureE*, the chaperone for assembly of the active enzyme (Clemens, Lee and Horwitz, 1995). Which means not all accessory proteins are necessary for urease activation.

It was proposed by Kim *et al.* (2005) that the accessory protein/s of *B. subtilis* urease may be distributed elsewhere in the genome (Kim, Mulrooney and Hausinger, 2005a) or as we propose, is it possible *B. subtilis* employs non typical accessory proteins to activate its structural proteins? It is apparent that further studies are necessary to clarify urease activation in *B. subtilis*.

1.4.1.1 Non-typical Accessory Proteins

The activation of urease in some microorganisms has been shown to be facilitated by non-typical urease accessory proteins. These additional accessory proteins can include transport systems such as the YntABCDE in *Yersinia pseudotuberculosis*. Upon deletion of the genes coding for the proteins Ni²⁺ uptake rate is reduced and urease activity was eradicated (Sebbane, Mandrand-Berthelot and Simonet, 2002). Recently, Brauer *et al.* (2020) demonstrated in *Y. pseudotuberculosis* YntA was more crucial in urease activity than the dedicated Ni²⁺ protein NikA (Brauer, Learman and Armbruster, 2020). The CbiKLMQO (Figure 1-6) complex of *A. pleuropneumoniae* are encoded by putative nickel transport genes which are also required for urease activity (Bossé, Gilmour and MacInnes, 2001).

These non-typical proteins could drive questions for urease activation in *B. subtilis*. There are also anomalies such as in the soil and water bacterium *Ralstonia eutropha* which in its genome includes, *hoxN*, a single gene responsible for Ni²⁺ transport. Could *B. subtilis* 168 include an unidentified protein interpreted as having a transport function, but, is responsible for the activation of urease, similar to HoxN? Comprehensive research is clearly required to investigate these questions further.

1.4.2 The Use of *B. subtilis* in MICP

B. subtilis is a model organism consisting of 4,215,606 nucleotides, coding for 4244 proteins (van der Steen, 2013). It has been extensively studied, much of its genomics, metabolic and developmental pathways have been identified. It is a non-pathogenic spore former, easy to cultivate and tolerant of extreme conditions. It also produces an active urease, albeit with poor efficiency (Cruz-Ramos *et al.*, 1997). The use of this bacterium in synthetic biology and metabolic engineering is notably advantageous, and we can exploit the unique metabolic pathways present (Song *et al.*, 2016). The engineering of *B. subtilis* into a next generation super engineered cell factory requires combined systems and synthetic biology approaches (van Dijl and Hecker, 2013). The research will enable a system that will promote the design of a competent and controllable promoter structure that responds appropriately to the imposed stress stimuli whereby the upregulation of urease in *B. subtilis* will be possible.

MICP studies have been primarily focused on the mechanical or structural properties of concrete. To understand the biological aspect of MICP is now critical. The ability to select a suitable organism or to even genetically select and enable the bacteria to survive and then facilitate a self-healing process such as MICP would be advantageous. There is therefore a great need in understanding urease regulation and activation pathways.

Once the regulation and activation of *B. subtilis* urease is understood, then along with synthetic biology, an engineered cell could be created. A cell in which urease activation could be controlled possibly alongside a pressure promoter that under undue stress would activate urease activity to promote high levels of MICP. Thus, creating enhanced precipitation and benefits to the construction industry.

1.5 Aims and Objectives

This PhD research project is one work package of the EPSRC funded ‘Thinking Soils’ project (EP/R003777/1), which is a collaboration between Newcastle and Northumbria Universities. The ‘Thinking Soils’ project aims to develop a bacterial system using *B. subtilis* in which urease expression is increased under mechanic pressure which leads to the production of CaCO₃ for soil improvement. Such systems potentially have wider civil engineering applications, for example it could be used as a riverbank floor defence or self-constructing foundations for the buildings. The overall project will be achieved through various working packages across various research disciplines. One of those work packages is to understand urease regulation and activation in *B. subtilis*. This PhD research project is set to achieve this aspect of the ‘thinking soils’ project and the results will link into the research of a synthetic biologist who will identify and develop a pressure sensitive promoter in *B. subtilis*. This promoter will link to the urease operon in *B. subtilis* and increase the expression of urease upon a stress being placed and the production of CaCO₃ will be increased as the result of MICP.

This aim of this PhD project is to understand the activation of urease in *B. subtilis* for the future application in construction materials. This aim will be achieved through a number of objectives including:

- 1) Defining a minimal media and suitable enzyme assay so that urease activity can be investigated in defined conditions such as a nitrogen limited condition and pH (Chapter 3);
- 2) Using a proteomic approach to investigate the proteins upregulated in *B. subtilis* cells during growth under the conditions in which *B. subtilis* has increased urease activity, and identify the proteins expressed (Chapter 3 and 4);
- 3) Investigating the potential role of the proteins identified in the objective 2 in the urease activation through urease enzyme assay using targeted knockout strains (Chapter 4 and 5)
- 4) Investigating the recombinant *B. subtilis* urease expressed in *E. coli* to understand the urease activity without accessory proteins (Chapter 6).

The accomplishment of the objectives will identify how urease in *B. subtilis* is activated and regulated. The understanding of urease activation by identifying potential urease accessory proteins in *B. subtilis* will not only enhance the knowledge database for this microorganism but also enable the engineered bacterium to be commercially utilised in the construction industry.

Chapter 2 Materials and Methods

2.1 Materials and Methods

2.1.1 Bacterial strains and growth conditions

The lab strain *B. subtilis 168* is used throughout this study. *B. subtilis* was cultivated in various media which will be detailed below following aseptic technique. All cultures were incubated in an orbital incubator (ANNOVA 44) at 30°C, 150 rpm.

2.1.2 Media Preparation

All media was produced with distilled water (unless otherwise stated) and autoclaved for sterilisation (unless otherwise stated). The autoclave (Rodwell, Gemini 316); maintained a temperature of 121° C for at least 15 minutes using saturated steam under at least 15 psi of pressure.

Luria Bertani Broth (L3022 Sigma)

The LB media (L3022 Sigma) was produced following the manufacturer's instructions (37 g/L).

Spizizens' Minimal Medium (SMM):

Cultivation of starter culture strains was achieved in SMM. The components of the medium are as follows:

	per litre
(NH ₄) ₂ SO ₄	2 g
Di-Potassium hydrogen phosphate	14 g
Potassium dihydrogen phosphate	6 g
Tri-sodium citrate.2H ₂ O	1 g
Magnesium sulphate.7H ₂ O	0.2 g
pH approx. 7.4 with 1 M KOH	

The following supplements of SMM were prepared in H₂O 18.2 MΩ/cm. They were filter sterilised and stored at 4°C.

Glucose	40 % (w/v)
MgSO ₄ .7H ₂ O	1 M
Casamino acids (CAA)	20 % (w/v)
Ammonium Iron citrate	0.22 % (w/v)
Tryptophan solution	2 mg/ml.

Final medium for overnight culture prepared fresh on the day consists

Per 10 ml

40 % (w/v) glucose	125 μ l
2 mg/ml Tryptophan	100 μ l
1 M MgSO ₄ .7H ₂ O	60 μ l
20 % (w/v) Casamino acids (CAA)	20 μ l
0.22% (w/v) Ammonium Iron Citrate	5 μ l

Glucose Glutamate Glycine Salts (GGGS) Minimal Media

The minimal media contains:

K ₂ HPO ₄	3.0 mM
KH ₂ PO ₄ .	5 mM
MgSO ₄ .7H ₂ O	0.8 mM
MnSO ₄ .4H ₂ O	0.04 mM
NaCl	0.2 mM
CaCl ₂	0.2 mM
ZnSO ₄ .7H ₂ O	0.05mM
FeSO ₄ .7H ₂ O	0.04 mM
Glycine	1.3 mM
Glutamic acid	70 mM
Glucose	5.5 mM

The pH was adjusted to 7.0 with addition of 1 M NaOH.

Media Basal Salt Solution BSS (JW)

The optimised media BSS (JW) was derived from a media described by Chasin and Magasanik

(Chasin and Magasanik, 1968). It contains:

	per L
K ₂ HPO ₄	14 g
KH ₂ PO ₄	6 g
MgSO ₄ .7H ₂ O	0.2 g
MnSO ₄	1 mg
FeCl ₃	1 mg

The pH was adjusted to 7.4 with addition of 1 M KOH

Once autoclaved the supplements were added as shown below.

	per 50 ml BSS
40% Glucose stock	0.5 ml
2 mg/ml Tryptophan stock	0.5 ml
5 g/L Glutamic acid*	0.5 ml
150 mM NaCl Stock	0.5 ml

*Glutamic acid was dissolved in 1 M HCl and using 4 M NaOH returned to pH 7

To optimise BSS (JW) growth medium, various concentrations of glutamic acid (as shown below) were tested

Normal [Glutamic acid]	5.0 g/L
Low [Glutamic Acid]	2.5 g/L
High [Glutamic acid]	10.0 g/L

BSS (JW) Nitrogen Excess Media

In addition to BSS (JW) media, 20 g/L Ammonium sulphate was added to create a nitrogen excess media.

2.1.3 Growth Conditions

To ascertain whether the growth media was suitable for the cultivation of *B. subtilis* basic inoculations were carried out. Per 10 ml of culture, 1 colony of *B. subtilis* 168 from an LB plate was inoculated. Cultures were incubated at 37°C 200 rpm overnight unless otherwise stated.

2.1.3.1 Growth analysis of *B. subtilis* 168

Growth media was inoculated with 1% (v/v) starter culture (SMM). Cultures were incubated at specified temperature and rpm. Initial growth curves were determined using the Biotek Synergy HT plate reader. The plate reader was set up with a 12 well plate (2 ml of BSS (JW) media per well).

The culture was incubated at 30°C, with linear shaking (approximately calculated as 150 rpm) for 72 hours. The absorbance at 600 nm ($OD_{600\text{ nm}}$) is measured at 2 hourly intervals. The data was saved and analysed in Excel document.

Final growth curve analysis was carried out in 500 ml BSS (JW) medium in 2 L conical flasks at 30°C, 150 rpm (ANNOVA 44). Time points were taken at hourly intervals, 1 ml of culture was aseptically removed and the absorbance at 600 nm was measured using an optical spectrometer (Spectronic unicam, Helios α). The OD was input into an Excel document and a growth curve produced for analysis.

2.1.4 Buffers used in Cell harvest and enzyme assay

Various buffers were tested to optimise the cell harvest and urease enzyme assay methods

All buffers in Table 2-1 were made up in 18.2 M Ω /cm H₂O.

Table 2-1. Buffers used in urease assay

Buffer	Concentration	pH
Sodium Phosphate	20 mM	7.4
Tris EDTA (TE)	1 M Tris, 1 mM EDTA	7.4
1x Tris-buffered Saline (TBS)	50 mM Tris-HCl;150 mM NaCl	7.8
HEPES	50 mM	7.4

2.1.5 Whole Cell assay of urease activity using Nessler reagent

B. subtilis 168 was cultured to exponential phase (OD_{600 nm} approx. 1.0) in shake flasks. To determine the urease activity, an aliquot per flask for was sampled. Cells were centrifuged at 5000 x g for 5 min at 4°C. The supernatant was removed, and the pellet washed in 1 ml of 20mM Sodium phosphate buffer (referred as Method 1 in Table 2-2). This was repeated 3 times. After the final wash, the pellet was resuspended in 0.95 ml of 20 mM Sodium phosphate buffer and then 50 μ l of Urea (20 g/L) was added. Zero time points were taken upon addition of urea. All other samples were incubated shaking at 37°C. The samples were taken at time points 1 h, 2 h, 5 h and 24 h, and then centrifuged at 5000 x g for 5 min 4°C. 25 μ l of supernatant was used for the reaction with 850 μ l of 18.2 M Ω /cm water and 125 μ l of Nessler Reagent (Sigma 72190). The OD was measured at 420 nm using a spectrometer (Helios). The reaction standard was set up as indicated in Table 2-3. All assays were performed in triplicates.

2.1.6 Optimization of Buffers for Whole Cell assay of urease activity using Nessler reagent

B. subtilis 168 was cultured to exponential ($OD_{600\text{ nm}}$ approx. 1.0) in shake flasks. To determine the urease activity, an aliquot of 20 ml (from a 50 ml culture) was centrifuged at 5000 x g for 5 min. The supernatant was removed, and the pellet washed in 20 ml of TBS (referred to as Method 2 in Table 2-2) Tris EDTA (TE) buffer (referred to as Method 3 in table 2-4) and 50 mM HEPES buffer (referred to as Method 4 Table 2-2) respectively. All the washes for each method was repeated 3 times. After the final wash, the pellet was resuspended in 20 ml TBS and 950 μ l aliquoted into micro centrifuge tubes (in triplicate for each time point) and 50 μ l Urea (20 g/L) added. Zero time points were taken upon addition of urea. All other samples were incubated shaken at 37°C. In each optimisation the samples were taken at time points 1 h, 2 h, 5 h and 24 h and centrifuged at 5000 x g at 4°C for 5 min. 25 μ l of supernatant was used for the reaction with 850 μ l of 18.2 M Ω /cm Water and 125 μ l of Nessler Reagent. The OD was measured at 420nm using a spectrometer as described in section 2.2.4. The reaction standard was set up as indicated in Table 2-3. In each optimisation all assays were performed in biological and technical triplicates.

2.1.7 Cell Free Extract (CFE) Assay of Urease using Nessler Reagent

B. subtilis 168 was cultured to exponential ($OD_{600\text{ nm}}$ approx. 1.0) in 50 ml in 250 ml shake flasks. Aliquots were centrifuged at 5000 x g for 15 min at 4°C. Cells were washed in 20 ml of the appropriate buffer (see Table 2-2). After the 3rd wash the pellets were resuspended in 3.80 ml buffer and sonicated on ice for 1 minute with 10 seconds on, and 10 seconds off at 13 KHz (MSE, Soniprep 150). This is referred as method 5 in Table 2-2. Samples were then centrifuged at 5000 x g at 4°C for 30 min. The supernatant was harvested for assay, using 25 μ l of supernatant was for the reaction with 850 μ l of 18.2 M Ω /cm water and 125 μ l of Nessler Reagent, the OD was measured at 420nm as mentioned in section 2.2. The reaction standard was set up as indicated in Table 2-3. All assays were performed in biological and technical triplicates.

2.1.7.1 Optimization of CFE for Urease Assay using Nessler Reagent

The method was optimised (Method 6 Table 2-2) by increasing the culture volume to 4 x 500 ml

in 2 L flasks. Aliquots were centrifuged at 5000 x g for 15 min at 4°C. Cells were washed in 20 ml of the appropriate buffer (see Table 2-2). After the 3rd wash the pellets were resuspended in 5 ml buffer and sonicated on ice for 1 minute with 10 seconds on, and 10 seconds off at 13 KHz. This is referred to as method 5 in Table 2-2. Samples were then centrifuged at 5000 x g at 4°C for 30 min. The supernatant was harvested for assay, using 25ul of supernatant was for the reaction with 850 µl of 18.2 MΩ/cm water and 125 µl of Nessler Reagent, the OD was measured at 420nm as mentioned in section 2.2. The reaction standard was set up as indicated in Table 2-3. All assays were performed in biological and technical triplicates.

2.1.7.2 Final Condition for CFE Assay

B. subtilis 168 was cultured (2 L – 4 x 500ml in 2 L flasks) to exponential ($OD_{600nm} > 1.0$) in conical flasks containing BSS (JW). Cells were harvested by centrifugation at 5000 x g for 10 min and pellets were resuspended in 5 ml of appropriate buffer. This was process was repeated three times. The final resuspension was in 5 ml of appropriate buffer. The samples were transferred to glass vials and sonicated for 1 minute with 10 seconds on and 10 seconds off at 3 KHz and kept on ice. A final centrifugation step was performed at 25,000 x g for 20 minutes at 4°C. The reaction standard was always set up as Table 2-3.

Table 2-2. Optimised methods for whole cell and Cell Free Extractions (CFE)

	Whole Cell	Cell Free Extract Method		
	Method	Sonication		
Buffer of Interest		13 kHz	6 kHz	3 kHz
20 mM Sodium Phosphate	1	x	x	x
TE	2	x	x	x
TBS	3	x	x	x
50 mM HEPES	4	5	6	7

Table 2-3. Reaction mixture standard for Nessler assay.

Solution	Reaction Volume/cuvette	Blank Volume/cuvette
Reaction Mixture	25 µl	0
Buffer	0	25 µl
18.2 MΩ/cm Water	850 µl	850 µl
Nessler Reagent	125 µl	125 µl

2.1.7.3 Determination of Protein Concentration in CFE (Bradford Assay)

CFE samples extracted using method in 3.5.2 were diluted with the appropriate buffer in the ratio of 1:10, 1:20 and 1:50. 5 µl of each dilution or standard with 250 µl Bradford reagent was used in a Bradford assay to confirm the protein concentration. Standard concentrations ranging from 0-1.4 mg/ml of bovine serum albumin (BSA) with appropriate buffer provided a standard curve to enable the concentration of protein in CFE to be calculated. 96 well plates were used. The absorbance at 595 nm was measured on a Biotek Synergy HT plate reader. The data was collected using Gen. 5 software and data was analysed using Excel. The standard curve produced enabled the protein concentration of the test CFE samples to be calculated using the equation of the line: $y=mx+c$.

2.1.8 Impact of Metal ion Additions in the growth medium on the urease activity

Divalent metal ions were incorporated into BSS (JW) media to ascertain their involvement in urease activation in *B. subtilis*. Those metals included Zinc (Zn^{2+}), Manganese (Mn^{2+}) and Iron (Fe^{2+}) at various concentrations dependent if they were already present in the media (Table 2-4). The growth media BSS (JW) was altered and those ions normally present in BSS (JW) at 1 mg/L (Mn^{2+} and Fe^{2+}) were increased to 2 mg/L which is in excess of normal BSS (JW) conditions. Zinc is not present in the media nor in any supplements and so was added at the same final concentration 2mg/L.

Table 2-4. Metal ion additions to growth media investigating urease activity.

Metal Addition	Concentration
Zinc Sulphate	2 mg/L
Manganous Sulphate	1 mg/L
Iron Chloride	1 mg/L

The cells are harvested at the end of exponential stage. The whole cell assay was performed following the method described in section 2.2.3 and CFE assay was performed following the method described in section 2.2.5.

2.1.9 Effect of pH in growth medium on the urease activity

Additions of 1 M HCl was added to BSS (JW) to provide various pH growth conditions: pH 5, pH6 and pH 7.4 (standard).

The cells were harvested at the end of exponential stage. The whole cell assay was performed following the method described in section 2.2.3 and CFE assay was performed following the method described in section 2.2.5.

2.1.10 Enzyme Assay Controls

The enzyme assay included the zero time point as a baseline control and also included a urea control. The standard reaction mix included 950 μ l sample + 50 μ l of 50 mM urea. The control reaction mix included 950 μ l sample + 50 μ l 50 mM HEPES.

To obtain the result = OD control - OD test reaction (converted to μM).

2.1.11 Enzyme Activity definition

To determine the enzyme activity Ammonium Chloride (NH_4Cl) standards were prepared 0-20mg/L (NH_4Cl Mol.wt. 53.491 g/mol). In order to determine the test samples a standard curve was produced to represent the relationship between OD and concentration of ammonium produced in the reaction solution. The relationship will be described by the equation of the line: $y = mx + c$. Where m is the gradient of the line and c is its intercept with the y-axis.

Whole cell enzyme activity of urease is determined by:

$$\text{Urease Activity} = \frac{\mu\text{M}}{\text{time} / \text{biomass (OD}_{600\text{nm}})} \\ (\mu\text{mol. ammonium present})$$

CFE urease activity is determined by:

$$\text{Urease Activity} = \frac{\mu\text{M}}{\text{time} / \text{mg of protein}} \\ (\mu\text{mol. ammonium present})$$

2.1.12 Culture for Proteomics Study

The comparative proteomics study utilised *B. subtilis* cultured in the NLM (BSS (JW)) and NPM as detailed in section 2.1.2. Overnight cultures were set up in SMM and 1% of this inoculated per 500 ml NLM or NPM. Cultures were grown until end exponential approximately $\text{OD}_{600 \text{ nm}}$ 1.5 and harvested as described in 2.1.7.1. A minimum of 4 replicates were used in the proteomics study. If more replicates were utilised, it is stated.

2.1.13 Buffer optimisation of method in Protein extraction for proteomics study

A gel LC-MS/MS proteomics approach was employed in this study. Before the comparative analysis of the proteome of *B. subtilis* cells cultured in the NLM (BSS (JW)) and the nitrogen enriched medium (BSS (JW) + Ammonium Sulphate), several steps were employed to optimise the proteomics methods.

2.1.13.1 Optimisation of buffers

In order to identify the optimum buffer for protein extraction a number of buffers were investigated. The buffered recipes are shown in Table 3-2.

Table 2-5. Buffers used in determining protein extraction method

Buffer	Components
20 mM Sodium Phosphate Buffer	3.27 g Na ₂ HPO ₄ , 0.94 g NaH ₂ PO ₄ Adjust to pH 7 up to 1L.
50mM HEPES Acid free buffer + 1 mM PMSF	11.9 g / L 0.174 g PMSF pH 7.4
TBS + 1 mM PMSF	6 g Tris 8.76 g NaCl pH 7.5 + 0.174 g PMSF
TE Buffer + 1 mM PMSF	1.2 g Tris 0.292 g EDTA pH 7.5 0.175 g PMSF

A stock solution of 100 mM of Phenylmethanesulfonyl fluoride (PMSF) in isopropanol was made and diluted into the specific buffer immediately before use at 1 mM.

The buffers were analysed via enzyme assays and the number of proteins identified via extraction processes. The buffer was used to wash cells and finally resuspend the cells for sonication to take place. Once the CFE process was complete a Bradford assay would be carried out and the protein concentration identified, as detailed in section 2.5.7.3.

2.1.13.2 Optimisation of buffer pH

Urease activity was tested at various HEPES buffer pH. Additions of 1 M NaOH created the more basic buffer solution.

2.1.14 Sodium Dodecyl Sulphate–Polyacrylamide Gel electrophoresis (SDS-PAGE)

CFE with a total protein concentration of 20 µg/ml was added to 7 µl of cracking buffer (Table 2-6). All samples were boiled for 3-5 minutes. The denatured protein samples were separated using Sodium dodecyl sulphate-polyacrylamide gel electrophoresis (SDS-PAGE) in a mini-gel tank (Miniprotean® II, Bio-Rad).

All the solutions required for SDS-PAGE are listed in Table 2-6. The 15% (w/v) polyacrylamide resolving gels were prepared to separate proteins on molecular weight. SDS-PAGE gels were made up by combining reagents detailed in Table 2-7 and Table 2-8 .

Table 2-6. Solutions SDS-PAGE.

Solution	Components
Coomassie blue protein stain R-250	1 g Coomassie blue (R-250) 400 ml Methanol (40%) 100 ml Acetic Acid (10%) Make up to 1 L with dH ₂ O
Coomassie Destain Solution	400 ml Methanol (40%) 100 ml Glacial Acetic Acid (10%) Make up to 1 L with dH ₂ O
SDS-PAGE Loading buffer	0.6 ml TRIS-HCl pH 6.8 (60mM) 5 ml 50% Glycerol 2 ml 10% (w/v) SDS 0.5 ml 14.4 mM β-Mercaptoethanol 1 ml 1% (w/v) Bromophenol Blue 0.9 ml 18.2 MΩ/cm H ₂ O
SDS-PAGE Cracking Buffer	7.6 ml SDS-PAGE Loading Buffer 2.4 g Urea
Solution B – Resolving Gel Buffer	In 100 ml add: 75 ml 2M TRIS HCl (pH 8.8) (1.5M) 4 ml 10% (w/v) SDS (0.4%) 21 ml dH ₂ O

Solution	Components
Solution C – Stacking Gel Buffer	In 100 ml add:
	50 ml 1 M TRIS – HCl (pH 6.8) (0.5 M)
	4 ml 10% SDS (0.4%)
	46 ml dH ₂ O
10 x Running Buffer	30 g Tris base
	144g Glycine
	10 g SDS
	Make up to 1 L
	pH 8.3

Table 2-7. Components for 15% SDS-PAGE gel

Component	15% gel
Polyacrylamide (40%)	3.75 ml
18.2 MΩ/cm H ₂ O	3.75 ml
Buffer B	2.50 ml
APS (10 %)	50 µl
TEMED	10 µl

Table 2-8. Components for 4% stacking gel

Component	Volume
Acrylamide (40%)	0.5 ml
18.2 MΩ/cm H ₂ O	2.5 ml
Buffer C	1.0 ml
APS (10%)	30 µl
TEMED	10 µl

2.1.14.1 Running and visualisation of SDS PAGE

10x running buffer was diluted to 1x with distilled water and used in the gel tank. CFE samples were loaded as in 2.1.14 (Table 2-6). The gel was run at 200 V for 45 minutes.

The protein staining was achieved by immersing the gel in Coomassie blue R-250 stain (Table 2-6) for 20 minutes. The gel was then rinsed with distilled H₂O and immersed overnight in Coomassie destain solution (Table 2-6).

Gel images were captured using the G:Box system (SYNGene) with GenSys imaging software.

2.1.15 In gel digestion

Gels were prepared following the method in section 3.2.2. The stained protein bands were excised from the gel with a clean scalpel, the gel was cut into approx. 1x1 mm pieces and placed in a LoBind microcentrifuge tube. The Coomassie stained gel pieces were washed three times with 200 μ l of 100 mM NH_4HCO_3 and 120 μ l of acetonitrile (ACN) for 15 min at room temperature (RT) or as long as required to remove all blue colour. Gel pieces were then dehydrated by adding at least 200 μ l of 100% ACN. Once all gel pieces were white in colour (about 5-10 min) all ACN was removed by pipetting.

The gel pieces were rehydrated in 100 μ l of 20 mM DTT for 30 min at 56°C. Any excess liquid was removed, and the gel pieces were dehydrated again with ACN as described before. The gel pieces were rehydrated in 100 μ l of 55 mM IAA (Iodoacetamide) for 20 min at RT in darkness. Any excess liquid was removed by pipetting and the gel pieces were washed twice with 100 μ l of 100 mM NH_4HCO_3 .

The gel pieces were dehydrated again with ACN as above. To remove (evaporate) all ACN and dry the samples, they were placed in a vacuum centrifuge at 4°C for 5 min.

To digest the protein mixture in the gel, 30 μ l of 20 μ g/ml trypsin solution (Trypsin Gold, Promega V5280 reconstituted in 50 mM acetic acid to 1 μ g/ μ l) was added to each sample tube and allowed to absorb for 20 min on ice. Then 50 μ l of 50 mM NH_4HCO_3 was added to completely cover the gel pieces. This was incubated up to 18 hours at 37°C.

To extract the peptides 50 μ l of 50% (v/v) ACN / 5% (v/v) formic acid (FA) was added and samples were shaken for 30 min at RT. The supernatant was collected in another LoBind microcentrifuge tube and the extraction repeated with 50 μ l of 83% (v/v) ACN / 0.2% (v/v) FA. The supernatant was added to the previously extracted supernatant.

2.1.15.1 Sample Lyophilisation

The supernatant was frozen at -80°C with a hole punched on the top of the LoBind microcentrifuge tube. Using a freeze-drier (Modulyo, Edwards) the frozen supernatant was freeze-dried, the resulting lyophilised samples were stored at -80°C until further analysis.

2.1.16 Liquid Chromatography and Mass Spectrometer analysis of Peptide Samples (LC-MS)

The digested peptide samples prepared following section 3.2.3 were re-suspended in 20 μ L of 5% (v/v) ACN, 0.1% (v/v) FA before LC-MS analysis.

2.1.16.1 LC Instrument Settings

The Nanoflow Dionex™ 3000 RSLC (Dionex, Sunnyvale, CA) linked to a Q-Exactive Plus (Thermo, Hemel Hempstead, UK) was utilised to characterise the extracted peptides. It is a high-resolution mass spectrometry system using a C18 EasySpray column, in a data-dependant acquisition. The LC-MS system was managed, maintained and processed by Dr William Cheung (Northumbria University).

A binary buffer system was utilised for the nanoflow liquid chromatographic protein separation. The buffers utilised are detailed in Table 2-9. Sample injection was set as a 5 μ l load; flow rate was set to 0.3 μ l / minute. The trap column used was Acclaim™ PepMap™ 100 C18 LC column (Thermo Scientific™), (5 μ m particle size; pore size 100 Å), maintained at 45 °C.

Table 2-9. Binary buffer system components.

Buffer	Components
Buffer A	95 % ultrapure water 5 % (v/v) ACN
Buffer B	0.1 % (w/v) formic acid 95 % (v/v) ACN 5% ultrapure water
Loading and Transport Buffer	0.1 % (w/v) formic acid 95 % ultrapure water 5% (v/v) ACN 0.1 % (w/v) Tetrafluoroacetic acid (TFA)

2.1.16.2 LC gradient elution

To generate the LC gradient elution the liquid chromatographic profile was performed as; starting condition 96% buffer A, 4% buffer B, 0 min (4% buffer B/ 96% buffer A), 3 min (8% buffer B/ 92% buffer A), 93 min (30% buffer B/ 70% buffer A), 98 min (80% buffer B/ 20% buffer A) as detailed in Table 2-10, held for additional 10 minutes and then returned to starting condition with 20 min allowed for column equilibration.

Table 2-10. Buffers required for specific time points to generate LC elution

Time point (min)	Duration (min)	Buffer A	Buffer B
0		96%	4%
3	3	92%	8%
93	93	70%	30%
98	98	20%	80%

2.1.16.3 MS Instrument settings

A full scan MS scanning was performed at 70,000 MS resolution with an automatic gain control (AGC) of 1E6 and injection time of 100 ms. The scan range was set to 375 to 1400 m/z. Data-dependent-MS2 was performed at 35,000 MS resolution with an AGC of 1E5 with a maximum injection time of 100 ms. The instrument isolation window was set to 1.3 m/z, with a ratio of 0.4 %. Dynamic exclusion was set to 15 seconds, the top 10 abundant ions are selected for MS/MS with a normalized Collision energy (NCE) level of 10, 30 and 50.

2.1.1 MASCOT MS/MS search for individual protein identification

Protein identification was performed by searching raw tandem mass spectral ion peak lists against a specific database. The thermo .RAW files were converted to mascot generic format (.mgf) using RawConverter (He *et al.*, 2015). Analysis was achieved using the MS/MS ion search function of the MASCOT server (Matrix Science) (Perkins *et al.*, 1999).

The following parameters were utilised when analysing with MASCOT: (1) database: B_S *Bacillus subtilis* 168, (2) enzyme: Trypsin, (3) missed cleavages: allow up to one, (4) fixed modifications: carbamidomethyl (C), (5) variable modifications: oxidative (M), (6) peptide tolerance: 25 ppm, (7) MS / MS tolerance: 50 ppm, (8) peptide charge: 2+, 3+ and 4+, (9) mass value: monoisotopic, (10) data format: Mascot generic, (11) instrument: ESI-TRAP.

MASCOT analysis provided a peptide score distribution which identifies the probability the observed match is a random event, identifying the quantity of peptide matches above the identity or homology thresholds. An average score is predicted for each analysis which indicates a greater value identity or extensive homology ($p < 0.05$). The MASCOT results were viewed using the

report builder which were ranked by score, which considers the peptide coverage and fragmentation pattern.

2.1.2 Bioinformatic analysis for comparative proteomics

Progenesis LCMS (Nonlinear Dynamics) along with MASCOT (Matrix Science) was utilised to identify biologically relevant changes in protein expression. Raw chromatography files (thermo. RAW) were imported into the Progenesis LC-MS software, the chromatographic profiles were then automatically aligned between samples. Sample filtering was performed using the default peak picking parameters. The peptide ions were filtered on the basis of charge. A normalisation reference is automatically selected when using the Progenesis (LC-MS) software.

An experimental design analysis was produced in order to analyse runs using a 'between-subject design' grouping of samples which was based upon appearance in a given condition being analysed. The validation and review of peptides was performed by selection filtering to exclusively identify statistically significant features (peptides with a fold change of ≥ 3 and ANOVA p-value ≤ 0.05). The Principal Component Analysis (PCA) and standardised expression profiles are then produced by the software to review the selected peptide ions.

The peptide ion peak list table created in Progenesis LC-MS was then exported to the MASCOT format to identify specific proteins. MASCOT MS/MS ion searching was performed as described in 2.1.1. The results were exported from MASCOT as an .xml file format and then imported into Progenesis LC-MS software. Peptide identifications were again refined based upon the batch detection option, removing results that have: (a) a peptide score of < 40 ; and/or (b) a peptide hit count of < 2 .

Validation of the peptides was then resolved at the protein level. This was achieved by resolving each peptide conflict. When a conflict occurs between peptides, they were resolved manually based upon the peptide score, peptide hits and mass error (ppm).

2.1.2.1 Protein filtering and statistical analysis

The proteins identified were then reviewed enabling the proteins to be tagged and filtered to identify statistically significant proteins with a fold change of ≥ 2 and ANOVA p-value ≤ 0.05 .

Finally, the identified proteins were ranked by highest mean which enabled the identification, tagging and filtering for proteins upregulated in a specific condition. Report outputs were transferred to Excel for further analysis.

A Progenesis LC-MS/MASCOT standard operating procedure (SOP) was created so that all peptide analysis followed the same standard input queries and parameters (see Appendix Figure 9-1).

2.1.3 Bioinformatic analysis to determine specific of genes of interest

The final report produced by Progenesis LC-MS details differentially expressed proteins present in each condition. The results are filtered according to specific parameters described 2.1.1. All proteins via their unique and stable identifier code were analysed using bioinformatic tools. Those tools utilised in this study are listed in Table 2-11.

Table 2-11. Bioinformatic tools and their function used in this study

Bioinformatic Tool	Function
UniProt https://www.uniprot.org/	Identify protein sequence and function (Consortium, 2018)
STRING https://string-db.org/	Establish protein-protein interaction networks (Franceschini <i>et al.</i> , 2012),
Subtiwiki http://subtiwiki.uni-goettingen.de/	Understand the genes and proteins of <i>B. subtilis</i> as well as the metabolic and regulatory pathways of identified proteins (Zhu and Stulke, 2018),
BioCyc https://biocyc.org/	Establish in the proteins of interest the protein features, operon in which they belong, metabolic pathways and regulatory networks (Karp <i>et al.</i> , 2019)
EggNOGv5 ‘Evolutionary Genealogy of Genes: Non-supervised Orthologous Groups’ (function bacteria) http://eggnog5.embl.de	Enable the cluster of orthologous proteins (COG) analysis proteins to be grouped by function; functions can be predicted in all completely sequenced microbial genomes

The COG database is a phylogenetic classification of proteins from complete genomes (Tatusov *et al.*, 2001). Every COG includes orthologous proteins, or those that are thought to be. The

COG database serves as a platform for functional annotation of newly sequenced genomes and with many broad ranging functional categories as detailed in Table 2-12.

Table 2-12. COG list and specific functional description.

Each COG consists of a group of proteins found to be orthologous across at least three lineages and likely corresponds to an ancient conserved domain

General COG Association	COG Specific Functional Description
Cellular processing and signaling	[D] Cell cycle control, cell division, chromosome partitioning [M] Cell wall/membrane/envelope biogenesis [N] Cell motility [O] Post-translational modification, protein turnover, and chaperones [T] Signal transduction mechanisms [U] Intracellular trafficking, secretion, and vesicular transport [V] Defence mechanisms [W] Extracellular structures [Y] Nuclear structure [Z] Cytoskeleton
Information storage and processing	[A] RNA processing and modification [B] Chromatin structure and dynamics [J] Translation, ribosomal structure and biogenesis [K] Transcription [L] Replication, recombination and repair
Metabolism	[C] Energy production and conversion [E] Amino acid transport and metabolism [F] Nucleotide transport and metabolism [G] Carbohydrate transport and metabolism [H] Coenzyme transport and metabolism [I] Lipid transport and metabolism [P] Inorganic ion transport and metabolism [Q] Secondary metabolites biosynthesis, transport, and catabolism
Poorly Characterised	[R] General function prediction only [S] Function unknown

2.1.4 Addgene knockouts

The genes of interest were purchased as knockouts as shown in Table 2-13 from a strain collection from Addgene. The *B. subtilis* Strain Collection (Addgene kit #1000000115) includes the Gene Deletion Library. The knockout library consists of every non-essential gene which has been individually replaced with a kanamycin resistance cassette. The entire protein coding region (not including start and stop codons) is replaced with a kanamycin resistance cassette (<https://www.addgene.org/kits/grosslab-bsubtilis-collections/>) (Koo *et al.*, 2017).

Table 2-13. Bacterial strains and knockouts used within the research and utilised in proteomics experiments.

Strains highlighted in blue were investigated by final-year undergraduate project students.

<i>B. subtilis</i> 168 Gene Deletion	Strain Name (BGSC No.)	Genotype
<i>ΔoppA</i>	BKK11430	<i>ΔoppA::kan trpC2</i>
<i>ΔoppB</i>	BKK11440	<i>ΔoppB::kan trpC2</i>
<i>ΔoppC</i>	BKK11450	<i>ΔoppC::kan trpC2</i>
<i>ΔoppD</i>	BKK11460	<i>ΔoppD::kan trpC2</i>
<i>ΔoppF</i>	BKK11470	<i>ΔoppF::kan trpC2</i>
<i>ΔyciC</i>	BKK03360	<i>ΔyciC::kan trpC2</i>
<i>ΔznuA</i>	BKK02850	<i>ΔznuA::kan trpC2</i>
<i>ΔznuB</i>	BKK02870	<i>ΔznuB::kan trpC2</i>
<i>ΔywpJ</i>	BKK36290	<i>ΔywpJ::kan trpC2</i>
<i>ΔyjoB</i>	BKK12420	<i>ΔyjoB::kan trpC2</i>
<i>ΔyhfE</i>	BKK10200	<i>ΔyhfE::kan trpC2</i>
<i>ΔyrdA</i>	BKK26780	<i>ΔyrdA::kan trpC2</i>
<i>ΔyydB</i>	BKK40220	<i>ΔyydB::kan trpC2</i>
<i>ΔyisK</i>	BKK10750	<i>ΔyisK::kan trpC2</i>
<i>ΔyufO</i>	BKK31550	<i>ΔyufO::kan trpC2</i>
<i>ΔyfiT</i>	BKK08390	<i>ΔyfiT::kan trpC2</i>
<i>ΔyjbM</i>	BKK11600	<i>ΔyjbM::kan trpC2</i>
<i>ΔyxeP</i>	BKK39470	<i>ΔyxeP::kan trpC2</i>
<i>ΔytrE</i>	BKK30420	<i>ΔytrE::kan trpC2</i>
<i>ΔytrF</i>	BKK30410	<i>ΔytrF::kan trpC2</i>
<i>ΔytlA</i>	BKK30595	<i>ΔytlA::kan trpC2</i>
<i>ΔyurM/frlM</i>	BKK32580	<i>ΔfrlM::kan trpC2</i>
<i>ΔureC</i>	BKK36640	<i>ΔureC::kan trpC2</i>

2.1.5 Proteomic and bioinformatics analysis

The comparative proteomic and bioinformatics analysis of each knockout was carried as described in Section 2.1.5. Comparative proteomics identifies the expression changes between

B. subtilis 168 (the wild-type in this study) and each knockout with particular focus on urease expression levels. Bioinformatic analysis using various tools such as Uniprot, Subtiwiki and EggNOG 5.0.0 was used to understand the regulation processes involved. The EggNOG (evolutionary genealogy of genes: Non-supervised Orthologous Groups) database is hosted by EMBL and is based upon the use of COGs but expands the idea to non-supervised (those genes that cannot be mapped) orthologous groups constructed from different organisms.

2.1.6 Plasmids and Bacterial Cells

The plasmids and host cells used in this research are listed in Table 2-14.

Table 2-14. Plasmids and host cells used in this research

Plasmid	Characteristics	Reference
pURE91	<i>B. subtilis ureABC</i> cloned into pET-23	(Kim, Mulrooney and Hausinger, 2005a) Prof. R. Hausinger MSU
pET22b	Cloning and expression vector used as control	Novagen
Host Cells		
<i>E.coli</i> BL21(DE3)	Used for recombinant expression	Novagen
<i>E.coli</i> TOP10	Used for transformation	Invitrogen

2.1.7 Maintenance of pURE91 plasmid

The 10 µl of plasmid (provided by Prof. Robert Hausinger, Michigan State University) was added to a 150 µl aliquot of competent *E. coli* TOP10 cells. Cells were left on ice for 30 min. The cells were then heat shocked at 42°C for 90s and the tube was immediately transferred onto ice for 2 min, 200 µl of LB was added and the mixture and incubated for 45 min at 37°C. The whole cell suspension was spread onto an LB + Amp (10 mg/ml) agar plate and incubated at 37°C overnight. Then 1 colony was grown in a 10 ml LB culture, 0.5 ml of this was used to create a glycerol stock by adding to 0.75 ml 50 % (v/v) glycerol and the remainder was used to produce a large quantity of plasmid extraction for transformation into BL21(DE3) using the NZY Tech Kit Miniprep (MB010) according to the manufactures protocol as shown in Appendix Section 5.1.

2.1.8 Transformation into *E.coli* BL21 (DE3) cells - Control

To transform *E. coli* BL21 (DE3) with pURE91, 2 µl of pURE91 containing the urease genes and pET22b as a control (vector map in Appendix Figure 9-2) were added to separate 150 µl aliquots of *E. coli* BL21 (DE3) cells. The transformation followed the same protocol as described in section 2.1.7.

2.1.9 Recombinant Protein Expression and Extraction

One colony from the *E.coli* BL21 (DE3) + pURE91 and pET22b control agar plate was inoculated into 10 ml of LB +AMP (10 mg/ml) medium and incubated at 37°C, 200 rpm overnight to form the starter culture. Then 500 µl of starter culture was transferred into 50 ml of LB + AMP (10 mg/ml), incubated at 37°C at 200 rpm. Once the culture had reached OD_{600 nm} between 0.6 and 1.0, IPTG was added into the culture to induce the expression of the urease. Two IPTG final concentrations were tested 0.5 M and 1 M IPTG. The induced culture was then incubated at 16°C, 30°C and 37°C at 100 rpm overnight, expression was visualised on SDS-PAGE (Appendix Figure 9-3).

After the protein is expressed, the cells were harvested and lysed as in section 2.1.7.2 with the sonication frequency at 12 KHz. The proteins were visualised by SDS-PAGE as described in section 2.1.14.

2.1.10 Western Blot Analysis to Detect *B. subtilis* UreC

Once the expression of urease was optimised, the recombinant *B. subtilis* urease was produced in *E. coli* BL21 (DE3) cells containing pURE91. Western blot analysis was performed to identify the structural unit α which contains the active site of urease.

Solutions and reagents for Western blot are listed in Table 2-15:

Table 2-15. Recipes for Western Blot solutions

Solution	Recipe
Tris-HCl	20 mM Tris-HCl
Laemmli 2X buffer/loading buffer	4% w/v SDS 10% 2-mercaptoethanol 20% w/v glycerol 0.004% w/v bromophenol blue 125 mM Tris-HCl pH to 6.8
Running buffer (Tris-Glycine/SDS)	25 mM Tris base 190 mM glycine 0.1% w/v SDS pH to 8.3
Transfer buffer (wet)	25 mM Tris base 190 mM glycine 20% methanol pH to 8.3
Blocking buffer	3–5% (w/v) milk or BSA (bovine serum albumin) Add to TBST buffer. Mix well and filter
Tris Buffered Saline + 0.1% Tween (TBST)	150 mM NaCl 3 mM of KCl 25 mM Tris base 0.1% Tween 20

2.1.10.1 Sample Preparation for Western blot

Protein concentration of recombinant proteins and *B. subtilis* was determined for the CFE using Bradford Reagent as shown in section 2.1.7.3. Protein concentration was standardised so each

well contained 20 µg/ml and equal volumes of loading buffer were added. The sample was reduced and denatured by boiling at 100°C for 5 min.

2.1.10.2 SDS-PAGE and transferring the proteins to the membrane

An equal amount of protein of each CFE sample in 20 µl was loaded into the wells of the 12% (w/v) SDS-PAGE gel, along with 5 µl of a molecular weight marker (ThermoScientific, PageRuler Product No. 11852124). The gel was ran for 55 minutes at 200 V.

Filter paper and the nitrocellulose membrane (ThermoFisher Cat. No. 88018) was cut to fit the measurements of the gel to be used in the stack. The stack contained layers prepared from the anode of sponge, filter paper, gel, 0.45 µM nitrocellulose membrane, filter paper, sponge to the cathode and any bubbles between gel and membrane removed. The clamp transfer case was closed and transferred to the tank with transfer buffer and ice packs. The power pack was switched on at 200V and protein transfer began. After one hour the gel was removed, and the membrane was ready for antibody treatment.

2.1.10.3 Antibody treatment and detection

The membrane was blocked for 1 h at room temperature using blocking buffer (rock at RT). The blocking buffer was removed, and the membrane placed in the primary antibody solution (1:10,000 dilution), Anti-*Helicobacter pylori* urease β antibody (Sigma Aldrich SAB2702130) for 15 min. The membrane was then washed in TBST (Tris-buffered saline, 0.1% (v/v) Tween 20) 3 x 10 min washes. The membrane was incubated with the recommended dilution (1:2000 x 1.0) of conjugated secondary antibody (2°) Polyclonal Goat Anti-Rabbit Immunoglobulins/HRP (Agilent P044801-2) in blocking buffer at RT for 1 h. The membrane was then washed again with TBST for 3 x 5 min each time and any excess reagent was removed.

The highly sensitive chemiluminescent detection reagent; enhanced chemiluminescence (ECL) was used as the detection reagent (GE Healthcare RPN3004). ECL mix was prepared following the proportion of solution A and B provided by the manufacturer. The membrane was incubated in the detection reagent for 1–2 minutes. The result was imaged using the G-box.

2.1.11 Analysis of Urease Conformation using Native Tris Glycine Gels

Native gels were initially used in the research to understand urease in its folded state in the recombinant and native samples. The native gel method was adapted from (Arndt *et al.*, 2012).

The solutions are listed in Table 2-16, Table 2-17 and Table 2-18.

Table 2-16. Solutions required for Native gel preparation

Solution	Recipe
4 x Separating Gel buffer	36.3 g TRIS (FW 121.1) 150 ml dH ₂ O Adjust pH to 8.8 using HCl Final Volume 200 ml
4 x Stacking Gel Buffer	15.1 g TRIS (FW 121.1) 40 ml dH ₂ O Adjust pH to 6.8 with HCl Final Volume 50 ml
10% Ammonium Persulphate	1.0 g Ammonium Persulphate 10 ml dH ₂ O
Electrophoresis Buffer	28.8 g 0.192 M Glycine 6.0 g 0.025 M TRIS (FW 121.1) De-ionised water added to final volume 2 L pH 8.3
2 x Sample Buffer	2.5 ml 4 x Stacking Buffer 2 ml 20% Glycerol 0.02% Bromophenol Blue (40 µl of 5% Bromophenol Blue) 5.5 ml dH ₂ O
Staining Solution	0.25 g Coomassie Brilliant Blue R250 125 ml Methanol 25 ml Glacial Acetic Acid 100 ml dH ₂ O
Destaining Solution	100 ml Methanol 100 ml Glacial Acetic Acid 800 ml dH ₂ O

Table 2-17. Separating Gel Mixture preparation

Solution	6%	12%
40% Acrylamide:Bis Solution (37.5:1)	1.5 ml	3 ml
4 x Separating Gel Buffer	2.5 ml	2.5 ml
dH ₂ O	6.0ml	4.5 ml
10 % Ammonium Persulphate	50 µl	50 µl
TEMED (N,N,N',N'- tetramethyl-ethylenediamine)	10 µl	10 µl

Table 2-18. Stacking gel solution preparation (4ml)

Solution	Volume Required
40% Acrylamide:Bis Solution (37.5:1)	0.4 ml
4 x Stacking Gel Buffer	1.0 ml
dH ₂ O	2.6 ml
10 % Ammonium Persulphate	30 µl
TEMED (N,N,N',N'- tetramethyl-ethylenediamine)	10 µl

The Bio Rad mini II system was used. 10 ml of specific separating gel mixture was prepared as in Table 2-17, 50 µl of 10% Ammonium persulphate (APS) and 10 µl of TEMED (N,N,N',N'-tetramethyl-ethylenediamine) was added, mixed and poured immediately. Water was overlaid to create a flat top to the gel. The stacking gel solution was prepared as Table 2-18, mixed and used immediately, inserting the comb.

Once polymerised the gel was placed in electrophoresis running buffer and the comb removed. The gel was loaded with 20 µl of loading dye without SDS which contained 20 µg of protein per well running at 200V for 1 h. The gel was removed from the glass plates and stained in staining buffer and visualised on the G-Box.

2.1.12 Analysis of Urease Conformation using Size Exclusion Chromatography (SEC)

The activated urease should be in the form of trimer of the trimer (ABC)₃. SEC was utilised to identify the conformation of the enzyme in both the urease produced by *B. subtilis* (referred to native sample hereafter) and the recombinant urease produced by *E.coli* (recombinant sample hereafter). Both HiPrep Sephacryl S-200 (GE Healthcare, Product Code 10106414) and HiPrep

Sephacryl S-300 (GE Healthcare Produce Code 10616695) high solution columns were utilised in this study (Table 5-6), and various protein standards were applied in the columns.

Table 2-19. Sephacryl columns and fraction ranges used in the study

Column	Fraction Ranges (proteins)
S-200 HR	5 kDa -250 kDa
S-300 HR	10 kDa – 1500 kDa

Both columns were linked to AKTA protein purification system (Amersham pharmacia biotech AKTA explorer), and the separated fractions were collected using fraction collector (Amersham pharmacia biotech, Frac-950). Before analysis, the HiPrep Sephacryl columns were washed utilising the AKTA with 2 column runs of 50% methanol in order to maintain solubility of the sample and then primed with 2 column runs of 50 mM HEPES + 0.5 mM NaCl buffer, pH 7.4.

2.1.12.1 Protein mixture separation using Sephacryl S-200 column

The Sephacryl S-200 column coupled with 100 µl loop was first calibrated with standard proteins of known molecular size using a gel filtration marker kit (Sigma Code: MWGF1000-1KT). The protein standards are detailed in Table 2-20. The purchased standard included two visible markers (vitamin B12 and myoglobin) to establish the column was properly packed and also that the sample was eluted evenly. Fractions were measured utilising UV-vis spectral analysis at 280 nm.

Initially the protein mixtures from the native sample and recombinant sample were analysed using the Sephacryl S-200 column coupled with 100 µl loop. Recombinant and native CFE of 100 µl was prepared as in 2.1.7 and loaded onto the column after equilibration at a flow rate of 0.5 ml/min. The collecting fraction volumes was set to 1ml.

2.1.12.2 Protein mixture separation using Sephacryl S-300

Following use of the S-200, a Sephacryl S-300 column coupled with 2 ml loop was utilised for this study. The column was equilibrated and calibrated as in 2.1.12.1. Standards were used as detailed in Table 2-20 and a BSA (A2153 Sigma Aldrich) standard was manually prepared at 5.0 mg/ml, estimated molecular weight: monomeric BSA (66 kDa) and dimeric BSA (132 kDa). CFE

of both recombinant and native of 2 ml was prepared as in 2.1.7 and loaded onto the column at a flow rate of 0.5 ml/min. The collecting fraction volumes was set to 1 ml.

Table 2-20 Gel filtration standards (Sigma 1511901) for S-200 and S-300

Component	Estimated Molecular Weight	Amount per vial, mg
Thyroglobulin (bovine)	670,000	5.0
γ -globulin (bovine)	158,000	5.0
Ovalbumin (chicken)	44,000	5.0
Myoglobin (horse)	17,000	2.5
Vitamin B12	1,350	0.5

2.1.13 Visualization and Protein ID Analysis of Peak Fractions from SEC

Once the recombinant urease was separated on the gel filtration column the protein contents for each peak were visualised through 12 % SDS-PAGE. The ID of the targeted protein band was analysed followed the method in section 2.1.15. To compare the urease quantity in different conformations (e.g. trimer of trimer, dimer of trimer, single trimer see Table 6-1) the fractions of each size range were pooled according to P1, P2 and P3 which represent the different molecular ranges. Proteins were concentrated through TCA precipitation.

2.1.13.1 Trichloroacetic acid precipitation (TCA) Protein precipitation

Protein precipitation of the SEC fractions was adapted from Sanchez *et al.* (Sanchez, 2001). One volume of TCA stock (100% w/v) was added to 4 volumes of protein sample. This was incubated for 10 min at 4°C. The sample was centrifuged at 14,000 x g, 5 min. The supernatant was removed, leaving the protein pellet intact. The pellet was washed with ice cold 80% Acetone and the centrifuged at 14,000 rpm, 5 min. This was repeated twice. The pellet was placed in 95°C for 10 minutes to drive off any residual acetone. Once dry, SDS-PAGE loading dye (Table 2-6) was added and boiled for 5 min at 95°C before analysis using 14% SDS-PAGE.

**Chapter 3 Understanding
urease regulation and
activity of *Bacillus subtilis*
cultured in a defined
minimal media**

3.1 Introduction

The expression of urease varies among microbes, suggesting different regulatory mechanisms of urease production. The induction and expression of urease differs not only from species to species but also within the same species.

3.1.1 Regulation of Urease Synthesis in Microorganisms

Regulatory mechanisms of urease are complex and expression of urease is regulated differently within different bacteria as detailed in Figure 3-1. There are four main established mechanisms of urease regulation for ureolytic bacteria (Mobley and Hausinger, 1989; Mulrooney, Pankratz and Hausinger, 1989; Atkinson and Fisher, 1991). They are constitutive urease expression, induction by urea, nitrogen regulation, regulation of urease by pH and in *H. pylori* the regulation by metal ions has now been proposed. The details for each mechanism will be discussed below. In some microorganisms, urease is regulated by a single mechanism, and in others, it is regulated by multiple mechanisms. The differences in regulation suggest the enzyme has a number of physiological roles (Wray, Ferson and Fisher, 1997b).

3.1.1.1 Constitutive Expression

The expression of urease in some organisms is unaffected by environmental conditions, for example the soil bacteria *Sporosarcina pasteurii* and *Sporosarcina ureae*, the cyanobacterium *Anabaena variabilis* and the opportunistic pathogen *Morganella morganii* (Mobley, Island and Hausinger, 1995). The bacterium *M. morganii* was considered to have constitutive regulation as Rosenstein *et al.* (1980) found no induction via urea (Rosenstein, Hamilton-Miller and Brumfitt, 1980). The work of Collins and Falkow (1988) determined that those bacteria that utilise constitutive expression all have a similar gene organisation (Collins and Falkow, 1988). Constitutive expression of genes can provide a higher fitness than responsive expression, as a constitutive strategy can confer significantly better growth than responsive expression especially when adaptation to environments are necessary, as there would be no requirement to adapt (Geisel, 2011). This may be true for those microorganisms that constitutively express urease as the expression is a survival tactic. Those microorganisms that constitutively express urease

normally include the 7 urease genes in specific order; *ureD*, *ureA*, *ureB*, *ureC*, *ureE*, *ureF* and *ureG* within the urease operon (Figure 3-1 A).

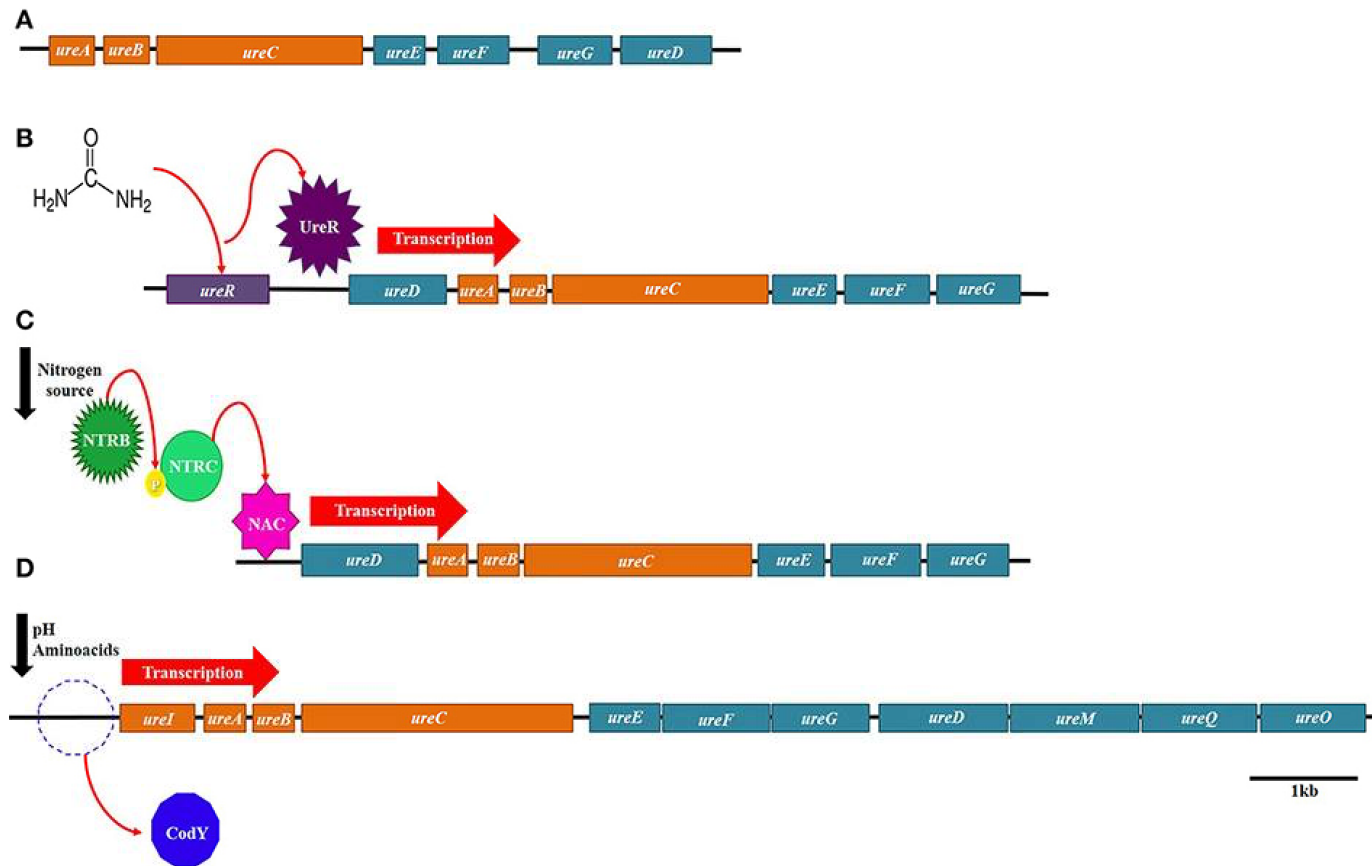


Figure 3-1. Regulatory mechanisms of urease in various bacteria.

A. The constitutive expression of urease (*S. pasteurii*). B) Urease induced by urea (*P. mirabilis*). C. Urease induced by nitrogen availability (*K. aerogenes*). D. Urease induced by pH (*S. salivarius*). (Castro Alonso *et al.*, 2019)

3.1.1.2 Induction by Urea

In some microorganisms urease is synthesised in response to various environmental conditions via a positive control of transcription of specific genes. There are numerous bacteria that only produce urease in the presence of urea and so are induced by urea. Those bacteria include *P. mirabilis*, *Providencia stuartii*, *Escherichia coli* and *Salmonella* (Gendlina *et al.*, 2002; Follmer, 2010) which are all well-known human pathogens where their virulence factors include urease. The urinary tract includes an abundance of urea which acts as an environmental signal to certain ureolytic bacteria. The ammonia produced by urea hydrolysis then raises the pH of the urine. This is an important biological function of urease as it enables the survival of the bacterium. However, the rise in pH causes precipitation of normally soluble anions and cations forming struvite ($\text{MgNH}_4\text{PO}_4 \cdot 6\text{H}_2\text{O}$) and carbonate apatite ($\text{Ca}_{10}(\text{PO}_4)_6\text{CO}_3$) crystals (Torzewska and Róźalski, 2015). These crystals can deposit on catheter surfaces which obstructs urine flow and can further develop into bladder and kidney stones (Torzewska and Róźalski, 2015).

Urease gene clusters which are urea-induced always begin with the regulatory gene (*ureR*) followed by *ureD* and then structural and accessory genes. In *P. mirabilis* *ureR* lies 400 bp upstream of *ureD* (Figure 3-1 B). UreR positively influences *ure* genes in the presence of urea (Mulrooney, Pankratz and Hausinger, 1989; Mobley, Island and Hausinger, 1995) and also initiates transcription of its own gene in a urea-inducible manner. Mobley *et al.* (1995) discussed that *ureR* is a positive activator which binds to the promoter of *UreD*. UreR is a member of the AraC/XylS family of transcriptional regulators and also an environmental sensor (Gendlina *et al.*, 2002). In high concentrations of urea, UreR is in its transcriptionally active form as it has a high binding affinity for urea at its N-terminal end, which promotes the binding on *ureD*. In contrast, in the absence of urea or in low concentrations it is not an efficient activator as it has lower DNA binding affinity (Thomas and Collins, 1999). Dattelbaum *et al.* (2003) discussed the expression of urease in *P. mirabilis* via the binding of UreR to urea, which causes the protein to then bind both *ureR* and *ureD* promoters. The binding sites have the consensus sequence T(A/G)(T/C)(A/T)(T/G)(C/T)T(A/T)(T/A)ATTG) within the 491-bp *ureR-ureD* region

(Dattelbaum *et al.*, 2003). The *ureR* gene is the only regulatory gene identified for urea-induced urease operons.

3.1.2 Nitrogen Regulation of Urease

In general nitrogen regulation is an accepted occurrence especially within *Enterobacteriaceae*, where a series of genes regulate many aspects of nitrogen assimilation in response to the nitrogen source (Chasin and Magasanik, 1968). Urease expression is affected by the levels of nitrogen in the environment. Nitrogen limitation is therefore an environmental condition whereby urease expression is positively regulated. The best characterised organism employing this mode of regulation is the Gram-negative bacterium *K. aerogenes*, which, in nitrogen-limiting conditions activates urease synthesis. In this instance urease production may be tightly regulated in conjunction with the nitrogen regulatory system, which is controlled by a complex cascade that ultimately triggers ribonucleic acid polymerase synthesis, recognizing specific promoters of nitrogen-regulated gene products (Mobley and Hausinger, 1989). This system is a cascade involving many components dependent on the products of the nitrogen-regulated genes such as: *ntrA*, *ntrB* and *ntrC*. NtrA is a sigma factor (sigma54) promoting transcription from certain promoters when bound to an RNA polymerase (RNAP) (Flores, 1996). The regulator NtrC is a member of the two-component regulatory system NtrB/NtrC. This system controls expression of the *ntr* genes in response to nitrogen limitation which includes transcription of glutamine synthetase and indirectly the *ure* promoters in *K. aerogenes*. The role of NtrB in the two-component regulatory system is to autophosphorylate and transfer the phosphoryl group to NtrC (Ninfa and Magasanik, 1986). This is detailed in Figure 3-1, whereby regulation of *ureABCDFG* is mediated by the nitrogen assimilation control protein (NAC), which is itself under the control of NtrC phosphate.

Another bacterium that has a similar urease regulation mechanism which does not belong to the *Enterobacteriaceae* is, *Saccharopolyspora erythraea*, an erythromycin producer. This soil bacterium has shown evidence that its urease synthesis is also subject to nitrogen levels (Flores, 1996), with ammonium being the effector in the mechanism, and the global system of nitrogen control (*ntr*) exists for this actinomycete to control the synthesis of the urease.

Urease gene expression in nitrogen regulated mechanisms is also dependent upon the transcriptional activator Nac (nitrogen assimilation control) an associate of the LysR family of transcriptional activators; whose transcription is governed by the Ntr system (Chasin and Magasanik, 1968). In theory, under NLC (nitrogen limited conditions) the Ntr system activates the transcription of Nac and in turn Nac induces the expression of urease (Figure 3-1 C) via strong Nac-dependent transcriptional activation of *ureD*. Mobley *et al.* (1995) discusses that mutants of *nac* vary in their expression of various nitrogen-regulated genes and Nac has been demonstrated as having a binding site close to *ureD* (Mobley, Island and Hausinger, 1995). Frisch *et al.* (2010) detailed the Nac binding site (ATAAGCGTTTCGTAT) is 47bp upstream of the *ureD* promoter of *K. pneumonia* {Frisch, 2010}. In some microorganisms such as *B. subtilis*, urease synthesis can also be regulated by the transcriptional factors PucR, TnrA and GlnR, which regulate gene expression in response to changes in nitrogen availability. The details of this regulation will be discussed later in this work.

3.1.1 Regulation by Metal Ions

Regulation of urease by metal ions occurs in some bacteria, the best studied is the bacterium *H. pylori*. The urease operon in *H. pylori* is regulated by the Ni²⁺-dependent sensor and transcription factor NikR (Zambelli *et al.*, 2011). This protein is metal responsive and controls the homeostasis of Ni²⁺, the essential cofactor of urease in *H. pylori*. Carter *et al.* (2009) describe how the supplementation of *H. pylori* growth medium with Ni²⁺ leads to an increase in the transcription of the urease genes. Ni²⁺ dependent regulation of urease is derived from *nikR* mutant experiments where mutant cells lacked the ability to increase urease expression in the presence of Ni²⁺ (Carter *et al.*, 2009). Ni²⁺ bound NikR of *H. pylori* can bind directly to specific sequences of the *ureA* promoter which results in the induction of transcription as detailed in Figure 2-2 (Ernst *et al.*, 2005; Jones, Li and Zamble, 2018).

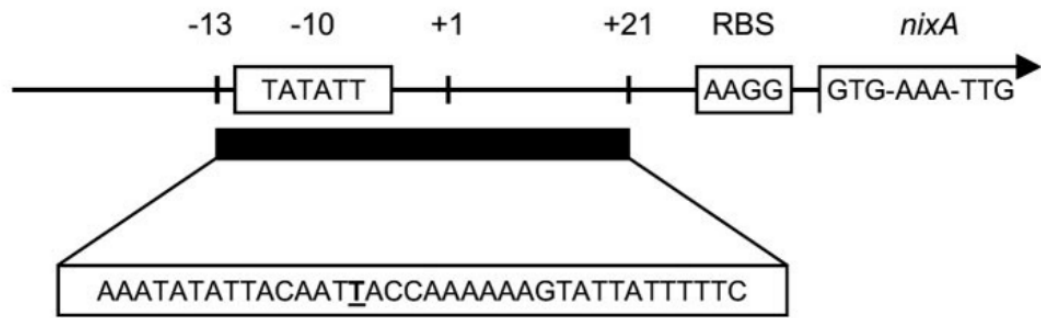


Figure 3-2. The *ureA* promoter region of *H. pylori*.

The location and sequence of the NikR-binding site indicated, where -91 and -56 indicate the boundaries of the NikR-binding site (Ernst *et al.*, 2005).

Interestingly in bacteria that utilise metal-dependent urease regulation, the bacteria possess two sets of urease genes, one which contains the complete urease gene cluster and a second containing only a second copy of the structural genes (termed *ureA2* and *ureB2*), as shown in Figure 1-6 for *H. musteleae* gene cluster. The copied urease gene cluster is more than 50% identical to the first, however *ureA1B1* is induced by nickel ions whereas *ureA2B2* is inversely regulated by nickel and increases with iron supplementation (Carter *et al.*, 2009). NikR also regulates gene expression in direct response to acidic pH, which will be discussed in next section.

3.1.2 Regulation by pH

pH is another environmental factor which can regulate urease gene expression; specifically low pH. Many ureases that function as acid ureases are associated with pathogenic microorganisms. It is understood that environmental adaptation is crucial to bacterial virulence and adaptability. Recent evidence suggests that urease is vital for acid resistance in various niches especially in the bacteria *H. pylori* and *S. salivarius* (Zhou *et al.* 2019; Jones, Li and Zamble, 2018). In conditions of low pH, urease genes are positively-controlled by acid-dependent activation of the promoter with increasing acidity (Pflock *et al.*, 2005).

The regulation of urease in *H. pylori* is complex and is a direct response to acidic pH. NikR regulates gene expression of urease linking acid adaptation and Ni²⁺ homeostasis (Jones, Li and Zamble, 2018). Jones *et al.* (2018) discussed that in response to acid shock, NikR-dependent upregulation of *ureA* occurred upon the addition of Ni²⁺ which is expected. However, transcription of *ureA* was also up-regulated at low pH in the absence of added Ni²⁺, which

indicated NikR is responding also to acidic pH which is another mechanism of urease regulation in *H.pylori*. NikR is able to bind to the corresponding DNA promoters at acidic pH. However, how the changes in pH affect the DNA binding activity by NikR is not known (Jones, Li and Zamble, 2018).

Bacteria that are acid-activated usually include *ureI* within the urease cluster which encodes an inner membrane protein that produces an acid-activated urea channel which in *H. pylori* and *S. salivarius* acts as a H⁺-gated urea transporter (Figure 3-1 D). The channel remains closed at neutral pH, however at acidic pH it opens to allow rapid urea access to cytoplasmic urease (Strugatsky *et al.*, 2013). In *H. pylori* *ureI* is regulated by the transcriptional regulatory protein ArsS. ArsS binds directly to the promoter regions of *ureA* and *ureI* to positively regulate their expression in response to acidic pH (Pflock *et al.*, 2005).

Urease is synthesised in *S. salivarius* to play a role in protection from the acidic environment of the oral cavity (Mobley, Island and Hausinger, 1995). The pH regulation of urease expression in *S. salivarius* is governed by the global regulator CodY, which regulates the *ureI* promoter in response to pH conditions by direct binding to the promoter. Huang *et al.* (2014) demonstrated that at neutral pH CodY is more active and represses *ureI*. At a lower pH the C-terminal domain of the RNA polymerase (RNAP) α subunit (α -CTD) interacts with the 5' sequence to the -35 element of *ureI* (5'-AATTTTCWGAAAATT) and further enhances the expression of *ureI* (Huang, Burne and Chen, 2014). This indicates that CodY and RNAP compete for the same binding to the *ureI* promoter region. This regulation ensures optimal urease expression when the enzyme is required most i.e. at acidic pH. The acid resistance of *S. salivarius* as a result of urease activity is achieved via the regulation of gene expression, rather than urea channel activation (Weeks and Sachs, 2001).

3.1.3 Complex regulation of urease

Urease regulation can be described as ambiguous, because exact mechanisms of its regulation are not known in many microorganisms. It has been shown in well-studied microorganisms, most of them pathogens, that there are many mechanisms involved. Bacteria may even switch which mechanism they use depending upon the environment. This complex regulation of urease has

likely evolved as a result of the need to tightly control the expression of the genes in response to multiple stimuli, which optimises growth and survival in a constantly changing environment (Huang, Burne and Chen, 2014). *H. pylori* is a perfect example of complex urease regulation. *H. pylori* consists of a compact genome with relatively few regulatory proteins. However, it is able to survive under harsh and variable conditions. This is *via* a complex and robust acid response that is centered on urease. This complex regulation maintains Ni²⁺ availability and acid adaptation survival (Jones, Li and Zamble, 2018). NikR coordinates both Ni²⁺ mobilisation and acid adjustment, providing the bacterium with two vital functions in one regulator. NikR regulates the uptake of Ni²⁺ and the expression of many systems required for the colonisation and adaptation of *H.pylori*. However, there is also the necessity for the response regulator ArsR in pH-responsive regulation of urease in *H.pylori* (Van Vliet, Ernst and Kusters, 2004).

3.1.4 Urease regulation in *B. subtilis*

As described in the previous section, the regulation of bacterial ureases is often related to the interactions with one of the urease promoters. As shown in Figure 1-6, there are no gene sequences annotated for urease accessory genes in the *B. subtilis* genome. Scientists have been studying urease regulation for more than 30 years. It was first thought that glutamine synthetase regulated urease expression in *B. subtilis* (Atkinson and Fisher, 1991). However, we now know that complicated transcriptional regulation mechanisms dictate the urease expression of *B. subtilis*.

3.1.4.1 Urease Promoters in *B. subtilis*

The *B. subtilis ureABC* operon includes 3 promoters: P1, P2 and P3. Immediately upstream of *ureA* is P1 as shown in Figure 3-3, a low level constitutive promoter, which generates low level urease expression.

Preceding P1 is the P2 promoter which lies 270 bp upstream of the *ureA* start Figure 3-3 (Wray, Ferson and Fisher, 1997a). The P2 promoter therefore starts transcription, further upstream of the *ureA* start codon than P1.

Figure-3-4 details the nucleotide sequence for the 210 and 235 regions of this promoter. Studies have shown that the P2 promoter is a σ^H -dependent promoter (Wray, Ferson and Fisher, 1997b;

Brandenburg *et al.*, 2002a). In *B. subtilis*, the function of σ^H is for transition to post-exponential phase in the cells during the start of the sporulation process and also to direct the transcription of some early stationary phase genes utilised in competence. The σ^H is an RNA polymerase whose function is as an activating/modifying subunit that is often not fully active in laboratory strains due to a mutation (V117A). It is therefore a non-essential gene involved in transcription of stationary phase genes and regulates 49 genes, for example *ureA-ureB-ureC* (Zhu and Stulke, 2018).

The *ureABC* promoter P3 lies 839 bp upstream of the *ureA* start codon (Wray, Ferson and Fisher, 1997a). The nucleotide sequence of the 210 and 235 regions of this promoter are detailed in Figure-3-4. The *ureABC* P3 promoter is a σ^A -dependent promoters. The essential housekeeping σ^A factor of *B. subtilis* is the prevalent σ factor during exponential growth and regulates 1194 genes, which include the utilisation of nitrate (*nasB-nasC-nasD-nasE-nasF*), purine utilisation (*pucA-pucB-pucC-pucD-pucE*) and those involved in the utilisation of urea as a nitrogenous source (*ureA-ureB-ureC*).

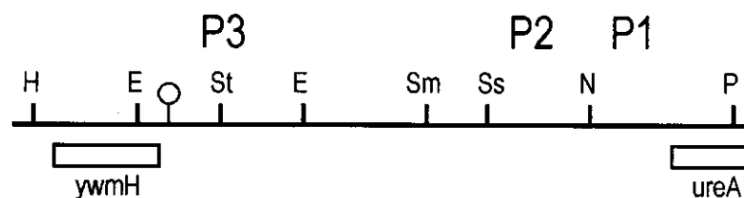


Figure 3-3. *B. subtilis ureABC* promoter region (Cruz-Ramos *et al.*, 1997).

Urease promoters lying upstream of *B. subtilis ureA*. P1 lies immediately upstream of *ureA* followed by P2 and finally P3.

A. *ureABC* P2

```

      SspI          -35          -10          *
AATATTTTACTTAATAAACAATTGGAAGGAATTCAGATTTTAATTGTCGAACTAGTCAGACAAG
      : : : : : : : : : : : : : : : : : : : : : : : : : : : : : : : : : :
      RVAGGAWWT          MGAAT
  
```

B. *ureABC* P3

```

          GlnR/TnrA          PucR
      TGT-A-----T-ACA          WWC-TTGGTTAA
      : : : : : : : : : : : : : : : : : : : : : : : : : : : : : : : : : :
TTTTTCTGATGTGAATAAATAACAACAAAAAAGAAGCTGATTGGTCAAGGTAACATAAATTTTTAAATA
  
```

```

      -35          -10          GlnR/TnrA
      TTGACA          TATAAT          TGT-A-----T-ACA
      : : : : : : : : : : : : : : : : : : : : : : : : : : : : : : : : : :
TTCTTTGAATTAATAGGCCTCTTCTATATAATGATGACATAAGTTGTAAACTTTTATAACATCATTGAA
  
```

Figure-3-4. Nucleotide sequences of *ureABC* P2 and P3 promoters in *B. subtilis*, and *GlnR/TnrA* and *PucR* binding sites of P3.

Adapted from (Wray, Ferson and Fisher, 1997a) (Brandenburg *et al.*, 2002a). A. Nucleotide sequences of *ureABC* P2 promoter with the consensus regions of the σ^H -dependent promoters are indicated below the nucleotide sequence. Transcriptional start sites labelled as asterisk. B. Nucleotide sequences of *ureABC* P3 promoter and *GlnR/TnrA* and *PucR* binding sites. The consensus sequences for the -10 and -35 regions of σ^A -dependent promoters, *GlnR/TnrA* sites, and *PucR* box are indicated above the nucleotide sequence. Transcriptional start sites labelled as asterisk.

3.1.4.2 Regulation of *B. subtilis* Urease by Nitrogen

The optimum source of nitrogen utilised by *B. subtilis* is glutamine, as it is easily converted to glutamate (Detsch and Stulke, 2003; Gunka and Commichau, 2012). Glutamate is the primary donor for amino acid and nucleotide synthesis and it is the central metabolite at the intersection of carbon and nitrogen metabolism. Similar to most urease-producing bacteria, the expression of urease in *B. subtilis* is also regulated by nitrogen. The regulation by nitrogen in *B. subtilis* also can be categorised into the global nitrogen-regulated and pathway specific regulated mechanism.

3.1.4.3 Regulation through Global Nitrogen Regulators GlnR and TnrA

In general, during nitrogen-limited growth in *B. subtilis*, GlnR and TnrA are responsible for increased gene expression (Table 3-1)(Fisher, 1999; Wray *et al.*, 1996). Both proteins include similar amino acid sequences in their N-terminal DNA binding domains and they bind to DNA sequences which house TnrA/GlnR sites with the common consensus sequence TGTNAN₇TNACA (Zalieckas, Wray and Fisher, 2006). GlnR represses gene expression during growth with excess nitrogen, while TnrA both activates and represses gene expression during nitrogen limitation.

The regulation of urease expression by GlnR is controlled through its interaction with GlnR/TnrA binding sites in P3. As (Figure 3-4) shows, P3 includes two GlnR/TnrA binding sites within its sequence. One GlnR/TnrA binding site is centred 91 bp upstream of the *ure* P3 transcriptional start site, while the other site is centred 15 bp downstream of the transcriptional start site. Brandenburg *et al.* (2002) has demonstrated that both binding sites are required for the regulation by GlnR. In the presence of glutamine, GlnR binds both GlnR/TnrA sites on P3 promoters. They also demonstrated the repression of urease expression is due to binding to the downstream GlnR site which inhibits the initiation of transcription at the *ure* P3 promoter and the binding of GlnR to the downstream site could be strengthened by a cooperative interaction with GlnR bound to the upstream GlnR site.

Table 3-1. Gene expression in nitrogen limited conditions of TnrA and GlnR in *B. subtilis*

<i>TnrA</i> Activates	
<i>pucR-pucJ-pucK-pucL-pucM</i>	<i>nrgA-nrgB</i>
<i>yzkB-ykoL</i>	<i>ureA-ureB-ureC</i>
<i>nasA</i>	<i>appD-appF-appA/1-appA/2-appB-appC</i>
<i>ansZ</i>	<i>oppA-oppB-oppC-oppD-oppF</i>
<i>glnQ-glnH-glnM-glnP</i>	<i>tnrA</i>
<i>gabP</i>	<i>ysnD</i>
<i>yrbD</i>	<i>yfiS-yfiR</i>
<i>ywrD</i>	<i>yxkC</i>
<i>nasB-nasC-nasD-nasE-nasF</i>	<i>pxpA-ycsG-ycsI-pxpB-pxpC-kipR-lipC</i>
<i>dtpT</i>	
<i>GlnR</i> Represses	
<i>glnR-glnA</i>	<i>alsT</i>
<i>ureA-ureB-ureC</i>	<i>tnrA</i>
<i>glnR</i>	

TnrA is in its active DNA binding state during nitrogen limitation, thus, turning on the transcription of genes required for nitrogen assimilation such as *tnrA*, *nasB-nasC-nasD-nasE-nasF* (Farazmand *et al.*, 2012)) and *pucR* (the *puc* operon contains two binding sites for Tnr (Doroshchuk, Gel'fand and Rodionov, 2006; Zhu and Stulke, 2018). Initially, Wray *et al.* (1997) showed that TnrA activated the expression of the P3 promoter in nitrogen limited condition. However, Brandenburg *et al.* (2002) demonstrated high-levels of *ureABC* P3 expression during nitrogen-limited growth does not require TnrA to bind to the upstream GlnR/TnrA site, and they suggested that TnrA regulates *ureABC* P3 expression indirectly. This indirect regulation is through the activation of PucR expression in the nitrogen limiting condition which will be discussed in the section below.

3.1.4.4 Regulation by Pathway specific PucR

PucR is the transcriptional regulator of the *puc* genes (*pucR-pucJ-pucK-pucL-pucM*) whose function is the regulation of degradation of purines and is expressed in the absence of good nitrogen sources (glutamine/ammonium). The *pucR* gene is transcribed from a promoter that overlaps the promoter of one of the regulated target genes *pucH* (Schultz, Nygaard and Saxild, 2001). Research carried out by Beier *et al.* (2002) on *puc* promoters identified two significant binding sites. The 1st one is the sequence of the PucR box 5'-WWWCNTTGGTTAA-3' which is upstream of the *puc* promoters Figure 3-5. The 2nd binding site is TnrA/GlnR box which lies 10 bp upstream of the -35 region *pucR* promoter. According to Beier *et al.* (2002) TnrA activates *pucR* expression by binding on this TnrA/GlnR box. The same year, Brandenburg and his colleagues show that upstream of the *ureABC* P3 promoter has a nucleotide sequence which is similar to the PucR box consensus sequence. Therefore, in nitrogen limiting conditions TnrA indirectly regulates *ure* P3 expression by binding to *pucR* therefore activating expression. Subsequently, the expression of urease is activated by PucR binding P3. The 2 GlnR/TnrA binding sites located in the *ure* P3 promoter region provided negative regulation by GlnR. Brandenburg (2002) identified via mutational analysis that the interaction between GlnR dimers at these binding sites, which show urease expression, is not only nitrogen regulated but also regulated by the enzymes involved in purine degradation and transport (Brandenburg *et al.*, 2002a). Beier *et al.* (2002) also found that PucR can induce transcription without purine degradation products, however, the induction is far more effective when the purine degradation products are available (Beier *et al.*, 2002). Urea is an intermediate produced during purine degradation, so the expression of *ureABC* by PucR enables purines to be completely degraded to ammonia providing an optimum source of nitrogen for *B. subtilis* (Brandenburg *et al.*, 2002b).

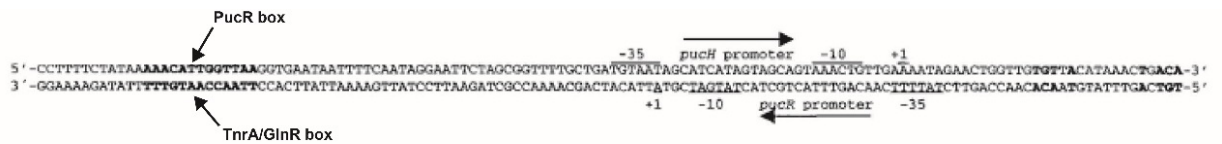


Figure 3-5. Nucleotide sequence in *pucH* and *pucR* regulatory region.

The PucR box (5'-WWWCNTTGGTTAA-3') and TnrA/GlnR box (5'-TGTNAN7TNACA-3') are shown and the -10 and -35 sequences are indicated (Beier *et al.*, 2002).

3.1.4.4.1 Regulation by Overall Nutrient Level Through CodY

The expression of urease is also regulated by the protein CodY. This protein was first identified in *B. subtilis* (Slack *et al.*, 1995) as a global regulatory protein and due to the number of genes it regulates it facilitates many adaptive mechanisms that enable *B. subtilis* to adjust to changes in the nutrient availability. In particular, CodY senses the level of Guanosine-5'-triphosphate (GTP) and branched chain amino acids (BCAA) and also modifies the expression of over 200 genes of which some encode nutrient transport, intracellular catabolism and metabolic pathways (Rutherford, 2014). The DNA binding activity is actually enhanced by the interaction with BCAAs and GTP. Those genes regulated by CodY (224) either repressed or less frequently induced, contain CodY binding sites (AATTTTCWGAAAATT) in their regulatory or coding sequence sites (Belitsky and Sonenshein, 2011).

Literature has detailed that CodY can mediate pH dependent expression of urease in some pathogens. The urease operon of *S. salivarius* consists of 11 genes (*ureIABCEFGDMQO*) and the expression is elevated in pH conditions. The expression of the 11 *ure* genes is due to a promoter located 5' of *ureI* (encodes acid activated urea channel) which interestingly contains a putative CodY binding site (5'-AATTTTCWGAAAATT) (Huang, Burne and Chen, 2014). Huang *et al.* (2014) determined CodY repressed the *ureI* promoter by direct binding to it as in the absence of CodY the RNAP (RNA polymerase) immediately interacted with the promoter suggesting CodY and RNAP compete to bind the promoter region.

As mentioned in 3.1.2, CodY can mediate pH-dependent expression of urease in some pathogens such as *S. salivarius* by competing with RNAP to bind the *ureI* promoter repressing urease expression. However, *B. subtilis* does not contain the *ureI* gene, and the mechanism of CodY

regulation is not fully understood. Molle *et al.* (2003) reported that the presence of CodY could reduce urease expression in *B. subtilis*. Wray *et al.* (1997) also detailed CodY repressed the expression of *ure* P2 and P3 promoters during growth in medium containing amino acids. As CodY is a DNA-binding protein they propose CodY functions directly as a repressor to inhibit transcription from these promoters, Figure 3-6 (Wray, Ferson and Fisher, 1997a). In summary CodY controls numerous genes required for the survival of *B. subtilis* in adverse conditions. During rapid and exponential growth CodY binds and represses these genes, however, once the cells reach the end of exponential phase. CodY loses affinity and the genes are activated.

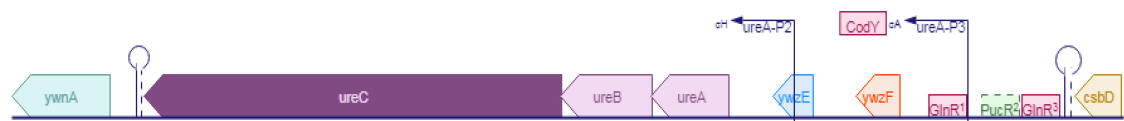


Figure 3-6. *B. subtilis ureABC* operon.

The *B. subtilis ureABC* operon including promoters and CodY, PucR and GlnR binding boxes (Karp *et al.*, 2019).

To summarise, expression of *B. subtilis* urease is synthesized at high levels during nitrogen limited growth (Atkinson and Fisher, 1991). The regulation of *ureABC* is complex (Table 3-2), involving various transcription factors and a regulatory protein along with sigma factors; it involves the transcription of a low level constitutive promoter P1 along with the P2 and P3 promoter which are induced in response to nitrogen limitation. Brandenburg *et al.* (2002) state that *B. subtilis* urease enzyme is a novel example of a urease enzyme whose expression is controlled by both a global nitrogen transcription factor (TnrA) and a pathway specific regulator (PucR) that responds to purine availability aiding survival under stressful conditions.

Table 3-2. Genes involved in urease regulation in *B. subtilis* during nitrogen limiting conditions (Wray, Ferson and Fisher, 1997b; Brandenburg *et al.*, 2002a; Fisher, 1999).

Regulatory protein	Growth conditions in which regulation occurs	Regulation	Regulated genes/promoters	Regulation of expression
<i>TnrA</i>	Nitrogen limitation	+	<i>pucR</i>	Indirect
<i>GlnR</i>	Excess Nitrogen	-	<i>ureABC</i> P3, <i>tnrA</i>	Direct
<i>CodY</i>	Increased growth with amino acids	-	<i>ureABC</i> P3, <i>ureABC</i> P2	Indirect
<i>PucR</i>	Nitrogen limited	+	<i>ureABC</i> P3	Direct

3.2 Urease Enzyme Assays

It can be difficult to compare the urease activity levels across studies due to the divergence of methods utilised for urease activity. The pH of the buffer; substrate concentration, incubation temperature and the time of incubation can differ greatly. Results of urease activity can also be expressed in a variety of units, which can create confusion in the comparison of results (Dharmakeerthi and Thenabadu, 2013).

3.2.1.1 Common Assay Methods for Urease Activity

There are various assay methods to study urease activity. The methods are based on the detection of the ammonium ions reaction products. In most studies, ammonia yields can be low and often the effect of interferants (such as impurity ions, N-containing molecules, and certain solvents) on NH₃ quantification is not considered (Zhao *et al.*, 2019b). Methods utilised for urease activity include: 1) **Berthelot's method**; Berthelot reagent is a solution of phenol and hypochlorite (Ngo *et al.*, 1982). Ammonia reacts with the reagent to form a blue product (indophenol) which is then used in the colorimetric analysis to determine ammonia at 670nm. Various groups utilise this method for urease analysis (Atkinson and Fisher, 1991; Pervez *et al.*, 2008) 2) **Nessler method**; Nessler reagent is the most common operating assay for ammonia/ammonium ion detection (Okyay and Rodrigues, 2013). The reagent measures the ammonium concentration using anhydrous mercuric iodide and anhydrous potassium iodide. It can also be prepared from potassium tetraiodomercurate that is dissolved in potassium hydroxide. Colourimetric analysis is

again used to determine the reaction product, which infers ammonium content at 420 nm. Various groups utilise this assay for urease analysis (Phang *et al.*, 2018; Jia *et al.*, 2013; Weaver, Chen and Burne, 2000) 3) **Phenol red**; this indicator can be used in solid and liquid media to identify urease activity. The production of ammonia from the catalysed reaction visually alters the indicator from light orange at pH 6.8 to magenta at 8.0. 4) **Conductivity Method**; the hydrolysis of urea produces ionic products from non-ionic substrates. A conductivity assay utilises the production of the ionic species which generates an increase in overall conductivity in the solution. The rate at which conductivity increases is proportional to the concentration of active urease present (Whiffin, 2004). This method is suitable for the detection of large concentrations of ammonium ions. 5) **Ion Chromatography method**; is mostly used to analyse ammonium ions in water and wastewater utilising a cation exchange column. This method is expensive and requires complex instrumentation, but offers the advantages of high sensitivity and excellent reproducibility of results (Zhao *et al.*, 2019b).

To fully evaluate urease activity, decisions regarding the optimal urease detection assay are vital. Each method listed includes its own limitations with regards to the detection. The use of spectrophotometric assays are more common-place due to their low cost, which includes Nessler's method and Berthelot's method.

3.2.2 Factors which influence Urease Assays

As urease is a multi-subunit enzyme, and it is challenging to purify from both native and recombinant cells. Many studies investigate urease activity in whole cells (Bachmeier *et al.*, 2002; Bauerfeind *et al.*, 1997) or cell free extracts (CFE) (Cruz-Ramos *et al.*, 1997; Kim, Mulrooney and Hausinger, 2005a). As whole cells and CFE are complex samples, the results of enzyme assays using these samples can be influenced by many factors. In the case of assays for urease activity, by measuring the production of the ammonium such as the Nessler method, many cell related factors could influence the detection of ammonium in the reaction.

There are various biological processes involving specific genes in *B. subtilis* which produce ammonium/ammonia products as seen in Table 3-3. This is of great interest as any design of urease assay that detects ammonium ions will need to consider these reactions. Urea hydrolysis

is not the only pathway in bacterial cells to produce $\text{NH}_4^+/\text{NH}_3$. Other pathways in *B. subtilis* are detailed in Table 3-3 and include the glutamate catabolic process (*rocG*). It is important to highlight the main nitrogen source in NLM is glutamic acid. RocG is the major glutamate dehydrogenase and only expressed in the presence of arginine and enables the bacteria to utilise (Belitsky and Sonenshein, 1998). However, this enzyme is expressed during spore germination and so should not affect analysis. There is also glutamate dehydrogenase (GudB) which is inactive in 168 due to a mutation during domestication (Gunka and Commichau, 2012). Cytidine deaminase (*cdd*) includes a function of pyrimidine interconversion and so is involved in nucleotide metabolism scavenging for exogenous and endogenous cytidine and 2'-deoxycytidine for UMP synthesis. This enzyme is under the *sigA* and *sigB* regulons and zinc is its cofactor (Song and Neuhard, 1989). Guanine deaminase (GuaD) synonyms *gde* and *yknA* is involved in the deamination of guanine to xanthine and associated with purine salvage and interconversion (Nygaard *et al.*, 2000). The enzyme is expressed during limited or partially limited nitrogen conditions and is induced in the presence of purines or intermediates of the purine catabolic pathway (Nygaard *et al.*, 2000) and the gene is a member of the PucR, SigA and Sig B (stress) regulons. The putative adenine deaminase YeaR is also listed and is involved in the adenine catabolic process and is identified as a hydrolase. Very little is known about this protein due to its putative annotation.

These processes will need to be considered and proteomic data analysed to determine their affect upon creating false positives in the enzyme assay, as NH_4^+ is detected.

Table 3-3. Known ammonium producers in *B. subtilis* and their corresponding reaction (Uniprot).

Gene/s	Reaction	Description
<i>guaD</i>	guanine + H ⁺ + H ₂ O → NH ₄ ⁺ + xanthine	Guanine Deaminase
<i>cdd</i>	cytidine + H ⁺ + H ₂ O → NH ₄ ⁺ + uridine or 2'-deoxycytidine + H ⁺ + H ₂ O → 2'-deoxyuridine + NH ₄ ⁺	Cytidine deaminase
<i>rocG</i>	H ₂ O + L-glutamate + NAD ⁺ → 2-oxoglutarate + H ⁺ + NADH + NH ₄ ⁺	Arginine and Orthinine Catabolism
<i>ure</i>	2 H ⁺ + H ₂ O + urea → CO ₂ + 2 NH ₄ ⁺	Urease
<i>yerA</i>	adenine + H ⁺ + H ₂ O → hypoxanthine + NH ₄ ⁺	Putative adenine deaminase

3.2.3 Ammonium transportation

At neutral pH, which is typical of a cell's cytoplasm, approximately 99% of ammonium is present as NH₄⁺, as NH₃ is a weak base. Therefore a decrease of one pH unit can cause a tenfold increase in the ratio NH₄⁺:NH₃ (Howitt and Udvardi, 2000). A ubiquitous family of integral membrane proteins drive NH₄⁺ back and forth across membranes; these are the ammonium transport proteins (Amts). Amts are found in all domains of life and enable the scavenging of environmental NH₄⁺ for uptake and assimilation of nitrogen and are part of the ammonia transporter channel (TC 1.A.11.2) family (Wacker *et al.*, 2014). The exact transport mechanism of Amts is still not understood. Amt proteins are slow transporters and are difficult to investigate experimentally, as they struggle to generate large currents for measurements (Wacker *et al.*, 2014).

We understand in *B. subtilis* there are two mechanisms to transport NH₄⁺. At high concentrations of NH₄⁺, a large portion of the NH₄⁺ present as NH₃ and enters the cell via diffusion (Detsch and Stulke, 2003). At low concentrations or low pH (the equilibrium of NH₃ and NH₄⁺ fluctuates) the membrane protein and NH₄⁺ transporter NrgA (synonym *amtB*) is required for a NH₄⁺ utilisation. Under nitrogen limited conditions (NLC) TnrA activates expression of the genes encoding NH₄⁺ transporter which form the *amtB-glnK* complex, originally named *nrgAB* (Wray, Ferson and

Fisher, 1997b). This complex therefore consists of a transmembrane NH_4^+ transporter and its cognate regulator which interacts with TnrA. Mutants of this gene struggle to grow at pH 5.5 and fail to grow at all at pH 5.0 when NH_4^+ is their sole nitrogen source. NrgB (homologue of GlnK) is present in the cytoplasm at low NH_4^+ concentrations, it would be recruited by AmtB under conditions of nitrogen excess. NrgB is a member of the PII proteins that function as signal transduction proteins and are of great importance in the nitrogen control in bacteria (Huergo, Chandra and Merrick, 2013). Interaction of NrgB with NrgA is needed to locate it correctly to the membrane, and under the NLC, NrgB is required for the full induction of the operon.

3.3 Nickel and Metalloenzymes

Ni^{2+} is an essential nutrient for selected microorganisms, where it engages in a variety of cellular processes. Innumerable microbes are able to detect cellular Ni^{2+} concentrations and assimilate the metal via Ni^{2+} specific permeases or ATP- binding cassettes- type transport systems (Mulrooney and Hausinger, 2003).

Only a third of enzymes are metalloenzymes and those with Ni^{2+} as a cofactor are less common (Siegbahn, Chen and Liao, 2019). There are ten known Ni^{2+} dependent metalloenzymes, seven of these enzymes belong to the oxidoreductase class which include: Hydrogenase, Methyl-Coenzyme M reductase, CO dehydrogenase, Acetyl-CoA synthase, Acireductone dioxygenase, Quercetin 2,4-dioxygenase, Superoxide Dismutase. The remaining three Ni^{2+} metalloenzymes include: Urease, Glyoxylase I and Lactate racemase.

An interesting question is why these enzymes use Ni^{2+} as their cofactor and not other divalent cations? One main reason for utilising Ni^{2+} as a cofactor maybe due to its flexible coordination geometry (Maroney and Ciurli, 2013).

3.3.1 Metal ion interactions with urease

Urease belongs to the hydrolase class and superfamily of amidohydrolases and phosphotriesterases which feature catalytically-active metal(s) in their active site (Kappaun *et al.*, 2018). Cofactors are often small organic molecules, if tightly bound they are prosthetic groups. If loosely bound they have the same function as the prosthetic groups but bind in a more temporal way, they can bind and be released from the enzyme.

Several other metal ions have been shown to bind to the urease apoproteins (Carter *et al.*, 2011). Those divalent metals include Zinc (Zn^{2+}), Copper (Cu^{2+}), Cobalt (Co^{2+}) and Manganese (Mn^{2+}). All inhibit Ni^{2+} urease activation at concentrations below that of Ni^{2+} , whereas Magnesium (Mg^{2+}) and Calcium ions (Ca^{2+}) do not inhibit the system (Park and Hausinger, 1996). However metal substituted urease has never been purified from Ni^{2+} deprived cells with the exception of Fe^{2+} i.e. ferrous urease has been purified but no others (Carter *et al.*, 2011). This substitution of metal ions may be attributed to the Irving Williams series: $\text{Mn}^{2+} < \text{Fe}^{2+} < \text{Co}^{2+} < \text{Ni}^{2+} < \text{Cu}^{2+} > \text{Zn}^{2+}$. The Irving Williams series indicates the relative stabilities of complexes formed by transition metals. The ions typically increase across the period to a maximum stability at copper.

3.3.1 Metal binding proteins that could affect urease activity

It is understood that Ni^{2+} are essential for catalytic activity of the majority of urease. Those proteins that bind divalent cations will therefore be investigated within this research, in the hope of understanding the activation of *B. subtilis* urease. The hypothesis that certain proteins will be identified through this research as accessory proteins for urease activity due to their metal binding properties will be investigated through gene knockouts. Therefore, if a specific identified gene is involved in activation, when the gene is knocked out via single gene deletion, urease activity should be affected.

The cytoplasmic membrane bound protein *NixA*, of *H. pylori* transports Ni^{2+} for the activation of urease. However, a *NixA* mutant retains some urease activity (Bauerfeind, Garner and Mobley, 1996). Also, the well-studied *H. pylori* mutants of the ferric uptake regulator (FUR) showed that Fur appears to be involved in acid resistance *H. pylori* urease activity. This is of interest as this regulator does not concern Ni^{2+} .

As Castro Alonso *et al.* (2019) discuss, with regard to MICP, further research is needed in order to understand the rates of urease expression and the regulatory strategies involved in environmental bacteria (such as *B. subtilis*) in order to understand further calcite precipitation.

3.4 Aims and Objectives

The aims of this chapter of research were to define a minimal media suitable for the cultivation of *B. subtilis* 168 whilst increasing urease activity, along with a suitable assay for urease detection.

Within this defined medium we would be able to control the urease activity level by controlling the nitrogen level. Literature has shown that urease activity increases in nitrogen limited conditions. This defined media would be designed to be nitrogen-limited in order to promote urease regulation in *B. subtilis*. A further minimal media would need to be developed to use as a comparative for the proteomic study on the differentially-expressed proteins which potentially are involved in the activation of urease. We understand *B. subtilis* urease activity is increased in nitrogen limited conditions. Therefore, the two different media would be one that is nitrogen limited and one of nitrogen excess. It would then be necessary to determine urease activity was greatest in the nitrogen limited minimal media, which would confirm previous research (Cruz-Ramos *et al.*, 1997; Fisher and Wray, 2002). The two different media will enable the identification of how urease expression is regulated and how urease is activated, as those proteins involved in urease activation in *B. subtilis* are proposed to be upregulated in the nitrogen limited media.

Urease activity in *B. subtilis* is known to be low, or inefficient (Cruz-Ramos *et al.*, 1997) and this needs to be considered when a specific enzyme assay is selected and developed to be suitable for this research. Therefore, after the defined minimum medium is developed, a reliable, accurate and robust method for the detection of urease activity in *B. subtilis* needs to be developed and optimised.

3.5 Results and Discussion

One objective of this chapter was to optimise a minimal medium (MM) that would achieve the growth of *B. subtilis* 168. This would enable the media to be controlled and provide an understanding of *B. subtilis* in specific limiting conditions in order to understand urease activation. As urease activity is greater in NLC, the media would include a limited nitrogen source and ideally the preferred nitrogen source (glutamine) of *B. subtilis*. Once the correct media was devised, it was necessary to understand the growth patterns of *B. subtilis* 168 in the specific growth media. The information from the growth curves would enable us to ascertain the different phases of growth, and also identify if the cells were under stress. Identifying the growth phases in the media would enable us to understand when urease activity was greatest in the cells.

3.5.1 Media optimisation and growth curves

To establish the appropriate media to be used in this research, we tested the growth in four media and with various supplements. Preliminary testing of media was assessed by the turbidity of the liquid culture and the results are shown in Table 3-4. The results from the preliminary media testing identified SMM and LB media as suitable for cultivation as good turbidity was achieved. The initial MM identified was SMM, a popular cultivation media for *B. subtilis* which includes a minimal base solution with supplements as described in methods 2.2.3. The media is commonly used to produce naturally competent cells, with low yield. As seen in Figure 3-7, specific growth curves were identified. They were achieved by inoculating one colony of *B. subtilis* 168 into 100ml of SMM and incubating at 30°C 150 rpm with 1 ml aliquots taken aseptically every hour to measure OD. This media, however, did not include a simple, controllable nitrogen source, as the base media contained $(\text{NH}_4)_2\text{SO}_4$ with additional supplements of ammonium iron citrate and tryptophan.

Table 3-4. Preliminary data identifying media suitable for growth of both *Bacillus* strains in use.

Growth of *B. subtilis* 168 (2.6.1.4) was achieved in SMM and in LB, with a greater OD in LB. No growth was visible in GGS media or those with supplements.

Media	<i>B. subtilis</i> 168 24h
SMM	+
LB	++
GGS	-
GGS + Glucose	-
GGS+ Ammonia	-
GGS+ Urea	-

Literature identified various minimal media for the cultivation of *Bacillus* sp. (Buono, Testa and Lundgren, 1966) (Demain, 1958) including GGS and BSS. The first MM trialled was GGS which consisted of a controllable nitrogen source. The controllable nitrogen source was deemed important as controlling the nitrogen source could possibly control urease expression. The GGS media was initially trialled for cultivation of *B. subtilis* without any supplements. Cultivation was then explored including supplements to the base media of suitable nitrogen and carbon sources. The initial trials of GGS media alone, and including supplements of suitable nitrogen compounds and carbon sources produced no growth (as shown in Table 3-4), presumably as tryptophan was not present and *B. subtilis* 168 is a tryptophan-requiring auxotroph (Zeigler *et al.*, 2008). Growth was visible in SMM and LB media, as all nutrients for growth would be provided including tryptophan, either as a supplement (SMM) or within the media (LB) containing tryptone, a stable product of protein digestion, rich in amino acids particularly tryptophan.

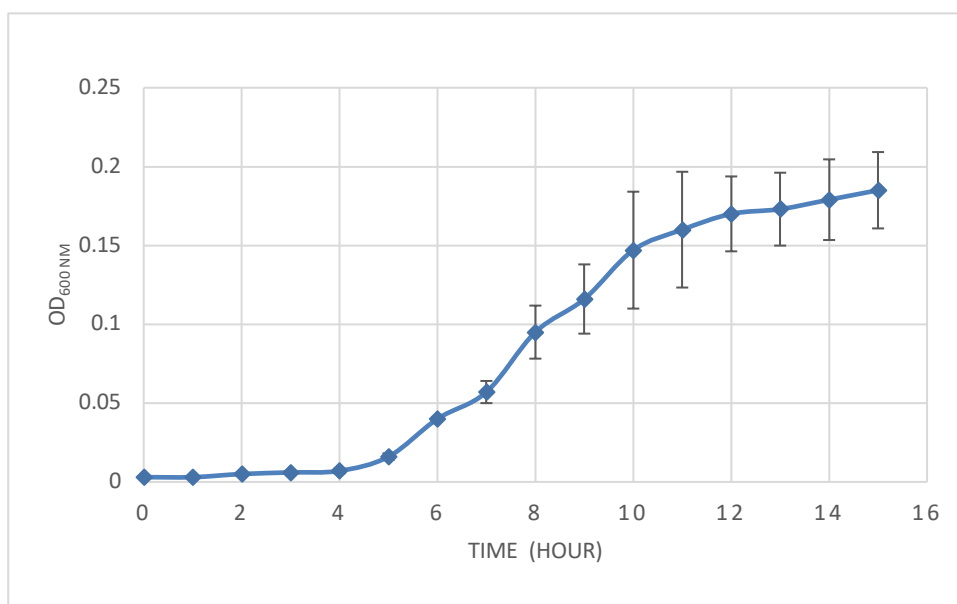


Figure 3-7. Growth curve of *B. subtilis* 168 in SMM.

Growth curve analysis of *B. subtilis* 168 in SMM media at 30°C 150 rpm over 15 hours. The growth phases can be identified at 7 hours for mid exponential and 12 hours for end exponential at 30°C 150 rpm. The test was performed with 4 biological and 2 technical replicates.

Another MM investigated was a Basal Salt Solution (BSS) (Chasin and Magasanik, 1968). We tested the growth in BSS and BSS with several supplements. As seen in Table 3-5, BSS alone, as detailed by Chasin and Magasanik achieved no growth of *B. subtilis*. As described (in section 2.5.4.4) the necessary supplements needed for growth and for nitrogen control were identified. The supplemented BSS incorporated glucose, tryptophan and the simple preferred nitrogen source glutamic acid, producing sufficient high cell density yield. As published data (Dawes and Mandelstam, 1970; Vasantha and FREESE, 1979) acknowledges, and our results show in Table 3-5, we confirm tryptophan is necessary for growth. In addition, the results show that glucose is required as a carbon source unless there is an excess of nitrogen in the media (from Ammonium Sulphate) as shown in Table 3-5 (9. BSS with Glutamic acid, Tryptophan, Ammonium Sulphate and Sodium chloride as supplements). This may be because, as Sonenshein *et al.* (2007) describe, glutamate connects carbon and nitrogen metabolism by supplying the carbon skeleton for α -ketoglutarate synthesis, which is the entry point for carbon metabolism for certain AA degradation pathways (Sonenshein, 2007). Ammonium assimilation in *B. subtilis* also involves 2 enzymes: glutamine synthetase, which catalyses the formation of glutamine from glutamate and ammonium, and glutamate synthase which converts 2-oxoglutarate and glutamine to two

molecules of glutamate. One of these glutamate molecules is recycled to glutamine whilst the other is available for anabolism, linking carbon metabolism (Krebs citric acid cycle) and nitrogen metabolism (Wacker *et al.*, 2003).

This medium provided the optimal nutrient source. However, it would be problematic to alter all nitrogen sources. Therefore, the media identified for optimal growth of *B. subtilis* 168 included the base media (BSS) along with glucose, tryptophan and glutamic acid (GA) achieving turbidity after 48 hours and included the controllable and preferred nitrogen source, GA. The media was named BSS (JW).

Research also suggested that when the concentration of NaCl is at high levels, the addition of extra can inhibit urease activity, however, at optimal concentrations (< 0.5 M) it can increase urease activity in some bacteria (Jabri *et al.*, 1995; Carter and Hausinger, 2010). Therefore, a minimal amount of NaCl was added as a supplement (150 mM) to BSS (JW).

Table 3-5. Growth of *B. subtilis* 168 in BSS MM with varying supplements identified as necessary for *B. subtilis* growth. (Dawes and Mandelstam, 1970; Vasantha and FREESE, 1979).

Medium	Growth of <i>B. subtilis</i> 168	
	24hr	48hr
Minimal Media BSS & Supplements		
1. BSS	-	-
2. BSS & Ammonium Sulphate	-	-
3. BSS & Ammonium Sulphate + Glucose	-	-
4. BSS & Glucose + Glutamic acid	-	-
5. BSS & Glutamic acid	-	-
6. BSS & Tryptophan	-	-
7. BSS & Glucose & Tryptophan	+	+
8. BSS, Glucose, Tryptophan & Glutamic acid BSS (JW)	+	+
9. BSS, Glutamic acid, Tryptophan, (NH ₄) ₂ SO ₄ & NaCl	++	++

It was necessary to ascertain growth phases in BSS (JW) and identify urease activity within these phases. Preliminary growth was investigated using the Biotek Synergy HT plate reader to gain an insight of the growth rate of *B. subtilis* 168 in BSS (JW). The growth curves were constructed in Excel (Figure 3-8). The growth analysis detailed mid exponential at approximately 22 hours and end exponential at approximately 40 hours. The final OD in this media is always below 1.

The use of the Biotek synergy plate reader was a guide to *B. subtilis* growth in BSS (JW), however the shaking activity could not be accurately replicated (only approximate) as the shaking was linear and characterised as ‘low, medium or high’ and the oxygen level is relatively low due to the plate set up. It was decided that growth would also be studied in large scale i.e. 500 ml media in 2 L flask at 30°C at a comparable orbital shaking of 150 rpm over 48 hours. The absorbance at 600 nm wavelength was manually measured using the spectrophotometer at each time point. Due to the length of growth, it was challenge to take the measurement every hour, so the time points were selected from 18 hours based on Figure 3-8. Figure 3-9 details growth curve analysis over a period of 18-47 hours with the end exponential phase visible at approximately 40 hours.

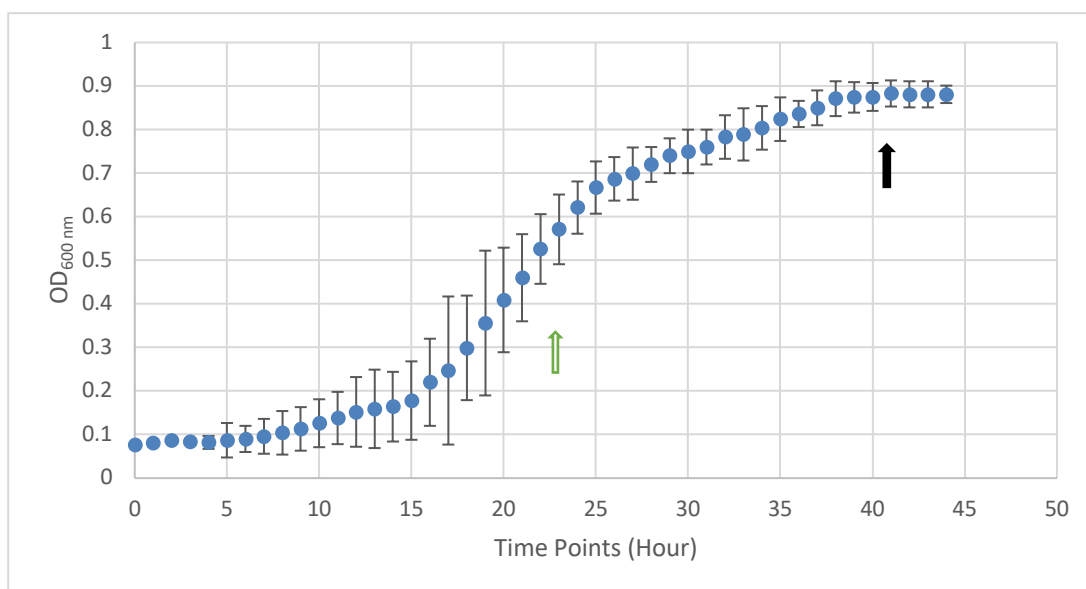


Figure 3-8. Growth analysis of *B. subtilis* 168 cultured in small scale BSS (JW).

Growth analysis of *B. subtilis* 168 using the Biotek Synergy HT plate reader over a period of 72 hours cultured a 12 well plate using 2 ml in BSS (JW) per well at 30°C, shaking; medium as in method 2.1.3.1. The green arrow identifies the mid exponential phase (approx. 22 hours), the black arrow identifies the end exponential phase (approx. 40 hours). The data represents the growth measurements from 8 biological and 3 technical replicates.

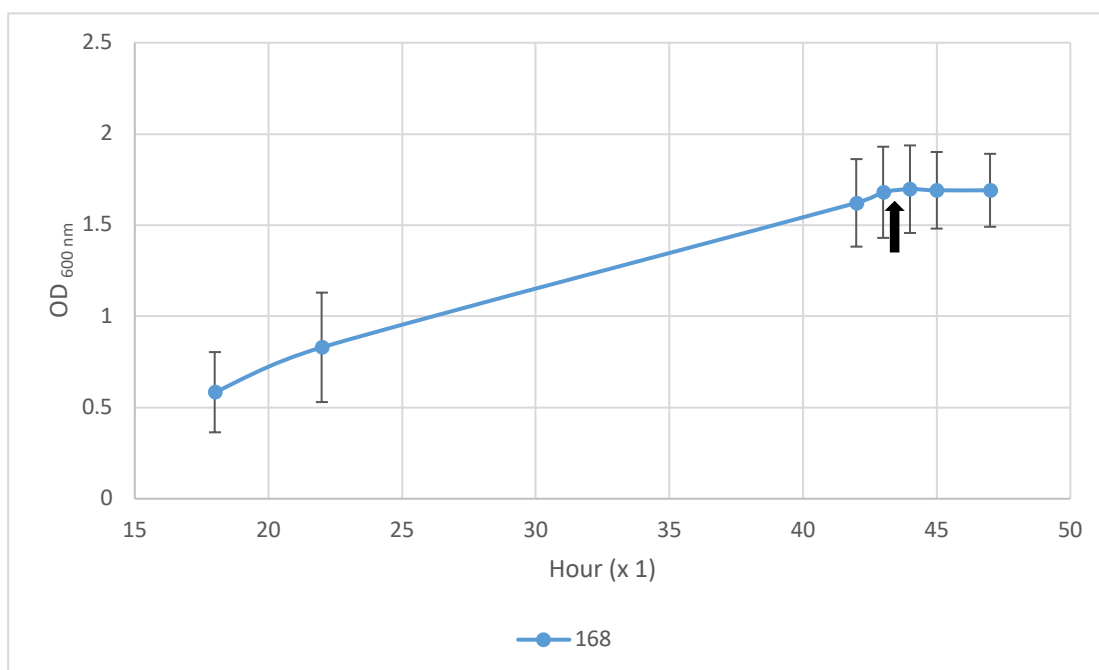


Figure 3-9. Growth analysis of *B. subtilis* 168 cultured in large scale BSS (JW).

Analysis of 5 replicates of *B. subtilis* 168 cultured in 500 ml (2 L conical flask) at 30°C at 150 rpm from 18 hours – 47 hours. End exponential (black arrow) visible at approx. 42 hours. The error bars detail the fluctuations in the absorbance readings of the replicates, yet a similar growth trend is followed. The data represents the growth measurements from 3 biological and 2 technical replicates.

The growth analysis of *B. subtilis* 168 cultured in BSS (JW) therefore detailed the mid exponential growth phase to be approximately 22 hours and end exponential at approximately 40 hours. This knowledge would aid the research in understanding urease activity at specific growth phases.

In order to understand the activation of urease in *B. subtilis*, previous urease expression and regulation data (Fisher, 1999; Cruz-Ramos *et al.*, 1997) enabled us to design suitable growth mediums. Nitrogen limitation is obviously a huge factor when considering the growth media required for urease activation (due to the increased urease presence in NLC). However, also of significance is the necessity of tryptophan for the growth of *B. subtilis* 168, as stated in Table 3-5, this also confirms the correct strain is being investigated. As stated, *B. subtilis* 168 is a tryptophan auxotroph strain (Zeigler *et al.*, 2008). It would be necessary to design a Minimal Media (MM) whereby all constituents needed for growth were available, however, limitation is key in order to enable growth but create a stress on the cells. Therefore, the media needed to consist of vital salts, a carbon source, tryptophan, and controllable nitrogen source such as

glutamate. In the lab setting glutamic acid is used; glutamic acid is also referred to as glutamate as it is the ionic salt of glutamic acid.

3.5.2 Determination of Urease Activity in Various Conditions

In order to determine urease activity in solution the Nessler method was followed. Nessler's reagent is an aqueous solution of potassium iodide, mercuric chloride, and potassium hydroxide, which is used to determine the presence of ammonium (NH_4^+) compounds in liquid states. Upon detection of NH_4^+ compounds the colour of the solution will change to red/brown. Nessler's reagent was optimum for the reaction for numerous reasons; the reagent is accurate in a range of pH, the colorimetric application and the ability to optimise the method for this research.

As seen in Figure 3-10 NH_4Cl standards 0 – 20 mg/L (NH_4Cl Mol.wt. 53.491g/mol) were produced. In order to determine the test samples a standard curve was produced using the standards to represent the relationship between OD and concentration of NH_4^+ produced in the reaction. Using $x = y - c/m$ the test sample concentrations of NH_4^+ are determined.

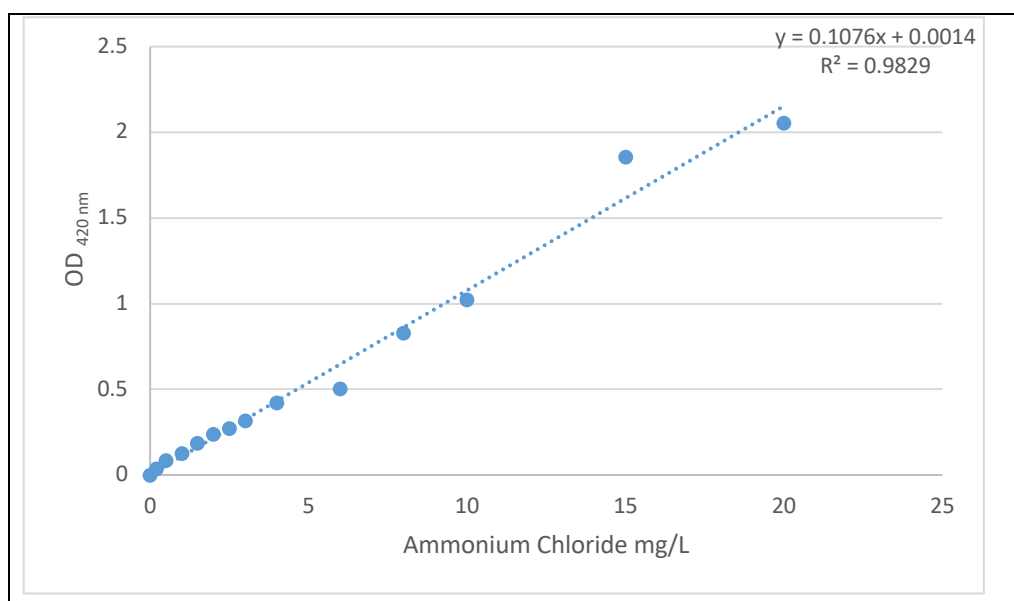


Figure 3-10. Ammonium Chloride standard curve (0-20mg/L) for Nessler Assay.

Various ammonium chloride solution standards (0-20 mg/L) were prepared in order to produce a standard curve to determine ammonium concentration in test samples. Of each standard 25 μl was added to 850 μl 18.2 M Ω /cm H_2O , then 125 μl of Nessler reagent was added. The OD of the mixture was determined at 420 nm and plotted. There R^2 value also determined confidence in the standard curve.

3.5.1 Urease Activity in Different Growth Phases

Once growth curves in specific media were attained, urease activity could be ascertained at each growth phase for BSS (JW) media.

The mid-exponential growth phase is evident at approximately 24 hours and end exponential phase at approximately 40 hours when *B. subtilis* 168 is cultured in BSS (JW) at 150 rpm 30°C (Figure 3-8 and Figure 3-9). The cells were harvested at both mid and end exponential growth phases and urease activity was examined using whole cells for both phases. Figure 3-11 details urease activity of *B. subtilis* 168 at both phases. The results detailed the urease activity trend in *B. subtilis* 168 was importantly higher at end exponential growth phase when compared to that of mid-exponential phase. This was consistent with the literature (Atkinson and Fisher, 1991).

The activity of urease at mid exponential was 0.368 U/OD and at end exponential is 0.588 U/OD.

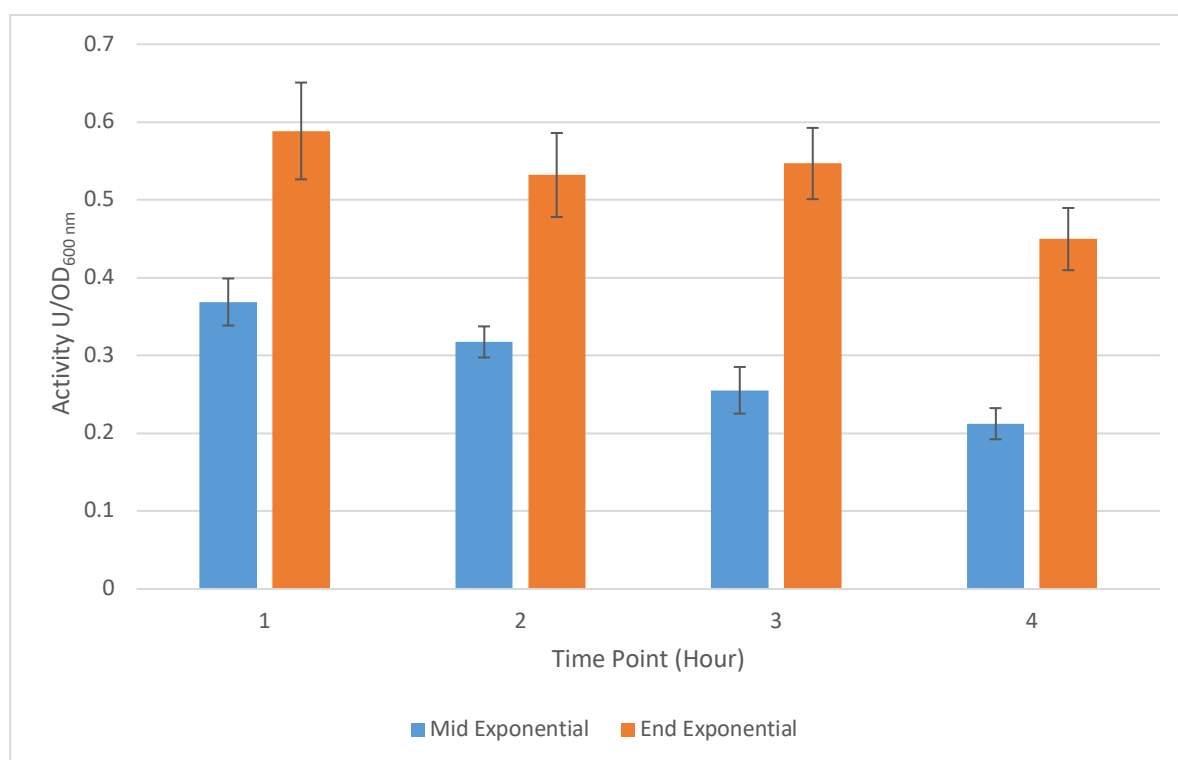


Figure 3-11. Urease activity of *B. subtilis* 168 at mid and end exponential growth phases in whole cells

A comparison of urease activity at mid and end exponential time points. Data is based on 4 biological and 2 technical replicates.

These results identified that the cell harvest time would be at end exponential for all enzyme assay and proteomics experiments.

3.5.2 Effect of Nitrogen upon urease activity in *B. subtilis*

It is understood the expression of *B. subtilis* urease is increased during nitrogen limited growth (Wray, Ferson and Fisher, 1997a; Brandenburg *et al.*, 2002a).

3.5.2.1 Media activation of urease in *B. subtilis* 168

The enzyme activity of urease refers to the number of micromoles of ammonia formed by urease per minute. Urease activity for whole cell assay was established as the amount of urease activity per unit of biomass and was calculated in accordance with the equation in methods 2.1.10.

Activity of urease in CFE assays was established via the equation in 2.1.10, where biomass was replaced with protein amount in mg, leading to U/mg. This establishes the micro moles of ammonia formed by urease per minute per mg of total proteins.

Urease activity was initially investigated in LB media and compared to the MM BSS (JW) to investigate how the media affect urease activity in *B. subtilis*. Urease activity was greater when the bacterium was cultivated in BSS (JW), compared to the general LB medium (Figure 3-12). At the one-hour time point, urease activity of the cells grown in BSS (JW) is approximately double that in LB. LB media is a general growth medium and compared to BSS (JW) is nitrogen 'rich'. The constituents of LB that make it nitrogen rich include tryptone and yeast extract. It was necessary to confirm the NLC produced by BSS (JW) would increase urease activity, as it was proven by previous research that urease activity is increased under nitrogen limiting conditions (Atkinson and Fisher, 1991). Confirmation of this hypothesis (Figure 3-15) would be the foundation of this research into understanding urease activation in *B. subtilis*.

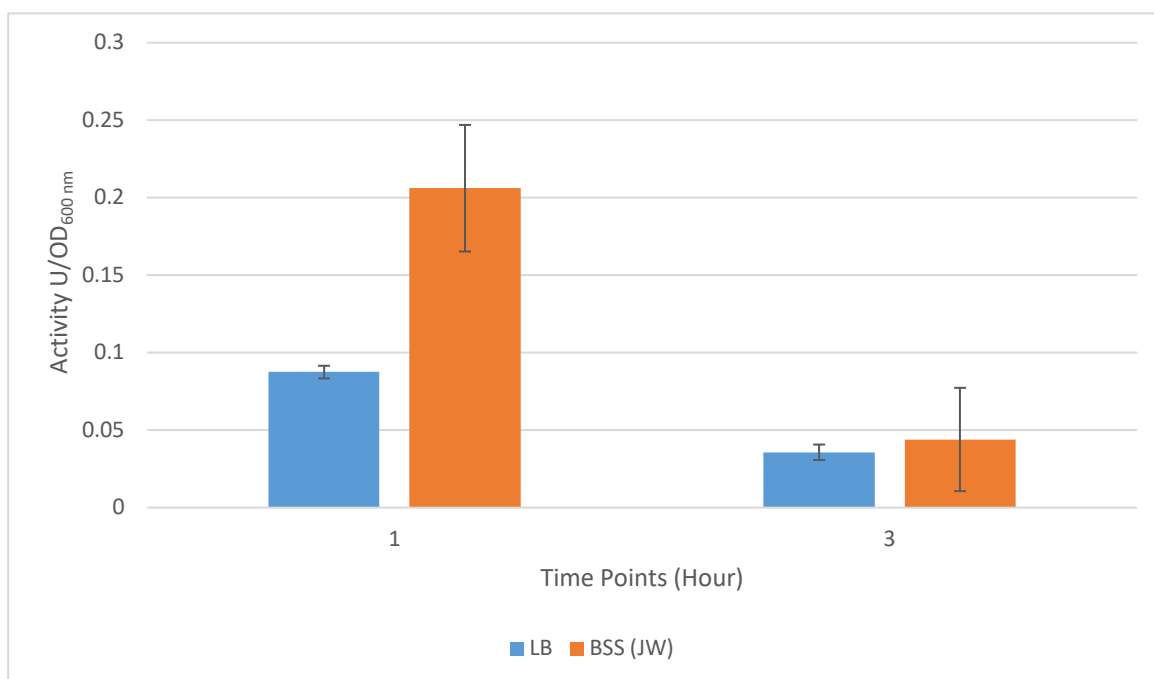


Figure 3-12. Urease activity of *B. subtilis* when cells are cultured in LB and BSS (JW).

Urease activity is greater (approx. double) in the nitrogen limiting condition (BSS (JW)) at 0.2 U/OD compared to LB at 0.75 U/OD. The assay was prepared in HEPES buffer and the data is based on 3 biological and 2 technical replicates.

Atkinson and Wray (1991) investigated the effect of different nitrogen sources in the growth medium and their impact on urease activity and found if the nitrogen source was classed as ‘poor’, urease activity would be elevated. A ‘poor’ nitrogen source would include any nitrogen source other than the optimum which is - glutamate or ammonium (Atkinson and Fisher, 1990, Hu *et al.*, 1999). In this study, the term nitrogen limitation is reflected from the work of Atkinson and Fisher (1990) where a nitrogen limited media (NLM) is one which consists of only one nitrogen source. A nitrogen excess media, or nitrogen plus (NPM) is therefore one which includes more than one nitrogen source.

Nitrogen availability plays an integral role in urease expression in *B. subtilis*. It was thought that altering the concentration of glutamic acid available in BSS (JW), may incur a difference in urease expression and/or activity. Firstly, the impact of the different concentrations of glutamic acid in BSS (JW) on the growth of *B. subtilis* were investigated. Growth curves were constructed for the comparison of low (2.5 g/L) and high (10 g/L) glutamic acid concentrations on the growth of *B. subtilis* 168 as seen in Figure 3-13. The differing concentrations of glutamic acid, follow a similar

trend in growth with the 'normal' (5 g/L) concentration growth of *B. subtilis* 168. Therefore the varying concentrations offer little change to bacterial cell growth.

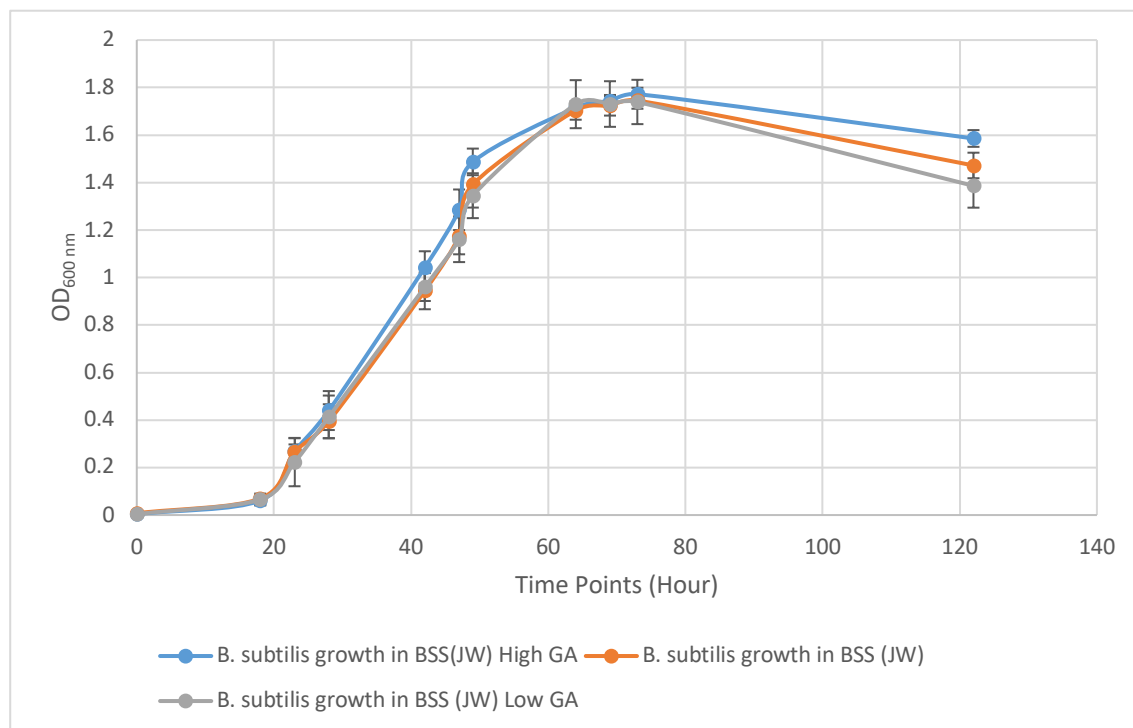


Figure 3-13. Growth comparison of *B. subtilis* 168 cultured in large scale BSS (JW) (500 ml) with varying concentrations of glutamic acid.

Growth curve analysis of *B. subtilis* 168 in BSS (JW) with various additions of Glutamic acid (Normal 5 g/L, high 10 g/L and Low 2.5 g/L). The data is based on 3 biological and 3 technical replicates.

Once growth curves of bacteria in the medium containing various glutamic acid concentrations were ascertained, urease activity in each condition was then investigated. Cell were harvested at end exponential and as Figure 3-14 demonstrates, initially, at one hour, the low glutamic acid condition included the highest urease activity. Overall, both low and high concentrations at the one-hour time point are greater than the normal condition. However, on reflection, when considering the standard deviations of the three conditions (low, normal and high GA), amending the concentration of glutamic acid did not incur great change in growth nor activity of the enzyme. The results shown here indicate that the concentration of GA at all levels tested in our experiments (low, normal and high) could still be classed as limited.

These results indicate that BSS (JW) is an appropriate medium which can be used as a nitrogen limited minimal medium to study urease activity, and it will form the basis for our proteomic studies.

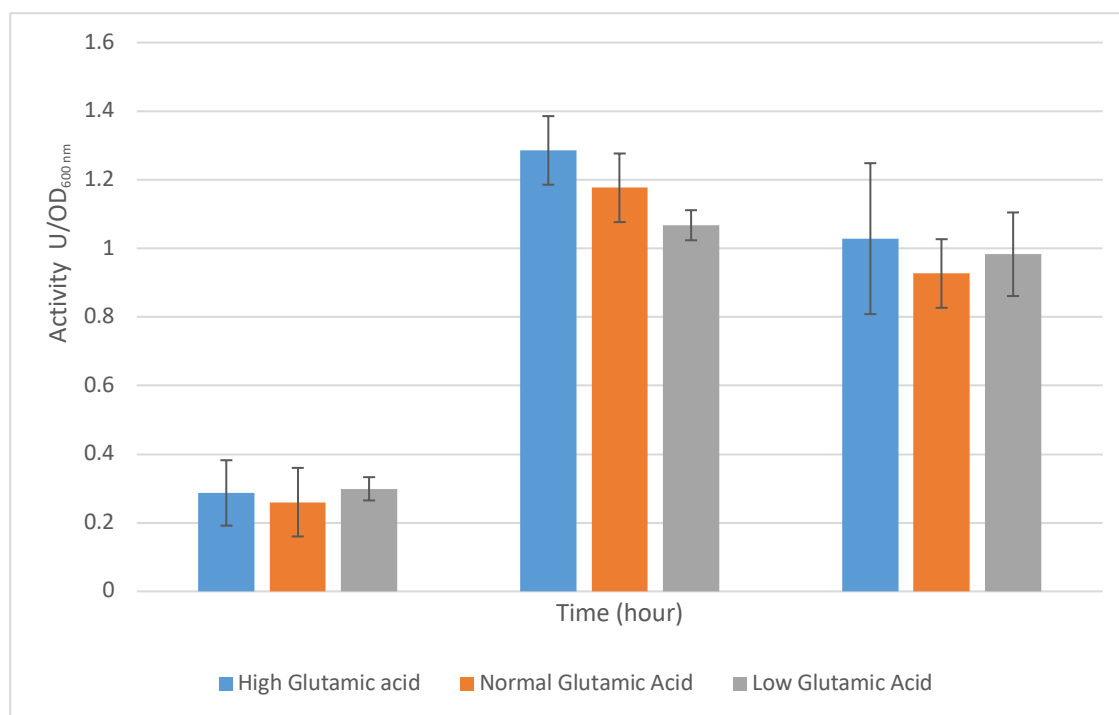


Figure 3-14. Urease activity of *B. subtilis* 168 cultured in various concentrations of glutamic acid (low 2.5 g/L, high 10 g/L and normal 2.5 g/L) in BSS (JW).

Urease activity is slightly increased in the lower GA condition however the error bars indicate deviations with normal being considered similar at the one-hour time point. The enzyme assay was carried out in HEPES buffer. Data is from 3 biological and 2 technical replicates.

3.5.1 Effect of Ammonium Sulphate in the Growth Medium on Urease Activity

It is well documented that urease activity in *B. subtilis* is elevated in nitrogen limited growth conditions (Cruz-Ramos *et al.*, 1997; Wray, Ferson and Fisher, 1997b; Brandenburg *et al.*, 2002a). The media BSS (JW) was devised with this knowledge, consequently, for detailed analysis of BSS (JW) a media of non- nitrogen limitation (i.e. nitrogen plus), that is, one in which nitrogen is in excess needed to be designed for comparison. We have tested the impact of different levels of glutamic acid (the preferred nitrogen source of *B. subtilis*) in the growth medium on urease activity, and did not observe differences in activity. NH_4^+ is also a preferred nitrogen source of *B. subtilis*. We aimed to test the impact of the addition of NH_4^+ in the growth medium on urease activity. This was simply generated by the addition of ammonium sulphate (20 g/L) to the

minimal media BSS (JW) (method in 2.1.2). The BSS (JW) media 2.2.6 was therefore altered to incorporate ammonium sulphate, producing a nitrogen rich condition. Cells were harvested at end exponential and HEPES buffer was used in the whole cell enzyme assay. As detailed in Figure 3-15, urease activity shows a marked difference from the cells grown in the two media, with the nitrogen rich media demonstrating a much lower activity than that in BSS (JW). Urease activity is decreased by approximately 0.15 U/OD in the (BSS (JW)) nitrogen rich media at the first hour of reaction. This is consistent with the literature, as the nitrogen limitation of BSS (JW) has increased urease activity and therefore this medium is sufficient to be used as a nitrogen rich medium for the future study of urease activation.

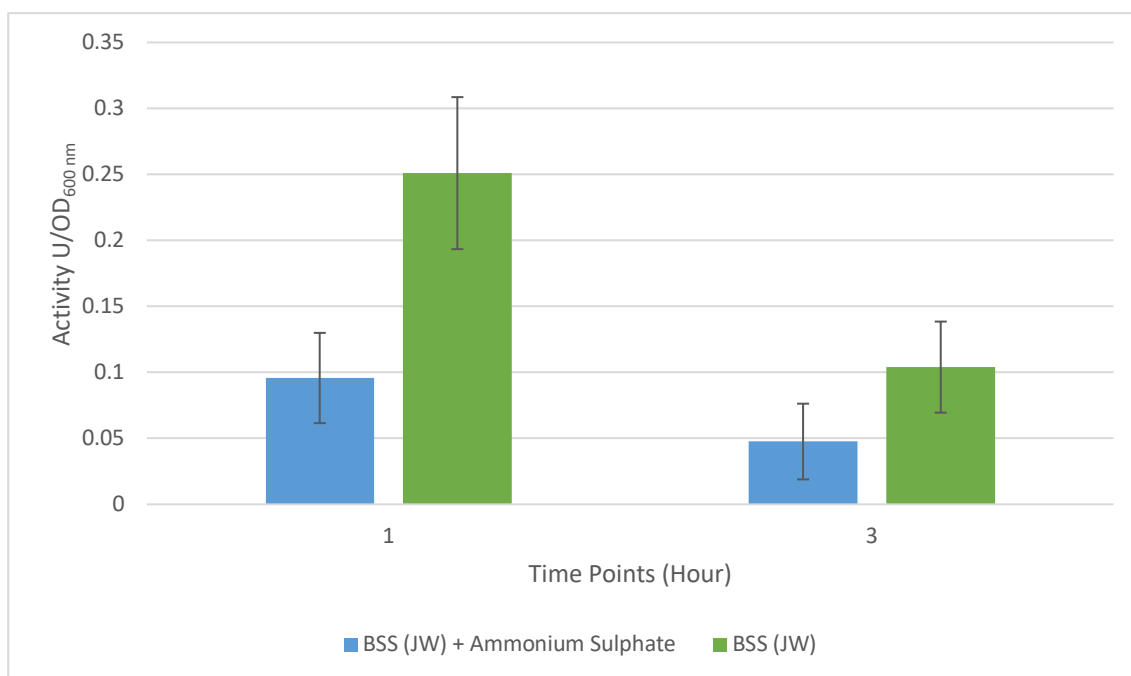


Figure 3-15. The effect of Ammonium Sulphate (nitrogen excess) on urease activity of *B. subtilis* 168.

Urease activity in four *B. subtilis* replicates cultured in a nitrogen limited media (BSS (JW)) and a nitrogen excess medium BSS (JW) + Ammonium sulphate. The data is based on 4 biological and 2 technical replicates.

3.5.1 Effect of metal ion additions on urease activity

It is understood in some species of ureolytic bacteria, that Ni^{2+} is not always the known cofactor of urease or in fact the only metal cofactor. The assembly and activation of the metalloenzyme requires a complex maturation machinery and in most cases involves several accessory proteins. The accessory proteins facilitate the incorporation of Ni^{2+} ions into the metalcentre. As

previously stated, there is evidence that some ureases are activated by other divalent metals. A close relative of *B. subtilis*, *Bacillus paralicheniformis* incorporates an iron-urease (Liu *et al.*, 2017) and Carter *et al.* (2011) describes how the gut pathogen of ferrets, *Helicobacter mustelae* combines a distinct iron-dependent urease (Figure 1-6) in addition to its archetypical Ni²⁺-containing enzyme (Carter *et al.*, 2011). With this knowledge it was important to investigate the effect of iron upon urease activity in *B. subtilis* 168. The media already contains a minimal amount of iron, as iron chloride.

In *S. pasteurii*, Zn²⁺ is needed for urease activation as the accessory protein UreG binds a maximum of 4 Ni²⁺ and 2 Zn²⁺ ions per homodimer, and the affinity for Zn²⁺ is 10-fold higher than for Ni²⁺ (Zambelli *et al.*, 2005a). If this was true for *B. subtilis* then an increase in urease activity may be seen when Zn²⁺ is added. With this in mind Moncrief *et al.* (1997) explain that the urease accessory complex UreDFG – apoprotein is inhibited by zinc, copper and cobalt (Moncrief and Hausinger, 1997). Carter *et al.* (2009) identified pretreating urease apoprotein with zinc, copper, cobalt and manganese led to the inhibition of the carbon dioxide and Ni²⁺ dependent activation. Magnesium and calcium ions had no effect on the activation process of urease (Carter *et al.*, 2009).

Previous experiments have identified that the addition of Ni²⁺ to *B. subtilis* growth conditions does not increase urease activity (Kim, Mulrooney and Hausinger, 2005a). The addition of other metal ions to the growth media and their effect on urease activity has not been ascertained in *B. subtilis*. As the activation of *B. subtilis* urease is unknown, it was decided to supplement the growing conditions with various divalent metal ions to determine their effect on urease activity.

The growth media BSS (JW) already contained certain metal ions. It was altered (see Table 2-4) to contain increased manganese or iron, as these ions are normally present in BSS (JW) at 1 mg/L this was increased to 2 mg/L which is in excess of normal BSS (JW) conditions. Zinc is not present in the media nor in any supplements and so was added at the same concentration 2 mg/L Table 2-4. Cells were harvested at end exponential and the enzyme assay carried out using 50 mM HEPES.

The addition of iron and manganese ions to the culture medium barely altered the effect on urease activity (Figure 3-16) at approximately 0.2 U/ OD. However, the addition of Zn^{2+} to the medium almost halved urease activity when compared to the normal BSS (JW) 0.13 U/OD (Figure 3-16). The activity may have been partially inhibited due to the binding of the incorrect metal cofactor to the active site, possibly in accordance with the Irving Williams series, as described in 3.3.1. As Foster *et al.* (2014) explain competitive metals must be kept out of the binding sites of the weaker binding sites, *in vivo* this is easier to achieve as the environment is more controlled (Foster, Osman and Robinson, 2014). As proteins are not rigid, their interactions with metal cofactors is not always correct and mismetallation can exploit certain ligands and even distort the native binding geometry. As Foster *et al.* (2014) stated, a protein will be inactive if one or more residues of an active metal site recruit incorrect metal ions via a more competitive metal creating an alternative geometry rendering the enzyme inactive.

Zn^{2+} is not present in the BSS (JW) media and the addition of 2 mg/L may have over saturated the urease system; perhaps causing some incorrect metalation. Ultimately, none of the metal additions increased urease activity in *B. subtilis* 168 in the first few hours of the enzyme assay.

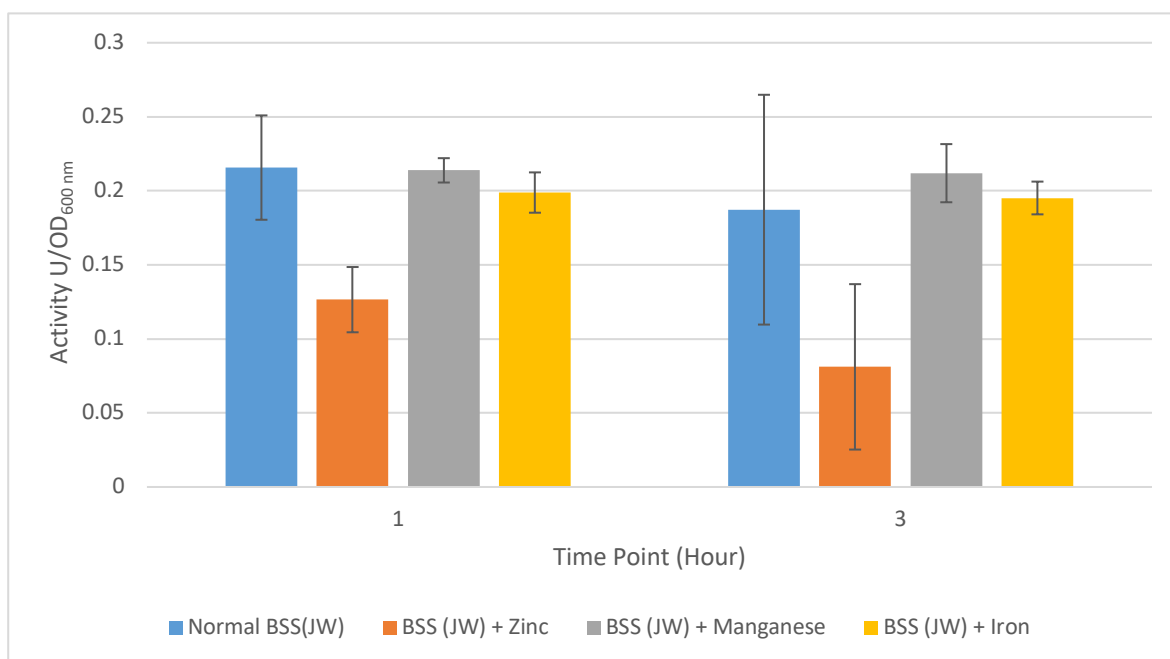


Figure 3-16. Addition of Zn^{2+} (2 mg/L), Mn^{2+} (2 mg/L) and Fe^{2+} (2 mg/L) to BSS (JW) to determine the effect on urease activity in *B. subtilis* 168.

Urease activity was determined in triplicate cultures of *B. subtilis* 168 cultured in BSS (JW) with extra divalent metals added (Zinc, Manganese and Iron). Cells were harvested at end exponential OD. Urease activity is still greatest in the normal condition, however very similar at 1 and 3 hour time point to the additions of manganese and iron. Zinc additions always indicate lower in activity than the normal. Data is based on 3 biological and 2 technical replicates.

3.5.2 Cell free extract (CFE) and urease activity

It was imperative to deduce whether results from the whole cell assay were higher at end exponential due to cell lysis produced by the growth phase or if indeed, urease activity was greatest at this phase. A CFE method would confirm this detail of urease activity in *B. subtilis*. As mentioned in the introduction, results from whole cells assay are significantly influenced via several cell mechanisms such as transportation e.g. of urea into the cells and ammonium out. Therefore, using CFE in an enzyme assay is another way to understand true urease activity, i.e. the rate of NH_4^+ produced due to enzyme activity. However, many factors could have an impact on the CFE leading to the various outcomes of the assay such as sample preparation methods particularly the sonication method. The CFE assay method was optimised and then used as a reliable method for future use in this study.

3.5.2.1 Effect of Sonication on urease activity

The aim of optimisation was to develop a method that is capable of breaking down the cell wall without inactivating the enzyme. To optimise the urease assay using CFE, we tested different sonication methods (Table 2-2) to lyse cells after they were harvested, and assessed the impact of each method on the urease activity. Methods utilised for cell disruption and protein release include; sonication, homogenisation, bead milling and nebulisation (Özbek and Ülgen, 2000). The use of a French pressure cell is the preferred method for lysing *B. subtilis* cells (Nakayama *et al.*, 1978; Marty-Mazars *et al.*, 1983), however sonication is also described as a preferred disruption method by others (Fisher and Wray, 2002; Kim, Mulrooney and Hausinger, 2005a), but rarely are the exact details defined.

Optimisations of frequency were necessary as sonication could conceivably disrupt the enzyme. LB media is one of the preferred culture conditions for *B. subtilis*, as it contains all necessary nutrients and produces a high yield in a short amount of time. In comparison, BSS (JW) does not produce a high yield of cells. Therefore, although the urease activity is known to be low in LB media it was decided to culture in LB to produce a high cell density and try various sonication frequencies followed by the enzyme assay.

Various sonication frequencies were therefore implemented to lyse the cells and then the consequential CFEs were used to test urease activity in *B. subtilis* cultured in LB. Figure 3-17 shows urease activity of *B. subtilis* using CFE prepared at different sonication frequencies. There was a clear impact of the sonication frequency upon urease activity. High frequency sonication (13 KHz) and mid frequency (6 KHz) produced far less urease activity (75% and 50% less respectively) when compared to the lower frequency (3 KHz). There are two potential reasons for this: 1) urease is a multisubunit complex enzyme, and the sonication at higher frequencies may have disturbed the folding of the holo enzyme and, 2) the Ni^{2+} was not bound sufficiently to the apoenzyme. Literature has documented the impact of sonication on enzyme stability (Özbek and Ülgen, 2000). One such impact is the rate of release of an enzyme, which is described as following first order kinetics. However, the rate of release of an enzyme by disruption, is dependent on the location of the enzyme in the cell. Those enzymes located in the membrane are

released slowly, whilst those, such as urease in the cytoplasm are released instantly into the surrounding buffer (Özbek and Ülgen, 2000). Various other factors can affect enzyme stability upon sonication, such as the sonication time, fluid viscosity, shear field forces and cavitation (Tarun, Metelitsa and Adzerikho, 2003; Islam, Zhang and Adhikari, 2014). However, these are specific for each enzyme. It is thought shear field forces within the fluid can have the greatest impact. Therefore, the large, cytoplasmic urease will be likely be affected by sonication. The effects would be to the protein structure or its ability to become active by disturbing the method of activation via Ni^{2+} binding, especially if Ni^{2+} was bound loosely.

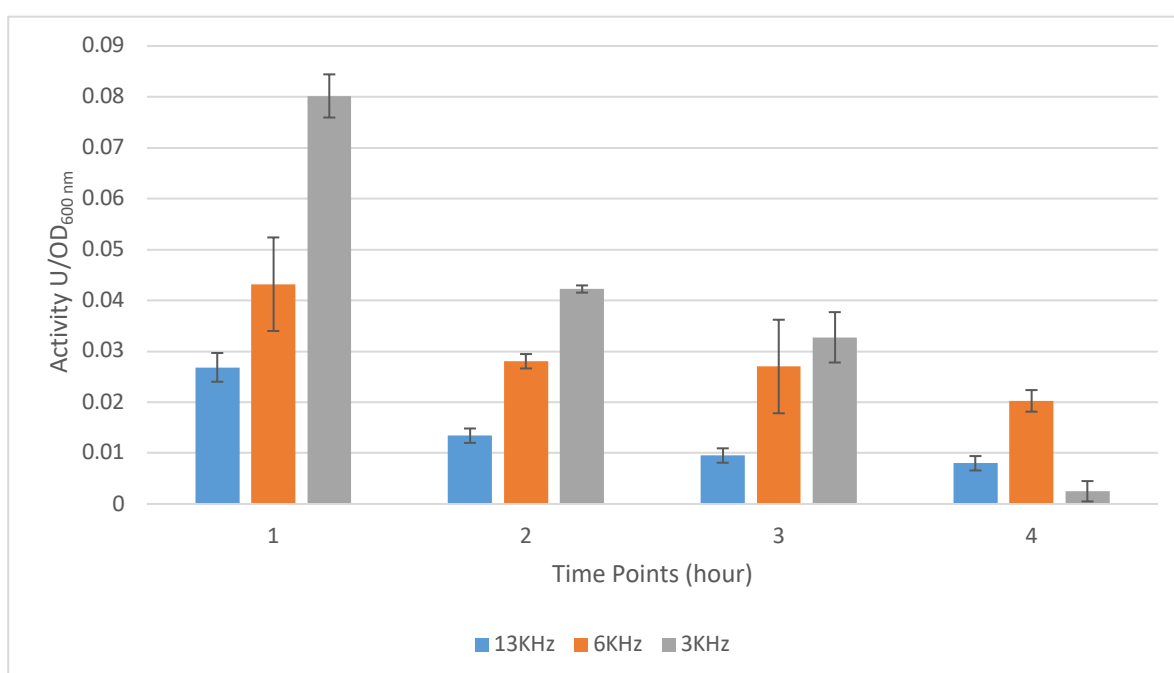


Figure 3-17. Urease activity of *B. subtilis* 168 using CFE prepared under various sonication frequencies.

B. subtilis cells were cultured in LB and harvested and CFE produced following method Table 2-2. Three sonication frequencies (13, 6 and 3 KHz) were tested with the CFE, the highest frequency that displayed urease activity was 3 KHz. Data is based on 3 biological and 2 technical replicates.

Following these tests 3 KHz sonication for 1 minute with 10 sec on and 10 sec off was identified as the optimum frequency to be applied to *B. subtilis* cells for preparation of cell lysate in the future studies.

3.6 Difference between Urease Assays using Whole Cell and CFE

Once optimum sonication frequency was attained, a method to prepare CFE could be composed to determine urease activity. A culture of *B. subtilis* was grown to optimum OD approximately

OD_{600 nm} 1.5 for urease expression, cells were then harvested and washed in HEPES buffer. Of the cell suspension 20 ml was used in urease assay using the whole cell, whilst the remainder was utilised in urease assay using CFE. Both WC and CFE enzyme assays were considered as the WC assay will take into account the transport of the substrate in and out of the cell whereas this is not considered in the CFE assay so the reaction rate may differ. Figure 3-18 and Figure 3-19 detail urease activity in CFE and WC respectively from the same sample. Urease activity in WC tests is described as NH₄⁺ production per OD or for CFE tests as NH₄⁺ production per mg. The results indicated a very similar urease activity trend. This confirmed the CFE method was also suitable for urease activity determination.

Figure 3-18 shows activity of *B. subtilis* urease at 1 and 3 hour time points. Urease activity is approximately 0.25 U/mg at 1 hour. This can be compared to the activity of *B. subtilis* urease determined by Kim *et al.* (2005). The activity in this work is higher than that produced by Kim *et al.* (2005) at 0.113 U/mg protein. An important note to make is that Kim *et al.* utilised the growth media MM S7 with *B. subtilis*. This MM consists of 100 mM morpholinepropanesulfonic acid (MOPS), 10 mM (NH₄)₂SO₄, 5 mM potassium phosphate (pH 7.0), 2 mM MgCl₂, 0.9 mM CaCl₂, 50 µM MnCl₂, 5 µM FeCl₃, 10 µM ZnCl₂, and 2 µM thiamine-hydrochloride (Saggese *et al.*, 2018) plus 0.2% (w/v) glutamate (Kim, Mulrooney and Hausinger, 2005a). This media is similar in its metal additions and GA supplementation to BSS (JW) however the addition of (NH₄)₂SO₄ in the S7 media creates a media that will be more nitrogen rich than BSS (JW) and so urease activity (U/mg) would be lower in this media. As Kim *et al.* discuss, the process to extract the protein will have included sonication of *B. subtilis* cells. The paper does not identify a specific frequency for sonication. As in Figure 3-17 the sonication frequency implemented may also incur a decrease in urease activity, which may also be why their U/mg differs from this research.

These results show that CFE assay Figure 3-19 and WC assay Figure 3-18 are consistent and reliable results. The CFE assay also shows urease activity is not affected by the process to produce the CFE for analysis.

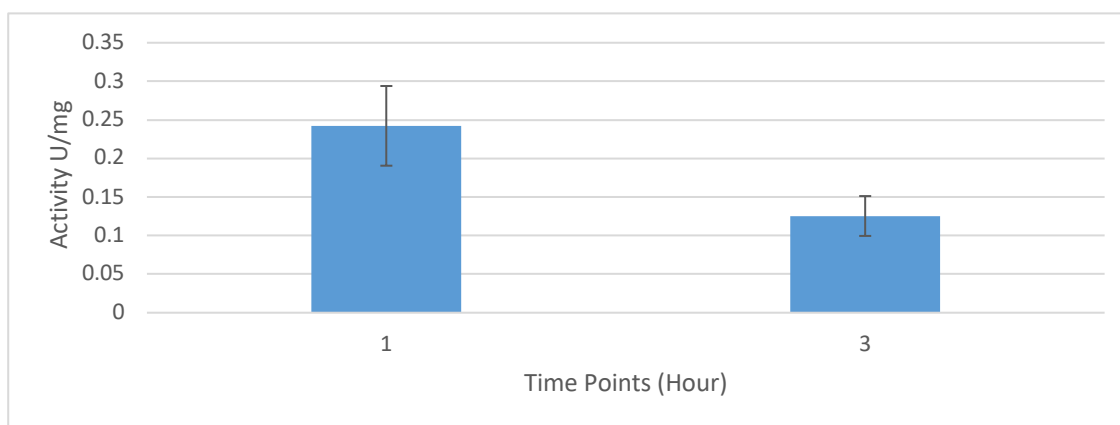


Figure 3-18. Urease activity of *B. subtilis* 168 in CFE from sample also analysed for activity in whole cells.

Data is based on 4 biological and 3 technical replicates.

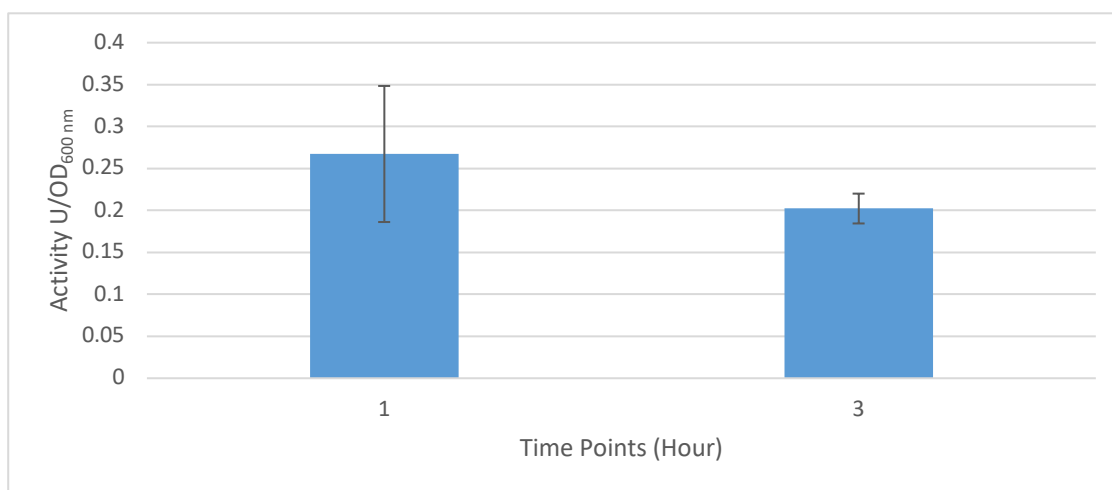


Figure 3-19. Urease activity of *B. subtilis* 168 in whole cells from sample also analysed for activity in CFE.

Data is based on 4 biological and 3 technical replicates.

3.6.1 Effect of pH on urease activity in *B. subtilis*

The pH of the environment can greatly affect urease activation in some bacteria such as *S. salivarius*. The effect of pH on *B. subtilis* urease has not been investigated. We know *B. subtilis* does not possess *ureI* which is often present in the genome of those bacteria which are activated by pH, however there may be another mechanism in *B. subtilis* which acts upon low pH. Acid activation of urease has been well studied in some bacteria for example *Helicobacter pylori* and other ureolytic species (Jones, Li and Zamble, 2018; Young, Amid and Miller, 1996). In understanding the role of urease expression and regulation, determining urease activity of *B. subtilis* 168 in acidic conditions was imperative to the research so we could determine a

mechanism of activation. *B. subtilis* 168 was cultured at two acidic pH conditions (pH 5 and pH 6) which would sustain growth and so the growth was monitored following the methods shown in 2.1.9. As shown Figure 3-20, the growth in the more acidic conditions achieved end exponential growth earlier than pH 7. The pH of an environment can greatly affect bacterial growth, as change to bacterial growth is largely based on the nature of the proteins of the bacterium. The pH will also affect microbial processes, for example microbial respiration which catalyses redox reactions in order to synthesize ATPs. The bacterium was able to grow at both pH 5 and pH 6, reaching a similar OD to those cultured in pH 7 and so the growth on pH 5, being the lowest pH tested, was used for the urease assay to ascertain acid activation of urease in *B. subtilis*.

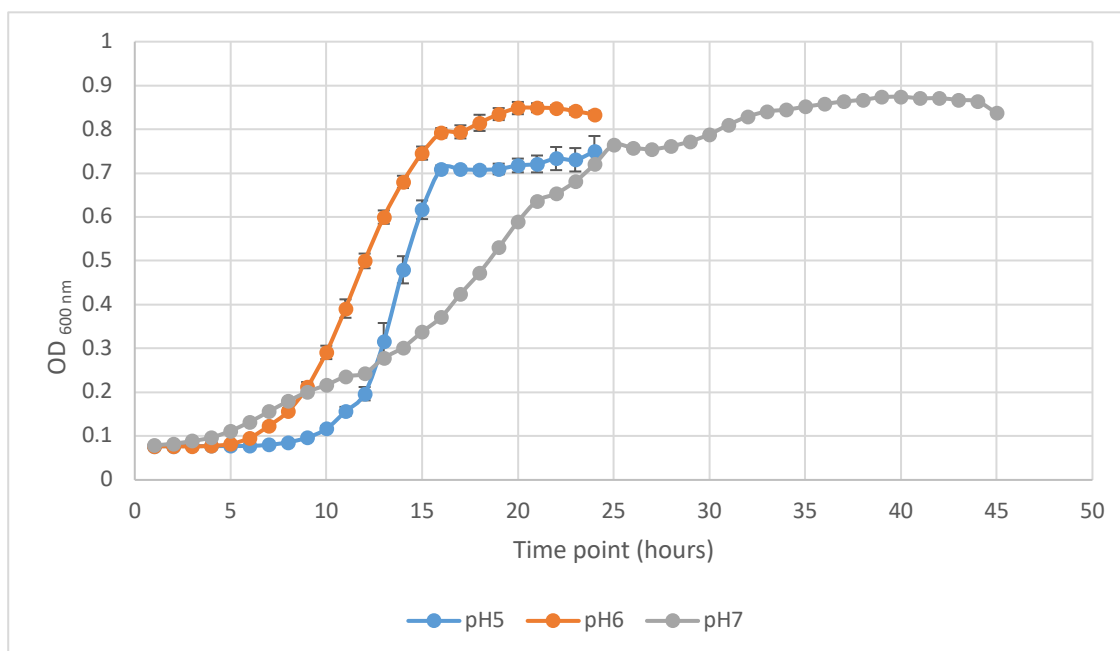


Figure 3-20. Growth of *B. subtilis* 168 in BSS (JW) media over approximately 20-45 hours under different pH conditions.

B. subtilis cultured at pH5, pH6 and pH7 using Biotek Synergy plate reader at 30°C medium shaking over 20+ hours. Bacterial cells in the more acidic pH (pH 5 and 6) enter stationary phase approx. 10 hours prior to those cells cultured at pH7. Data is based on 4 biological and 2 technical replicates.

Urease activity from those cells cultured at pH 5 and pH 7 is detailed in Figure 3-21. There is a difference in urease activities of the two pHs. The lower pH (pH5) produces lower urease activity (0.15 U/OD) compared to pH 7 (0.22 U/OD) on average. This data suggests urease activity in *B. subtilis* is not regulated via acidic pH conditions and therefore not an acid activated urease.

Although activity is lower in pH 5, it is not markedly lower. However, the low pH may inhibit the expression of urease in *B. subtilis* at or indeed, the activation. Proteomics data (Appendix) also confirmed urease activity was downregulated in the more acidic condition when compared to pH 7.

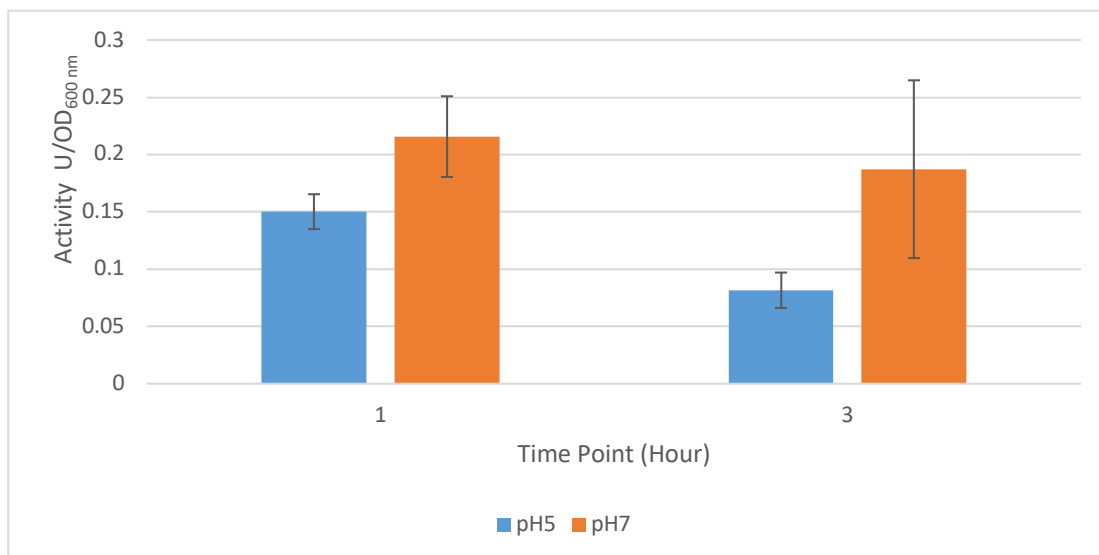


Figure 3-21. Urease activity of *B. subtilis* 168 in whole cells at pH 5 and pH 7.

Comparison of urease activity in *B. subtilis* 168 cultured in BSS (JW) at pH 5 and pH 7. Activity is slightly greater at pH 7 however when considering the deviations they are quite comparable. Data is based on 4 biological and 2 technical replicates.

Optimal urease activity therefore differs not only from microbe to microbe, species to species but also regulation and environments play huge roles in the activation of this enzyme. Therefore, any buffers used in this research would need to be investigated thoroughly before use. These buffers are discussed in more detail in chapter 4 (4.2.1.1).

3.6.2 Summary

The aims of this chapter were to define a MM which was suitable not only for the cultivation of *B. subtilis* 168 but also promoted urease activity and then use a suitable enzyme assay to detect urease activity. The defined medium would include a suitable limited nitrogen source as urease activity in *B. subtilis* has been identified as increased in NLC. The media would also enable the control of urease activity by controlling the nitrogen source. A further minimal media would need to be developed to use as a comparative for the proteomic study on the differentially expressed proteins which potentially are involved in the activation of urease.

Various media were investigated however, BSS (JW) was chosen as it was the most minimal media which could be designed with optimisations 2.5.4.4 containing the favored nitrogen source of *B. subtilis* in its ionic form but in limitation along with the necessary amino acid tryptophan (Zeigler *et al.*, 2008). Growth analysis of this newly defined media was utilised to determine urease activity at both mid exponential and late exponential growth phases. Urease activity was demonstrated to be higher at end exponential as shown in Figure 3-11, confirming the work of Fisher *et al.* (1999) whereby urease activity was also deemed optimum at the end exponential growth phase. The optimisations of both enzyme assays produced a robust and reliable assay for use throughout the research and all assays afterwards were performed using cells or CFE harvested at end exponential.

Then the impact of nitrogen level and source on urease activity were tested using this BSS (JW) as control conditions. As stated NLC increase urease synthesis in *B. subtilis* (Brandenburg *et al.*, 2002a; (Cruz-Ramos *et al.*, 1997), therefore, with the increase of the nitrogen level, the urease expression should be decreased. Although changing the concentration of glutamic acid did not change the nitrogen level (Figure 3-14), the addition of ammonium sulphate in BSS (JW) has shown an increase in urease activity Figure 3-15 . The urease activity values are of interest as Kim *et al.* (2005) determine urease activity in *B. subtilis* to be low but detectable at 0.113 U/mg. This value is more comparable to the urease activity in this research of the ammonium excess media, which when investigated Kim *et al.* (2005) growth media (S7) included not only 0.2% (w/v) glutamate but also 10 mM (NH₄)₂SO₄. Based on these results, we concluded that BSS (JW) would be considered nitrogen limited which was essential, and the base BSS (JW) with the addition of 20 g/L ammonium sulphate created a nitrogen excess media compared to BSS (JW). This nitrogen 'excess' media (BSS (JW) + ammonium sulphate) was not only essential in confirming the nitrogen limitation hypothesis but would also be necessary for future proteomic approaches of the research. The two media would enable the identification of how urease is activated and regulated in *B. subtilis* by identifying proteins of interest which could then be investigated further.

The work also included the necessity of a suitable enzyme assay to determine urease activity in *B. subtilis*. The enzyme assay utilised Nessler reagent which was identified as the preferred spectrophotometric method from the literature (Zhao *et al.*, 2019b; Mobley and Hausinger, 1989). WC assays were optimised as described in 2.5.6.5 according to volumes used. It was also determined that urease activity was greater at end exponential compared to mid exponential. However, much optimisation was needed for CFE assays, as described in 2.5.7.3. This included the increased biomass, using 4 x 500 ml resuspended in a final volume of 5 ml. The effect of sonication had great impact on urease activity and results from Figure 3-17 determined 3 KHz was optimum. Various metal additions (Figure 3-16) and pHs (Figure 3-17) of the growth media in *B. subtilis* were also investigated in order to increase urease activity, however very little change was determined. In fact, the addition of increased Zn^{2+} showed a decrease in urease activity and the growth of *B. subtilis* in lower pH conditions did not affect urease activity greatly. Various additions of GA were also added to BSS (JW) in order to determine the effect on urease activity, however all 3 conditions were comparable detailing the 'normal' GA concentration already present as a constituent of BSS (JW) was low enough to produce a NLC. The production of the 2nd medium, BSS (JW) + Ammonium sulphate was necessary as this detailed a marked difference in urease activity confirming urease activity is increased under NLC, as detailed in the literature.

The aims and objectives of this chapter laid the foundations of the methods required for the research in this thesis. The designing of a robust media for cultivation and urease expression and a reliable enzyme assay was essential in order to enable consistent data production in understanding urease activation in *B. subtilis*.

**Chapter 4 A proteomics
approach to understanding
the activation and
regulation of *B. subtilis*
urease in nitrogen limiting
conditions.**

4.1 Introduction

Transition metals are essential for enzyme activity but can be limited in the environment which lead to the evolution of mechanisms for metal ion sensing and utilisation. Metal-dependent transcription factors recognise changes in metal ion concentrations and produce appropriate cellular responses. These responses regulate metal ion homeostasis and metalloenzyme activation. The ions can induce toxicity effects within the cell and so regulated intracellular trafficking of the ions is carried out by specific chaperones. Bacterial cells make use of Ni²⁺ chaperone/storage histidine proteins *via* different Ni²⁺ metalloenzyme biosynthetic systems.

4.1.1 Nickel and urease activation

Urease activation is discussed in 1.3.3.2, which identifies the importance of Ni²⁺ binding accessory proteins involved in the maturation process. The Ni²⁺ binding is via specific protein-protein interactions which avoids the toxic release of the metal into the cytoplasm. Guanosine triphosphate (GTP) hydrolysis plays a role in this sequential binding via conformational changes and thus regulating the binding/release of the Ni²⁺ in forming the active enzyme.

4.1.1.1 UreD

UreD is the least characterised of the accessory proteins, as UreD and its *Helicobacter* homologue UreH is a relatively insoluble protein which binds directly to urease but is not competent for urease activation without the other accessory proteins (Carter and Hausinger, 2010). Despite the insolubility researchers have overcome this issue in *K. aerogenes*. A maltose-binding protein (MBP) fusion variant of UreD is soluble and has been shown to functionally replace UreD (Carter and Hausinger, 2010). In the case of *H. pylori ureH*, solubilisation is achieved by coexpression with *ureF*, which provides a UreH:UreF complex (Fong *et al.*, 2011). UreD has been identified as a scaffold protein in the complex for recruiting other accessory proteins and a direct facilitator of Ni²⁺ insertion into the active site. Studies have provided experimental evidence for a Ni²⁺ transport channel through UreD, identifying its unique role in supplying Ni²⁺ to urease apoprotein (Farrugia, Macomber and Hausinger, 2013).

4.1.1.2 UreF

UreF, like UreD is insoluble when overproduced alone, leading to difficulty in characterising this protein. Although heterologous expression of UreF is insoluble, research using UreF of *K. aerogenes* enables a soluble product when synthesised with MBP-UreF (Carter and Hausinger, 2010) and UreE-UreF (Farrugia, Macomber and Hausinger, 2013) fusion proteins. UreF binds to the UreD: UreABC complex and acts as a GTPase modulator to the GTPase UreG (Boer *et al.*, 2010). UreF appears to gate the GTPase activity of UreG so as to promote efficient coupling of GTP hydrolysis and metallocentre biosynthesis, thereby enhancing the fidelity of urease activation.

The C-terminal tail of *H. pylori* UreF contains highly conserved residues, detailed in Figure 4-1, which were shown to be essential for the interaction with UreD, the assembly of an activation complex and urease activation (Fong *et al.*, 2011; Kim, Mulrooney and Hausinger, 2006). Upon binding to UreD, the C-terminal residues become structured and form an extra helix-10 and a loop structure stabilized by hydrogen bonds involving a conserved Arg-250 residue (Fong *et al.*, 2011; (Nim and Wong, 2019). The crystal structure of the *H. pylori* UreFD complex revealed it is a heterodimer with UreF in the middle, providing the dimerization interface as detailed in Figure 4-1. These conformational changes were shown to be important for recruiting UreG to form the UreGFD complex by mutagenesis studies.

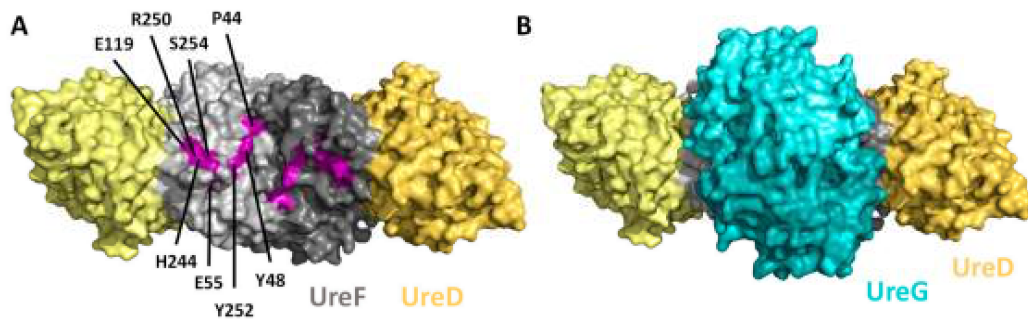


Figure 4-1. Conformational changes in UreF recruit UreG to the UreGFD complex in *H. pylori*.

A. Crystal structure of UreFD where a saddle like structure is formed at the UreF dimer surface. The essential residues of UreF are detailed. B. Crystal structure of the UreGFD complex. UreG is bound to the saddle like structure of UreF. (Nim and Wong, 2019)

4.1.1.3 UreE

In urease activation, UreE is the metallochaperone which binds Ni^{2+} with high affinity and enables the incorporation of two adjacent Ni^{2+} in the active site of urease. Most UreE contain a histidine-rich C-terminal motif that is concerned with binding Ni^{2+} which consists of distinct peptide-binding and metal-binding domains (Brayman and Hausinger, 1996). Homologues of UreE are conserved in almost all urease-producing bacteria and partial deletions creates reduced urease activities in *K. aerogenes* (Mulrooney, Ward and Hausinger, 2005) or abolished urease activity in *H. pylori* (Benoit *et al.*, 2007; Volland *et al.*, 2003) which could be partially restored by adding Ni^{2+} . The results from the various research groups proposed that UreE was not essential to urease activation but facilitated the process.

According to Zambelli *et al.* (2013) UreE of *S. pasteurii* includes binding sites where 2 Ni^{2+} binds via a high affinity site which includes the conserved solvent-exposed His¹⁰⁰ and the C-terminal His¹⁴⁵. The low affinity site includes the binding site C-terminal His¹⁴⁷. They identified zinc (Zn^{2+}) binding to UreE in the same regions and with similar affinity as Ni^{2+} , which caused dimerization of the protein, however metal ion experiments with different metal ions detailed the high affinity binding sites preferentially bound Ni^{2+} to Zn^{2+} (Zambelli *et al.*, 2013).

4.1.1.4 UreG

The urease accessory protein UreG is a Signal Recognition Particle (SRP), MinD, and BioD (SIMIBI) type nucleoside triphosphate-binding protein involved in the regulation of Ni^{2+} delivery.

This family is an ancient subfamily of nucleotide binding proteins which are involved in numerous cellular processes. This class of protein mainly includes ATPases and GTPases. The GTPases are a superfamily of proteins that provide the molecular switches to regulate a number of cellular processes (Shan, 2016) and SIMIBI GTPases are often regulated by dimerization (Fong *et al.*, 2013b). The GTPase activity of UreG is essential for urease maturation, as findings show the replacement of the GTPase P-loop motif or the nonhydrolyzable GTP analogue during urease activation results in a non-active urease (Shan, 2016).

UreG proteins contain a metal binding invariant motif: Cys-Pro-His (Figure 4-2). If this motif is substituted then there is complete abolition of urease maturation, as seen in *K. aerogenes* (Boer *et al.*, 2010). It is understood from suggested maturation mechanisms that UreG interacts with UreE incorporating nickel into the urease nickel metallocentre (Shi *et al.*, 2010; Song *et al.*, 2001). The process of urease maturation requires GTP hydrolysis, which is thought to be catalysed by UreG.

SpUreG	----MKTIIHLGIGGPGVSGKTTLVKTLSEALKEEYSIAVITNDIYTREDANFLINENILE
HpUreG	-----MVKIGVCGPVGSGKTALIEALTRHMSKDYDMAVITNDIYTKEDA EFMCKNSVMP
KaUreG	MNSYKHPLRVGVGGPVGSGKTALLEALCKAMRDWQLAVVTNDIYTKEDQRILTEAGALA
PmUreG	MQEYNQPLRIGVGGPVGSGKTALLEVLCKAMRDSYQIAVVTNDIYTQEDAKILTRAQALD
	:.:*: *****:*.:. * : . :.:**:*:*:*.* ** : :
SpUreG	KDRIIGVETGGCPHTAIREDASMNFEAIEELKNRFDLDLEIILLESGGDNL SATFSP ELVD
HpUreG	RERIIGVETGGCPHTAIREDASMNLEAVEEMHGRFPNLELLLI ESGGDNL SATFNPELAD
KaUreG	PERIVGVETGGCPHTAIREDASMNLAAVEALSEKFGNLDLIFVESGGDNL SATFSP ELAD
PmUreG	ADRIIGVETGGCPHTAIREDASMNLAAVEELAMRHKNLDIVFVESGGDNL SATFSP ELAD
	:**:*
SpUreG	AFIYVIDVSEGGDIPRKGPGVTRSDFLMVNKTELAPYVGVLDLTMKNDTIKARNGRPFT
HpUreG	FTIFVIDVAEGDKIPRKGPGITRSDLLVINKIDLAPYVGADLKV MERDSKKMRGEKPF I
KaUreG	LTIYVIDVAEGEKIPRKGPGITKSDFLVINKIDLAPYVGASLEVMASDTQRMRGDRPWT
PmUreG	LTIYVIDVAEGEKIPRKGPGITHSDLLVINKIDLAPYVGASLEVM EADTAKMRPVKPYV
	::*:*:*.* .*****:*.***:*:*:*:* :*****.*.*.* * : . * .*:
SpUreG	FANIKTKKGLDEIIAWIKSDLLLEGKTNESASESK
HpUreG	FTNIRAKEGLDDVIAWIKRNALLED-----
KaUreG	FTNLKQGDGLSTIIAFLEDKGM LGK-----
PmUreG	FTNLKEKVGLETIIDFIIDKGM LRR-----
	::. ** . : * : : . : *

Figure 4-2. UreG protein sequences of various bacteria.

Protein sequences of UreG in *S. pasteurii* (SpUreG), *H. pylori* (HpUreG), *K. aerogenes* 9KaUreG) and *P. mirabilis* (PmUreG) 'CPH' metal binding motif highlighted.

Studies therefore suggest that UreG, UreF and UreD are required for urease maturation, while UreE facilitates the process. The molecular functions and biological processes associated with urease accessory proteins are detailed in Table 4-1.

Table 4-1 Molecular functions and biological processes associated with urease accessory proteins including Gene Ontology (GO) terms associated with each function and process

Molecular Function	GO term	Associated Accessory Protein	Biological Process	GO term	Associated Accessory Protein
Nickel Cation Binding	0016151	UreD, UreE, UreF, UreG	Nitrogen compound metabolic process	0006807	UreD, UreF, UreG
Ammonium Transmembrane Transporter Activity	0008519	UreD	Enzyme Active Site Formation	0018307	UreE
Unfolded Protein Binding	0051082	UreE	Protein Folding	0006457	UreE
GTPase	0003924	UreG	Urea Metabolic Process	0019627	UreE
GTP binding	0005525	UreG	Protein-Containing Complex Assembly	0065003	UreE
Zinc ion Binding	0008270	UreG	Pathogenesis	0009405	UreE, UreF
Protein Homodimerization Activity	042803	UreG			
Magnesium Ion Binding	0000287	UreG			
Urease Activity	0009039	UreG			

4.1.1.5 Other accessory or associated proteins required for activation

Urease accessory proteins belonging to the UreH family are a group of Ni²⁺ specific permeases encoded in microbes such as *Yersinia pseudotuberculosis* and *Geobacillus stearothermophilus* and some *Bacillus* sp gene clusters. The assumed permease structure of these proteins consists of six transmembrane domains with the amino (N) and carboxyl (C) termini located to the outside of the cell (Eitinger *et al.*, 2005). Interestingly, the structure includes a histidine rich section between TMH (trans membrane helices) III and TMH IV. There is a conserved motif [H(A/S)X(E/D)XDH] in TMH I which corresponds to the nickel binding motif of NiCoT (Nickel and cobalt transporter family) proteins (Culotta and Scott, 2016).

The third distinct family are HupE/UreJ proteins which are assigned as nickel/cobalt permeases and are usually localized in hydrogenase (HupE) and urease (UreJ) gene clusters. Bacteria which include these proteins include *Cupriavidus metallidurans* and *Paenibacillus* sp. HupE and UreJ proteins are often produced as precursors which include an N terminal signal peptide. The proteins contain six TMHs, and like NiCoT and UreH proteins include a binding motif (HPXXGXDH). This motif is present in TMH I and is considered to be essential for metal transport (Zambelli *et al.*, 2011).

It is understood that in some species urease activation also requires proteins alongside urease accessory proteins. Transition metals such as Ni²⁺ are essential components of specific enzymes and therefore are taken up by specific transport systems. Nickel and Cobalt, which is another important co-factor in cells, often share the same binding sites and therefore transport system. They are both divalent cations and have similar protein binding affinity. In fact, there is much literature mislabelling nickel transport systems as cobalt transport system. There is also similar misannotation within the urease accessory proteins of certain bacterial strains, for example, *A. pleuropneumoniae*, which requires the putative Ni²⁺ transport proteins NikKLMQO (was formerly CbiKLMQO) for urease activation (Bossé, Gilmour and MacInnes, 2001). Rodionov *et al.* 2006, identified via *in silico* analysis that CbiMNQO and NikMNQO were the most widespread group of microbial nickel and cobalt transporters (Rodionov *et al.*, 2006). Rodionov *et al.* (2006) demonstrated in *Salmonella enterica serovar typhimurium* that significant metal

transport activity was via the basic CbiMN complex without the need of a SBP, which could also be investigated in *B. subtilis* (Rodionov *et al.*, 2006).

Chen *et al.* (2003) established that in NLCs two NikMQO like systems were now identified which were previously named UreMQO in *S. salivarius* in CbiKLMQO *A. pleuropneumoniae* and are now considered to provide Ni²⁺ for urease activation (Chen and Burne, 2003). As Rodionov explains some bacterial genomes encode no homologues of any known nickel/cobalt transporters, yet they encode Ni²⁺ dependent enzymes. Such bacteria include *B. subtilis*, *Campylobacter jejuni* and *Neisseria meningitidis*. This indicates that unknown Ni²⁺ transporters/transport systems exist in these bacteria.

Recently identified by Benoit *et al.* (2011), is the Mua protein which is an essential nickel binding protein that regulates urease activity in *H. pylori*, as it represses urease transcription when Ni²⁺ levels are elevated. This mechanism counterbalances the NikR-mediated activation of urease in *H. pylori* ensuring the presence of a high Ni²⁺ concentration, so urease activation is limited and does not lead to an increased production of detrimental ammonia (Benoit and Maier, 2011).

The literature is constantly being updated regarding novel proteins involved in urease activation. Those novel proteins are usually identified in pathogenic ureolytic bacteria (Bossé, Gilmour and MacInnes, 2001; de Koning-Ward and Robins-Browne, 1997; Benoit and Maier, 2011). The consistent updating of novel proteins involved in urease activation means there could be proteins in *B. subtilis* not annotated as such but acting as accessory proteins in urease activation. If this is true, when urease overexpresses and has increased activity then there is a significant chance that ‘accessory’ proteins would be over expressed too.

4.1.1.6 Nickel Transport

Evidence has therefore shown that some transport systems are required for urease activation and in many bacterial cells, Ni²⁺ transport is misannotated either as cobalt transport or peptide transport. Therefore, some of the ABC type transport proteins may be of interest to us.

4.1.2 Proteomics

An organism or system produces a set of proteins termed the proteome. It was Wilkins *et al.* (1995) who first used the term ‘proteome’ to describe the protein complement of the genome, “PROTein complement of a genOME.” Since the first use of this term its definition and understanding has simplified. The proteome is complex and dynamic; and will differ over time and from cell to cell within the same system, conferring dynamic scope. Proteomics is the scientific study of proteins, focusing on their roles, localisation and interactions. Modern proteomic tools enable large-scale, high-throughput analyses for the detection, identification, and functional investigation of proteome.

Proteomics approaches have been used to study various aspects in molecular microbiology, for example where and when proteins are upregulated, the rate of protein production and degradation, modification of proteins (post-translational modifications (PTMs) such as phosphorylation), how proteins move within the cell, their involvement in metabolic pathways and, essentially for this research, how they interact with each other.

Understanding the proteomics of the cell enables the researcher to be informed of what the proteins do, rather than just what proteins are being produced. Baysal *et al.* (2013) utilised a proteomics approach to determine the inhibitory effects of *Bacillus sp.* upon the cell wall of the fungal plant pathogen *Fusarium oxysporum*, as a form of biocontrol mechanism (Baysal *et al.*, 2013).

Proteomic approaches can also be used to understand cellular responses to antimicrobial compounds. Bandow *et al.* (2003) utilised proteomic techniques to determine the cellular responses of *B. subtilis* to classical and emerging antibiotic classes (Bandow *et al.*, 2003). Proteomics-based methods are therefore utilized in various capacities for different research requirements.

4.1.2.1 Challenges of Proteomics

The accurate determination of proteins of interest, such as the analysis of low abundance proteins is a definite challenge. These proteins can often be concealed due to the high concentration of other proteins present (Krasny *et al.*, 2018). Any improvements to proteomic techniques need

to consider all aspects of the process to avoid protein loss. The use of complex samples by researchers also leads to a challenge regarding the repeatability of peptide identification and also the consistency of quantification. The mass spectrometer is vital in proteomics experiments, however the results recovered can be limited by the sample quality. A high quality sample is necessary for successful proteomic experiments (Feist and Hummon, 2015).

4.1.2.2 **Proteomic methods**

There are three essential technological components when utilizing a proteomic method. This includes a method whereby the protein is fractionated, the use of mass spectrometry (MS) to collect the data to enable identification of particular or individual proteins and then bioinformatics to evaluate the MS data.

The backbone of most proteomics experiments utilises a qualitative or bottom up proteomic approach, enabling the identification of as many proteins as possible in a sample. The method flow in bottom up proteomics is to first digest the protein mixture to its peptide components. This is achieved by enzymatically cleaving the proteins using proteases into their resulting peptides. Then using liquid chromatography (LC), the peptide mixture is separated and peptides analysed by MS. In this step the peptide mixture is subjected to ms/ms fragmentation to obtain the raw ms to charge data. The final raw data enables the determination of the protein ID in the biological sample. In some cases, the bottom-up proteomics technique is also referred to as a shotgun proteomics method. The unique feature of shotgun proteomics is that it enables the identification and comparative quantification of a wide range of proteins at the same time. GeLC-MS/MS is a widely used method in shotgun proteomics. The protein mixture from a sample, often CFE, are denatured and separated using electrophoresis, then in gel digestion utilising the protease trypsin is performed. The peptides would be further separated via nanoflow HPLC, and finally analysed by MS. The resulting MS data would determine the original protein components of the sample by compared with predicted MS data derived from defined protein databases.

The alternative method is a top down proteomics approach, which consists of the intact protein being separated from the mixture before digestion and fragmentation. The method utilises an ion trapping spectrometer for mass measurement and tandem mass spectrometry analysis or other protein purification methods such as 2-D gels in conjunction with MS/MS.

The analysis and interpretation of large amounts of raw data requires various bioinformatic technologies and genomic and protein knowledge databases are essential for recording and storing this data, enabling the understanding of the proteins and their involvement in certain processes. There are databases utilised in proteomic research that collate and assemble their data from gene sequences (e.g. Ensemble) and annotation tools (e.g. Interpro). The use of these databases enables an understanding by identifying protein sequences and function, establishing protein-protein interactions, metabolic pathways and regulatory networks in which they belong.

4.1.3 Proteomic studies of *B. subtilis*

B. subtilis is a well-established model system for physiological proteomic analysis (Dreisbach *et al.*, 2008). There is much proteomic data analysis of *B. subtilis* published which details the proteins and or gene expression to understand the specific biological functions. Much research has been conducted in proteomic analysis of stress responses in *B. subtilis*, such as heat shock and general stress responses (Hecker, Schumann and Völker, 1996), glucose starvation (Bernhardt *et al.*, 2003), tryptophan and ammonium starvation (Tam le *et al.*, 2006) and salt stress (Hahne *et al.*, 2010). Research related to this thesis by Tam le *et al.* (2006) analysed the global gene expression of *B. subtilis* under tryptophan and ammonium starvation using proteomic and transcriptomic techniques. Utilising DNA microarray hybridization, mass spectroscopy (MS) and 2D gel electrophoresis their results indicated that both starvation conditions induced definitive, overlapping responses of general starvation (Tam le *et al.*, 2006).

4.1.4 Aims and Objectives

In order to understand urease activation and regulation in *B. subtilis* the work of this chapter was based on two hypotheses:

- 1) *B. subtilis* urease activity was investigated in NLCs (3.5.1) where it was demonstrated that there was a substantial increase in urease activity which was corroborated by previous research. We hypothesise that the proteins involved in urease activation in *B. subtilis* may be upregulated in this particular condition.
- 2) As detailed in the literature, some accessory proteins are involved in nickel binding (UreE) and others are associated with nickel transport (UreH and UreJ). The upregulated

proteins present in NLM which have a metal binding capacity may play an important role in the urease activation.

The research aim of identifying the activation of urease in *B. subtilis* would be determined by analysing the proteins upregulated in NLC. The proteins of interest will be investigated fully, and specific proteins highlighted for further study.

To achieve the aim of this chapter, three objectives are set as below:

- 1) Proteomic Method optimisation, which will include optimisations of protein extraction methods including specific buffers for use in both extraction and enzyme assay.
- 2) Perform reliable proteomic data analysis,
- 3) Identify specific proteins of interest from NLC which may be connected to urease activation in *B. subtilis*.

4.2 Results and Discussion

The research carried out in this chapter was to confirm urease activity was greater in NLM. We hypothesise that if urease activity is greater in NLC then those proteins upregulated in this condition may be involved in urease activation in *B. subtilis*. To test our hypothesis, we have conducted several comparative proteomics studies. Those studies initially comprised of proteomic method optimisations in order to identify the optimum buffer for protein extraction. Once a suitable buffer was identified proteomic analysis was conducted between the two nitrogen media conditions. This enabled the production of a set of data which identified those proteins upregulated in NLC in *B. subtilis* and those proteins downregulated in the said condition.

As the literature states, some accessory proteins are involved in Ni²⁺ binding. Therefore, any possible candidate genes that may be metal binding were to be investigated initially. Then any proteins whose molecular function included a transport function, permease and ATPases, see Table 4-1 were investigated.

There are numerous ABC transport systems in *B. subtilis* that transport a variety of nutrients including the *opp* and *app* and *dpp* systems. The *opp* operon, formerly Spo0K (LeDeaux, Solomon and Grossman, 1997) of *B. subtilis* encodes an oligopeptide permease that is required for uptake of oligopeptides, development of genetic competence, and initiation of sporulation.

The oligopeptide transport system belongs to the nickel/peptide/opine PepT subfamily of ABC-transporters. The *app* and *opp* systems can transport tetra and pentapeptides, however tripeptides are not transported by the *app* system. According to Koide *et al.* (1994) the *app* system can substitute completely for the *opp* system in both sporulation and competence for genetic transformation (Koide and Hoch, 1994b). Unlike the *app* and *opp* systems, the *dpp* system is not as involved in sporulation, but is linked to an adaptation in nutrient deficiency such as nitrogen (Cheggour *et al.*, 2000). The importance of highlighting these specific ABC transport systems of *B. subtilis* is because Ni²⁺ transporters can often be misannotated as simply peptide transporters, as they fall into the same family of proteins, PepT - peptide/opine/nickel ABC transporter family (Eitinger *et al.*, 2005).

4.2.1 Buffer Optimisation

Before using GELC-MS/MS a comparative method was needed to study urease activation in *B. subtilis*. Several buffers were explored to achieve the maximum protein identification and the optimum enzyme assay outcome.

4.2.1.1 Optimisation of buffer for protein extraction.

An appropriate buffered system would protect the integrity of the proteins whilst separating them from other cell components. The buffer solution would need to be compatible with urease, the pH balance must be similar to that in vivo and needs to be used at every stage from harvesting cells to the extraction of proteins. A number of buffers are routinely used with *B. subtilis* and they include Tris-HCl, HEPES-NaOH, and Sodium dihydrogen phosphate (Cruz-Ramos *et al.*, 1997; Kim, Mulrooney and Hausinger, 2005a).

The literature search of suitable buffers was narrowed to investigate three at approximately pH 7. They included Tris EDTA buffer, Tris buffered saline and 50mM HEPES (Table 2-5). Initially the buffers were tested without PMSF, then each buffer was used to harvest the cells and the cell associated proteins were extracted following the method in section 2.1.7.2. GeLC-MS/MS methods were applied to identify the proteins in each buffer choice. There were low numbers of proteins identified in each buffer condition. TBS buffer identified the maximum number of proteins, 281, in TE buffer 150 proteins were identified and 189 were identified in HEPES buffer.

After further reading it was decided that all buffers should include the addition of the protease inhibitor PMSF at 1 mM which would increase the extraction potential and avoid protein degradation (Deutscher, 1990) as shown in Table 4-2. This was confirmed via proteomics methods and a greater number of proteins were extracted (including urease structural subunits) when PMSF was added Table 4-2. PMSF is used by many to prevent protein degradation during protein extraction (Lopez, 2007; Biochemicals, 2006). PMSF has a short half-life, poor stability and solubility in aqueous solutions. Despite the disadvantages it is used routinely in urease proteomic studies at 1 mM and is also suitable for tryptic digestion at this concentration (Lerm *et al.*, 2017; Soriano, Colpas and Hausinger, 2000; Uberti *et al.*, 2013) (Yang *et al.*, 2018; Singh *et al.*, 2013; Eymann *et al.*, 2004).

Table 4-2. Comparison of different buffers with the addition of 1 mM PMSF for proteomics evaluation.

Buffer	Number of Proteins extracted
TBS + PMSF	345
TE + PMSF	181
HEPES + PMSF	255

B. subtilis 168 was cultured in BSS (JW) and harvested in each buffer (with the addition of 1mM PMSF) and a number of proteins were identified.

TE + PMSF buffer extracted the least number of proteins (181), HEPES + PMSF was second with 255 proteins identified however, TBS buffer showed a greater extraction potential (345). All buffers were used at a similar pH.

Another way of detailing the results of the protein extractions of each particular buffer can be seen from the simplified Venn diagram in Figure 4-3, which compared the proteins extracted from each buffer to a blank sample. The buffers extracted similar proteins which would be expected, importantly all urease subunits (UreABC) were identified in both TBS buffer and HEPES buffer, and only UreA and UreC were identified in TE buffer. TBS + PMSF showed a greater number of proteins extracted overall; 41.4% were also extracted with TE+PMSF and 30.8% with HEPES + PMSF. HEPES + PMSF details the second greatest number of proteins extracted; 72.2% were also extracted with TBS + PMSF and 44.4% with TE + PMSF. TE + PMSF details the smallest number of proteins extracted. Both TBS and HEPES buffer are suitable for the extraction.

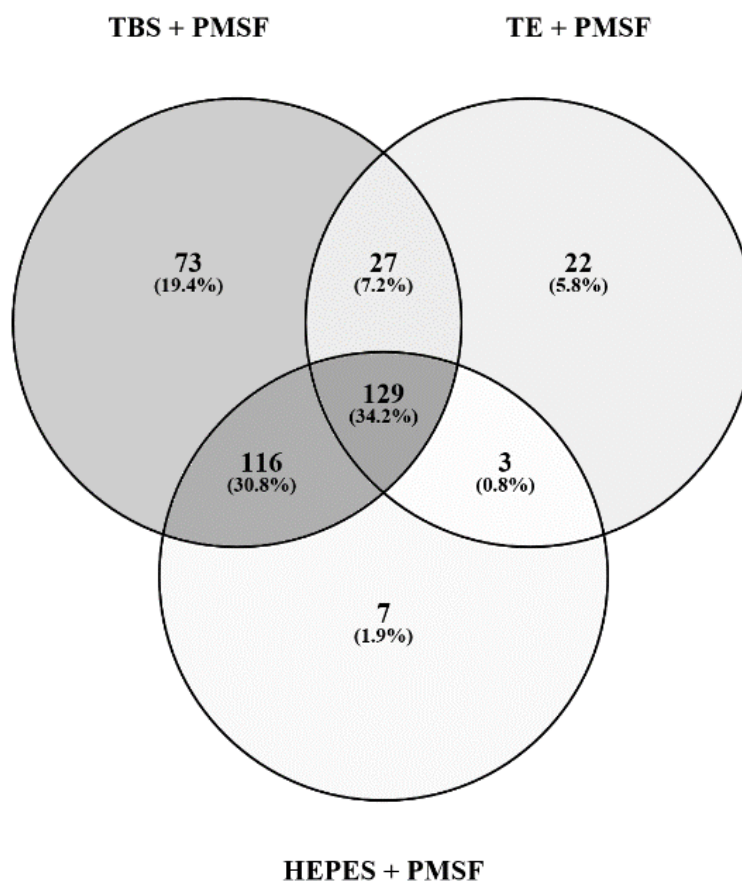


Figure 4-3. Venn diagram indicating all proteins extracted using the three buffers compared to the blank; TE, TBS and HEPES all with the addition of 1 mM PMSF.

TBS buffer identifies more proteins however, both TBS and HEPES buffers are suitable for the extraction.

4.2.1.1 Suitable Buffer for Enzyme Assay

The buffer suitable for optimum protein extraction also needed to be suitable for the urease enzyme assay. Therefore, we performed the enzyme assay using Nessler reagent and the CFE which was harvested using all the buffers listed in Table 3-2. The assay followed the methods mentioned in section 2.1.5.

As shown in Fig 4-4, CFE extracted in HEPES buffer has shown greatest urease activity compared to the other two buffers. Urease activity was 60% greater using HEPES buffer than when using TE buffer and there was 40% more activity in HEPES buffer than in TBS. The decrease in activity in TE buffer may be due to the EDTA component which is a chelating agent for divalent ions, therefore binding free Ni^{2+} in the environment.

The number of proteins expressed in the three buffers + PMSF differed, as seen in Table 4-2. TE + PMSF buffer extracted the least number of proteins (181) and also showed less activity when used in the Nessler assay (Figure 4-4). TBS buffer showed a greater extraction potential (345) and was suitable for the Nessler assay, however HEPES + PMSF was the optimum buffer for both extraction (255) and assay (Figure 4-4) and was comparable to most literature (Kim, Mulrooney and Hausinger, 2005a; Nim and Wong, 2019). Therefore, to move forward 50 mM HEPES + 1 mM PMSF buffer was applied to the comparative proteomic study.

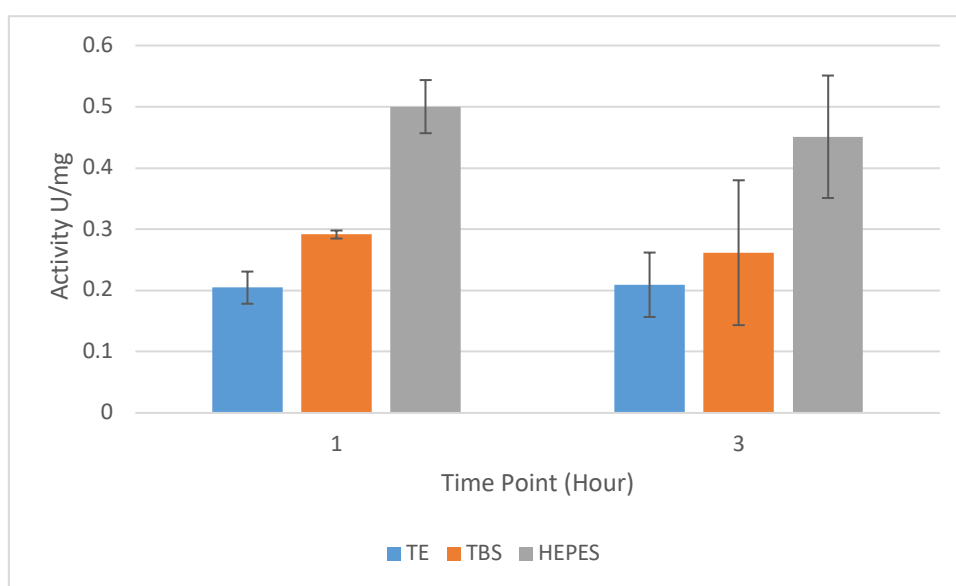


Figure 4-4. Urease activity of *B. subtilis* urease using different buffers for cell harvest.

B. subtilis 168 CFE was extracted in three buffers TE/TBS/HEPES to determine the optimum the buffer (TE/TBS/HEPES) for protein extraction and assay. The assay was performed in 5 biological and 3 technical replicates.

4.2.1.2 Effect of pH on urease activity

It was noted in the literature (and discussed in this thesis) that various conditions may activate urease expression and activity and Ugwu *et al.* (2004) stated that determining the correct buffer for the process can be challenging. The buffer should exhibit little or no change in pH with temperature, yet still have maximum buffer capacity at a pH where the protein exhibits optimal stability (Ugwu and Apte, 2004). The effect of pH on urease activity in *B. subtilis* 168 has not been clearly defined. Similar studies used HEPES buffer pH 7.8 (Kim, Mulrooney and Hausinger, 2005b). Buffer studies (section 4.2.1) in this research indicated that HEPES buffer was suitable for enzyme assays, however various buffer pHs 7.4, 8 and 10 were then investigated. The results,

as shown in Figure 4-5, detailed that urease activity was optimum between pH 7.4 – 8.0 and at pH 10 urease activity decreased. These results enabled us to use a working pH of 7.4 for HEPES buffer.

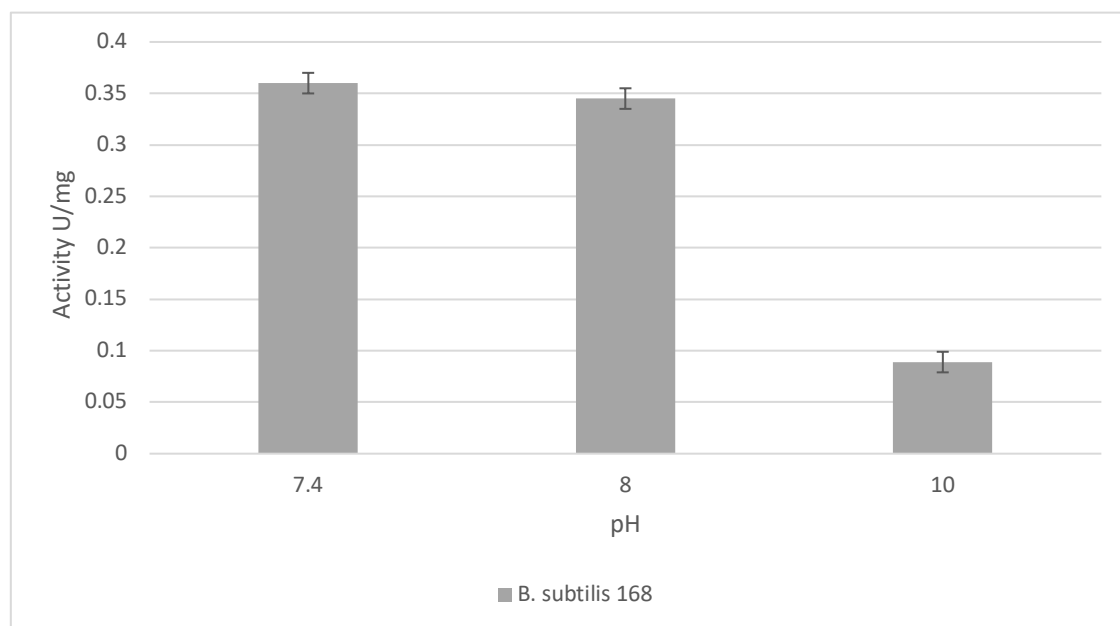


Figure 4-5. Urease activity in CFE of *B. subtilis* 168 at various pH.

Urease activity is greatly affected by the increase of pH as seen by the decrease in activity at pH 10. Data is based on 3 biological and 2 technical replicates.

4.2.1.1 COG analysis using EggNOG

The database of Clusters of Orthologous Groups of proteins (COGs) is an attempt to phylogenetically classify of all proteins encoded in 21 complete genomes of bacteria, archaea and eukaryotes (<http://www.ncbi.nlm.nih.gov/COG>). The COGs were created by applying the principle of consistency of genome-specific best hits to the results utilising a comprehensive comparison of all protein sequences in the genomes. The COG database is comprised of 2091 COGs which include 56–83% of the gene products from the complete bacterial and archaeal genomes, with approximately 35% from the genome of the yeast *Saccharomyces cerevisiae*. The COG database is also supplemented by the COGNITOR programme which enables new proteins to be added to the correct COG, so that newly sequenced genomes can be annotated functionally and phylogenetically (Tatusov *et al.*, 2000).

There are 26 functional COG categories which are determined in accordance with the cellular roles of the particular COG. An important feature of the COG approach is that a protein (or domain) either belongs or does not belong to it (Galperin *et al.*, 2019). EggNOG ('Evolutionary genealogy of genes: Non-supervised Orthologous Groups', <http://eggnoG.embl.de>) is a popular database and applies the same approach as COGs to a much greater number of genomes, but the database relies fully on the automated assignment of orthologues and does not annotate the orthologous gene clusters (Galperin *et al.*, 2019).

To determine urease activation in *B. subtilis* proteomic methods were followed. The NLM (BSS (JW) and the nitrogen excess media (BSS (JW) + Ammonium Sulphate), enabled the proteins differentially expressed in the two conditions to be investigated, initially via COG analysis which lead on to bioinformatics analysis.

4.2.2 Comparative Proteomic analysis of *B. subtilis* 168 cultured under Nitrogen limited conditions (NLC).

The use of proteomics is an effective approach for observing the responses of bacteria to stress and starvation stimuli. In this study two media: BSS (JW) and BSS (JW) + (NH₄)₂SO₄ provided the conditions for proteomic comparison of the bacterial responses of nitrogen-limited gene expression.

B. subtilis 168 was cultured in both media until end exponential approximately OD_{600nm} 1.4. Cells were harvested, in-gel digestions carried out and then the proteomes from each condition analysed by comparing the MS data for each medium with the MS data for a blank (Loading Buffer with no peptide sample). It can be seen from the simplified Venn diagram in Figure 4-6 that there are more proteins identified under 'normal' NLC compared to the media with nitrogen excess (NPM). There are 297 proteins identified in the NLM and 117 proteins identified in the NPM. There are 235 proteins that overlap both conditions.

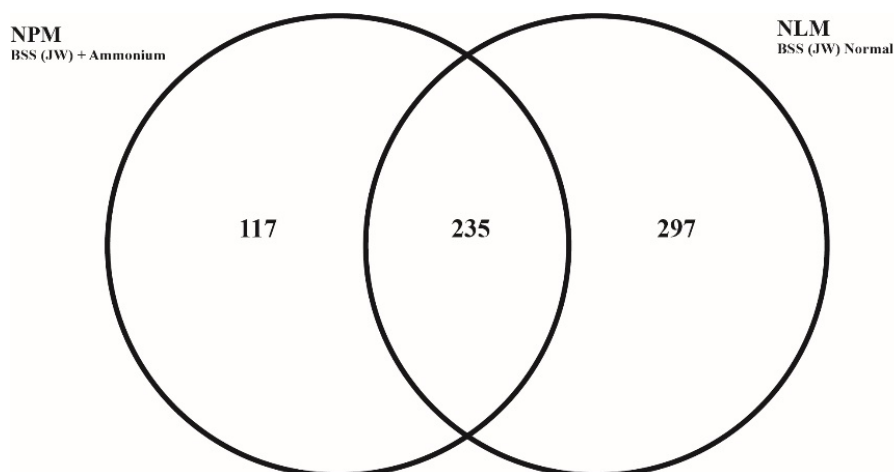


Figure 4-6. Venn diagram detailing number of proteins identified in NLM (BSS (JW)) and NPM (BSS (JW) + (NH₄)₂SO₄).

The samples were analysed using GeLC-MS/MS proteomic approach. Each condition was compared to a blank (loading buffer), to identify the proteins upregulated in that particular condition. The Venn diagram then compares those in each specific condition. This data was based on 4 biological replicates.

The differentially expressed proteins from each nitrogen condition were investigated using a comparative method through Progenesis analysis, i.e. the MS data from the NLM was compared to that from NPM. The differentially expressed proteins are defined via the initial parameters used included fold change > 3 and an annova p score <0.05. The detailed identification of the differentially expressed proteins identified fold change >3, annova p <0.05 is detailed in Table 4-3 (those upregulated of fold change < 3 see Appendix 9-1). There were 146 upregulated in NLM and 88 down regulated in NLM medium. The differentially expressed proteins were further analysed using COG analysis through EggNOG (various groups and functions are listed in Table 2-12).

Table 4-3. Proteins upregulated in the nitrogen limited condition of BSS (JW) compared to BSS (JW) + Ammonium Sulphate.

The proteins upregulated in this condition were filtered via peptide score, fold change >3 and p< 0.05. Urease subunits are highlighted red

UniprotKB	Accession	COG	Anova (p)*	Fold	Description
O34737	Probable flavodoxin 1 <i>ykuN</i>	C	1.30E-11	28.5	Probable flavodoxin
O34482	L-asparaginase <i>ansZ</i> <i>Paralogous protein: •AnsA</i>	E	0	16.73	Utilization of asparagine. Catalyses the conversion of L-asparagine to L-aspartate and ammonium.
O32144	Probable xanthine dehydrogenase subunit D <i>pucD</i>	C	0	22.83	Oxidizes hypoxanthine and xanthine to uric acid. Probable xanthine dehydrogenase subunit D.
P42432	Nitrate transporter <i>nasA</i>	x	3.05E-11	22.73	Nitrate transporter , positively regulated by TnrA under nitrogen-limited conditions
O32141	Uric acid degradation bifunctional protein <i>pucL</i>	Q	4.44E-16	18.14	Urate degradation/Purine Utilisation
P77837	Urease subunit alpha <i>ureC</i>	E	0	20.16	Urease subunit ALPHA
O32142	5-hydroxyisourate hydrolase <i>pucM</i>	F	6.99E-07	14.41	Catalyzes the hydrolysis of 5-hydroxyisourate (HIU) to 2-oxo-4-hydroxy-4-carboxy-5-ureidoimidazoline
O32060	Putative sodium/proton-dependent alanine carrier protein <i>yrbD</i>	E	8.66E-12	13.56	Putative sodium/proton-dependent alanine carrier protein
P12425	Glutamine synthetase <i>glnA</i>	E	7.77E-16	12.41	Trigger enzyme •feedback inhibition by glutamine, glutamine binds the entrance site for
Q07428	Nitrogen regulatory PII-like protein <i>nrgB</i>	E	5.95E-10	11.44	Regulation of ammonium uptake. Required for full induction of the nrgAB operon under conditions of ammonium limitation.
P42437	Uroporphyrinogen-III C-methyltransferase <i>nasF</i>	H	2.13E-03	10.57	Uroporphyrinogen methyltransferase. Nitrate Respiration.

UniprotKB	Accession	COG	Anova (p)*	Fold	Description
P24138	Oligopeptide transport permease protein <i>oppB</i> synonym <i>spo0KB</i>	P	5.84E-08	9.61	Oligopeptide ABC transporter (permease).
P42085	Xanthine phosphoribosyltransferase <i>xpt</i>	F	3.33E-16	9.34	Purine Salvage and interconversion. Xanthine phosphoribosyltransferase.
Q45604	Uncharacterized zinc-type alcohol dehydrogenase-like protein	C	1.98E-09	8.85	Similar to formaldehyde dehydrogenase. Uncharacterized zinc-type alcohol dehydrogenase-like protein
P94390	Proline dehydrogenase <i>putB</i>	E	1.08E-09	7.71	Proline dehydrogenase 2 Converts proline to delta-1-pyrroline-5-carboxylate.
O32145	Probable xanthine dehydrogenase subunit C <i>pucC</i>	C	7.05E-14	7.34	Probable xanthine dehydrogenase subunit
P00497	Amidophosphoribosyltransferase <i>purF</i>	F	3.72E-06	7.26	Amidophosphoribosyltransferase involved in purine biosynthesis.
P45744	Isochorismate synthase <i>dhbc</i>	H	3.50E-13	7.23	Isochorismate synthase. Bacillibactin biosynthesis.
P12044	N5-carboxyaminoimidazole ribonucleotide mutase <i>purE</i>	F	1.07E-09	7.05	N5-carboxyaminoimidazole ribonucleotide mutase. Purine biosynthesis
P42434	Assimilatory nitrate reductase catalytic subunit <i>nasC</i>	C	9.30E-09	6.69	Utilisation of nitrate.
O31449	Uncharacterized HTH-type transcriptional regulator <i>YbfI</i>	K	8.46E-11	6.5	Uncharacterized HTH-type transcriptional regulator
O07939	Uncharacterized protein <i>yisT</i> synonym <i>bstC</i>	S	7.56E-10	6.47	Uncharacterized protein YisT. Possible bacillithiol S-transferase
Q45666	HTH-type transcriptional regulator <i>tnra</i>	K	0.00026	6.4	Transcription regulator that activates the transcription of genes required for nitrogen assimilation

UniprotKB	Accession	COG	Anova (p)*	Fold	Description
O06736	Probable sulphate adenylyltransferase <i>sat</i> <i>paralogous protein: YitA</i>	P	3.04E-10	6.33	Sulfate adenylyltransferase. ATP + sulfate = diphosphate + adenylyl sulfate.
P53556	8-amino-7-oxononanoate synthase 2 <i>bioF</i>	H	8.82E-03	6.2	8-amino-7-oxononanoate synthase 2. Biosynthesis of Biotin
P45857	Acyl-CoA dehydrogenase <i>yqjN</i>	E	3.44E-15	6	Uncharacterized protein Paralogous protein RocB (subtiwiki)
P24139	Oligopeptide transport system permease protein <i>oppC</i>	P	2.70E-10	5.93	Oligopeptide transport system permease protein
P75030	Urease subunit gamma <i>ureA</i>	E	9.51E-06	6.67	Urease subunit gamma catalytic activity
P50619	Uncharacterized protein <i>ymaB</i>	S	1.50E-06	5.62	Uncharacterized protein YmaB
O34632	<i>sirB</i> synonym: <i>ylnE</i> , <i>cbiX</i>	H	3.26E-07	5.62	Sirohydrochlorin ferrochelataase. Chelates iron to the siroheme precursor. .
P39641	<i>bacD</i>	I	2.21E-13	5.52	Alanine--anticapsin ligase Part of the bacABCDEFG operon responsible for the biosynthesis of bacilysin, a
Q07429	<i>nrgA</i>	T	3.34E-07	5.49	Functions as an ammonium and methylammonium transporter in the absence of glutamine. Required for ammonium utilization at low concentrations
P70972	Energy-coupling factor transporter transmembrane protein EcfT	P	5.26E-05	5.49	Transmembrane (T) component of an energy-coupling factor (ECF) ABC-transporter complex. Unlike classic ABC transporters this ECF transporter provides the energy necessary to transport a number of different substrates
P28820	<i>pabB</i>	EH	4.91E-08	5.41	Part of a heterodimeric complex that catalyzes the two-step biosynthesis of 4-amino-4-deoxychorismate (ADC), a precursor of p-aminobenzoate (PABA) and tetrahydrofolate (PabB) to produce ADC. biosynthesis of folate
P39581	<i>dltA</i>	Q	1.30E-09	5.38	D-alanine--D-alanyl carrier protein ligase D
P42435	<i>nasD</i>	C	2.04E-08	5.37	Required for nitrite assimilation. Ammonia + 3 NAD(P) ⁺ + 2 H ₂ O = nitrite + 3 NAD(P)H.

UniprotKB	Accession	COG	Anova (p)*	Fold	Description
O07619	<i>yhfT</i>	IQ	2.57E-07	5.33	Uncharacterized acyl--CoA ligase May be involved in fatty acid metabolism.
C0SPA7	<i>yukB</i>	S	1.56E-06	5.27	ESX secretion system protein. Required for YukE secretion
Q45460	<i>opuBA</i> paralogous protein:• <i>OpuCA</i>	E	2.37E-13	5.18	Choline transport ATP-binding protein
O31581	<i>yfhM</i>	S	7.99E-07	4.8	AB hydrolase superfamily protein general stress protein,
O31840	<i>rapk</i>	T	2.26E-11	4.75	Response regulator aspartate phosphatase K
P50842	<i>kduD</i>	S	1.25E-06	4.67	2-dehydro-3-deoxy-D-gluconate 5-dehydrogenase
P24136	<i>oppD</i> Paralogous proteins: • <i>AppD</i> , <i>DppD</i>	EP	6.77E-15	4.56	Oligopeptide transport ATP-binding protein OppD. .
O05253	<i>yufO</i> synonym: <i>nupO</i>	S	2.54E-08	4.55	ABC transporter for guanosine (ATP-binding protein).
O34741	<i>bceB</i> synonym <i>ytsD</i>	V	2.60E-10	4.23	Bacitracin export permease protein Bce.
O31611	<i>yjbm</i> paralogous <i>sasb</i>	S	1.04E-04	3.9	Functions as a (p)ppGpp synthase; GDP can be used instead of GTP, resulting in an increase of (p)ppGpp synthesis (PubMed:18067544). The enzyme binds ATP, then GDP or GTP and catalysis is highly cooperative
P71002	<i>rapF</i>	T	2.95E-10	3.88	Response regulator aspartate phosphatase
O32157	<i>frlB</i>	G	2.90E-13	3.82	Catalyzes the conversion of a range of fructosamine 6-phosphates to glucose 6-phosphate and a free amino acid. Carbohydrate Metabolism
P24141	<i>oppA</i> paralogous to <i>DppE</i>	E	7.24E-11	3.72	Oligopeptide-binding protein OppA. .
P11018	<i>ispA</i>	H	2.14E-06	2.2	Farnesyl diphosphate synthase protein degradation
P39639	<i>bacB</i>	S	1.08E-08	3.62	H2HPP isomerase.
Q08787	<i>srfAC</i> synonym <i>comL</i>	Q	6.47E-11	3.59	Surfactin synthase subunit 3.
P77837	<i>ureB</i>	E	3.22E-07	4.56	Urease subunit beta
O32117	<i>yutJ</i>	C	5.74E-09	3.52	Uncharacterised NADH dehydrogenase-like protein YutJ.

UniprotKB	Accession	COG	Anova (p)*	Fold	Description
O34666	<i>ctpA</i>	M	1.08E-07	3.5	Carboxy-terminal processing protease Is expressed only during vegetative growth
P94391	<i>putC</i> Paralogous proteins: <i>YcbD, DhaS, RocA, IolA, YwdH, GabD, YfmT, AldX, AldY, GbsA</i>	C	8.74E-10	3.49	1-pyrroline-5-carboxylate dehydrogenase 2. Important for the use of proline as a sole carbon and energy source or a sole nitrogen source
P80865	<i>sucD</i>	C	1.85E-08	3.37	Succinyl-CoA synthetase functions in the citric acid cycle (TCA), coupling the hydrolysis of succinyl-CoA to the synthesis of either ATP or GTP and thus represents the only step of substrate-level phosphorylation in the TCA
O32138	<i>pucR</i>	K	4.68E-08	3.31	Transcriptional regulator of puc genes. Purine catabolism regulatory protein. Activates the expression of pucFG, pucH, pucI, pucJKLM and guaD, while it represses pucABCDE and its own expression.
P45931	<i>yqbQ</i>	S	3.43E-08	3.31	Uncharacterized protein
08788	<i>srfAD</i>	Q	5.60E-09	3.27	Surfactin synthase thioesterase subunit Probable thioesterase involved in the biosynthesis of surfactin.
P39845	<i>ppsA</i>	Q	5.08E-08	3.24	This protein is a multifunctional enzyme, able to activate and polymerize the amino acids Glu and Orn as part of the biosynthesis of the lipopeptide antibiotic lipastatin.
P54420	<i>asnB</i>	E	1.42E-12	3.23	Main asparagine synthetase in vegetative cells
O05218	<i>ywrD</i>	E	8.35E-09	3.23	Glutathione hydrolase-like proenzyme
P27206	Surfactin synthase subunit 1 <i>srfAA</i>	IQ	3.48E-10	3.18	This protein is a multifunctional enzyme able to activate and polymerize the amino acids Leu, Glu, Asp and Val.
P71007	Antilisterial bacteriocin subtilosin biosynthesis protein <i>albE</i>	O	1.91E-05	3.09	Antilisterial bacteriocin subtilosin biosynthesis protein.
P17865	<i>Cell division protein ftsZ</i>	D	1.03E-08	3.07	Essential cell division protein that forms a contractile ring structure (Z ring) at the future cell division site Binds GTP and shows GTPase activity

UniprotKB	Accession	COG	Anova (p)*	Fold	Description
P39847	Plipastatin synthase subunit C <i>ppsC</i>	Q	5.45E-09	3.07	Function: production of the antibacterial compound plipastatin.
Q07833	tRNA nuclease <i>wapA</i>	M	1.17E-04	3.03	tRNA nuclease WapA.
P12011	Gluconokinase <i>gntK</i>	G	5.62E-05	3.03	Gluconokinase. D-gluconate degradation
O07576	Uncharacterized amino acid permease <i>yhdG</i> or <i>bcaP</i> <i>paralogous protein •MtrA</i>	E	6.31E-06	3.02	Branched-chain amino acid transporter.

The 146 upregulated proteins (Table 4-3) were grouped into 19 functional COG groups as shown in Figure 4-7. It is interesting to note that of those proteins upregulated the highest number are involved in amino acid metabolism and transport (E). This is understandable as the cells are under nitrogen limitation and thus trying to degrade and transport all possible forms of nitrogen. It is also the category in which urease proteins are associated and is consistent with the findings of Tam *et al.* (2006). The second group with the most protein change are of unknown function (S). This group consists of many 'y' genes, where the function has not been ascertained.

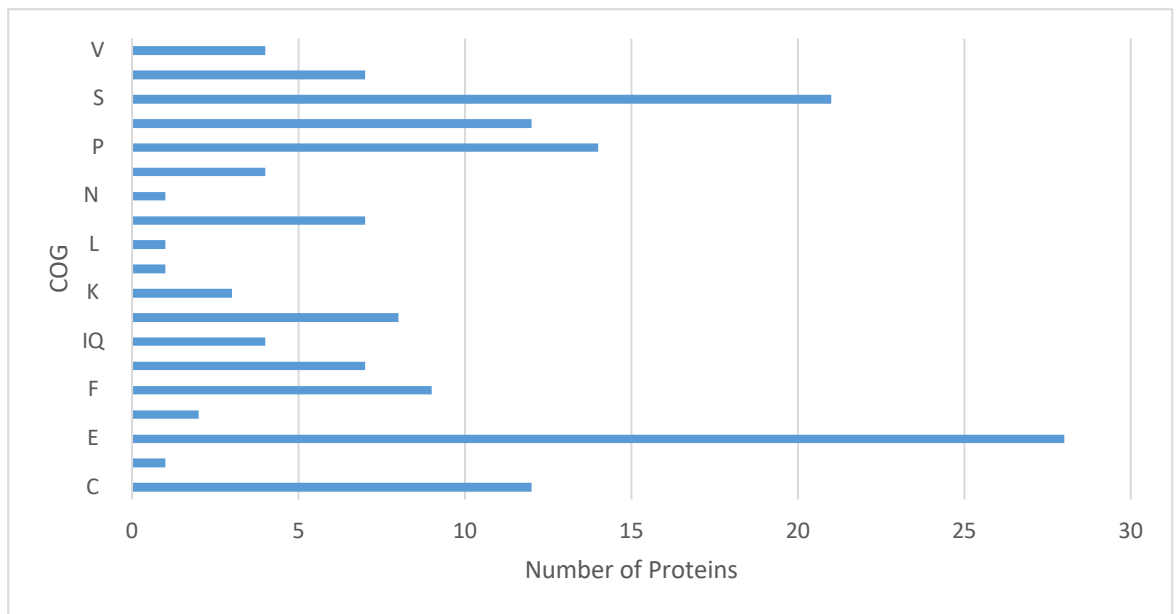


Figure 4-7. COG analysis of proteins upregulated in nitrogen limited media.

The total number of proteins upregulated were 146, with the most proteins (28) present in COG E and second most 21 in COG S. Table 3-9 includes all COG.

There are 88 proteins identified which are downregulated in the NLC (Figure 4-8 and Table 4-4). Of those proteins downregulated the highest number, 18 in total, fall into the COG C - Energy production and conversion. The second group with the most protein change are of unknown function (S) with 14 proteins in this category.

Table 4-4. Proteins downregulated in the nitrogen limited condition of BSS (JW) compared to BSS (JW) + Ammonium Sulphate.

Protein Accession and Description	COG	Anova (p)*	Fold
P36948 Ribose import permease protein RbsC	G	5.36E-09	566.98
O34738 Putative HMP/thiamine permease protein YkoE	S	2.08E-08	255.69
P36949 Ribose import binding protein RbsB	G	4.21E-04	87.57
O34967 50S ribosomal protein L31 type B	JT	6.85E-04	79.27
P40410 Iron-uptake system permease protein FeuB	P	1.11E-05	68.87
O31728 Cell division protein SepF	S	7.00E-05	55.53
P42317 Uncharacterized oxidoreductase YxjF	C	4.63E-09	49.66
P18156 Glycerol uptake facilitator protein	G	4.07E-11	36.18
P94367 ATP-binding/permease protein CydD	V	1.64E-10	35.01
O34742 Glycine betaine/carnitine/choline transport system permease protein OpuCD	E	2.55E-15	31.84
O34591 Acetoin:2,6-dichlorophenolindophenol oxidoreductase subunit beta	C	6.55E-15	31.39
P24812 Uncharacterized protein YqxI	S	7.25E-09	25.33
O31550 Dihydrolipoyllysine-residue acetyltransferase component of acetoin cleaving system	C	1.11E-15	23.31
P42413 5-deoxy-glucuronate isomerase	G	1.01E-03	20.51
P39600 Uncharacterized protein YwcB O	S	1.28E-06	15.48
P46318 Lichenan-specific phosphotransferase enzyme IIB component	G	9.72E-09	15.29
O34421 Probable acyl-CoA dehydrogenase YngJ	I	7.77E-16	14.97
O06989 Maltodextrin-binding protein MdxE	G	5.71E-11	13.58
O34425 Glyceraldehyde-3-phosphate dehydrogenase 2	G	4.32E-12	13.08
P54948 Uncharacterized protein YxeI	M	2.46E-05	12.62
O34909 Putative adenine deaminase YerA	F	3.31E-12	11.94
O34345 Uncharacterized protein YflJ	S	7.98E-07	11.63
P39216 Methyl-accepting chemotaxis protein TlpA	S	3.20E-08	11.55
O31436 Uncharacterized protein YbdN	S	8.49E-03	11.55
P36947 Ribose import ATP-binding protein RbsA	P	7.74E-11	10.9
P42316 Probable succinyl-CoA:3-ketoacid coenzyme A transferase subunit B	I	5.89E-13	10.87
O06988 Intracellular maltogenic amylase	G	6.80E-09	10.76
P39635 U Protein RocB	E	2.05E-10	10.72
O34895 N-acetyltransferase YodP	S	6.36E-12	10.64
P42314 Uncharacterized transporter YxjC	S	0.01	9.78
P45857 Acyl-CoA dehydrogenase	I	1.40E-10	9.75
P12946 Heme A synthase	C	1.99E-09	9.3
P37561 Uncharacterized protein YabS	S	1.94E-04	8.67
P06533 HTH-type transcriptional regulator SinR		0.01	8.54
O32180 Uncharacterized protein YusN	S	8.60E-08	8.36
P71009 Putative ABC transporter ATP-binding protein AlbC	S	5.63E-10	8.2
P39124 Glycogen biosynthesis protein GlgD	G	3.39E-09	7.9
P37525 Uncharacterized protein YaaB	S	5.41E-05	7.88
Q45497 UPF0223 protein YktA	S	6.56E-05	7.86
P39634 1-pyrroline-5-carboxylate dehydrogenase	C	1.67E-10	7.41
O31725 Uncharacterized protein YlmC	S	2.50E-04	7.25
O31826 Putative acyl-CoA synthetase YngI	S	6.68E-06	6.49
P42108 Uncharacterized protein YxaI	S	1.72E-05	6.48

Protein Accession and Description	COG	Anova (p)*	Fold
P70949 Fe-S protein maturation auxiliary factor YitW	S	5.82E-07	6.34
O34726 Putative malate transporter YflS	K	1.21E-05	6.07
P54716 Maltose-6'-phosphate glucosidase	G	1.07E-13	6
P39579 D-alanyl carrier protein	I	2.00E-03	5.99
P18157 Glycerol kinase	C	2.17E-12	5.68
P71066 Uncharacterized protein YvfG	S	0.01	5.58
O34873 Hydroxymethylglutaryl-CoA lyase YngG	E	1.69E-06	5.5
O34324 Dihydrolipoyl dehydrogenase O	C	9.59E-08	5.36
ACCC2_BACSU Biotin carboxylase 2	I	2.28E-11	5.31
P36945 Ribokinase	G	1.03E-06	5.3
O06475 Uncharacterized protein YfmQ	S	4.58E-05	5.09
O31643 Uncharacterized protein YjdB	N	2.28E-03	5.05
P45859 2-methylcitrate dehydratase	S	3.37E-11	4.98
O34745 Uncharacterized symporter YodF	E	1.14E-09	4.87
P94531 Intracellular exo-alpha-(1->5)-L-arabinofuranosidase 1	G	8.68E-04	4.75
P49937 Iron(3+)-hydroxamate import system permease protein FhuG	P	1.09E-06	4.6
P32397 Protoporphyrinogen oxidase	H	6.84E-05	4.55
O31850 Uncharacterized protein YojN	M	1.44E-07	4.54
sp O34697 BCEA_BACSU Bacitracin export ATP-binding protein BceA O	P	1.57E-07	4.52
O05508 6-phospho-beta-glucosidase GmuD	G	9.76E-09	4.38
P50727 Ferredoxin	C	8.79E-04	4.36
O31684 Uncharacterized protein YkvS	S	1.98E-04	4.28
P39802 Chemotaxis protein CheW	NT	2.18E-07	4.09
P71067 L-lactate permease	C	1.10E-08	4.07
O32089 Uncharacterized protein YuzC	S	7.77E-08	4.03
P55910 L-lactate permease	C	2.55E-07	4.02
O34662 Uncharacterized aminotransferase YodT	E	1.89E-07	3.99
P35161 Cytochrome c biogenesis protein ResB	O	4.26E-04	3.96
P45858 2-methylcitrate synthase	C	3.77E-09	3.95
O34926 Pulcherriminic acid synthase	Q	1.72E-08	3.83
O34362 Putative HMP/thiamine import ATP-binding protein YkoD	P	2.79E-07	3.8
P94431 Uncharacterized protein YcnI	S	1.74E-08	3.74
O34949 Uncharacterized HTH-type transcriptional regulator YkoM	K	1.98E-03	3.68
P54596 L-cystine uptake protein TcyP	S	1.58E-05	3.67
O34563 ABC transporter glutamine-binding protein GlnH	E	1.11E-08	3.64
P24809 Uncharacterized protein YqxJ	S	1.16E-06	3.64
O32254 Uncharacterized protein YvbT	S	7.32E-07	3.61
P34957 Quinol oxidase subunit 2	C	3.77E-06	3.59
O31777 8-amino-7-oxononanoate synthase 1	H	2.62E-09	3.57
O07635 Uncharacterized protein YlaK	T	4.22E-07	3.49
P37550 4-diphosphocytidyl-2-C-methyl-D-erythritol kinase	I	6.53E-09	3.49
O34433 Putative phage-related protein YobO	S	3.17E-08	3.48
P45855 Acetyl-CoA acetyltransferase	I	1.06E-11	3.44
C0SPC0 Probable 4-hydroxyphenylacetate 3-monooxygenase	S	0.03	3.41
P50865 Probable polysaccharide deacetylase PdaB	S	4.91E-04	3.4
P54477 Uncharacterized protein YqfT	S	6.31E-04	3.37
P16397 Bacillopeptidase F	O	1.13E-05	3.32

Protein Accession and Description	COG	Anova (p)*	Fold
O34468 Uncharacterized N-acetyltransferase YlbP	S	1.42E-06	3.28
O31845 Uncharacterized membrane protein YozB	S	0.02	3.27
O05248 Putative membrane protease YugP	S	1.44E-05	3.27
P28599 10 kDa chaperonin	O	2.61E-07	3.18
O07533 Putative enoyl-CoA hydratase/isomerase YhaR	S	7.03E-04	3.15
O32127 Uncharacterized protein YutD	S	5.68E-03	3.14
O07539 Stress response protein YhaX	S	2.05E-08	3.12
P54720 Putative oxidoreductase CatD	S	1.55E-05	3.12
O34984 Uncharacterized metallohydrolase YodQ	O	5.75E-13	3.11
P39116 Pectate lyase	G	1.35E-07	3.1
O34788 (R,R)-butanediol dehydrogenase	E	5.90E-09	3.07
O34469 Putative ATP-dependent helicase YeeB	L	4.63E-06	3.07
O34588 Uncharacterized protein YkuJ	S	1.66E-07	3.04

For each category, the number of proteins upregulated and downregulated were compared. There were some significant changes in several categories. Comparing the changes in those proteins downregulated the greatest change can be seen in COG E – amino acid transport and metabolism with a decrease of approximately 2/3 (27 proteins down to 8). This is understandable as the addition of $(\text{NH}_4)_2\text{SO}_4$ will maintain the growth of *B. subtilis* and so many proteins involved in nitrogen assimilation will not be required in such large quantities, e.g including peptide transporters, etc., as those proteins that fall into COG E, including those of peptide transport systems, urease and glutamate synthase. The COG which displays the second most decrease was Q, which involves secondary metabolites biosynthesis, transport, and catabolism, which are involved in all aspects of the cell's metabolism. The proteins belonging to this category include those that produce antibiotics and those involved in purine utilisation. The need for upregulation of these specific proteins would coincide with a culture condition of stress and nitrogen limitation and are therefore understandably down regulated in the NPM (Figure 4-8). The downregulation of these proteins maintains growth and cell division. The proteomic evaluation of cells in NPM leads to the assumption the cells seem less stressed than those in NLM. Importantly, the COGs in which the urease accessory proteins and structural proteins belong, are all upregulated in this condition as shown in Table 3-11.

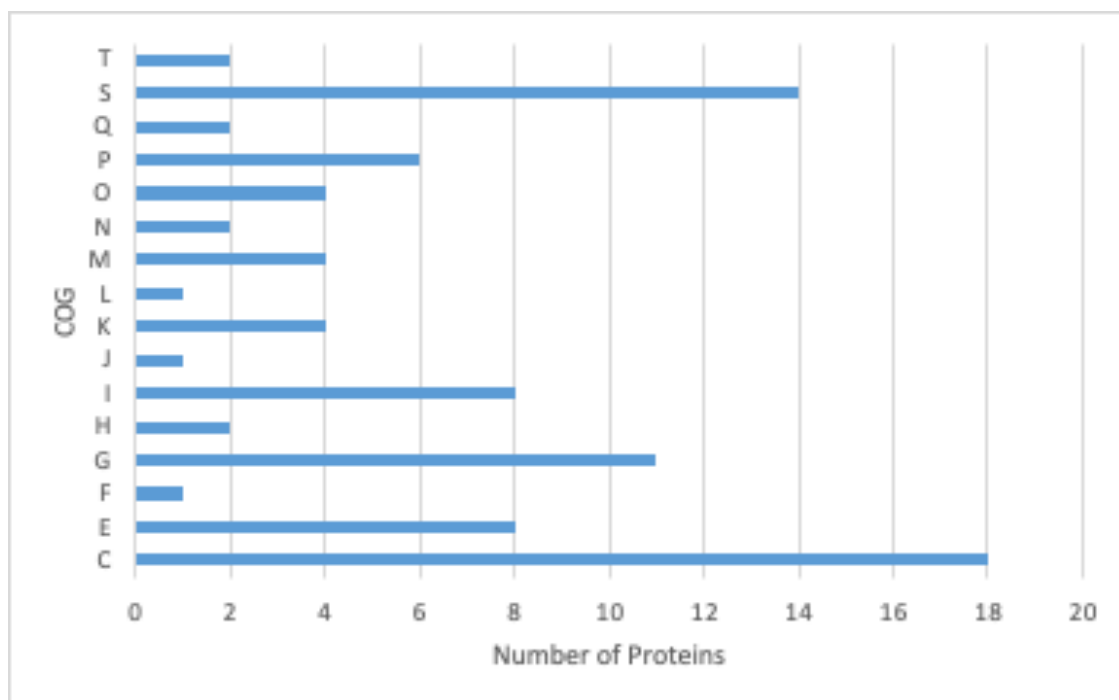


Figure 4-8. COG analysis of proteins downregulated in the NLM BSS (JW).

The total number of proteins downregulated was 88, with the most proteins (88) present in COG C and second most 14 in COG S (Methods: 4.2.1.1).

4.2.3 Functional Analysis of Proteins Upregulated in Nitrogen Limited Media (NLM)

The differentially expressed proteins are categorised into various COGs as detailed in Table 2-12. Understanding why particular proteins are upregulated in the NLM, by identifying which processes they are involved in, will enable the identification of candidate proteins that may be involved in urease activation in *B. subtilis*. The upregulated proteins which had a significant fold change (over 3) are presented in Table 4-3. The proteins that have fold change less than 3 are presented in Appendix table 9-1.

Amino acid transport and metabolism (E) is the most relevant COG associated with the urease structural units. It is also the COG which includes the most upregulated proteins of various fold change (30 proteins) in the nitrogen limiting media. UreC, which houses the active site of urease was the second highest fold change protein in the NLM at 20.16. The presence of all subunits of urease is in line with the observation with proteomics study conducted by Tam le *et al.* (2006) and again it confirms the correct growth conditions are nitrogen limited.

To help identify the potential proteins involved in urease activation, COG analysis was performed on the well-studied urease structural proteins and accessory proteins. As shown in Table 4-5, urease and its associated proteins are most commonly characterised in the COG groups of (E) amino acid and transport, (O) molecular chaperones and related functions, (K) transcription, (V) defense systems and (S) function unknown. Therefore, it is reasonable to make an assumption that the proteins acting as accessory protein have a high possibility to belong to one of these categories. In addition, the main function of accessory proteins is to aid the insertion of Ni²⁺ into the urease structural proteins, therefore those proteins of *B. subtilis* 168 identified as upregulated in NLM which can bind Ni²⁺, should be interesting and need further investigated. This may also include proteins with multiple binding metal domains which could possibly lead to UreE and UreG identifications.

Table 4-5. Known Urease accessory proteins and their associated COG's.

Urease Accessory Protein/s	Associated COG
UreABC	(E) Amino acid transport and metabolism
UreD	(O) Posttranslational modification, protein turnover and chaperones (S) Function Unknown
UreE	(O) Posttranslational modification, protein turnover and chaperones
UreF	(O) Posttranslational modification, protein turnover and chaperones (V) Defense Systems
UreG	(K) Transcription (O) Posttranslational modification, protein turnover and chaperones
UreJ	(O) Posttranslational modification, protein turnover and chaperones (S) Function Unknown

4.2.3.1 Purine Synthesis and Degradation

Upregulated in NLM is the purine catabolism regulatory protein PucR (fold change 3.31), belonging to COG O - Post-translational modification, protein turnover and chaperones. As discussed in section 3.1.4.4, PucR is the transcriptional regulator of *puc* genes and activates

the expression of various genes such as *pucFG*, *pucH*, *pucJ-pucK-pucL-pucM*, *guaD* and *ureA-ureB-ureC* (Brandenburg *et al.*, 2002a). Our finding that PucR was upregulated is in line with previous literature. The cells are experiencing nitrogen limitation and so *B. subtilis* utilises low molecular weight compounds, as a nitrogen source, when the preferred sources such as glutamate plus ammonia are not present (Schultz, Nygaard and Saxild, 2001). Schultz *et al.* (2001) via experimentation with knockouts, identified that under nitrogen limitation PucR acts as a positive regulator (Figure 4-9) for the purine catabolic pathway. Those genes listed in Figure 4-9 encode enzymes or proteins for protein degradation, of those the uricase PucL (fold change 18.14) belongs to COG Q (Secondary metabolites biosynthesis, transport, and catabolism) and catalyses the two step degradation of uric acid, and PucM (fold change 14.41) which also encodes uricase activity, are upregulated. Purines are the major constituents of nucleic acids and nucleotides. The degradation of nucleotides to nucleobases and nucleosides enable them to be reused in purine salvage pathways. As detailed in Figure 4-9, urea is produced by the final step in purine catabolism, and this can be further degraded to ammonia as an optimum nitrogen source under these growth conditions by urease (Brandenburg *et al.*, 2002a). The overexpression of PucR could also explain the upregulation of urease in NLM (shown in Table 3-10) as it positively regulates the expression of the urease operon in *B. subtilis*.

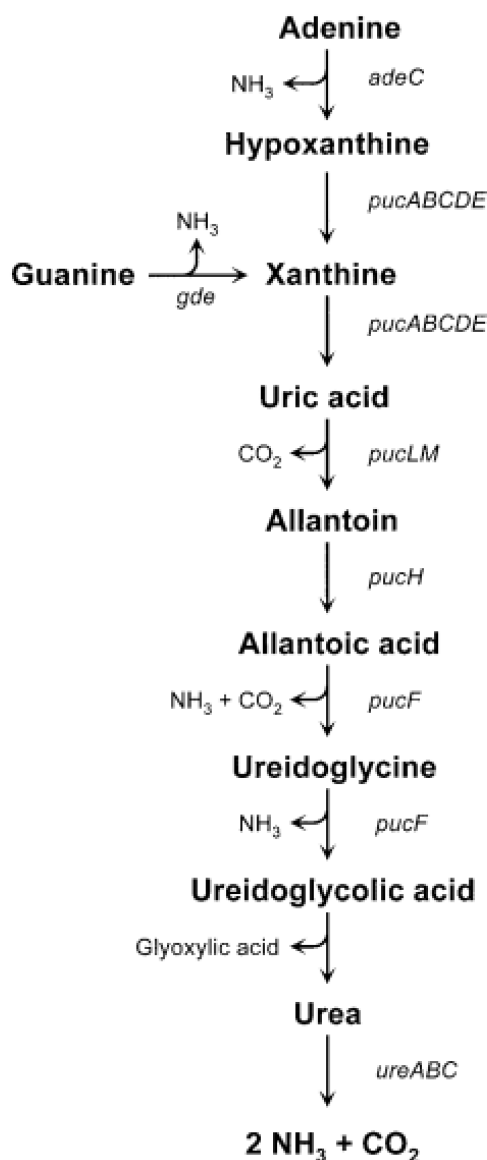


Figure 4-9. Purine-degradative pathway in *B. subtilis* (Brandenburg *et al.*, 2002a)

The upregulation of purine utilization proteins is also evident; PucC a xanthine dehydrogenase with fold change 7.34 and PucD a xanthine dehydrogenase with fold change 22.83 which oxidise hypoxanthine and xanthine to uric acid (Schultz, Nygaard and Saxild, 2001), are also evident. These proteins are detailed in Figure 4-9 and are part of the purine degradation pathway (which occurs under NLCs) in *B. subtilis*, which establishes that purines are degraded to ammonia that is utilized as a nitrogen source.

Also upregulated in NLM and characterised in COG F- nucleotide transport and metabolism, are those proteins necessary for purine salvage: CmK, fold change 16.35, and Xpt, fold change 9.34. CmK is a cytidylate kinase and is involved in the pyrimidine nucleotide metabolic process and

Xpt a Xanthine phosphoribosyltransferase which converts xanthine, a product of nucleic acid breakdown, to xanthosine 5'-monophosphate (XMP), so that it can be reused for RNA or DNA synthesis. Both were upregulated in NLCs.

4.2.3.2 Nitrate Assimilation

There are proteins upregulated in the NLM that are required for nitrate assimilation. Those proteins are positively regulated by TnrA in aerobic growth (Nakano *et al.*, 1998) and include the nitrate transporter NasA (fold change 22.73), the assimilatory nitrite reductase NasD (fold change 5.37) and nitrate reductase NasC (fold change 6.69) which are characterised in COG C. Ogawa *et al.* (1995) describe how *B. subtilis* utilizes nitrate or nitrite, as a sole source of nitrogen and NasD, NasC and NasE are vital in this process (Ogawa *et al.*, 1995). The assimilatory nitrate reductase catalytic subunit, NasC, is the key enzyme involved in the initial steps of nitrate assimilation in *B. subtilis*. Nitrate reductase reduces nitrate to nitrite in nitrate respiration, which is then reduced to ammonia by nitrite reductase. This does highlight that ammonia is produced by enzymes other than urease, which potentially may cause false positives in the enzyme assay, however assay controls are present to solve this.

4.2.3.3 Other Nitrogen Related Proteins

Nitrogen regulation in *B. subtilis* is complex. TnrA is upregulated in NLM with a fold change of 6.4. Interestingly, TnrA, as described in 3.1.4.3, is expressed in NLCs mirroring literature. TnrA activates a number of genes which will be discussed in this section, such as *oppA-oppB-oppC-oppD-oppF*, *nrgA-nrgB*, *ansZ*, *pucJ-pucK-pucL-pucM*, *nasA* and importantly *ureA-ureB-ureC*.

As detailed above, purines are degraded to ammonia. This links to the upregulation of GlnK (formerly NrgB) in NLM (fold change 11.44,) whose function is ammonium uptake and is necessary for the induction of the AmtB-GlnK (formerly *nrgAB*) operon. Fedorova *et al.* (2013) propose the action of AmtB, which is an ammonium transporter and required at low ammonium concentration, is regulated by GlnK as it is able to sense NH_4^+ in the cell. Glutamine synthetase (GS) or GlnA thereafter is upregulated, fold change 12.41, and this protein binds NH_4^+ coming into the cell and converts it into glutamine (Fedorova *et al.*, 2013). As Detsch *et al.* (2003) stated,

B. subtilis uses glutamine as its preferred source of nitrogen, but in its absence, ammonium can be utilised.

Another protein, GuaD, is also upregulated (fold change 15.05). It catalyzes the hydrolytic deamination of guanine (one of two forms of purine), producing xanthine and ammonia (Nygaard *et al.*, 2000). The upregulation of these proteins indicated the bacteria is utilizing the purine bases as nitrogen sources when there is a limited nitrogen source available.

Atkinson *et al.* (1991) identified the levels of urease and asparaginase were elevated in NLCs which is confirmed in this work (Atkinson and Fisher, 1991). AsnB is upregulated with a fold change of 3.23 and codes for an asparagine synthetase which controls peptidoglycan hydrolysis in vegetative cells. AsnZ is also upregulated with fold change 16.73. It catalyses the conversion of L-asparagine to L-aspartate and NH_4^+ . Again, NLCs must be evident, as TnrA, in nitrogen limiting conditions, positively regulates *ansZ* expression by binding to a DNA site located upstream of the *ansZ* promoter (Fisher and Wray, 2002).

4.2.3.4 Transport

In NLM the upregulation of several transport proteins was observed. Bacterial high affinity transport systems are involved in active transport of solutes across the cytoplasmic membrane. There are some ABC transport systems that are specific for the transport of peptides and amino acids and these systems are comprised of a membrane-spanning channel through which the peptide passes, a pair of ATPases which couple ATP hydrolysis to peptide translocation and a lipid-modified, membrane-anchored extracellular "binding-protein" that serves as the receptor for the system (Solomon *et al.*, 2003). As discussed, there are three main peptide transport systems in *B. subtilis*, a dipeptide permease (*Dpp*) and two oligopeptide permeases (*Opp* and *App*) with overlapping specificity and all belonging to the ABC transporter family.

The data from the COG analysis details the upregulation of peptide transporters such as OppA, fold change 3.72, OppB, fold change 9.61, OppC, fold change 5.93, OppD, fold change 4.56, and DppA (fold change 2.22), OppF (fold change 2.95) and YkfD (fold change 2.56). Included are those proteins upregulated but with a fold change <3, see Appendix Table 9-2. In addition, DppA,

fold change 3.22, was upregulated in NLM. As described these proteins have similar molecular functions but are different units of transport systems. The multicomponent proteins have various functions and can be placed in 2 COGs with regards to this data analysis, and this includes the COG E - amino acid transport and metabolism and P- inorganic ion transport and metabolism. Peptide transporters are important in numerous cellular processes, and especially in times of nitrogen deprivation and this may be the main reason for their upregulation.

opp operon

The *B. subtilis opp* operon encodes five proteins and is a binding protein dependent transport system —OppA, OppB, OppC, OppD, and OppF (Figure 4-10). It can bind up to five amino acids long with high affinity and is also required for sporulation and competence (Perego *et al.*, 1991). OppA is a substrate binding protein (SBP) and is tethered to the extracellular face of the cell membrane via a lipid anchor. OppB and OppC are membrane-spanning permease proteins that create the transmembrane pore through which oligopeptides are imported. OppD and OppF are ATPases, which hydrolyzes ATP to provide the energy to transport the molecules. OppA binds to the peptide substrate and facilitates its uptake by interacting with and delivering the peptide to the OppBCDF complex. The *app* system is another oligopeptide transport system, and it has a similar arrangement as *opp* system, but, unlike Opp the App system is incapable of transporting tripeptides. In *B. subtilis* the *app* system, as described, is not active due to a frameshift mutation. Unlike *opp* and *app*, *dpp* is a dipeptide permease system.

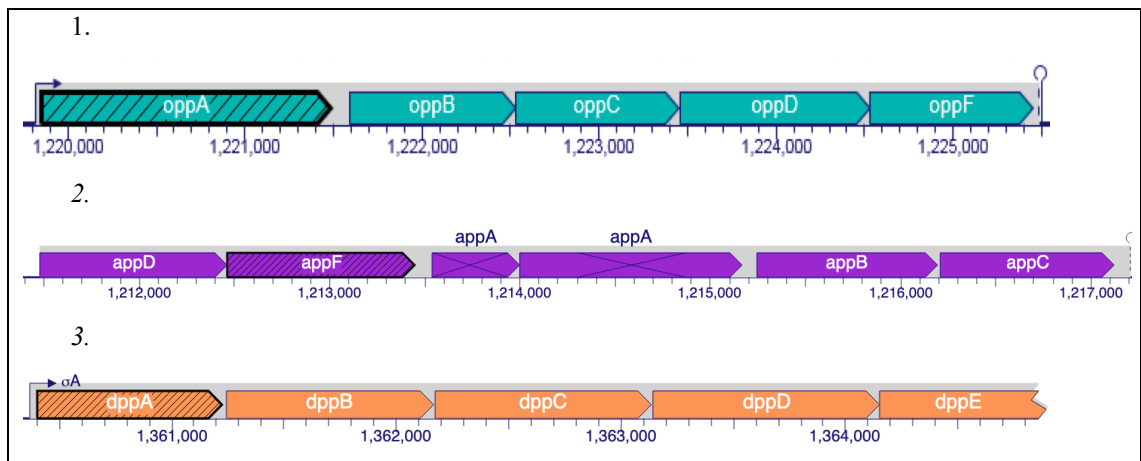


Figure 4-10 ABC transport system operons in *B. subtilis* 168.

1. *opp* operon of *B. subtilis* 168. 2. *app* operon featuring the inactive pseudogene *appA* in *B. subtilis* 168 due to mutation. 3. *dpp* operon of *B. subtilis* (Karp *et al.*, 2019). Hatched lines indicate binding protein.

The *opp*, *app* and *dpp* systems are upregulated under NLCs by TnrA due to them possessing a TnrA box which corresponds to the TnrA binding site TGTNANAWWWTMTNACA. It is important to note that *opp* transport systems can often be annotated incorrectly, as their function is not necessarily peptide transport but is indeed the transport of Ni²⁺. The reason for this is the *opp* system of *B. subtilis* belongs to the nickel/peptide/opine PepT subfamily of ABC-transporters, which are annotated with potential functions but not necessarily confirmed in all cases. As detailed previously, one of the *opp* systems in the Gram-positive organism *S. aureus*, was in fact renamed NikABCDE due to its function of Ni²⁺ transport and delivery for urease activation (Hiron *et al.*, 2010). Further investigations (detailed in Appendix 9-1) identified that the sequence alignments of *S. aureus opp2* genes were similar to the *opp* genes in *B. subtilis* with sequence homology ranging from 27% for the OppA comparison to 42% for OppD. In addition, very recently Hughes *et al.* (2019) identified OppA of the pathogenic spore former *Clostridium difficile* likely to be the receptor protein for a Ni²⁺ uptake system (Hughes *et al.*, 2019). *B. subtilis* OppA was compared to *C. difficile* OppA and demonstrated low homology, however, the SBP is still worth investigating.

When considering urease activation in *B. subtilis* it would be ideal to identify a Ni²⁺ transport system. Although there is no literature to show that the Opp system in *B. subtilis* is responsible for Ni²⁺ transport, it is plausible to consider the Opp system may have some involvement in Ni²⁺ transportation. Therefore, we have performed bioinformatic analysis to explore the possibility of

Opp proteins playing a role in Ni²⁺ transport and/or urease activation. Figure 4-11 details the protein sequence comparison of the ATPase of *B. subtilis* OppD and the reannotated NikD from *S. aureus* and reveals they share 42.22% homology.

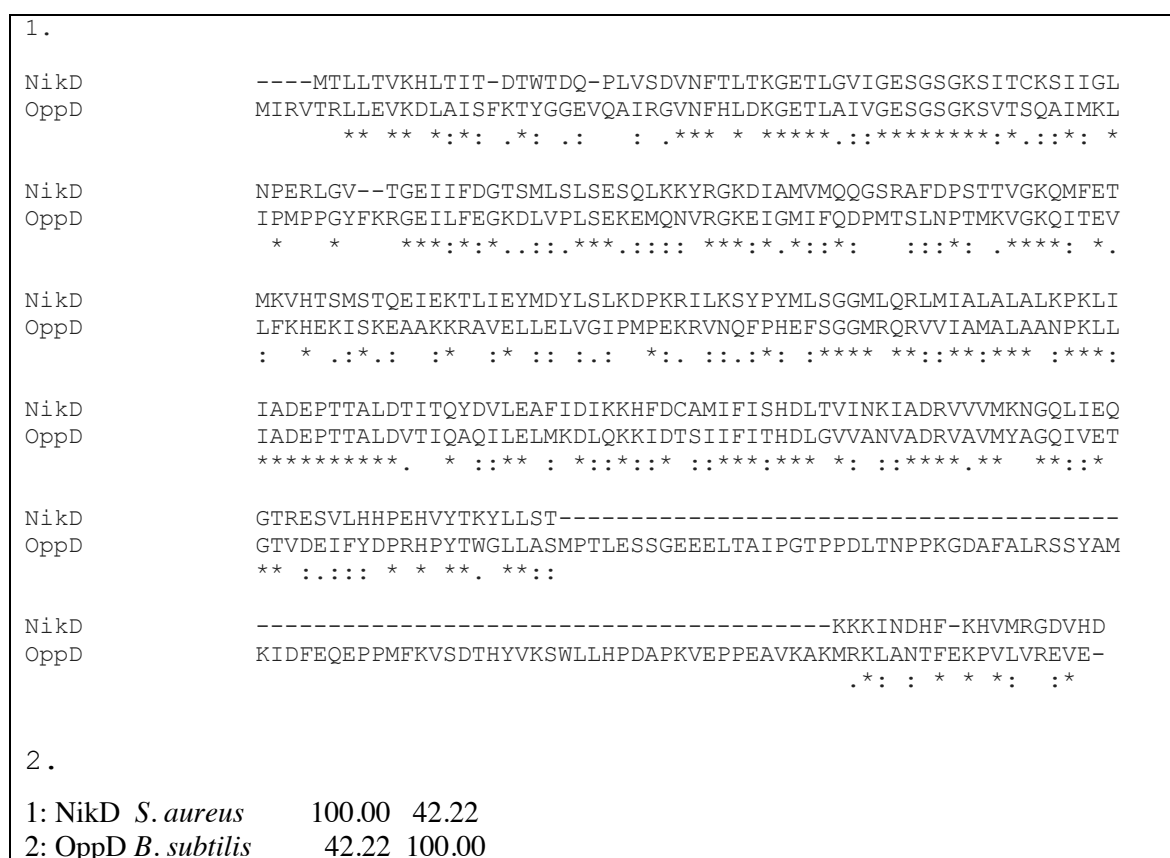


Figure 4-11. MUSCLE alignment comparison of the *B. subtilis* OppD and NikD of *S. aureus* which detailed 42.22%.

The comparison of sequences highlighted a 42.22% homology similarity which may indicate functional, structural and/or evolutionary relationships between two biological sequences.

OppF is an ATPase in the *B. subtilis opp* system. Although not greatly upregulated, with a fold change of 2.95, the protein was still investigated as part of the permease system. The protein sequence of UreE of *S. pasteurii* was compared to OppF of *B. subtilis* using the MUSCLE alignment tool. As shown in Figure 4-12, the sequence alignment score is only 25.69%, however they do show similar placement of His residues highlighted in green (Figure 4-12), which have been noted to be involved in metal binding. According to Won *et al.* (2004) they identified Ni²⁺ binding sites of UreE as Gly⁹⁷-Cys¹⁰³ (Figure 4-12 highlighted red) and in the C - terminal tail region Lys¹⁴¹-His¹⁴⁷ (highlighted blue) and for the first time these were confirmed as Ni²⁺ binding sites in UreE. The conserved sequence that includes fundamental Ni²⁺ binding consists

¹⁴⁴GHQH¹⁴⁷ (underlined red Figure 4-12) (Won *et al.*, 2004). When considering the protein sequence in OppF, the possible Ni²⁺ binding motifs can be identified as: **KYDPSVH** and **KLLEIKH** which would be Lys¹⁴¹-His¹⁴⁷ motif. There are shorter motifs in OppF of the Gly⁹⁷-Cys¹⁰³ which are highlighted red.



Figure 4-12. Sequence comparison of ureE *S. pasteurii* and *B. subtilis* 168 oppF.

1. Protein Sequence of UreE from *S. pasteurii*. 2. Protein sequence of OppF in *B. subtilis* 168 3. Muscle alignment of both sequences. 4. Muscle alignment score. Although the sequence homology is only 25.69% the amino acid sequences share similar His locations which may confer nickel binding.

Since we have observed the upregulation of urease in NLCs, it is reasonable to hypothesised that the Opp system is upregulated in response to the upregulation of the urease structural subunits

and therefore could be the system that delivers the nickel to activate the urease. Further protein analysis and molecular biology techniques will need to be utilised to understand this upregulation pattern.

dpp operon

The *dpp* operon previously named *dci* of *B. subtilis* 168, is regulated by CodY and expressed in late exponential and early stationary phase, in a nutrient rich medium (Serror and Sonenshein, 1996). In NLM, DppA, a D-aminopeptidase, which is part of the *dppA-dppB-dppC-dppD-dppE* operon, is upregulated with a fold change of 2.22. The degradation of cell wall peptides is carried out by this Zn²⁺ binding protein and the purpose is thought to be an adaptation to nutrient deficiency in which the hydrolysis that occurs releases D-alanine which could be used as a metabolic fuel (Remaut and Goffin, 2004). The carbon catabolite control protein A (CcpA) regulates expression of the *ilvB* (acetolactate synthase) operon altering intracellular levels of branched chain amino acids (BCAA), thus CcpA indirectly controls *dpp* expression (Shivers and Sonenshein, 2005). Interestingly, in *E. coli*, DppA proteins share similar conservations in their protein folding when compared to the Ni²⁺ binding protein NikA. Using the muscle alignment tool, *E. coli* DppA and *B. subtilis* DppA only share 25.27% homology. Even with low homology it is still important to consider this protein and its role in nickel transport for the activation of urease in *B. subtilis*.

The *app* system of *B. subtilis* has not been well characterised, since *appA* of the *B. subtilis* reference strain 168 and its derivatives is inactive due to a frameshift mutation (Picon and van Wely, 2001). In *Bacillus amyloliquefaciens subsp. plantarum* UCMB5113, AppF is a Ni²⁺ importing protein (its function is based on a conserved amino acid motif) and, as seen in Figure 4-13, there is evidence of great sequence homology between *B. amyloliquefaciens AppF* and *B. subtilis YkfD* proteins. More interestingly, a fold change increase of 2.39 for YkfD is seen in NLM and this is a paralogous protein to OppF and AppF in *B. subtilis*.

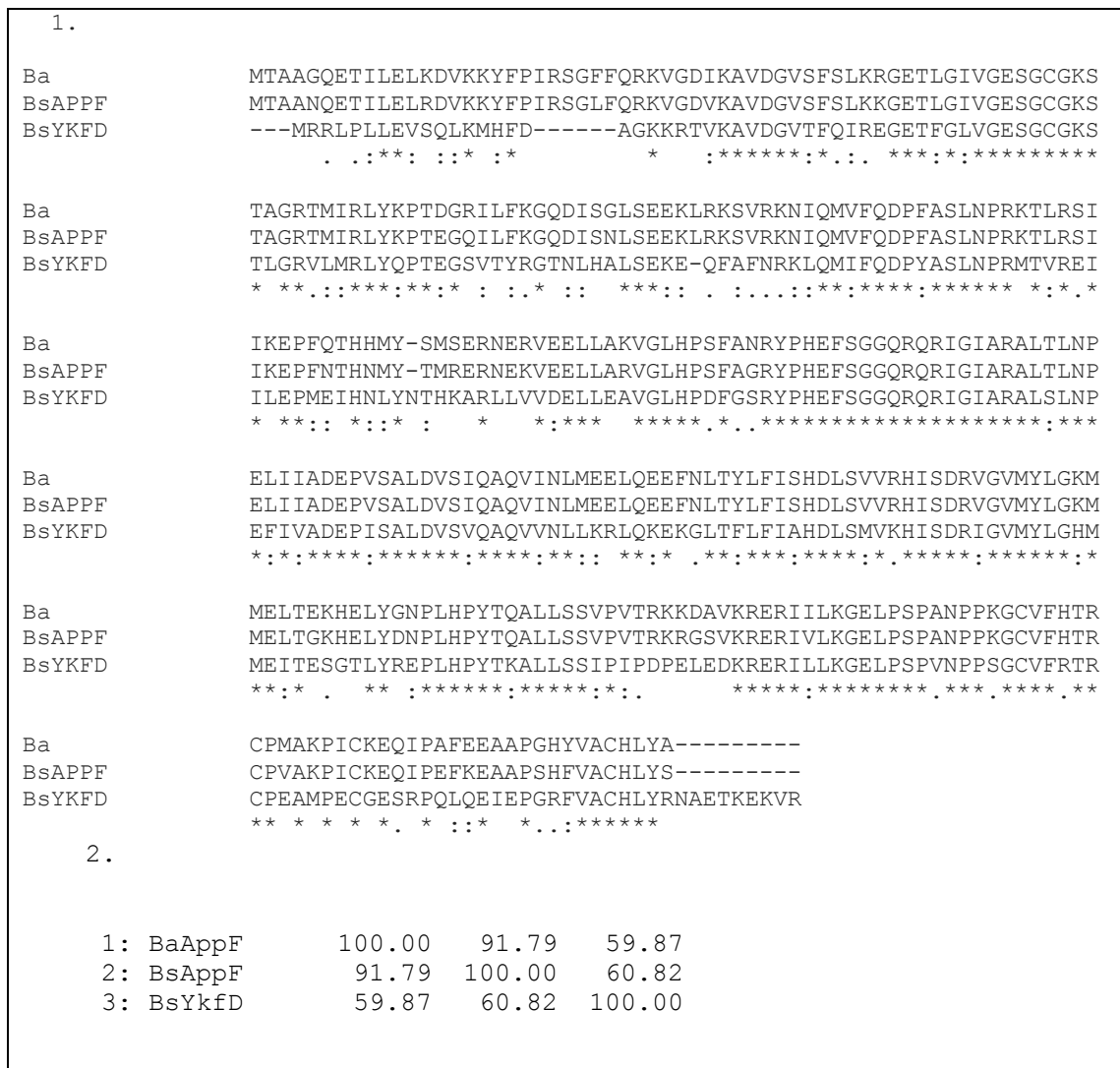


Figure 4-13. Comparison of AppF and Ykfd in *B. subtilis* and AppF in *Bacillus amyloliquefaciens*.

1. MUSCLE alignment of *B. subtilis* AppF (BsAPPF), *B. subtilis* Ykfd (BsYKFD) and *Bacillus amyloliquefaciens* AppF (Ba). 2. MUSCLE alignment percentage identity of *B. subtilis* AppF (BsAPPF), *B. subtilis* Ykfd (BsYKFD) and *Bacillus amyloliquefaciens* AppF (BsAppF). There is great homology between all 3 proteins with the highest between *B. subtilis* AppF and *Bacillus amyloliquefaciens* AppF at 91.79%.

In addition to the upregulation of Opp, interestingly Dpp systems, were also observed; i.e. the upregulation of EcfT (fold change 5.49), an energy-coupling factor transporter transmembrane protein part of a transporter complex. This is of interest as unlike the classic ABC transporters of Opp, App and Dpp this ECF transporter provides the energy necessary to transport a number of different substrates. ECF transporters are involved in the uptake of vitamins and micronutrients in bacterial cells. Ni²⁺ transporters have been identified which are EcfTs, which include for example CbiQ of *Salmonella typhimurium* and NikQ of *Rhodobacter* species, which can transport both Co²⁺ and Ni²⁺ but with low affinity (Rodionov *et al.*, 2006). EcfTs are considered

conformationally dynamic, supporting its function as a scaffold to moderate the interactions of the ECF module with various EcfS (Energy-coupling factor transporter substrate-binding protein) proteins to form different transporter complexes (Zhang *et al.*, 2014). It is, however, the S component of the complex that is the Ni²⁺ binder, but in order to transport the substrate the T component and the ATPases are required. However, sequence similarity of *B. subtilis* EcfT with NikQ or CbiQ shows approximately 26% homology, so may not be involved in urease activation in *B. subtilis*.

Some proteins are associated with multiple COG's. Those proteins are upregulated in COG I and Q (Lipid transport and metabolism and Secondary metabolites biosynthesis, transport, and catabolism, respectively) include SrfAB (fold change of 2.54) and SrfAA (fold change of 3.18). Surfactin has numerous roles and is involved in biofilm formation, has bio surfactant properties and also possesses antimicrobial activity (Luzzatto-Knaan, Melnik and Dorrestein, 2019). Davis *et al.* (1999) studied surfactin in batch culture and determined that *B. subtilis* requires an organic source of nitrogen for growth, and that nitrate is involved in 'switching on' secondary metabolism such as surfactin. They also describe how the increased production of some secondary metabolites is linked to increased levels of nitrate-induced glutamine synthetase (GlnA) (Davis, Lynch and Varley, 1999) which is upregulated in the NLM (fold change 12.41, discussed separately). The production of surfactin is also often associated with stationary phase. It increases aerobic yield growth, as it increases oxygen diffusion. Also in conditions of oxygen depletion, surfactin maintains viability by depolarising the membrane (Arjes *et al.*, 2020). An interesting note is that exopolymeric substances (EPS) such as surfactin can transport divalent cations, which could include Ni²⁺. The work of Li *et al.* (2009) identifies that the structure of surfactin adopts a specific structure in aqueous solutions, and within the peptide ring a 'claw' forms which has the potential to bind divalent cations (Li *et al.*, 2009). Surfactin may therefore be involved in Ni²⁺ transport and the Srf proteins may contribute to the activation of the urease in *B. subtilis*.

Interestingly upregulated in COG H (Coenzyme transport and metabolism), is SirB (fold change 5.62), a Sirohydrochlorin ferrochelatase involved in cobalamin biosynthetic process. Interestingly, in *S. salivarius* there are proteins involved in cobalamin biosynthesis and cobalt

transport (CbiMQO) that also transport Ni²⁺. These genes encode a Ni²⁺-specific ATP-binding cassette transporter (Chen and Burne, 2003). Interestingly, Fujishiro (2019) also deposited a protein structure of *B. subtilis* SirB with Ni²⁺ bound in the RCSB protein data bank database (Fujishiro, 2019). This indicates that SirB, from the CbiX family (involved in the salvage pathway of cobinamide), may play some role in Ni²⁺ transportation in *B. subtilis* and potentially have a role in urease activation.

There are many proteins involved in transport listed above that may be involved in urease activation in *B. subtilis*. These transport systems need to be studied in further detail.

4.2.3.5 Chemotaxis

Also upregulated in NLM and involved in signal transduction mechanisms is DegU. This protein has a fold change of 2.43 in NLM (Appendix table 9-1) and is part of DegS-DegU regulatory system which controls many processes that characterise the growth phase transition from exponential to stationary, i.e. the end exponential phase (Mäder *et al.*, 2002). DegU is also responsible for the control of expression of certain cellular functions, such as flagella formation, biofilm formation and competence. Therefore the upregulation of the DegU regulon regulates specific genes including the *ylxF-fliK-flgD-flgE-swrD-fliL-fliM-fliY-cheY-fliZ-fliP-fliQ-fliR-flhB-flhA-flhF-flhG-cheB-cheA-cheW-cheC-cheD-sigD-swrB* operon. Such proteins as CheA are also upregulated in NLM (fold change of 2.59) (Appendix Table 9-1) and are involved in the transmission of sensory signals from chemoreceptors to the flagella motors which are needed in order to find nutrient sources. This also links to the upregulated putative flagellin YvzB, with a fold change of 2.85, which is involved in cell motility and chemotaxis. Interestingly, McGee *et al.* (1999) hypothesized that flagella biosynthesis and urease activity in *H. pylori* were linked (McGee *et al.*, 1999). A recent study by Gu *et al.* (2017) also tried to establish this link of flagella and urease. It is speculated that flagella play an important role in the colonization of the gastrointestinal mucosa. Those strains with mutant chemotaxis showed less motility and reduced colonisation of *H. pylori*. Further investigation is required to confirm the association between flagella and pathogenicity including urease in *H. pylori* (Gu, 2017).

4.2.3.6 Unknown Function

There are a number of proteins upregulated in the NLM of unknown function. Those proteins that are poorly characterized and therefore poorly annotated are of great interest with regard to understanding urease activation. The proteins under discussion fall only into COG S, function unknown. Often urease accessory proteins have been identified and characterised as COG S, see Table 4-5. These are of interest as even though they fall into the function unknown category, some for example are associated with certain biological roles that could be linked to urease activation in *B. subtilis*, such as metal binding and transport. Some of these interesting proteins observed a fold change of < 3 , so are detailed in Appendix Table 9-1. The proteins include: YufO, an uncharacterised ABC transporter (fold change of 4.55); YfiT, a metal dependent hydrolase with the ability to bind Zn^{2+} and Ni^{2+} (fold change of 2.2), YrdA, a metal ion binding protein (fold change of 1.96), possibly a bacillithiol S-transferase, which often play a protective role in superoxide stress; YydB, an uncharacterized metallophosphoesterase (fold change of 2.45). Other putative proteins upregulated, include YhfE, a putative aminopeptidase with metal ion binding function (fold change of 2.12); YhdG, an uncharacterised amino acid permease (fold change of 3.02) and YxeP, an acetylcysteine deacetylase which binds Ni^{2+} (fold change of 2.28). Potentially, these proteins may play a part in the maturation of urease in *B. subtilis*. These proteins are of great interest for further study due to their basic annotation and possible involvement in urease activation in *B. subtilis*.

4.2.4 Significant Proteins for further analysis

After the further analysis of proteins upregulated in NLM, in terms of the molecular function and metal binding capacity, a list was created including a set of proteins that have potential to play a role in urease activation in *B. subtilis* Table 4-6.

The 1st group in this table of upregulated proteins in NLM are involved in peptide transport. Opp proteins are of interest in this work as it is known that some, such as the Opp2 permease complex (Opp2BCDF) and Opp5A of *Staphylococcus aureus* are involved in Ni^{2+} uptake and determine the urease activity (Hiron *et al.*, 2010). The protein CntA of *S. aureus* formerly Opp1 is part of the ABC transporter complex CntABCDF (Opp1) (Tanaka *et al.*, 2018; Remy *et al.*, 2013). The

complex is involved in the import of divalent metals ions such as Ni^{2+} , Co^{2+} and Zn^{2+} and essential for urease activity (Remy *et al.*, 2013).

There are also other proteins involved in transportation systems selected within this list which include the *dpp* dipeptide transport system and *ecfT*. Certain components of the *dpp* system in *H. pylori* have been investigated for Ni^{2+} transport and its effect upon urease activity (Davis and Mobley, 2005).

Another group of interesting proteins are unknown function proteins which were upregulated in NLM. These proteins were selected based on 1) their COG analysis is the same COG category with existing urease accessory proteins and 2) they can be placed into one of 4 molecular/biological functions i.e. metal binding capability, ATPases, hydrolases or chaperones, as these functions fit with those of current annotated urease accessory proteins.

Table 4-6. *B. subtilis* genes of interest for further study identified from comparative analysis of upregulated proteins in NLM.

Gene/s	Function	COG
<i>dppA-dppB</i>	Permease	EP Amino acid transport and metabolism, Inorganic ion transport and metabolism
<i>oppA-oppB-oppC-oppD-oppF</i>	Permease	EP Amino acid transport and metabolism, Inorganic ion transport and metabolism
<i>sirB</i>	Metal Binding	H Coenzyme transport and metabolism
<i>ecfT</i>	Transmembrane Transporter activity	P Inorganic ion transport and metabolism
<i>yfit</i>	Metal binding	S Function unknown
<i>yhfe</i>	Metal binding	E Amino acid transport and metabolism
<i>yisk</i>	ATPase	Q Secondary metabolites biosynthesis, transport, and catabolism
<i>yjob</i>	ATPase and Metal binding	Post-translational modification, protein turnover, and chaperones
<i>ykfD (oppF/AppF)</i>	Permease	E Amino acid transport and metabolism
<i>ypnp</i>	Metal binding	V Defence mechanisms
<i>ypwa</i>	Metal binding	E Amino acid transport and metabolism
<i>ytID</i>	Permease	P Inorganic ion transport and metabolism
<i>ytrE</i>	ATPase	V Defence mechanisms
<i>yufO (nupO)</i>	ATPase	S Function unknown
<i>yxep</i>	Metal binding	E Amino acid transport and metabolism
<i>yycR</i>	Metal binding	C Energy production and conversion
<i>yydb</i>	Metal binding	S Function unknown

4.3 Summary

This chapter of research focused on the proteomic findings when using NLM (BSS (JW)) compared to using nitrogen excess media (BSS (JW) + Ammonium Sulphate). Proteomic methods were optimised to produce optimum conditions for protein extraction and the enzyme assay. Three buffers (TE, TBS and HEPES) were investigated from similar research methods. The buffer chosen to go forward in this research was 50 mM HEPES, pH 7.4. Although this buffer did not facilitate the greatest number of extracted proteins, it was the buffer in which urease activity was greatest (Figure 4-4), which is important for further analysis, in later chapters, and importantly all 3 urease structural subunits were identified in the proteomic analysis.

The role of nitrogen is important for urease activity in *B. subtilis*. In the 1990s Fisher *et al.* (1999) published numerous papers regarding nitrogen limitation in *B. subtilis* (Fisher, 1999; Wray *et al.*, 1996; Cruz-Ramos *et al.*, 1997; Atkinson and Fisher, 1991). Although the work did not pursue the activation of urease in *B. subtilis*, the work created the foundations of the knowledge regarding nitrogen limitation in *B. subtilis* and importantly described the upregulation of urease in NLC and identified possible regulation involved (Atkinson and Fisher, 1991). There was also research carried out by Eymann *et al.* (2007) which investigated the global gene expression profiling of *B. subtilis* in response to ammonium and tryptophan starvation as revealed by transcriptome and proteome analysis (Eymann *et al.*, 2007). Their work was based on the research by Tam Le (2006) which created the publication 'Proteome signatures for stress and starvation in *Bacillus subtilis* as revealed by a 2-D gel image colour coding approach'. This work detailed novel insights into the two starvation responses of ammonium and tryptophan. They briefly mentioned the *ure* operon of *B. subtilis* and stated that during ammonium starvation there is greater *ureA* transcription than in tryptophan starvation. They carried out Northern blot analysis and determined that, of the 3 promoters of *B. subtilis ureABC*, the majority of the induced *ureABC* mRNA of ammonium starvation samples resulted from the sigma_H-dependent P2 promoter that is controlled by CodY (Tam le *et al.*, 2006). However, it is known from other literature, P2 promoter is positively regulated by TnrA and indirectly by CodY. Their results demonstrated that both starvation conditions induce specific, overlapping and general starvation responses (Eymann

et al., 2007). TnrA the transcriptional regulator of many nitrogen metabolism genes in *B. subtilis*, is also known to be activated in glucose-glutamate medium i.e. similar to the NLM used in this study (Belitsky *et al.*, 2015).

The NLM - BSS (JW) is proven to demonstrate increased urease activity compared to the NPM - BSS (JW) + Ammonium Sulphate (Figure 3-15). The compiled proteomics and bioinformatics data produced a large number of proteins upregulated in NLM compared to NPM. The data was filtered according to annova p score <0.05, max fold change > 3 in order to produce reliable data. Although some proteins are discussed whose fold change is < 3. Notably, consistent with NLM was the upregulation of *amtB/glnK* (formerly *nrgAB*), *nas* genes, *gabP*, *ureABC* and *pucR* (Wray, Ferson and Fisher, 1997b; Brandenburg *et al.*, 2002c).

There were many proteins upregulated in NLM and they have been discussed in specific groups for this study. Those proteins upregulated and involving purine synthesis and degradation confirm the NLC of the media. Importantly PucR is present along with various *puc* genes and AsnZ, Cmk and Xpt. All of which are upregulated due to the NLCs the cells are facing.

There were proteins upregulated in NLM which were involved in nitrate assimilation. Those proteins are activated by TnrA and include NasA, NasD and NasC. Again, these proteins are providing nitrogen sources for the cells due to the NLC the cells are facing in this media. As mentioned previously there are nitrogen related proteins upregulated such as TnrA. The ammonium transporter GlnK and AmtB is also upregulated which transports NH₄⁺ at low concentrations across the cell.

There are numerous proteins upregulated in NLM which involve transport of various substrates. Those of great interest include the *opp* and *dpp* transport systems. There are proteins of these multicomponent systems which may bind Ni²⁺ and have been shown to be involved in urease activation on other species and therefore may be involved in urease activation in *B. subtilis*.

Some upregulated proteins are involved in chemotaxis in NLM, such as DegU, CheA and YvzB. Under NLC the cells will be looking for nutrient availability and so chemotaxis and flagella proteins are activated. Our interest in these regarding urease activation comes from the link to

H. pylori in which chemotaxis and flagella are considered to be involved in urease activation in this bacterium.

There are many proteins upregulated in NLM which include unknown function. Such proteins are YfiT, which binds both Zn^{2+} and Ni^{2+} . This is interesting, as we know UreG proteins also bind both these ions and YxeP binds Ni^{2+} . However, very little is known about these proteins experimentally, hence their unknown function tag.

The proteomic and bioinformatic analysis identified a number of proteins which may be involved in urease activation in *B. subtilis* 168. Table 4-6 lists those genes which encode proteins identified for further investigation regarding their association to the possible activation of urease in *B. subtilis*. The association to urease activation may be via their molecular function being similar to urease accessory protein functions, for example metal binding, and also due to literature searches regarding the misannotation of nickel importers and the identification of nickel binding motifs in a protein. Ni^{2+} transporters can often be misannotated as simply peptide transporters, as they fall into the same family of proteins, PepT - peptide/opine/nickel ABC transporter family (Eitinger *et al.*, 2005). Of those identified, many are proteins defined as part of the peptide transport systems within the cell, which can often be misannotated. A number of unknown function proteins were also identified. Understanding the function, pathways and their impact on urease activity is now imperative in order to identify a possible activation system of urease in *B. subtilis*.

The further work within this thesis will concern those proteins of interest identified as upregulated in NLM. The proteins of interest will include molecular functions that are associated with urease accessory proteins (Table 4-1) or may be identified via literature and Ni^{2+} binding motifs. Further analysis will include knocking out the gene of interest. If the candidate gene is associated with urease activation in *B. subtilis* it will produce reduced or complete abolishment of urease activity. Once this gene is determined, it will be cloned back into the genome and activity will resume to normal levels.

In conclusion, the results of this chapter indicate the relevance of both the culture medium composition and the synthesis of urease during nitrogen starvation in *B. subtilis*. The proteomic

techniques and bioinformatic analysis have identified potential proteins which include those that have Ni²⁺ dependent functional and regulatory connections and ATPases between differentially classed proteins which were investigated further.

**Chapter 5 Investigation of the
roles of specific genes of *B.*
subtilis in urease activation.**

5.1 Introduction

Kim *et al.* (2005) postulated there were unknown proteins that could act as accessory proteins to activate urease in *B. subtilis*. We hypothesised that increased urease activity could associate with the higher expression of urease structural proteins and accessory proteins. Therefore, we utilised a proteomics approach to investigate the upregulated proteins in NLM. We have identified 146 proteins upregulated in this condition. To focus on the activation of urease, we have selected approximately 20 proteins of interest for further analysis as shown in Table 4-6. There are 4 categories including: transporters, metal binding, ATPases and those with unknown functions.

5.1.1 ABC Transporter genes of interest

ABC transporters of *B. subtilis* were of interest from the proteomics and bioinformatics analysis. ABC transporters utilised ATP hydrolysis to drive the import of nutrients into the cell or export toxic compounds or lipids across the membrane.

Peptide transporters enable *B. subtilis* to recognise and understand the environment the cells are in, and so can adjust and adapt to these conditions by the expression of specific genes. In *B. subtilis* 168 the peptide transporters oligopeptide permease (OppABCDF) and the dipeptide permease (DppABCDF) are the main uptake routes for peptides from the environment and are known to have rather relaxed substrate specificities (Kuenzl *et al.*, 2018). The receptor for the system is a lipid-modified membrane anchored binding protein. Oligopeptide transporters, may have thousands of different substrates, and so the binding pocket in the receptor protein has to accommodate ligands of diverse size and structure (Levdikov *et al.*, 2005). Interestingly for this study, these multicomponent systems encode proteins which have similar relationships to proteins that bind Ni²⁺. Those proteins which are known to bind Ni²⁺ include: 1) a solute-binding protein family 5, 2) a peptide/nickel binding protein, MppA-type, 3) an ABC transporter, substrate-binding protein, 4) a Ni²⁺ ABC transporter, substrate-binding protein Nika, 5) a periplasmic oligopeptide-binding proteins (*oppA*) of Gram-negative bacteria and homologous lipoproteins in Gram-positive bacteria (*oppA*, *amiA* or *appA*) and a periplasmic dipeptide-binding proteins of *Escherichia coli* (*dppA*).

5.1.1.1 Misannotation

Misannotation occurs due to computational predictions until experimental validations occur. As stated, peptide transporters are often misannotated due to the family of proteins in which they belong. An example of such misannotation occurred in the Gram-positive pathogen, *S. aureus*. This organism has 4 putative Opps and Opp5A that resembles a substrate binding protein. The *opp2* permease complex (Opp2BCDF) and Opp5A was annotated as an *opp* system, yet, has now been renamed NikBCDE and NikA respectively as they are involved in Ni²⁺ uptake (Hiron *et al.*, 2010).

5.1.2 Zn²⁺ binding proteins

Ni²⁺ are vital in urease activation, however, it is also stated Zn²⁺ is an important metal ion in the activation of urease (Bellucci *et al.*, 2009; Ciurli *et al.*, 2002). UreG is a Ni²⁺ chaperone and as stated a SIMIBI class GTPase. Zambelli *et al.* (2005) detailed that UreG of *S. pasteurii* binds a maximum of 4 Ni²⁺ and 2 Zn²⁺ ions per homodimer. The affinity for Zn²⁺ is 10-fold higher than that for Ni²⁺ (Zambelli *et al.*, 2005b). In *H. pylori* Zn²⁺ enables the stabilisation of the *H. pylori* UreE – UreG complex. The surface exposed Cys⁶⁶ and His⁶⁸ conserved residues in *H. pylori* UreG bind Zn²⁺. Bellucci *et al.* (2009) detailed that the Zn²⁺ dependent interaction between *H. pylori* UreE-UreG and the interdependence between Ni²⁺ and Zn²⁺, suggest a functional role for the metal binding to these accessory proteins, essential for urease maturation (Bellucci *et al.*, 2009). The structure of the *H. pylori* Ure-UreG complex is interesting as the Cys⁶⁶ and His⁶⁸ of UreG, and the His¹⁰² of UreE are in neighbouring positions within the complex. Bellucci *et al.* (2009) hypothesise that this is a novel metal binding site between the two proteins.

D'Urzo *et al.* (2014) identified that UreG of *S. pasteurii* also binds both Ni²⁺ and Zn²⁺ to enable the interactions with the other accessory proteins (D'Urzo *et al.*, 2014). D'urzo *et al.* (2014) identified both *S. pasteurii* and *H. pylori* UreG binds Zn²⁺ with a lower stoichiometry and higher affinity than Ni²⁺. This shows functional conservation in metal selectivity. Experiments by D'urzo *et al.* (2014) identified that the binding of one Zn²⁺ was enough to cause a conformational change in protein structure. When Zn²⁺ was added at higher concentrations (140 µM), disordered protein conformations accumulated and would be consistent with protein destabilisation in the presence of excess metal ions. Merloni *et al.* (2014) described the precipitation of *S. pasteurii*

UreG in conditions of high Zn^{2+} concentrations (Merloni *et al.*, 2014). Metal ion binding is thought to favour protein folding and stability by aiding the proteins structural flexibility (Breydo and Uversky, 2011). Past studies (Fong *et al.*, 2013a; Bellucci *et al.*, 2009) demonstrated that the Zn^{2+} or Ni^{2+} binding enables UreG interactions with UreF and UreE. The conformational changes that occur upon binding of the metal ions proposes that the specific metal binding dictates the specific protein-protein interactions that could affect the protein and also catalytic activity. This was confirmed by Nim *et al.* (2019) in which they stated urease activity can be inhibited by Zn^{2+} , Cu^{2+} , Co^{2+} and Mn^{2+} (Nim and Wong, 2019). This work also confirms the theory in Section 3.5.1, where the addition of Zn^{2+} greatly affected urease activity in *B. subtilis* by causing a decrease in urease activity.

5.1.3 Aims and Objectives

The aim of this research is to understand the activation and regulation of urease in *B. subtilis*. In *B. subtilis* urease activity is greater in NLM, as described in literature, and confirmed in the work reported in Chapter 4. Our hypothesis is that if *B. subtilis* utilises urease accessory proteins to activate urease, then these proteins will also be upregulated in NLM and these proteins may be of current unknown function or misannotated. The upregulated proteins of interest from the proteomic and bioinformatics data will be analysed as knockouts in this chapter, to establish their impact on urease activation in *B. subtilis*.

By utilising knockouts of genes listed in Chapter 4 (Table 4-6), the aim is to understand urease activation in *B. subtilis*. The aim is to evaluate the impact of the gene knockout on urease activity. The hypothesis is that if a protein is involved in the activation of urease in *B. subtilis* then we will see a diminished or even abolishment of activity in the knockout strain.

To achieve this aim there are several objectives or steps: 1) evaluate the knockouts growth by selecting the end exponential growth phase which produces the highest urease activity; 2) carry out an enzyme assay to measure the urease activity in individual knockout strains and 3) follow a proteomics approach to understand the factors that cause the urease activity change.

5.2 Results

The aim of this chapter was to utilise knockouts of specific genes we have highlighted that may be involved in urease activation due to their upregulation in NLM. We aim to understand urease activation in *B. subtilis* by evaluating the impact of the gene knockout on urease activity. The hypothesis that if a protein is involved in the activation of urease in *B. subtilis* then we will see a diminished or even abolishment of activity in a knockout strain. Growth analysis was determined for all knockouts at the end of exponential growth, where urease activity should be greatest determined. If urease activity differed from the wild-type of this study, 168, then proteomic analysis was carried out to identify the role of these knockouts regarding urease activity in *B. subtilis*.

5.2.1 Ammonium Producing proteins

There are a number of proteins identified that may produce ammonia e.g. GuaD and Cdd, under certain conditions. However, only UreABC utilises urea as a substrate. To avoid the detection of NH_4^+ that is not the product of urease a control in the enzyme assay was utilised. The control is simply the removal of urea from the assay, this value is calculated per time point:

$$\text{Baseline OD}_{420 \text{ nm}} = (\text{OD}_{420 \text{ nm}} + \text{Urea}) - (\text{OD}_{420 \text{ nm}} - \text{No Urea})$$

This control removes any possibility of false positives for the enzyme assay.

5.2.2 Analysis of Urease Activity of $\Delta ureC$

The first knockout investigated was $\Delta ureC$. UreC houses the active site of urease. In all ureolytic bacteria, if the active site is knocked out then urease activity is abolished (Murphy and Brauer, 2011; Lin *et al.*, 2012; Hausinger, 2011; Della Scala *et al.*, 2019).

5.2.2.1 Growth analysis of $\Delta ureC$

Growth analysis of $\Delta ureC$ was initially conducted in a 12 well plate using Biotek Synergy plate reader at 30°C and medium linear shaking. The measurement of $\text{OD}_{600 \text{ nm}}$ was taken every 2 hours. Growth analysis detailed a dip in growth at approximately 34 hours in NLM, as shown in Figure 5-1. The dip in growth is most likely due to oxygen levels when using the plate reader. Some cells will die and those that don't will switch on mechanisms for survival which are not reliant on urease and will increase in growth, as seen. The large scale growth curve 500 ml in 2 L flasks at

30°C and 150 rpm did not show this dip in growth as determined in Figure 5-1. End exponential for $\Delta ureC$ was deemed to be similar to 168 at 40 hours.

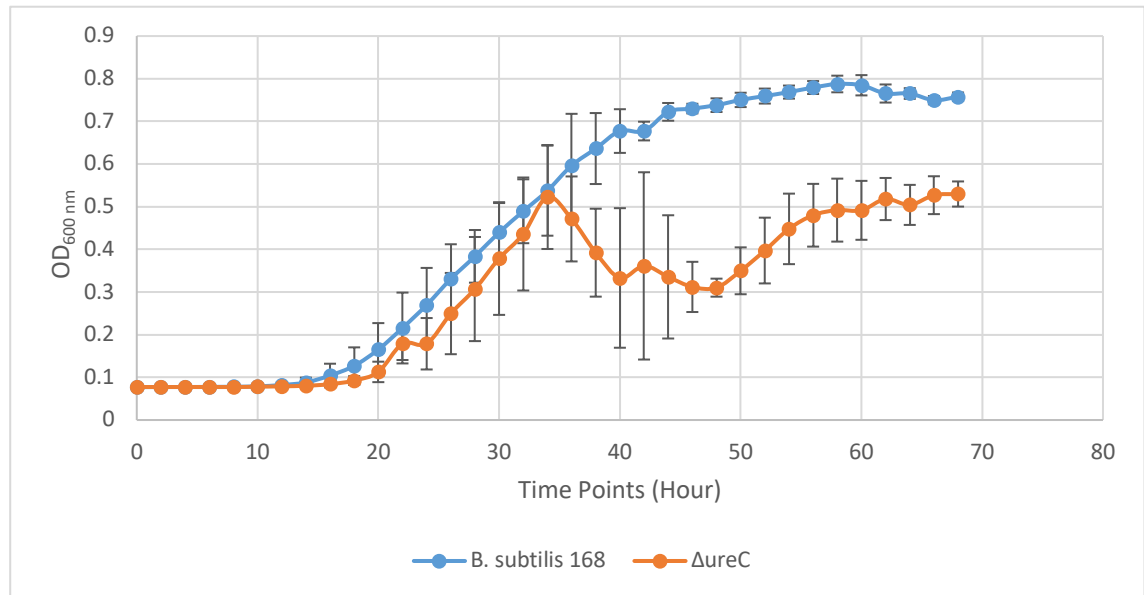


Figure 5-1. Small scale growth curve of $\Delta ureC$ in BSS (JW).

To identify end/late exponential phase of $\Delta ureC$, 2 ml of culture was monitored using the Biotek Synergy plate reader. Data is based on 4 biological replicates.

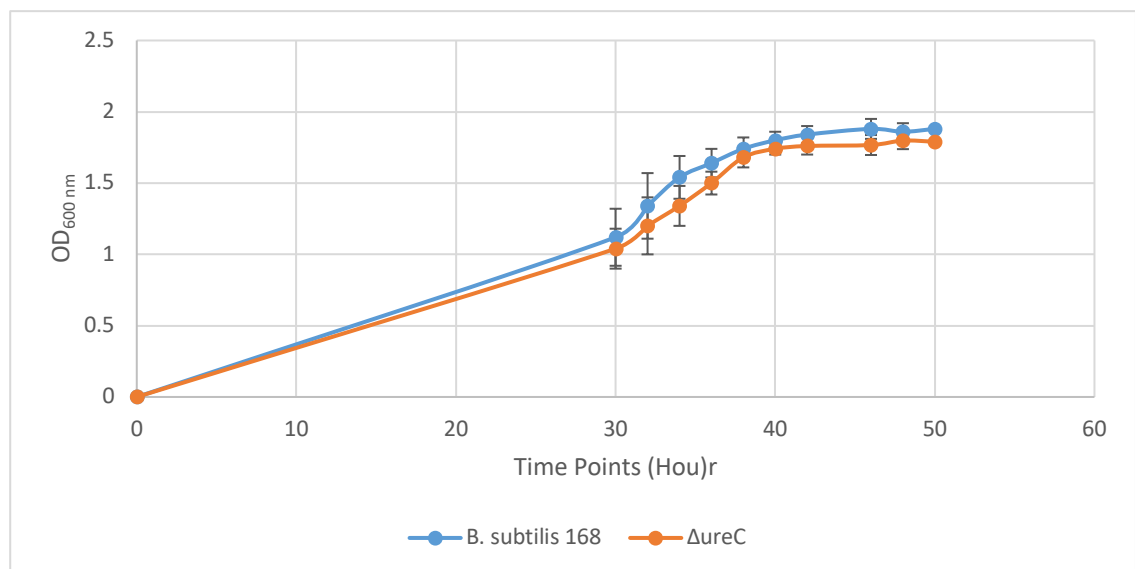


Figure 5-2. Large scale growth curve of $\Delta ureC$ in BSS (JW).

To identify end/late exponential phase of $\Delta ureC$, 500 ml of culture was monitored over 20 hours from time point 30 – 50 hours. Data is based on 4 biological replicates.

5.2.2.2 Enzyme assay of *ΔureC*

Once end exponential was determined urease activity assays were carried out. Whole cell urease activity was determined at both 1 hour and 3 hour time points, and urease activity was negligible in the *ΔureC* compare to strain 168 (Figure 5-3). Figure 5-3 shows negligible activity in *ΔureC* at both 1 and 3 hour time points, whereas activity for 168 is approximately 0.25U/OD at 1 hour.

Mutations involving the urease active site show complete abolishment of urease activity especially in acid resistant organisms (Murphy and Brauer, 2011; Lin *et al.*, 2012; Yamauchi *et al.*, 2019; Della Scala *et al.*, 2019; Brayman and Hausinger, 1996). However, accessory genes involved in the activation of urease may be substituted by other proteins or even possibly might not be essential for full urease activation. It must be noted that this is not true for all accessory proteins, some mutants do diminish all urease activity (Witte, Rosso and Romeis, 2005; Lee *et al.*, 1992). However, these are known, and annotated as specific accessory genes. This knowledge will be of use throughout this research, as a mutant may affect activation efficiency demonstrating diminished activity yet still be a part of the activation pathway in *B. subtilis*.

The enzyme assay results confirmed that the knockout of *ureC* results in the abolishment of urease activity.

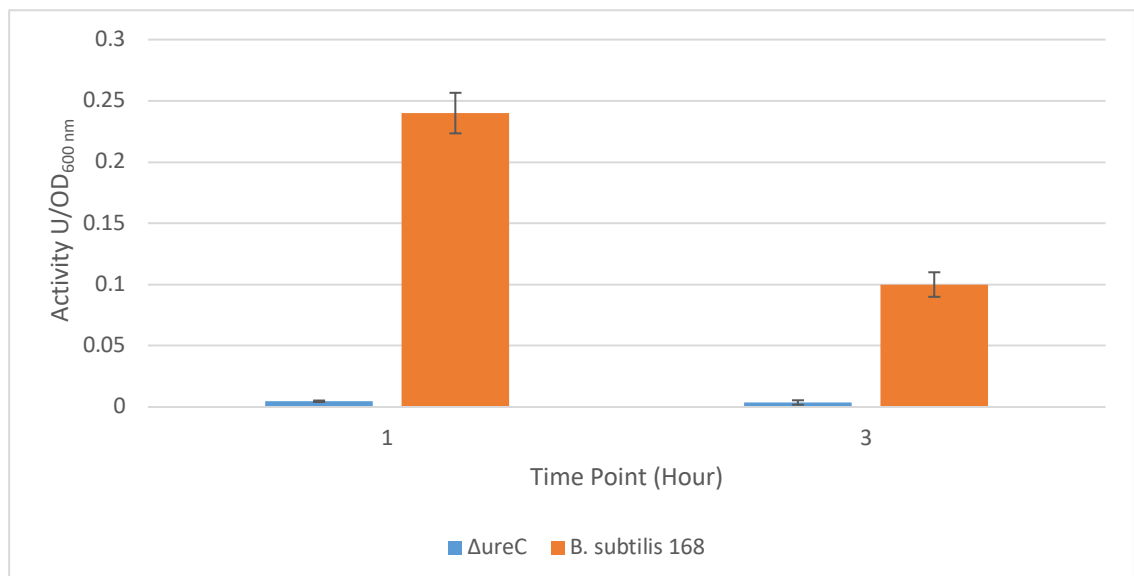


Figure 5-3. Urease activity of *B. subtilis* 168 and *ΔureC* urease in whole cells.

Whole cell urease activity comparison of wild-type *B. subtilis* 168 and *ΔureC* at 1 hour and 3 hour time points. Data is based on three biological and three technical replicates.

5.2.3 Analysis of urease activity of the *opp* operon knockout strains

There were several proteins involved in ABC transport systems that were identified as having potential to be involved in urease activation. They were analysed according to their operon system. The *opp* operon was the first peptide transporter to be investigated as the cumulative results from chapter 4 indicated this transport system may be involved in urease activation in *B. subtilis*. The *opp* transport system (*oppA-oppB-oppC-oppD-oppF*) is regulated by TnrA the nitrogen sensing transcriptional regulator which we know regulates *ureA-ureB-ureC*, *nasA-nasB-nasC-nasD-nasE-nasF*, *pucJ-pucK-pucL-pucM*, *ansZ*, *glnQ-glnH-glnM-glnP*, *gabP*, *pucR-pucJ-pucK-pucL-pucM*, *yrbD*, *nrgA-nrgB*, *tnrA* and *appD-appF-appA/1-appA/2-appB-appC*. *Opp* system is important for the uptake of oligopeptides from growth medium. The *opp* operon in *B. subtilis* is denoted as a peptide transporter, however in other species it has been reclassified as a Ni²⁺ importer, as Lebrette *et al.* (2015) stated; genes encoding Ni²⁺ importers are often misannotated as peptide transporters.

5.2.3.1 Growth analysis of *opp* knockout strains

As previously described, *B. subtilis* shows the optimum urease activity at end of exponential phase. In order to investigate the impact of specific gene knockouts on urease activity the measurement for growth curves of all knockout strains was carried out. Initially the measurement of OD_{600 nm} for the *opp* knockouts was conducted in a 12 well plate using Biotek Synergy plate reader at 30°C and medium linear shaking. However, the *opp* knockouts failed to grow, which was possibly due to oxygen limitation in the wells of the plates. Then, larger volumes (50 ml media in 250 ml conical flask) culture was set up and the knockout strains were grown successfully, as shown in Figure 5-4, which indicated that the limited availability of oxygen in the plate reader may have been a contributing factor to the lack of growth. Then the growth was monitored in larger volumes (500 ml in 2 L conical flask) between 24 to 48 hours to determine the end exponential time point. As shown in Figure 5-5, most *opp* knockouts reach the end of exponential growth phase quicker than *B. subtilis* 168. However, $\Delta oppF$, in particular, was very similar in its growth compared to *B. subtilis* 168. The end of exponential growth took approximately 28 hours to reach end exponential in $\Delta oppA-D$, whereas alike *B. subtilis* 168, $\Delta oppF$ reached the end of exponential growth just before 40 hours. The difference in the growth

between knockout strains and 168 strain will be due to the decreased ability for oligopeptide uptake.

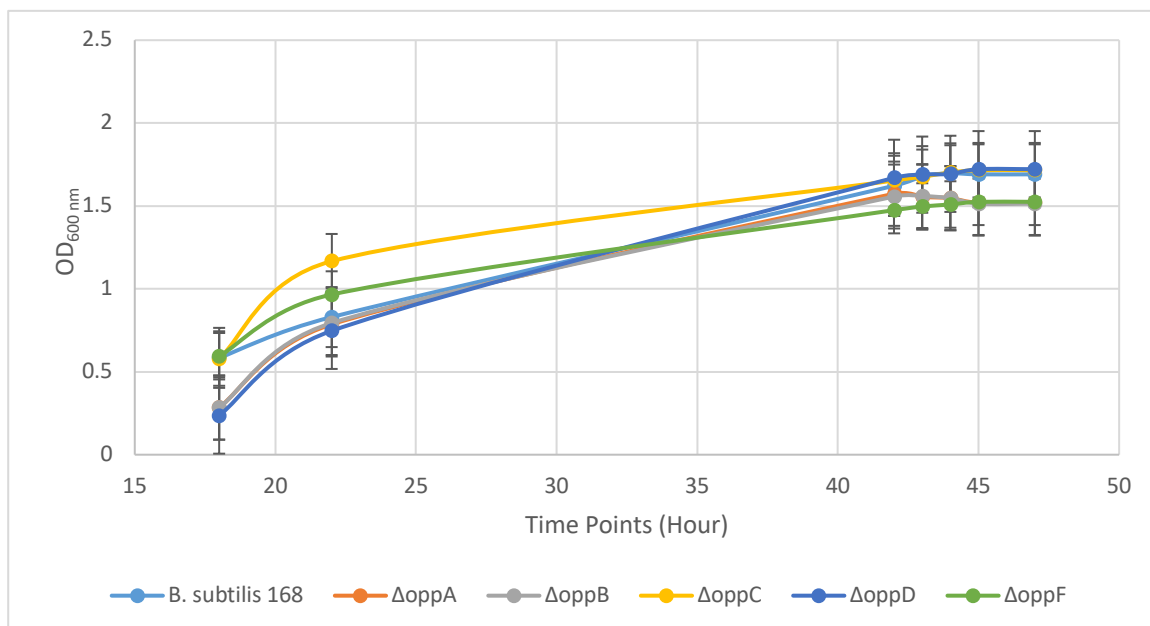


Figure 5-4. Preliminary growth analysis of 5 *B. subtilis opp* knockout strains cultured in 50 ml of BSS (JW) at 30°C and 150 rpm.

Estimated growth phases of *B. subtilis opp* knockout replicates cultured in BSS (JW) 50 ml at 30°C 150 rpm. Time points selected 17, 22, 42, 43, 44, 45 and 47 hours. Data is from 3 biological and two technical replicates.

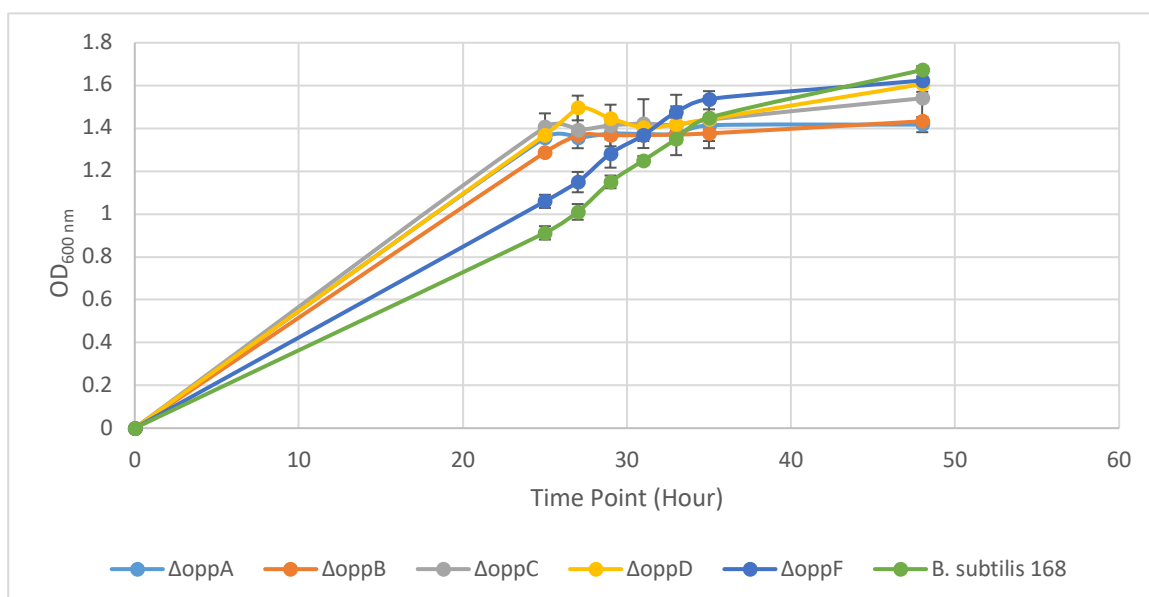


Figure 5-5. Growth curves of *B. subtilis opp* knockout strains in 500 ml of BSS (JW) at 30°C and 150 rpm.

Growth phases of 5 *B. subtilis opp* knockout replicates cultured in BSS (JW) 500 ml at 30°C 150rpm. Time points selected 24, 26, 28, 31,33, 35 and 48 hours. Data is from three biological and two technical replicates.

5.2.3.2 Enzyme assay *ΔoppA* (Whole Cell and CFE)

Oligopeptides play vital roles in bacterial nutrition and cell signalling. The hypothesis that the *opp* system may be involved in urease activation would mean that OppA the SBP could be the Ni^{2+} BP of a Ni^{2+} import system and play a role in urease activation in *B. subtilis*.

B. subtilis ΔoppA was grown in larger culture, as shown in Figure 5-5 and the cells were harvested at 28 hours, which is the end of exponential growth phase. The enzyme assay of *ΔoppA* was conducted in whole cell and CFE. Surprisingly, the results indicated an increase in activity of urease compared to the wild-type. At the 1 hour time point in the whole cell assay, urease activity in the *ΔoppA* is increased from 0.2 U/OD to 0.28 U/OD of the wild-type strain 168 shown in Figure 5-6. The increase is also statistically significant with a p value of 0.018 using t-test analysis. This increase in activity is also mirrored via CFE enzyme assay activity analysis, as shown in Figure 5-7, where urease activity is greater again (approximately 60%) and statistically significant with a p value of 0.009 at the one hour time point in *ΔoppA* compared to the 168 strain.

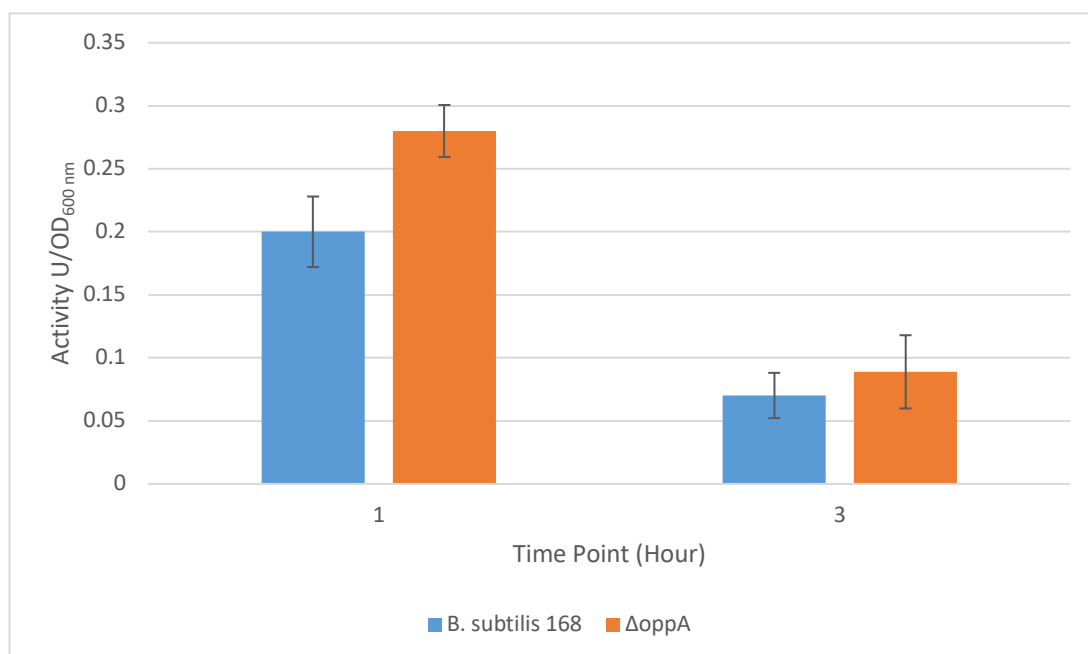


Figure 5-6. Urease activity of *B. subtilis* 168 and $\Delta oppA$ urease in whole cells.

Urease activity is greater in the $\Delta oppA$ compared to the 168 strain at the 1 hour time point. A t-test was carried out from the data at 1 hour, which determined a significant difference ($p = 0.018975192$) between whole cell urease enzyme activity between the wild-type and $\Delta oppA$. Data is based on three biological and two technical replicates.

This increase in urease activity may be due to the increase in nitrogen limitation caused by the knockout. OppA is the SBP of the peptide transport system, a system linked to nutrition by supplying bacteria with essential amino acids and also involved in peptide-mediated signalling (Hiron *et al.*, 2010). If there is reduced import of peptide concentrations in the cytoplasm, the cell is under further nitrogen stress and so will be attempting to re-direct nitrogen from other cellular processes, including urea degradation via urease activity. The increase in urease activity in $\Delta oppA$ may simply be due to the regulation of the enzyme in conditions of nitrogen limitation not only created by the media but also by the knockout. If the transcriptional regulators are upregulated in this knockout condition, this will affect urease expression and therefore urease activity. Still, the proposed hypothesis that OppA was the Ni^{2+} importer for use in urease activation can now be ruled out.

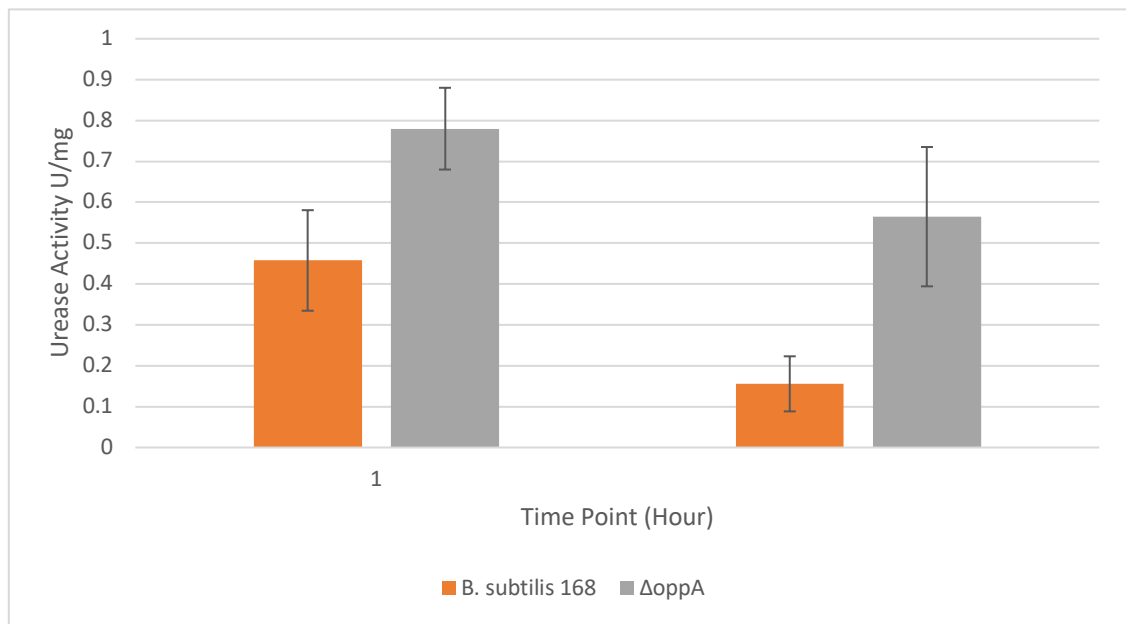


Figure 5-7. Urease activity of *B. subtilis* 168 and $\Delta oppA$ urease in CFE.

Data is based on 3 biological and 3 technical replicates.

There is also the possibility that another protein may be substituting for OppA, for example AppA or DppE. We know the *opp* and *apps* can substitute regarding cellular process such as sporulation and competence (Koide and Hoch, 1994a). However due to a frameshift mutation *B. subtilis* does not include *appA* (Koide, Perego and Hoch, 1999). So, the substitution of AppA can be ruled out. However, the paralogous (different specificity) protein to OppA is DppE (dppE synonym is dciAE). DppE is part of the binding-protein-dependent transport system for dipeptides; probably responsible for the binding of dipeptides with high affinity. It is expressed to facilitate adaptation to nutrient deficiency conditions, which also induces sporulation. The hypothesis is DppE, which belongs to the bacterial solute-binding protein 5 family, may be substituting for OppA.

As detailed in Figure 5-8, there is some shared homology (approximately 42% identity) between DppE and OppA. It could be hypothesised that if DppE is greatly upregulated in $\Delta oppA$ then the protein may be substituting. If this is confirmed, DppE could be expressed under this knockout stress as a scavenging mechanism and enabling the activation of urease efficiently leading to greater urease activity. Proteomic analysis will confirm this hypothesis.

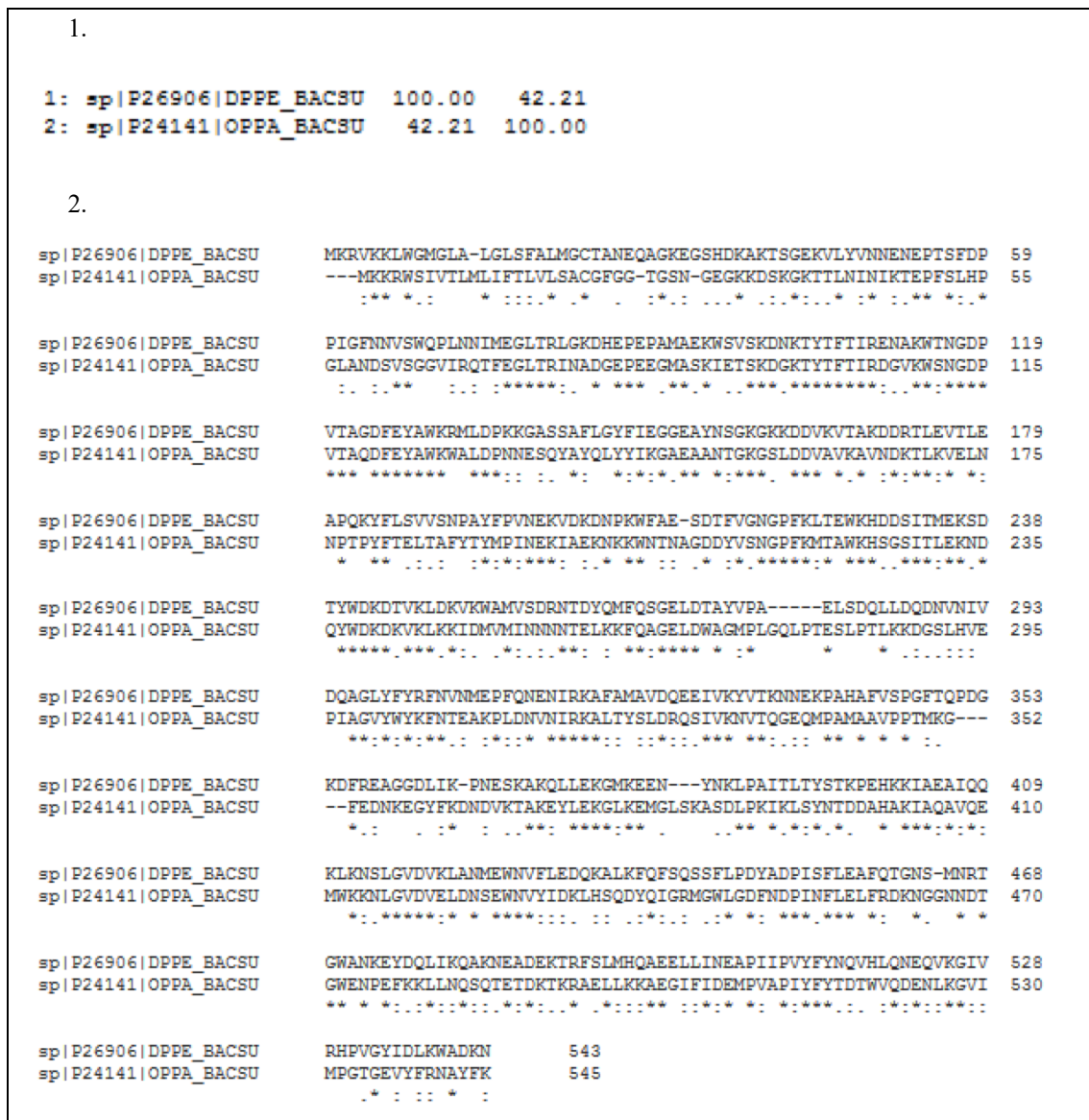


Figure 5-8. Sequence comparisons of DppE and OppA of *B. subtilis* 168.

DppE and OppA are paralogous proteins and share some homology between protein sequences. 1. Percentage Homology of both DppE and OppA 2. Protein sequence comparisons of OppA and DppE detailing homology*.

5.2.3.3 Proteomic analysis of $\Delta oppA$

To investigate the mechanism causing the increase of urease activity, a comparative proteomic analysis between $\Delta oppA$ and 168 strain was applied. In addition to aiding the understanding of the influence of $\Delta oppA$ on urease activity, the comparative proteomics analysis can also further detail the analysis of potential proteins involved in urease activation. It is important to note, urease activity in *B. subtilis* 168 is increased in NLM compared to NPM and also in the $\Delta oppA$ knockout strain compared to the 168 strain. Any proteins upregulated in the wild-type 168 cultured in

NLM, and then upregulated in $\Delta oppA$ condition should be considered important in urease activation in *B. subtilis*.

The proteins upregulated in $\Delta oppA$ were identified via Progenesis LC-MS software ($\Delta oppA$ cultured in NLM and 168 cultured in NLM) and analysed via the same parameters of 2.1.5 and 4.2.1.1. The proteins upregulated were compared to each other under NLC. Initial analysis identified 218 upregulated proteins (Table 5-1) and 324 downregulated proteins in $\Delta oppA$ with a fold change >3 . As seen in Figure 5-9, the upregulated proteins of $\Delta oppA$ were collated into COGs using EggNOG analysis. Those COGs with the greatest number of proteins include E, amino acid transport and metabolism; F, nucleotide metabolism and transport; C, energy production and conversion and S, function unknown. Cells were cultured in a NLM and subjected to further nitrogen limitation by the $\Delta oppA$ condition (i.e. a lack of a SBP in a peptide transport system). The upregulation of proteins in these COGs reflect this limiting condition.

Table 5-1. Proteins upregulated in $\Delta oppA$ cultured in BSS (JW). Proteins were filtered by fold change >3, peptide score >2 and annova p <0.05.

UniprotKB	Accession	COG	Anova (p)*	Fold	Description
P94400	Putative metal chaperone YciC (ZagA)	S	0.00000342	136.3	Zinc chaperone cobalamin synthesis protein
O31619	Sulfur carrier protein ThiS	H	0.000124	46.97	Catalyses the adenylation by ATP of the carboxyl group of the C-terminal glycine of sulphur carrier protein ThiS
O34966	High-affinity zinc uptake system binding-protein ZnuA	P	0.02	18.05	Part of the high-affinity ABC transporter complex ZnuABC involved in zinc import
P80873	General stress protein 39 YdaD	S	0.00000037	15.1	General stress protein
P13243	Probable fructose-bisphosphate aldolase FbaA	G	0.00592	12.63	Catalyzes the aldol condensation of dihydroxyacetone phosphate (DHAP or glycerone-phosphate) with glyceraldehyde 3-phosphate (G3P) to form fructose 1,6-bisphosphate (FBP) in gluconeogenesis and the reverse reaction in glycolysis
P37599	Chemotaxis protein CheV	NT	1.81E-08	11.35	Involved in the transmission of sensory signals from the chemoreceptors to the flagellar motors
P24072	Chemotaxis protein CheY	T	0.000322	11.06	Involved in the transmission of sensory signals from the chemoreceptors to the flagellar motors
Q04789	Acetolactate synthase AlsS	E	0.00000127	10.65	Catalyses the attachment of alanine to tRNA(Ala) in a two-step reaction.
P39810	Flagellar hook-associated protein 1FlgK	N	0.00000133	10.21	Flagellar hook-associated protein

UniprotKB	Accession	COG	Anova (p)*	Fold	Description
P13714	L-lactate dehydrogenase Ldh	C	2.61E-07	10.07	L-lactate dehydrogenase Induced under anaerobic conditions Carbon metabolism
O34610	High-affinity zinc uptake system membrane protein ZnuB	P	0.01	10.04	Part of the high-affinity ABC transporter complex ZnuABC involved in zinc import
P96740	Gamma-DL-glutamyl hydrolase PgdS	M	3.18E-08	9.96	Cleaves, in an endo-type manner, the gamma-glutamyl bond between D-glutamate and L-glutamate of poly-gamma-glutamate (PGA).
O31489	Uncharacterized protein YdcI	K	0.01	9.29	Uncharacterised
P94560	Stress response protein YsnF	S	5.98E-08	9.28	General stress protein.
P28368	Ribosome hibernation promotion factor YvyD	J	1.67E-07	8.38	General stress protein
P18255	Threonine--tRNA ligase 1 ThrS	J	0.00126	8.21	Catalyzes the attachment of threonine to tRNA(Thr) in a two-step reaction: L-threonine is first activated by ATP to form Thr-AMP and then transferred to the acceptor end of tRNA(Thr).
P80866	Vegetative protein 296 SufC	O	8.51E-07	8.09	FeS assembly ATPase feS assembly ATPase SufC
O34833	Uncharacterized protein YceH	P	7.24E-10	7.99	Uncharacterised
O34366	Putative flagellin YvzB	N	0.000121	7.96	Flagellin
P42435	Nitrite reductase [NAD(P)H] NasD	C	0.0000908	7.86	Assimilatory nitrite reductase (subunit) Function: utilization of nitrite as nitrogen source
O06477	Putative sensory transducer protein YfmS	S	2.05E-07	7.25	Soluble chemotaxis receptor
P42175	Nitrate reductase alpha chain NarG	C	5.67E-07	7.09	The alpha chain is the actual site of nitrate reduction

UniprotKB	Accession	COG	Anova (p)*	Fold	Description
O32214	Sulphite reductase [NADPH] flavoprotein alpha-component CysJ	P	0.00817	7.04	Sulfite reductase
P12043	Phosphoribosylformylglycinamide cyclo-ligase PurM	F	4.32E-07	6.5	Part of the phosphoribosylformylglycinamide synthase complex involved in the purines biosynthetic pathway.
P54169	Uncharacterized protein YpgR	C	3.84E-09	6.45	Uncharacterised
P49852	Flavo-hemoprotein hmp	C	0.00000142	6.2	Is involved in NO detoxification in an aerobic process, termed nitric oxide dioxygenase (NOD) reaction that utilizes O ₂ and NAD(P)H to convert NO to nitrate, which protects the bacterium from various noxious nitrogen compounds. Therefore, plays a central role in the inducible response to nitrosative stress.
Q04777	Alpha-acetolactate decarboxylase AlsD	Q	5.77E-08	6.15	Converts acetolactate into acetoin, which can be excreted by the cells.
P54382	Bifunctional protein FOLD	H	2.81E-09	6.03	Catalyzes the oxidation of 5,10-methylenetetrahydrofolate to 5,10-methenyltetrahydrofolate and then the hydrolysis of 5,10-methenyltetrahydrofolate to 10-formyltetrahydrofolate
P24073	Flagellar motor switch phosphatase FliY	N	0.00000037	5.91	Component of the flagellar switch
P12039	Phosphoribosylamine--glycine ligase PurD	F	0.000271	5.84	Phosphoribosylglycinamide synthetase - Purine Biosynthesis

UniprotKB	Accession	COG	Anova (p)*	Fold	Description
P80698	Trigger factor tig	O	0.0000378	5.71	Involved in protein export. Acts as a chaperone by maintaining the newly synthesized protein in an open conformation.
P12042	Phosphoribosylformylglycinamide synthase subunit PurL	F	4.19E-08	5.71	Part of the phosphoribosylformylglycinamide synthase complex involved in the purines biosynthetic pathway.
P09124	Glyceraldehyde-3-phosphate dehydrogenase GapA	G	0.00131	5.68	Involved in the glycolysis.
P96591	Putative thiamine pyrophosphate-containing protein YdaP	E	2.33E-08	5.68	Putative thiamine pyrophosphate
P50735	Cryptic catabolic NAD-specific glutamate dehydrogenase GudB	E	0.000373	5.52	GudB seems to be intrinsically inactive. The cryptic GudB serves as a buffer that may compensate for mutations in the rocG gene and that can also be decryptified for the utilization of glutamate as a single carbon source in the absence of arginine. It is unable to synthesize glutamate $H_2O + L\text{-glutamate} + NAD^+ = 2\text{-oxoglutarate} + H^+ + NADH + NH_4^+$
P96614	DEAD-box ATP-dependent RNA helicase CshA	L	0.0000541	4.94	The most abundant DEAD-box RNA helicase. An ATP-dependent RNA helicase with RNA-dependent ATPase activity
P37942	Lipoamide acyltransferase BfmBB	C	0.00000436	4.82	The branched-chain alpha-keto dehydrogenase complex catalyzes the overall conversion of alpha-keto acids to acyl-CoA and CO ₂ .
P40409	Iron-uptake system-binding protein FeuA	P	1.12E-07	4.6	Involved in the uptake of iron.
P30949	Glutamate-1-semialdehyde 2,1-aminomutase HemL	H	0.03	4.52	heme biosynthesis

UniprotKB	Accession	COG	Anova (p)*	Fold	Description
P11742	Methylated-DNA--protein-cysteine methyltransferase ogt	L	7.76E-07	4.48	Constitutive, DNA repair
O06745	Bifunctional homocysteine S- methyltransferase/5,10-methylenetetrahydrofolate reductase YitJ	E	0.0000388	4.47	Bifunctional homocysteine S-methyltransferase/5,10-methylenetetrahydrofolate reductase. Methionine biosynthesis,
O06478	Putative aldehyde dehydrogenase YfmT	C	8.49E-08	4.35	
P45740	Phosphomethylpyrimidine synthase ThiC	H	3.19E-09	4.33	Condenses 4-methyl-5-(beta-hydroxyethyl)thiazole monophosphate (THZ-P) and 2-methyl-4-amino-5-hydroxymethyl pyrimidine pyrophosphate (HMP-PP) to form thiamine monophosphate (TMP). I
P23446	Flagellar basal-body rod protein FlgG	N	1.47E-10	4.26	Structural component of flagellum, the bacterial motility apparatus
P02968	Flagellin hag	N	0.00151	4.25	Flagellin protein - motility and chemotaxis
P39821	Gamma-glutamyl phosphate reductase ProA	E	0.00554	4.22	Catalyzes the NADPH-dependent reduction of L-glutamate 5-phosphate into L-glutamate 5-semialdehyde and phosphate.
P28366	Protein translocase subunit SecA	U	0.0000227	4.19	preprotein translocase subunit (ATPase). Part of the Sec protein translocase complex. Interacts with the SecYEG preprotein conducting channel.
P94356	Uncharacterized protein YxkC	S	8.04E-09	4.1	Transcriptionally regulated by SigD. Negatively regulated by TnrA under nitrogen-limited conditions

UniprotKB	Accession	COG	Anova (p)*	Fold	Description
P37524	Nucleoid occlusion protein noc	K	0.00000134	3.94	DNA-binding protein- Control of cell division
O32138	Purine catabolism regulatory protein PucR	K	0.00000385	3.94	Activates the expression of pucFG, pucH, pucI, pucJKLM and guaD, while it represses pucABCDE and its own expression TRANSCRIPTIONAL REGULATOR
O07513	Protein hit	FG	0.03	3.72	Hit-like protein involved in cell-cycle regulation
P37869	Enolase eno	G	0.000254	3.71	Catalyzes the reversible conversion of 2-phosphoglycerate into phosphoenolpyruvate. It is essential for the degradation of carbohydrates via glycolysis.
O31620	Hydroxymethylpyrimidine/phosphomethylpyrimidine kinase ThiD	H	2.32E-08	3.64	Catalyzes the phosphorylation of hydroxymethylpyrimidine phosphate (HMP-P) to HMP-PP, and of HMP to HMP-P. Shows no activity with pyridoxal, pyridoxamine or pyridoxine
sQ05852	UTP--glucose-1-phosphate uridylyltransferase GtaB	M	0.000364	3.63	Catalyzes the formation of UDP-glucose from glucose-1-phosphate and UTP.
O32165	FeS cluster assembly protein SufD	O	0.00302	3.63	The SufBCD complex acts synergistically with SufE.
P05649	Beta sliding clamp DnaN	L	0.0000452	3.54	DNA polymerase III
P37512	Uncharacterized protein YyaL	O	0.00138	3.51	Uncharacterised
P35136	D-3-phosphoglycerate dehydrogenase SerA	E	0.0085	3.46	Phosphoglycerate dehydrogenase
P29072	Chemotaxis protein CheA	T	0.000285	3.42	Two-component sensor kinase, chemotactic signal modulator

UniprotKB	Accession	COG	Anova (p)*	Fold	Description
P71011	Antilisterial bacteriocin subtilosin biosynthesis protein AlbA	S	0.02	3.41	Radical S-adenosylmethionine enzyme, antilisterial bacteriocin (subtilosin) production
Q9KWU4	Pyruvate carboxylase pyc	C	0.000637	3.38	Catalyzes a 2-step reaction, involving the ATP-dependent carboxylation of the covalently attached biotin in the first step and the transfer of the carboxyl group to pyruvate in the second
P42434	Assimilatory nitrate reductase catalytic subunit NasC	C	0.0000296	3.35	Nitrate reductase (catalytic subunit)
O07621	Heme-based aerotactic transducer HemAT	C	1.84E-07	3.31	molybdopterin oxidoreductase
P54419	S-adenosylmethionine synthase MetK	H	0.000614	3.3	S-adenosylmethionine synthetase
P42980	Methylglyoxal synthase MgsA	G	0.000045	3.3	methylglyoxal synthase
P39645	Putative heme-dependent peroxidase Ywfl	S	0.0000562	3.2	biosynthesis of heme
P54482	4-hydroxy-3-methylbut-2-en-1-yl diphosphate synthase (flavodoxin) IspG	I	0.0000349	3.16	MEP pathway of isoprenoid biosynthesis
P42974	NADH dehydrogenase AhpF	O	0.000105	3.13	NADH dehydrogenase - resistance against peroxide stress
P12048	Bifunctional purine biosynthesis protein PurH	F	0.00000833	3.12	Phosphoribosylaminoimidazole carboxamide formyltransferase - Purine Biosynthesis
P35163	Transcriptional regulatory protein ResD	T	0.000424	3.11	Member of the two-component regulatory system ResD/ResE. Required for the expression of resA, ctaA, qcrABC and fnr; activation role in global regulation of aerobic and anaerobic respiration also nas genes
P70999	Agmatinase SpeB	E	0.00000232	3.07	Catalyzes the formation of putrescine from agmatine CREATES UREA
O06483	Uncharacterized glycosyltransferase YfnE	M	0.02	3.05	Similar to chondroitin synthase

UniprotKB	Accession	COG	Anova (p)*	Fold	Description
P54551	Uncharacterized protein YqjN	E	0.00036	3.04	Uncharacterised
P45694	Transketolase tkt	G	0.0000422	3	Transketolase

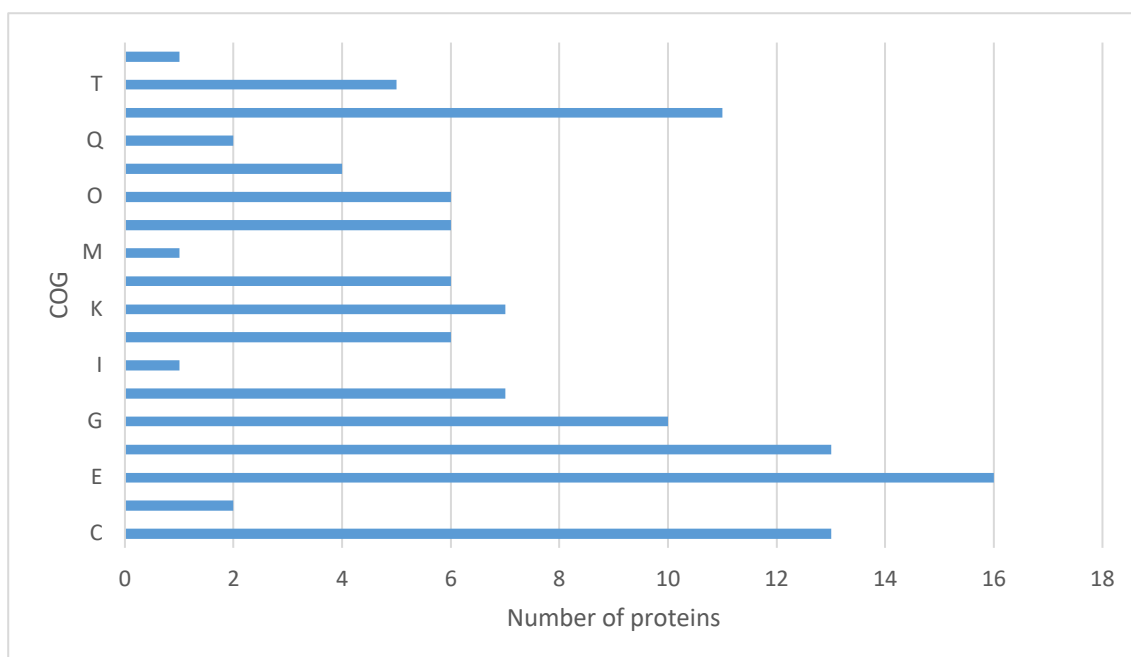


Figure 5-9. COG analysis of proteins upregulated in $\Delta oppA$.

The upregulated proteins cover a range of COGs with E, amino acid transport and metabolism the highest followed by F, nucleotide metabolism and transport and C, energy production and conversion.

The downregulated proteins of $\Delta oppA$ were grouped into COGs as shown in Figure 5-10. Figure 5-10 details many proteins downregulated in $\Delta oppA$ as characterised as COGs S and E. Interestingly, downregulated in $\Delta oppA$ are all the Opp transport system and Dpp transport system which are placed in (E). Which erases the hypothesis DppE may be substituting for OppA as it is downregulated in $\Delta oppA$ and unlikely to be contributing to urease activity. This downregulation of the peptide transporter systems is clearly linked to OppA and its involvement in the expression of these proteins. Also downregulated is CodY with a fold change of 6.63. As CodY represses expression of the P2 and P3 promoters of *ureABC* (Wray, Ferson and Fisher, 1997b) its downregulation is interesting regarding the expression and activity of urease as it is downregulated then urease is greatly expressed.

Table 5-2. Proteins downregulated in $\Delta oppA$ with fold change >3

Protein Accession and Description	COG	Anova (p)*	Fold
P24141 Oligopeptide-binding protein OppA	E	8.33E-10	Infinity
O06484 Uncharacterized protein YfnF	S	0.00000513	43.49
O31542 Uncharacterized protein YfnD	S	0.00000516	21.24
C0SP84 Putative binding protein YtlA	P	0.00000014	21.18
O06486 Probable glucose-1-phosphate cytidylyltransferase	m	0.000000228	16.18
O31449 Uncharacterized HTH-type transcriptional regulator Ybfl	K	3.86E-10	14.98
P54598 Lipoprotein YhcN	S	0.000781	14.46
P39123 Glycogen phosphorylase	G	2.73E-09	13.08
O06485 Putative sugar dehydratase/epimerase YfnG	m	1.58E-10	13.07
O34984 Uncharacterized metallohydrolase YodQ	E	3.2E-11	12.92
O08336 Bifunctional cytochrome P450/NADPH--P450 reductase 2	O	0.0000025	12.41
Q04809 Dipicolinate synthase subunit A	S	3.06E-12	11.75
O06997 Uncharacterized FAD-linked oxidoreductase YvdP	C E	9.87E-08	10.87
Q08352 Alanine dehydrogenase	E	4.08E-09	10.29
O3142 Uncharacterized protein SkfG	S	4.43E-09	10.27
O34704 Uncharacterized protein YxnB	S	2.15E-08	10.14
P46328 Uncharacterized protein YxbD	S	8.11E-09	9.82
P39638 Prephenate decarboxylase	S	0.0000107	9.64
O31663 Methylthioribose kinase	S	2.4E-14	9.38
O34677 Glutamine transport ATP-binding protein GlnQ	E	0.0000028	9.22
O34722 Uncharacterized protein YfmG	S	0.000000794	9.15
P31847 Uncharacterized protein YpuA O	S	0.00000178	8.43
P96722 Putative ribonuclease YwqJ	S	0.000000845	8.29
O31662 Methylthioribose-1-phosphate isomerase	J	2.17E-10	8.26
P39118 1,4-alpha-glucan branching enzyme GlgB	G	0.000762	8.13
O05242 Probable oligo-1,6-glucosidase 3	G	0.000000025	8.1
P39152 Uncharacterized protein YwlB	E	0.0000019	8
Q59HN8 Response regulator aspartate phosphatase	S	0.000000169	7.98
P39640 Dihydroantcapsin 7-dehydrogenase	S	1.04E-09	7.86
P39643 Transaminase BacF	E	1.66E-11	7.82
P39630 dTDP-glucose 4,6-dehydratase	m	1.84E-11	7.77
O32177 3-ketoacyl-CoA thiolase	I	0.00000165	7.65
P39790 Extracellular metalloprotease	O	9.5E-09	7.63
Q08787 Surfactin synthase subunit 3	Q	3.05E-08	7.27
P39696 ComE operon protein 4 O	E	0.0000572	7.24

Protein Accession and Description	COG	Anova (p)*	Fold
O32137 Allantoinase	F	7.81E-10	7.13
O34431 Calcium-transporting ATPase	P	0.000000874	7.1
P12310 Glucose 1-dehydrogenase	S	8.78E-09	7.03
C0SPC3 Putative ADP-ribose pyrophosphatase YjhB	F	0.0000144	6.88
P45913 Uncharacterized protein YqaP	S	0.0000205	6.87
Q04810 Dipicolinate synthase subunit B	H	8.01E-10	6.84
O34538 Uncharacterized lipoprotein YcdA	S	0.000000322	6.78
P71002 Response regulator aspartate phosphatase F	S	0.00000015	6.75
O31782 Polyketide synthase PksN	Q	0.00000024	6.74
P39779 GTP-sensing transcriptional pleiotropic repressor CodY		0.03	6.63
O35002 Carboxy-terminal processing protease CtpB	m	0.0000033	6.54
O31666 2,3-diketo-5-methylthiopentyl-1-phosphate enolase	G	1.96E-08	6.47
Q04747 Surfactin synthase subunit 2	I Q	0.00000632	6.39
P39641 Alanine--anticapsin ligase	I	6.73E-11	6.38
P39639 H2HPP isomerase	S	0.000000471	6.37
P0CI78 50S ribosomal protein L24	J	0.000218	6.32
P54477 Uncharacterized protein YqfT	S	8.28E-10	6.32
P07860 RNA polymerase sigma-F factor	K	0.000000488	6.31
O34767 Oxalate decarboxylase OxdD	K	0.000541	6.28
O34932 Dephospho-CoA kinase	J	0.000000565	6.25
O32201 Protein LiaH	KT	3.32E-08	6.2
O31455 Putative hydrolase YbfO O	S	0.00000334	6.16
P08838 Phosphoenolpyruvate-protein phosphotransferase	G	0.0000949	6.1
O31506 Putative ribonuclease YeeF	U	0.00199	6.08
P24809 Uncharacterized protein YqxJ O	S	0.000857	5.94
C0SPB6 Single-stranded DNA-binding protein B	L	0.0000174	5.9
O3471 Oxalate decarboxylase OxdC	G	8.78E-08	5.89
O31784 Polyketide synthase PksR O	Q	3.87E-10	5.78
P39134 Protein PrkA	S	0.000000274	5.72
P27206 Surfactin synthase subunit 1		0.00000503	5.66
P54586 Uncharacterized protein YhcB	S	0.00002	5.62
P94551 Electron transfer flavoprotein subunit alpha	C	0.0000193	5.61
P46327 Uncharacterized protein YxbC O	S	0.00000253	5.6
O05272 Asparagine synthetase [glutamine-hydrolyzing] 3	E	0.000000114	5.51
P46911 Menaquinol-cytochrome c reductase iron-sulphur subunit	C	0.000000161	5.47
C0SPB4 Uncharacterized ABC transporter ATP-binding protein YhaQ	S	0.00000568	5.42

Protein Accession and Description	COG	Anova (p)*	Fold
P54497 Uncharacterized protein YqgT	E	0.0000794	5.4
O32148 (S)-ureidoglycine--glyoxylate transaminase	E	0.000000884	5.35
P08065 Succinate dehydrogenase flavoprotein subunit	E	0.04	5.28
P96649 Response regulator aspartate phosphatase I	S	0.0082	5.25
sP80865 Succinate--CoA ligase [ADP-forming] subunit alpha O	C	0.00451	5.19
P12669 DNA-entry nuclease inhibitor	S	0.0000356	5.05
O34676 L-lysine 2,3-aminomutase	E	0.0000329	5.04
P42113 Asparagine synthetase [glutamine-hydrolysing] 2	E	0.0000248	4.9
P96723 Putative antitoxin YwqK	S	0.0000297	4.86
O34508 L-Ala-D/L-Glu epimerase	M	0.000000197	4.85
O34389 Probable NAD-dependent malic enzyme 3	C	0.000247	4.83
O34969 Uncharacterized oxidoreductase YfjR	K	0.00000392	4.82
P39120 Citrate synthase 2	C	0.00000112	4.77
O34482 L-asparaginase 2	E	0.00214	4.72
O07564 Glucose-6-phosphate 3-dehydrogenase	S	0.000171	4.66
O34725 Uncharacterized lipoprotein YjhA	S	0.0000152	4.63
O32141 Uric acid degradation bifunctional protein PucL	S	2.27E-08	4.63
P45742 Stress response UPF0229 protein YhbH	J	0.0000911	4.58
Q45595 Putative peptide biosynthesis protein YydG O	S	0.00000152	4.58
O07566 3-oxo-glucose-6-phosphate:glutamate aminotransferase 1	E	0.0000574	4.51
P20429 DNA-directed RNA polymerase subunit alpha	K	8.76E-08	4.49
P26906 Dipeptide-binding protein DppE	E	0.000000818	4.48
P49814 Malate dehydrogenase	C	0.00335	4.43
O31649 Uncharacterized protein YjdH	T	0.00000019	4.42
O32178 Probable 3-hydroxyacyl-CoA dehydrogenase	I	0.0000416	4.37
Q05873 Valine--tRNA ligase O	J	0.00158	4.29
O35010 Gamma-D-glutamyl-L-lysine dipeptidyl-peptidase	M	0.0000385	4.28
P23446 Flagellar basal-body rod protein FlgG	N	1.47E-10	4.26
P94391 1-pyrroline-5-carboxylate dehydrogenase 2	C	3.04E-08	4.25
P17631 Chaperone protein DnaJ	O	0.000000804	4.23
O34544 Biotin carboxylase 2	I	0.00015	4.17
P45942 Ribonuclease YqcG	S	0.000000415	4.06
P54542 Uncharacterized protein YqjE	E	0.00582	3.97
P39124 Glycogen biosynthesis protein GlgD	G	0.00000043	3.85
O34948 Uncharacterized oxidoreductase YkwC	I	0.00725	3.84
P39629 Glucose-1-phosphate thymidyltransferase	M	0.000027	3.83
P96579 Putative ribosomal N-acetyltransferase YdaF	S	9.37E-08	3.81

Protein Accession and Description	COG	Anova (p)*	Fold
O34851 Probable murein peptide carboxypeptidase	V	0.00000151	3.8
P37464 Serine--tRNA ligase	S	0.000966	3.78
P33166 Elongation factor Tu	J	0.02	3.75
P26905 Dipeptide transport ATP-binding protein DppD	E A	0.000188	3.69
Q04795 Aspartokinase 1	S	0.000163	3.69
P40397 Uncharacterized oxidoreductase YhxC	S	0.000018	3.67
P46326 Uncharacterized protein YxbB	S	0.000717	3.63
O34592 AB hydrolase superfamily protein YdjP	S	0.000000162	3.62
O0756 NTD biosynthesis operon regulator NtdR	K	7.03E-08	3.61
O07635 Uncharacterized protein YlaK	S	0.000317	3.6
P42407 Putative UTP--glucose-1-phosphate uridylyltransferase	S	0.0000027	3.46
Q45493 Ribonuclease J1	S	0.000000329	3.46
O32176 Probable acyl-CoA dehydrogenase	I	0.00000197	3.44
O31788 Serine protease AprX O	O	0.0000476	3.43
P26902 D-aminopeptidase	E	0.0000118	3.43
Q45598 Uncharacterized protein YydD	S	0.000172	3.31
P32399 Uncharacterized protein YhgE	S	0.00000328	3.3
Q00828 Response regulator aspartate phosphatase	S	0.00000297	3.28
O07597 D-alanine aminotransferase	E	0.01	3.24
P24136 Oligopeptide transport ATP-binding protein OppD	E	0.0000329	3.19

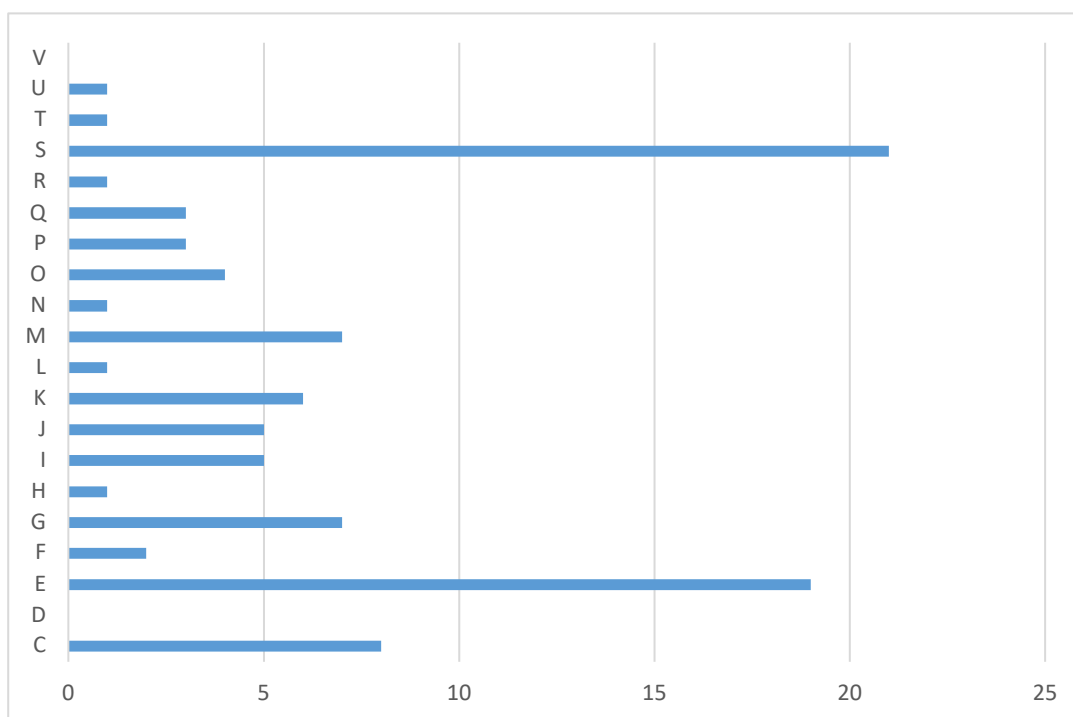


Figure 5-10. COG analysis of proteins downregulated in $\Delta oppA$ cultured in NLM BSS (JW).

Proteins in wild-type 168 and $\Delta oppA$

There are 12 common proteins upregulated in wild-type 168 and in $\Delta oppA$, as described in Figure 5-11. As urease activity is increased in wild-type 168 in NLM and also in $\Delta oppA$, these proteins may be responsible for the activation of urease. The 12 proteins were filtered via fold change >3, listing 7 common proteins in Table 5-3.

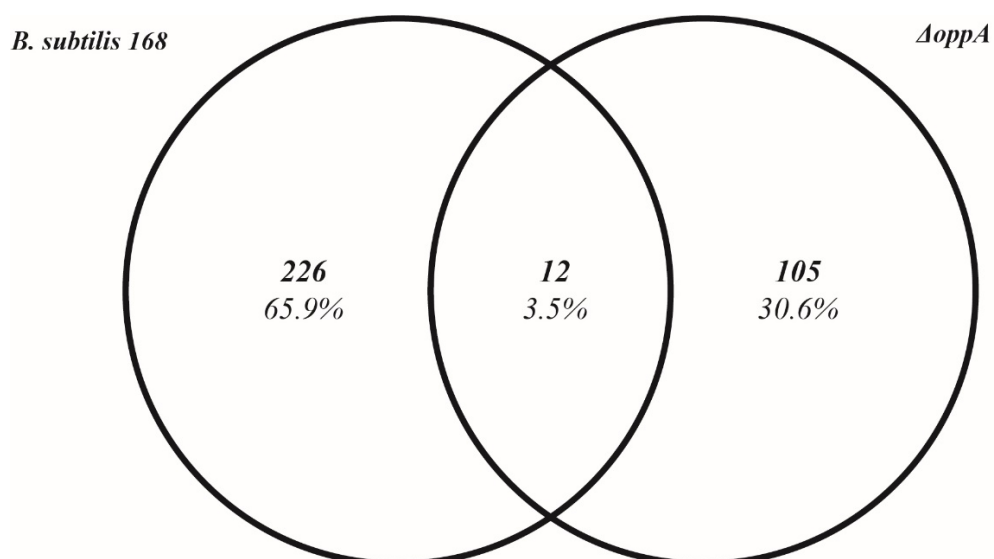


Figure 5-11. Proteins upregulated in $\Delta oppA$ compared to wild-type 168 both cultured in NLM.

These common proteins will be discussed further below regarding their place in the biological systems of the cell and their COG association, noting any association of urease activation. It is important to note UreC is upregulated in this condition, fold change 3.12.

The upregulated proteins of $\Delta oppA$ not present in wild-type 168 will also be discussed regarding their biological relationships, interactions and COG category associated to possible urease activation in *B. subtilis*.

Table 5-3. Proteins upregulated in both wild-type 168 and $\Delta oppA$.

Common proteins in both wild-type 168 and $\Delta oppA$ are identified with fold change and COG listed.

Protein Description	COG Designation	Fold Change in 168	Fold Change in $\Delta oppA$
Urease (UreC)	E	20.16	3.12
Glyceraldehyde-3-phosphate dehydrogenase (GapA)	G	2.26	5.68
Assimilatory nitrate reductase catalytic subunit (NasD)	C	5.37	7.86
Assimilatory nitrate reductase catalytic subunit (NasC)	C	6.69	3.35
Putative flagellin (YvzB)	S	2.85	7.96
Purine catabolism regulatory protein (PucR)	K	3.31	3.94
Chemotaxis protein (CheA)	T	2.53	3.42
Transcriptional Regulator TnrA	K	6.4	3.42

UreC

The enzyme assay results of wild-type 168 and $\Delta oppA$ indicated increased urease activity in NLM compared to NPM and increased urease activity in $\Delta oppA$ when compared to the wild-type when cultured in BSS (JW). Significantly it was important to see an upregulation of UreC, the fold change in NLM compared to NPM was 16.16 and for $\Delta oppA$ compared to the wild-type was 3.12. It is important to reiterate that urease belongs to the hydrolase class of proteins and super family of amidohydrolases and phosphotriesterases. An important reason these proteins are grouped together is they contain active sites that closely resemble each other. Phosphotriesterases contain an active site extremely similar to urease; a carbamylated lysine bridging two metal ions, in the case of a phosphotriesterase, commonly Zn^{2+} . Interestingly there are no accessory proteins that

have been proven biochemically or genetically that are utilised to activate these enzymes (Latip *et al.*, 2019). It is possible urease of *B. subtilis* could be the link between these two systems (Kim, Mulrooney and Hausinger, 2005a).

PucR

The transcriptional regulator, PucR, is also upregulated in both the wild-type 168 and $\Delta oppA$. The function of this protein is the regulation of purine utilisation, regulating the *puc* genes and urease structural units in *B. subtilis* and has been previously discussed in regard to urease regulation in Section 3.1.4.4. The upregulation of PucR in this condition indicates nitrogen is not being efficiently transported due to the knockout and so the cells are utilising other processes to produce nitrogen. However, although PucR is upregulated, the genes it activates (Appendix Table 9-1) are not upregulated in the knockout apart from UreC. We know urease activity is greater in $\Delta oppA$, and this is determined via enzyme assay analysis. We also know ammonia is the by-product of most of the *puc* genes (Figure 4-9) via the purine degradation pathway, so the downregulation of these and upregulation of UreC involved in urea degradation indicates greater urease activity alone in $\Delta oppA$.

TnrA

In both wild-type 168 and $\Delta oppA$, TnrA is upregulated. TnrA is discussed in detail, regarding the regulation of *B. subtilis* urease, in Section 3.1.4.3 and the fold change in $\Delta oppA$ was 3.42. TnrA belongs to the MeR family of proteins and is greatly involved not only in the regulation of urease but in the regulation of nitrogen in *B. subtilis*.

GapA

GapA is upregulated in wild-type 168 and $\Delta oppA$, which both produce an increase in urease activity. GapA is involved in glycolysis and in carbohydrate degradation and is the catabolic enzyme in glycolysis synthesising pyruvate from D-glyceraldehyde 3-phosphate. Although the function of GapA is in glycolysis, it is renowned as a moonlighting protein and also recruits RNases (Gimpel and Brantl, 2016). This protein is most likely upregulated due to the presence of glucose in the media. As Charpentier *et al.* (1998) demonstrate in *E.coli*, when glucose is

present in the growth medium, the expression of specific genes are required for its uptake and metabolism, which include *gapA* and *gapB-pgk* (Charpentier *et al.*, 1998). It is unlikely this protein is involved in urease activation in *B. subtilis* and is simply upregulated due to the growth conditions the cells are encountering.

NasD and NasC

Also upregulated in wild-type 168 and $\Delta oppA$ are the nitrate assimilatory enzymes NasD and NasC, discussed previously in Section 4.2.3.2. In $\Delta oppA$, as detailed in Table 5-3, NasD has a fold change of 7.86 and NasC has a fold change of 3.35. The conditions the cells are facing are nitrogen limiting in both wild-type 168 and $\Delta oppA$, when cultured in NLM. The literature identifies that the nitrate assimilatory enzymes (NasABCDEF) are elevated during nitrogen limitation, in *B. subtilis*, due to being activated by TnrA (Atkinson and Fisher, 1991; Nakano *et al.*, 1998). They are placed in COG C, energy production and conversion and function in nitrate utilization.

CheA

CheA is upregulated in both wild-type 168 and $\Delta oppA$, with a fold change in $\Delta oppA$ of 3.42. This protein is controlled by CheV, which is also upregulated in $\Delta oppA$ with a fold change of 11.35. CheA is a two-component kinase which functions as a chemotactic signal modulator. Linked to this protein is CheV which is involved in the transmission of sensory signals from the chemoreceptors to the flagellar motors and involved in the modulation of CheA in response to attractants. Modulators are able to bind to receptors in order to change the receptors response to a specific stimulus. CheY is another protein upregulated in $\Delta oppA$ with a fold change of 11.06 and it is a two-component response regulator of the flagella switch in the cells. The upregulation of CheA, along with CheV and CheY, identifies that the cells are in survival mode utilizing chemotactic solutions as an adaptive approach to sustain vegetative growth. It is unlikely CheA is upregulated in association with urease activity, but more connected to the growth limitations the cells are encountering.

YvzB

The putative flagellin, YvzB, is also upregulated (fold change 7.96) in both wild-type 168 and $\Delta oppA$ and relates to the upregulation of CheA. This protein is related to movement and chemotaxis when nutrients are low. In order to move to nutrient supply *B. subtilis* has two forms of active movement: swimming and swarming motility, which are powered by rotating flagella. The flagellar structure is complex and is thought to include three architectural domains: the basal body, the hook, and the filament. The filament is the helical propeller composed of the repeating protein monomer flagellin (Yonekura, Maki-Yonekura and Namba, 2003). *B. subtilis* includes in its genome two homologues of flagellin: *yvzB* and *hag* (H-antigen). YvzB is not required for motility and has no known function. It is paralogous to *hag* which is a flagellin protein involved in motility and chemotaxis (Mukherjee and Kearns, 2014). It seems unlikely this protein is upregulated for urease activation and more due to the conditions the bacteria are sustaining.

Importantly the upregulation of PucR and TnrA in both the wild-type 168 and $\Delta oppA$ explain the increased urease activity in both conditions.

5.2.3.1 Transport

There are proteins upregulated in $\Delta oppA$ that are involved in intracellular trafficking, secretion, and vesicular transport according to COG analysis. One of the upregulated proteins of interest is the Zn²⁺ binding protein SecA (fold change 4.19). The protein is an ATPase, and part of the Sec protein translocase complex. SecA has an essential role in coupling the hydrolysis of ATP to the transportation of proteins into and across the membrane. SecA may be upregulated as the *opp* operon will not be functioning to its optimum, as most of the annotated peptide transporters are downregulated in $\Delta oppA$ and so SecA upregulation may enable the translocation of polypeptide chains across the membrane (Bolhuis *et al.*, 1998).

5.2.3.1.1 Metal Transport

YciC, now renamed *ZagA*, was also upregulated in $\Delta oppA$. It was the protein with the greatest fold change of 136.3. Shin *et al.* (2016) identified that YciC (*ZagA*) and the high-affinity Zn^{2+} importer ZnuABC transporter are expressed together (Shin and Helmann, 2016). *ZagA* is a putative metal chaperone considered to be an ATPase and Zn^{2+} metallochaperone and a member of SIMIBI class G3E GTPase family in which UreG is known to belong to. The ATPase is also associated with cobalamin synthesis and repressed under conditions of Zn^{2+} limitation. This protein is of great interest as many UreG proteins are also annotated as involved in cobalamin synthesis (Chen and Burne, 2003). As urease activity in $\Delta oppA$ is greater than we have witnessed in wild-type 168, there is the possibility that *ZagA* is in fact acting as the GTPase (UreG) for urease activation in *B. subtilis* and needs to be investigated further. BLAST analysis carried out revealed that *ZagA* shared 66% homology to CobW/HypB/UreG, of *Kurthia sp. 11kri321*.

PHYRE2 analysis was also carried to predict the structure and function of the protein sequence. The results shown in Appendix Figures 9-2 and Figure 9-3 demonstrate a similarity of the protein folding between *ZagA* and UreG in *K. pneumoniae*, with a 99.5% confidence match and 24% ID match. *ZagA* protein folding structure includes a 99.7% confidence and 20% ID with the crystal structure of HypB (required for maturation of urease) from *H. pylori* in complex which binds two Ni^{2+} . Lastly, *ZagA* also includes 99.4% confidence and 22% ID to the crystal structure of *H. pylori* urease accessory protein UreF/H/G complex (Kelley *et al.*, 2015). Although the IDs are low, this protein was still selected for further analysis on urease activation, due to the high fold changes seen in $\Delta oppA$ and relatively high sequence similarity to UreG in *Kurthia sp. 11kri321*.

As previous research has shown the Opp proteins could be acting as metal transport proteins in other bacteria such as *S. aureus*, therefore proteins upregulated in $\Delta oppA$ cells which are involved in metal transport, are particularly interesting. ZnuA, of the high affinity Zn^{2+} transporter ZnuABC, was upregulated in $\Delta oppA$ to a fold change of 18.5. ZnuB was upregulated in $\Delta oppA$ to a fold change of 10.04. ZnuA is a SBP, hydrophilic lipoprotein anchored to the membrane and ZnuB a permease. Orgura (2011) proposed that the Zn^{2+} transporter ZnuABC is linked to competence in *B. subtilis*. In 2019, it was published that ZnuA was identified in the spore

membrane proteome of *B. subtilis* and, although the function was unknown, the protein was considered to play distinct roles in the accumulation of ions during sporulation (Chen *et al.*, 2019b). ABC transporters transport a wide range of substrates including sugars, metals, peptides, amino acids, and other metabolites (Berntsson *et al.*, 2010). It is possible the SBP ZnuA and ZnuB are upregulated due to the SBP OppA being knocked out and so there is a strong demand on metal transport to be upregulated to compensate for this.

5.2.3.2 General and Nutritional Stress

There are many proteins upregulated only in $\Delta oppA$, which will be a reflection of the mutant strain missing a SBP of the main peptide transporter. The knockout is under stress and many proteins upregulated in this condition relate to both general and nutritional stress. The upregulated trigger factor protein, tig (fold change 5.71) is a ribosome associated chaperone and belongs to COG O - Post-translational modification, protein turnover, and chaperones and is involved in protein folding and export. This protein is able to act as a chaperone by maintaining the newly synthesised protein in an open formation. Newly synthesized proteins often require the assistance of molecular chaperones to efficiently fold into functional 3-D structures. This chaperone may be involved in the protein folding of urease, as it has been identified as being involved in the formation of oligomeric protein complexes (Hoffmann, Bukau and Kramer, 2010) so should be considered for further work.

There are also numerous other proteins of unknown function (COG S) upregulated in $\Delta oppA$. Many of those include YdaD (fold change 15.1), YtxJ (fold change 2.34; see Appendix) and YsnF (fold change 9.28), which are considered to be general stress proteins. It is clear that many stress proteins are upregulated in this particular knockout, and so it seems the cells are creating alternative strategies for survival in this condition of nutrient limitation, which the wild-type uses more effectively than this knockout.

Many anaerobes use pyruvate formate lyase fermentation utilising external electron acceptors. *B. subtilis* can carry out fermentation in the absence of these acceptors and pyruvate dehydrogenase is utilized to metabolize pyruvate (Nakano and Hulett, 1997). As nitrogen is limited in this growth condition and exacerbated by the absence of a SBP in a peptide transport system, the $\Delta oppA$

knockout cannot efficiently utilise nitrogen compared to wild-type. During oxygen limitation, genes transcribed include *narGHJI*, which are respiratory nitrate reductases (Nakano and Zuber, 1998). My results indicate NarG (fold change 7.09) is upregulated in $\Delta oppA$. *B. subtilis* incorporates two specific nitrate reductases; one involved in the assimilation of nitrate nitrogen and the second for nitrate respiration. In nitrate respiration, nitrate reductase reduces nitrate to nitrite, which is then reduced to ammonia by nitrite reductase. Linking back to NasC and NasD upregulation in both wild-type 168 and $\Delta oppA$ is the NasBC complex, of which NasB was upregulated to a fold change of 2.48 (see Appendix). NasB catalyses nitrate reduction and anaerobic respiration is catalysed by, as discussed, NarGHJI enzymes. The transcription of *nasDEF* is also activated by TnrA during nitrogen limited aerobic growth (Nakano and Hulett, 1997); like *ureABC*. This links to anaerobic respiration as the *nasDE* and *narGHI* complexes are induced under low oxygen supply (Nakano *et al.*, 1998). However, the *narGHI* genes are induced by oxygen limitation only (Nakano *et al.*, 1998) which may be a condition $\Delta oppA$ is creating. A condition of anaerobic growth due to its inability to transport certain peptides of nutritional value into the cell.

5.2.3.2.1 Cell Motility

Proteins that enable cell motility respond to changes in the concentration of attractants and also repellents in the growing environment. Proteins upregulated in $\Delta oppA$ can be assigned to COG N - Cell motility, are also assigned to the sigD regulon.

In both wild-type 168 and $\Delta oppA$ 2 specific chemotaxis proteins, CheA and YvzB, were upregulated. This also explains the upregulation of a group of proteins involved in flagellin formation in *B. subtilis* cell movement and chemotaxis, the flagellar basal-body rod protein FlgG with a fold change of 4.26, the flagellar hook-associated protein FlgK with a fold change of 10.21, and FliY with fold change of 5.91. Also upregulated in $\Delta oppA$ was YfmS (fold change of 7.25) annotated with the potential function of a putative soluble chemotaxis receptor. Importantly, relationships between urease activity and flagella have been considered in *H. pylori* as urease and the motility created by flagella in *H. pylori* are essential factors for colonization of the stomach. However, the link between urease and flagella in *H. pylori* is still not understood (Gu, 2017).

5.2.3.3 Nitrogen Assimilation

The growth media is nitrogen limited and the cells are missing a peptide SBP and so are under more of a nitrogen limitation stress. There are processes within the cells in place to enable the cells survival, such as the stringent response, and the transcriptional factors PucR and TnrA.

5.2.3.4 Uncharacterised – Y genes

Numerous proteins were upregulated in COG [S] whose function are described as ‘unknown’. The proteins upregulated which are completely uncharacterised include YxkC (fold change of 4.1) and YobJ (fold change of 2.29).

As $\Delta oppA$ showed greater urease activity when compared to the wild-type 168 in NLM and increased expression of UreC was seen, this directed the research towards understanding the proteomics of the remaining *opp* transport system components and determine their involvement in urease activation as well as those proteins in Table 5-4 . The proteins in Table 5-4 were those considered for further analysis from the $\Delta oppA$ proteomic and bioinformatics analysis, regarding urease activation in *B. subtilis*.

Table 5-4. Proteins of interest identified from $\Delta oppA$ proteomic and bioinformatic analysis proposed to be involved in urease activation in *B. subtilis*.

Proteins of Interest	Fold Change
YciC (ZagA)	136.3
ZnuA	18.5
ZnuB	10.4

5.2.3.5 Urease Enzyme Assays of other *opp* transporter knockout strains

The enzyme and proteomic analysis from $\Delta oppA$ detailed interesting proteins for further investigation. The analysis of the remainder of the *opp* operon was conducted in a similar manner. Cells were harvested at the correct time point for end exponential relating to their strain (Figure 5-5) $\Delta oppB-D$ at approximately 28 hours and $\Delta oppF$ at 40 hours similar to the 168. Cells were washed in 50 mM HEPES, pH 7.4 and an aliquot was used for the WC assay whilst the remainder of the cells were processed further for CFE assay.

Enzyme assays relayed interesting findings as shown in Figure 5-12. Urease activity in WC was slightly elevated in all *opp* knockouts A-D when compared to the 168, however when standard deviations were considered and t-tests was performed, the difference was not statistically significant ($p = >0.05$) in any knockout compared to the 168 strain. $\Delta oppF$ has shown very similar enzyme activity to the 168. The similarity of the growth of $\Delta oppF$ and wild-type along with the enzyme assay results confirm the work of Perego *et al.* (1991) that $\Delta oppF$ was not required for peptide transport in this system.

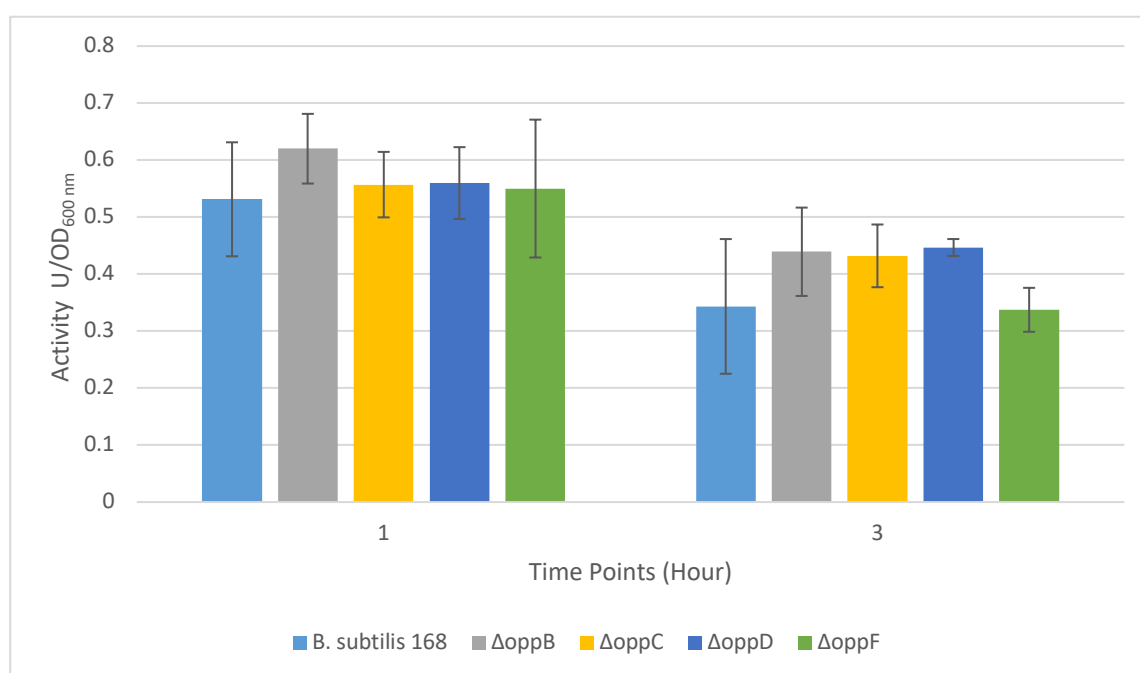


Figure 5-12. Activity of *B. subtilis* 168 and $\Delta oppB-F$ urease in whole cells.

Urease activity in whole cell is comparable amongst $\Delta oppB-F$ and wild-type 168. Data is based on 4 biological and 2 technical replicates.

Urease activity displayed a similar trend between WC and CFE enzyme analysis (Figure 5-13). Urease activity in CFE is still slightly increased in $\Delta oppB$, $\Delta oppC$ and $\Delta oppD$ compared to the 168, and comparable in $\Delta oppF$. However, the difference in urease activity between 168 and $\Delta oppB$, $\Delta oppC$, $\Delta oppD$ and $\Delta oppF$ is not statistically significant ($p = > 0.05$). Based on the results of these urease enzyme assay, we believe the OppB, OppC, OppD and OppF do not play any role in urease activation in *B. subtilis*

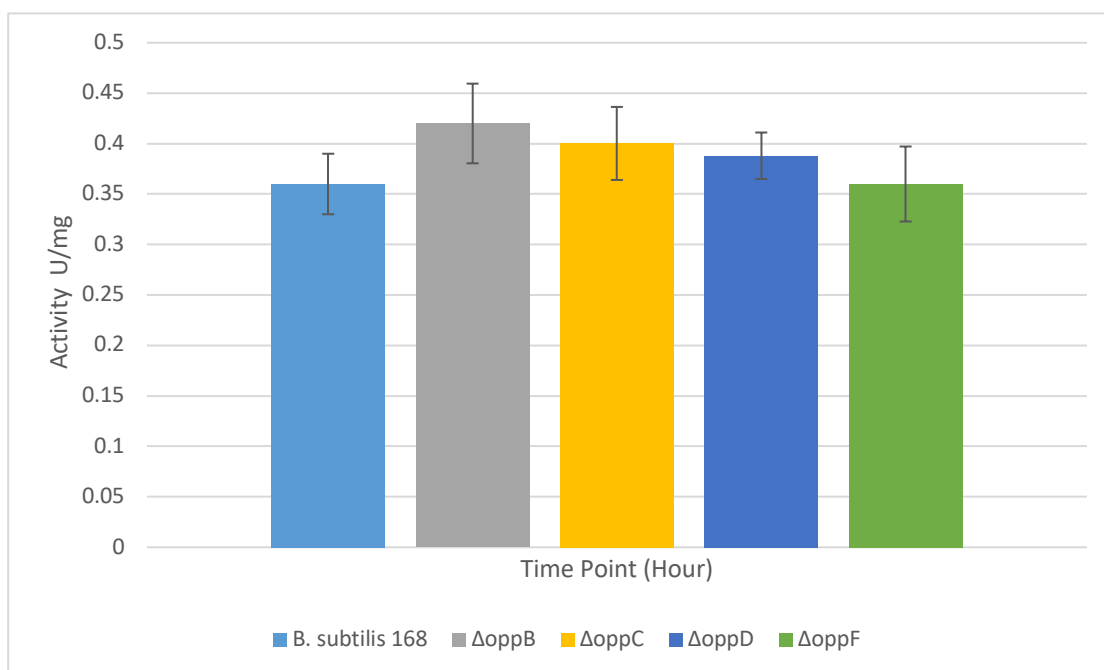


Figure 5-13. Activity of *B. subtilis* 168, $\Delta oppB$, $\Delta oppC$, $\Delta oppD$ and $\Delta oppF$ urease in CFE.

Activity is slightly increased in $\Delta oppB$ compared to the wild-type 168 however not of statistical significance as t test value p 0.176) and $\Delta oppC$, $\Delta oppD$ and $\Delta oppF$ show comparable activity to 168. Data is based on 3 biological and 3 technical replicates (0.6166mg).

Regarding these knockouts, urease expression was first needed to understand the activity. As detailed in Appendix Table 9-4, the comparative proteomic analysis identified UreC in $\Delta oppB$ was upregulated 2.24 fold which details no marked difference in $\Delta oppC$ - $\Delta oppF$ there was no difference in expression. The lack of consistent difference in urease activity between $\Delta oppB$ - F compared to strain 168 meant no in depth proteomic analysis was performed.

5.2.4 Analysis of urease activity of *dpp* operon knockout strains

The *dpp* operon is the 2nd group of transport proteins analysed to investigate the potential role in urease activation using gene knockout strains. Located in the cytoplasmic membrane is the dipeptide permease. The Dpp system is capable of transporting into the cell a variety of di- and tripeptides with structurally and chemically diverse amino acid side chains which detail a low degree of specificity (Kuenzl *et al.*, 2018). Like the *opp* system, the *dpp* system is annotated as peptide transporters. It was important to identify the role of the *dpp* system in urease activity, as other researchers have also tried to identify a link in other bacteria (Davis and Mobley, 2005).

5.2.4.1 Growth Analysis of $\Delta dppA$

Growth curve analysis was carried out on $\Delta dppA$. The result in Figure 5-14 shows that the lag phase in $\Delta dppA$ is much longer than in the wild-type of this study, 168. It demonstrates a shorter exponential phase and does not reach a similar OD as the wild-type. The growth reaches the end exponential at 48 hours. The $\Delta dppA$ displays no distinct stationary phase and cells diminish quickly in this condition. Cheggour *et al.* (2005) discuss the physiological role of the D-aminopeptidase, DppA, which hydrolyses N-terminal residues in D-amino acids containing peptides (D-Ala-D-Ala dipeptide) and is required in peptidoglycan biosynthesis, so cells lacking this gene find it difficult to synthesise the cell wall. The growth analysis of $\Delta dppA$ details a knockout which is stressed in nitrogen limited conditions and struggles to grow.

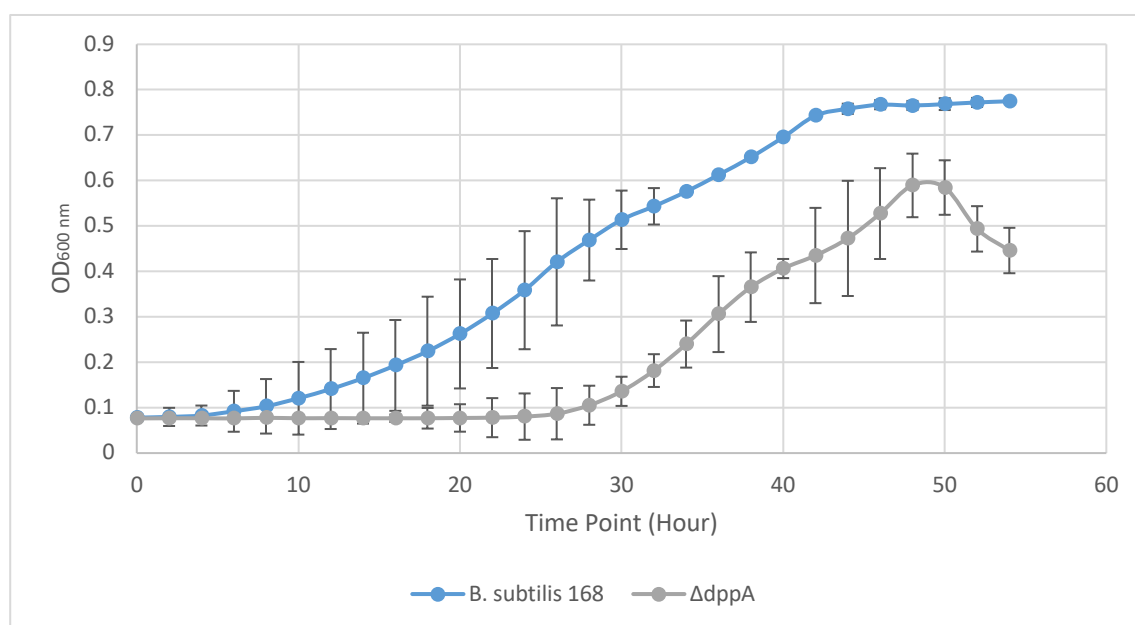


Figure 5-14. Growth analysis of *B. subtilis* 168 and $\Delta dppA$ cultured in BSS (JW) at 30°C 150 rpm.

Growth curve analysis was determined of *B. subtilis* 168 and $\Delta dppA$ in BSS (JW) using the Biotek Synergy Plate reader. End exponential was determined. Data was based on three biological and one technical replicate.

5.2.4.2 Enzyme Assay of $\Delta dppA$

The impact of the knockout of DppA in urease activity was investigated via enzyme assay utilising Nessler reagent in both WC and CFE as it is a transport protein. The whole cell enzyme assay has shown that $\Delta dppA$ presented a decrease in urease activity compared to the strain 168 (Figure 5-15). A decrease in urease activity from a knockout is valuable in understanding urease activation as it may indicate a potential protein capable of activation. Further analysis, using CFE,

has shown even further decrease in the knockout strain (Figure 5-16). Urease activity in the wild-type is approximately 0.35U/mg whereas in $\Delta dppA$ is less than 0.1U/mg.

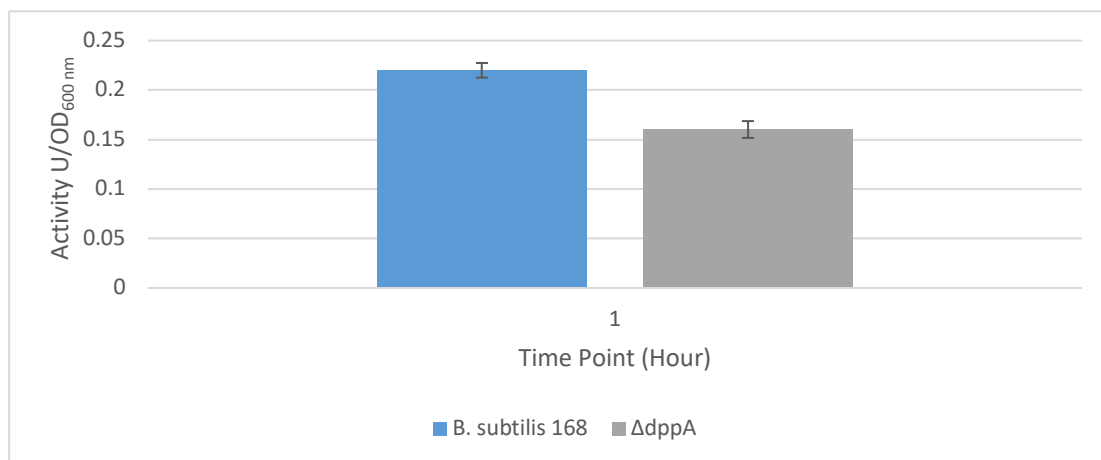


Figure 5-15. Activity of *B. subtilis* 168 and $\Delta dppA$ urease in whole cells.

Urease activity is consistently decreased in the $\Delta dppA$ compared to the wild-type. Data is based on three biological and two technical replicates.

The decrease in activity of $\Delta dppA$ in both CFE and WC enzyme assays highlighted our interest in this protein. There are two potential reasons that could cause the decrease we observed in the assay; 1) the downregulation of the urease structural proteins in $\Delta dppA$ or 2) the lack of activation of the urease structural proteins. This was further analysed through a comparative proteomic approach detailed below.

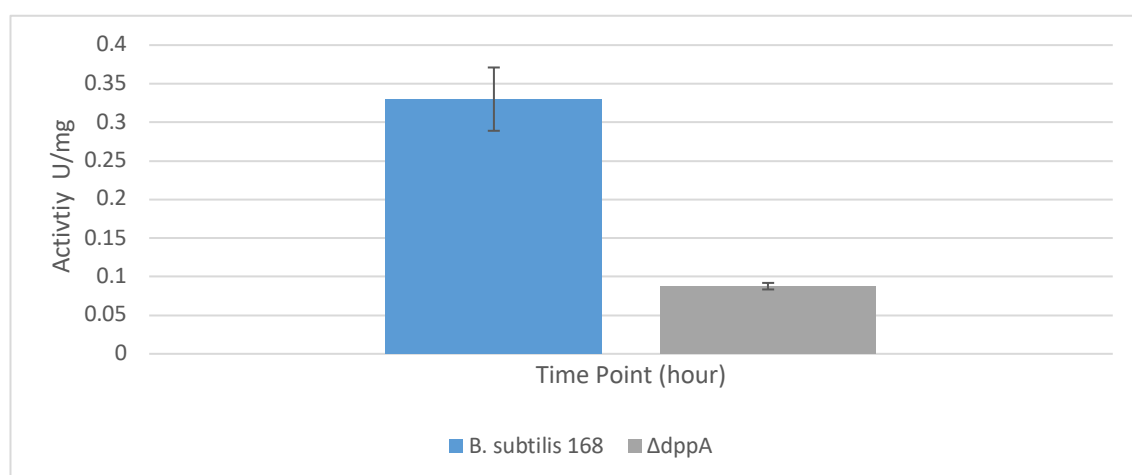


Figure 5-16 Urease activity of *B. subtilis* 168 and $\Delta dppA$ in CFE (0.756mg/ml protein).

Urease activity in the CFE assay is much greater in the wild-type compared to $\Delta dppA$ which is different to the whole cell assay but follows the same trend. Data is based on 3 biological and 2 technical replicates.

5.2.4.3 Proteomic analysis of $\Delta dppA$

It was necessary to ascertain the presence of urease in the *dpp* knockout, as the decrease in urease activity for $\Delta dppA$ as shown in Figure 5-16 was of great interest, as the protein encoded by this knockout gene may be involved in urease activation. As detailed in Appendix Table 9-4, the proteomic results detail that in $\Delta dppA$ urease structural subunits UreB and UreC were downregulated by 15.18 and 3.45 fold respectively, as interestingly was the sigma factor sig^A. The sigA regulon includes *ureABC*. This indicates the decrease of urease activity in $\Delta dppA$ is due to a decrease in the expression of urease in the cells, rather than the lack of the activation in the knockout cells. The DppA knockout therefore has an impact on urease activity but is not involved in the activation of the enzyme.

Interestingly, proteins upregulated in $\Delta dppA$ include OppC with a fold change of 599.98 and OppF with a fold change of 142.1, which indicates OppC-OppF may act as a broad substrate specific permease.

5.2.5 Analysis of urease activity of the High Affinity Zinc Transport System knockout strains

The results from the metal ion additions experiments, in section 2.1.8, and the proteomic knockout analysis of $\Delta oppA$, identified a Zn²⁺ transport system of interest. Zn²⁺ is an essential trace element for all forms of life and serves as structural cofactor for protein folding with the identification of numerous proteins that possess one or more Zn²⁺-stabilized structural motifs (Cox and McLendon, 2000). The divalent metal is a cofactor in many enzymes and DNA-binding proteins. Zn²⁺ sensing by transcriptional regulators almost always involve allosteric regulation (Blindauer, 2015). The binding of Zn²⁺ stabilises protein conformation or creates a conformational change which can increase or decrease an affinity to DNA.

The proteomic and assay results from $\Delta oppA$ indicated that *yciC* (*zagA*) and therefore the *znuABC* complex, as it is often upregulated alongside YciC (Shin and Helmann, 2016), would be of great interest to investigate regarding urease activation in *B. subtilis*.

The *znuA* SBP binds Zn^{2+} and was upregulated by a fold change of 18.5 in $\Delta oppA$, where urease activity was increased compared to wild-type strain 168. As detailed in section 5.1.2, we understand Zn^{2+} , along with Ni^{2+} , is essential for UreG (Ciurli *et al.*, 2002). As stated, the UreG of *S. pasteurii* binds four Ni^{2+} and two Zn^{2+} ions per homodimer. We have hypothesised that ZnuA is upregulated in $\Delta oppA$, due to the demand for metal ions. Interestingly, it is understood that the affinity for Zn^{2+} is 10-fold higher than that for Ni^{2+} ions (Soriano, Colpas and Hausinger, 2000).

5.2.5.1 Growth Analysis of $\Delta znuA$ and $\Delta znuB$

Growth analysis of $\Delta znuA$ was carried out to ascertain late exponential growth phase. The $OD_{600\text{ nm}}$ of the $\Delta znuA$ small scale culture were carried out in the Biotek synergy plate reader, which detailed a slower lag phase and a dip in growth at approximately 30+ hours (Figure 5-17). This was consistent over 3 runs. To confirm the dip in growth, a large-scale analysis was set up in 500 ml media (2 L flasks). The dip in growth observed in the small scale was not present at larger scale (Figure 5-18), therefore we proposed that the reason for the dip in growth, which has been witnessed in other knockouts may be attributed to the lack of oxygen.

The large-scale growth analysis of both $\Delta znuA$ and $\Delta znuB$ identified end exponential to be approximately 40+ hours (Figure 5-18), similar to that of 168.

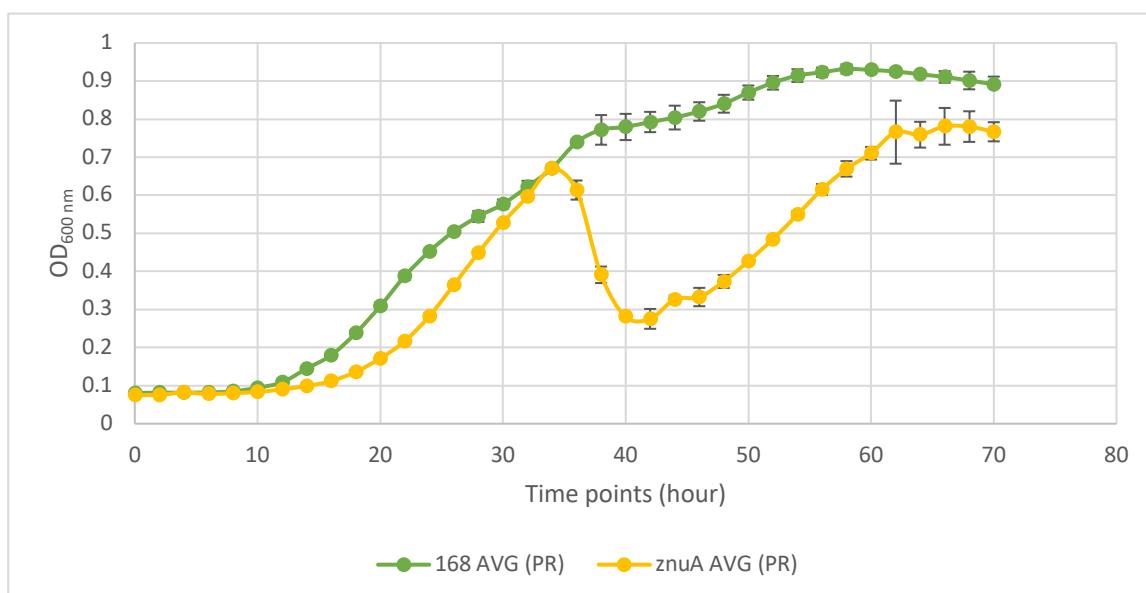


Figure 5-17. Growth of $\Delta znuA$ in BSS (JW) carried out in Biotek Synergy Plate Reader at 30°C and medium shaking.

Data points are based on 3 biological and 3 technical replicates.

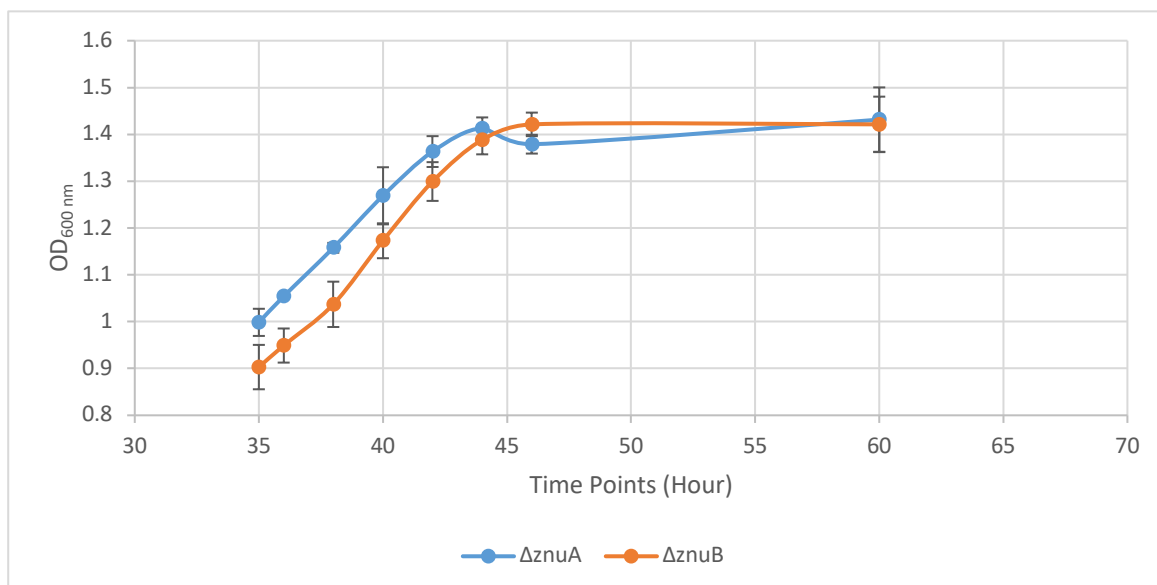


Figure 5-18. Growth analysis of $\Delta znuA$ and $\Delta znuB$ from 35 – 60 hours cultured in BSS (JW) at 30°C 150 rpm.

Data points are based on 4 biological and two technical replicates.

5.2.5.2 Urease Enzyme Assay of $\Delta znuA$ and $\Delta znuB$

Urease activity was analysed at late exponential in $\Delta znuA$ and $\Delta znuB$. Urease activity was seen to detail a marked decrease in both WC (Figure 5-19) and CFE (Figure 5-20) analysis in both knockout strains. As stated, a decrease in urease activity was investigated further to understand the cause, either due to the lack of the activation or the downregulation of urease in knockout strains.

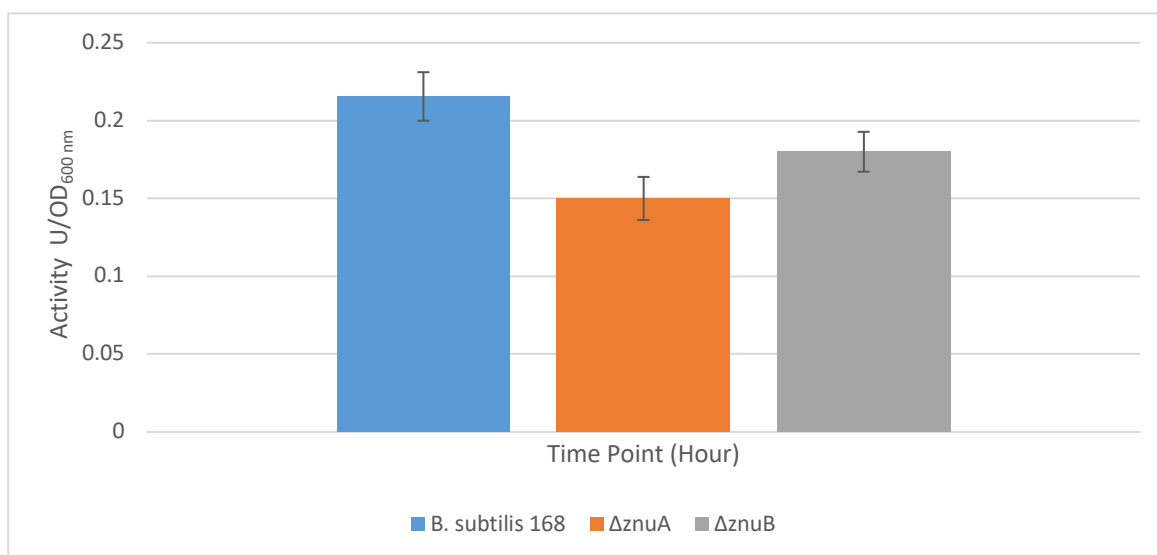


Figure 5-19. Urease activity of *B. subtilis* 168, $\Delta znuA$ and $\Delta znuB$ in whole cells.

Data points are based on 3 biological and 2 technical replicates.

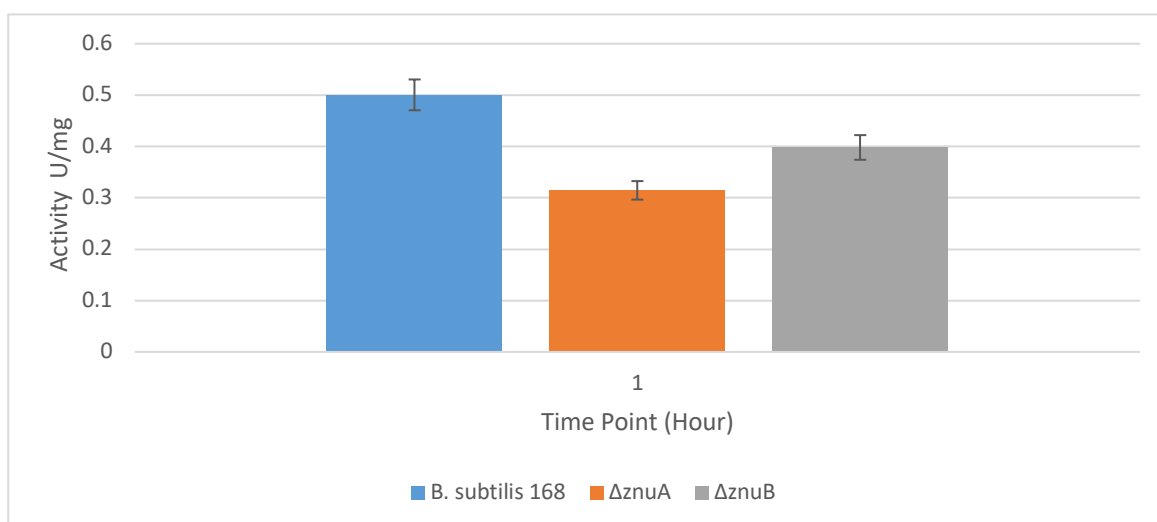


Figure 5-20. Urease activity of *B. subtilis* 168, $\Delta znuA$, $\Delta znuB$ urease in CFE.

Data points are based on 3 biological 2 technical replicates.

5.2.5.3 Proteomic analysis of $\Delta znuA$ and $\Delta znuB$

To investigate the mechanism causing the decrease of urease activity, a comparative proteomic analysis between $\Delta znuA$ and 168 strain, and $\Delta znuB$ and strain 168 was applied.

The proteins upregulated in $\Delta znuA$ and $\Delta znuB$ were identified via Progenesis LC-MS software and analysed via the same parameters in Sections 2.1.2 and 4.2.1.1. Initial analysis identified 125 upregulated proteins in $\Delta znuA$ and 216 downregulated proteins in $\Delta znuA$, with a fold change >3.

In $\Delta znuB$ analysis identified 108 upregulated proteins and 160 downregulated proteins with a fold change >3. As seen in Figure 5-21, the upregulated proteins of $\Delta znuA$ and $\Delta znuB$ were collated into COG's using EggNOG analysis. Those COGs with the greatest number of proteins include E, amino acid transport and metabolism and S, function unknown. It was necessary to identify urease expression in these knockouts as urease activity was lower in both *znu* knockouts. The proteomic data reflected this (see Appendix Table 9-4), as urease expression of UreA, UreB and UreC was downregulated in both $\Delta znuA$ and $\Delta znuB$ compared to the wild-type.

In $\Delta znuA$ UreA, UreB and UreC were downregulated 2.96, 4.24 and 4.71 fold respectively, as was PucR (downregulated 9.69 fold), which positively regulates *ureABC*. Various components of the peptide transport systems of *B. subtilis* are also downregulated in the *znu* knockouts. Downregulated in $\Delta znuA$ are OppA (fold change of 5.23), OppC (fold change of 8.46) and OppD (fold change of 6.43). DppA was downregulated (6.65 fold), as was DppE (8.07 fold). The ammonium transporter, *nrgA*, previously discussed in Section 3.2.3, is also downregulated 68.05 fold in $\Delta znuA$.

In $\Delta znuB$, UreB and UreC were downregulated 3.01 and 3.15 fold, respectively (see Appendix Table 9-4). Regarding the peptide transporters, many were downregulated, including OppA (fold change of 3.07), OppC (fold change of 3.93), OppD (fold change of 2.5), DppA (fold change of 2.66) and DppE (fold change of 2.91). Also downregulated by 4.5 fold was NrgB, which is associated with the regulation of ammonium uptake.

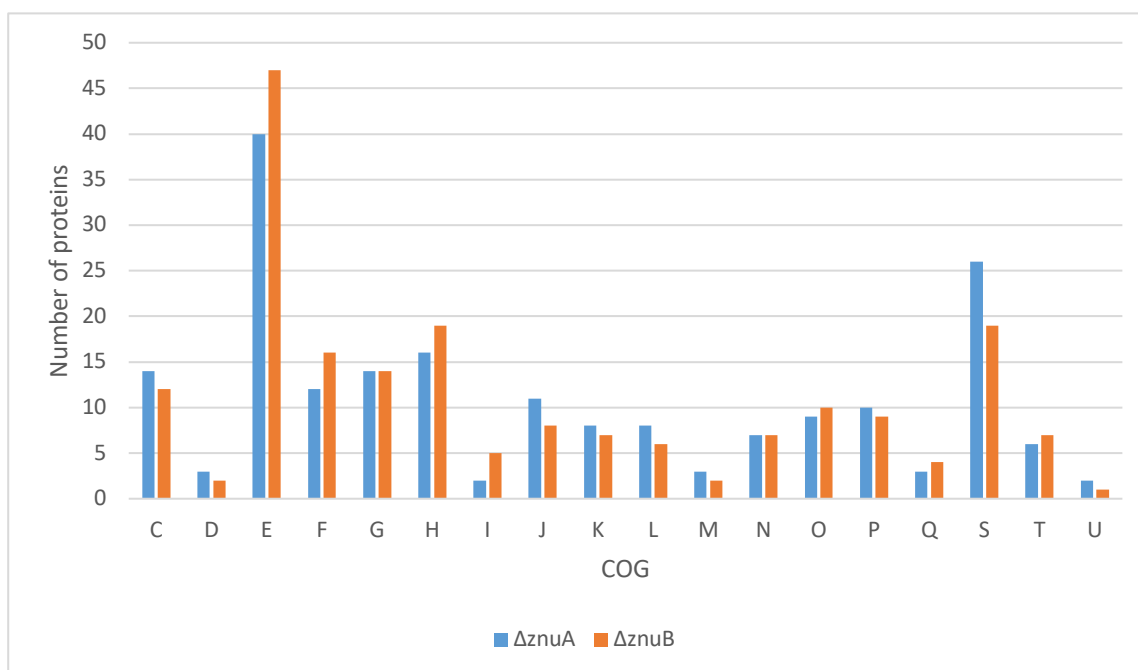


Figure 5-21. COG analysis of proteins upregulated in $\Delta znuA$ and $\Delta znuB$.

Urease activity is decreased in both $\Delta znuA$ and $\Delta znuB$ due to the downregulation of urease (see Appendix Table 9-4) in the knockout strains.

5.2.6 Bioinformatic analysis of YciC and analysis of urease activity in $\Delta yciC$.

The YciC protein was of great interest, as it was upregulated with a fold change of 136 in the $\Delta oppA$ condition and it belongs to the SIMBI class G3E GTPase family and CobW subfamily, which is the same as UreG (GTPase) from other ureolytic microorganisms. Previous researchers have hypothesised that the activation of the apo urease results in the carbamylation of the active site lysine and Ni^{2+} is inserted by a process that requires carbon dioxide and GTP hydrolysis (catalysed by UreG). Ni^{2+} are delivered to UreG by UreE, which receives the metal from an imported pool of Ni^{2+} . YciC, which was renamed as *zagA* (ZagA: "ZTP-activated GTPase A") in 2019 (Chandrangsu *et al.*, 2019) is known to bind GTP, act as a Zn^{2+} chaperone and is involved in cobalamin synthesis (Gabriel *et al.*, 2008). Research has indicated YciC contributes to optimal growth under starvation for Zn^{2+} (Gabriel *et al.*, 2008). Current research identifies YciC as a Zn^{2+} chaperone and a cobalamin synthesis protein. Chen *et al.* (2003) identified previously annotated proteins involved in cobalt transport uptake, and those identified as being involved in cobalamin synthesis, were in fact Ni^{2+} transporters (Chen and Burne, 2003).

5.2.6.1 Bioinformatics analysis of YciC

Urease activity is greater in $\Delta oppA$ compared to the 168 strain and the proteomic data identifies YciC is upregulated by 136.3 fold in $\Delta oppA$ as seen in Section 4.3.1. Based on the previous literature, we hypothesised that this protein may share some similar function as UreG in urease activation. To test this hypothesis, we initially conducted some bioinformatics analysis on this protein. Amino acid sequence alignment analysis has shown that there is 23% sequence similarity between YciC and UreG from *Betaproteobacteria* bacterium *HGW-Betaproteobacteria-13* (Figure 5-22 A). UreG from this organism is a multifusion protein of UreF and UreG. The urease operon of *HGW-Betaproteobacteria-13* consists of UreABCDGF, and UreC from this bacterium shares 67% sequence similarity with UreC from *B. subtilis* (Figure 5-22 B).

Won *et al.* (2004) proposed that the Ni^{2+} binding sites are Gly⁹⁷ – Cys¹⁰³ and Lys¹⁴¹ – His¹⁴⁷. YciC contains Gly⁹⁷ – Cys¹⁰⁴ which is highlighted in green in Figure 5-22 A and Lys¹⁴¹ – His¹⁴⁷ highlighted in purple in Figure 5-22 A. Although conservation of binding sites is low, it is still important to consider the hypothesis that YciC could act as the UreG in *B. subtilis* to activate urease and to investigate further.

A.	
BHGW	--MLPLVRL---LQLASPALPVGAYTYSQGLEWAV-----ECGRVKTEADTQRWI
YCIC	MKKIPVTVLSGYLGAGKTTLLNSILQNREGLKIAVIVNDMSEVNI DAGLVKQEGGLSRTD
	:*:. * * * . . . : * . : * * : * * : * * * * * . *
BHGW	GDLLEWSVARFEAPLVACLLEAWAQGDDDAVRRLNDDFVASRETSELRAETVQMGYSLVR
YCIC	EKLVEMSNGCICCTLRDLLIEVEKLAQDG--RFDYIVIESTGISEPI PVAQTFYSYIDEE
	. * : * * . : . * * * : . * . * : : . : * * * . : : * *
BHGW	MLVELDAWSSLPGWRARLQALDTPAFPTAWTAAAAAW--KVPVADALAAYLWAWLENQV-
YCIC	MGIDLTKFC QLD---TMVTVDANRFWHDYQSGESLLDRKEALGEKDERE IADLLIDQIE
	* : * * : . . * : : . * : * : : : * : . . : : * : * : *
BHGW	MAAVKTVPLGQSAGQRMLAVLGARIPDLVPLAIALPEDDWSNYTPGLALASSHETQYSR
YCIC	FCDVLI LNKC DLVSEQEQLEQLENVLRKLPRA-----RFIRSVKGNV KPEILHTG
	: . * : : : . . . * * : . * * * . : . : . : * : *
BHGW	LFRSGKTALTALCQALRDKYNIAVVTNDIYTAEDAQF-----LVRNE
YCIC	LENFEEASGSAGWIQELTAGHAEHTPETEEYGISSFVY KRRLPFH STRFYRWLDQMPKNV
	* . : : : . * * : . : * . . : : : : : * : *
BHGW	ALAADRIIGVETGGCPHTAIRE DASINLEAVDRLNRSFPGLEIIFVESGGDNLAATFSPE
YCIC	VRAKGIVWCASHNNLALLMSQAGPSVTIEPVSYWVAALPKLEQE QVQEQEPEILEEWDPE
	. * . : * : * * * . : * * * * * : * * *
BHGW	LSDLTLYVIDVSAGDKIPRKGPGITKSDLLVINKIDLAPLVGASLEVMDRDARKMRGER
YCIC	F-----GDRLTQLVFIGTDLDEETITKELDQCLL TEYEF---DSDWSLF--ED
	: * * . . . * . : : : * * . * . : : * * : *
BHGW	PFIFSNLKTGQGLAEIIDFVERQGLLR TVEA
YCIC	PFKWK-----LNQ
	* * : . : :

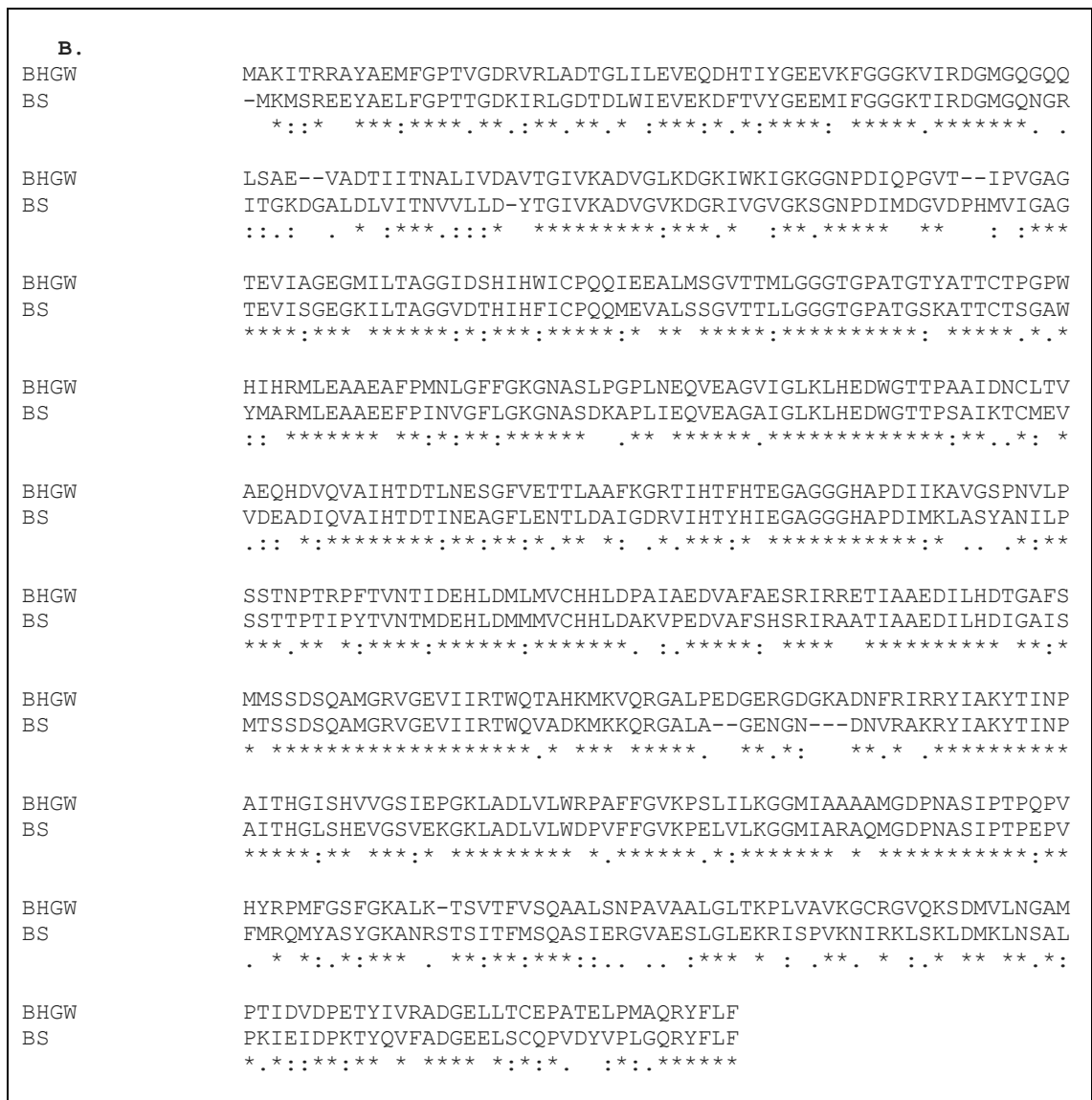


Figure 5-22. Amino acid sequence alignments.

A. *B. subtilis* YciC and UreG from *Betaproteobacteria* bacterium *HGW-Betaproteobacteria-13*. B. *B. subtilis* UreC (BS) and UreC from *Betaproteobacteria* bacterium *HGW-Betaproteobacteria-13* (BHWG) sharing 67% homology.

The software Phyre2 was utilised predict the structure and/or function of YciC. The results of the PHYRE2 analysis were interesting with regards to the function and structure of YciC. The YciC amino acid sequence of *B. subtilis* showed 77% protein folding homology to HypB (urease Ni²⁺ incorporation protein) of *H. pylori* with 99.7% confidence and 24% protein folding homology to UreG of *K. pneumonia* with 99.4% confidence (Figure 5-23).

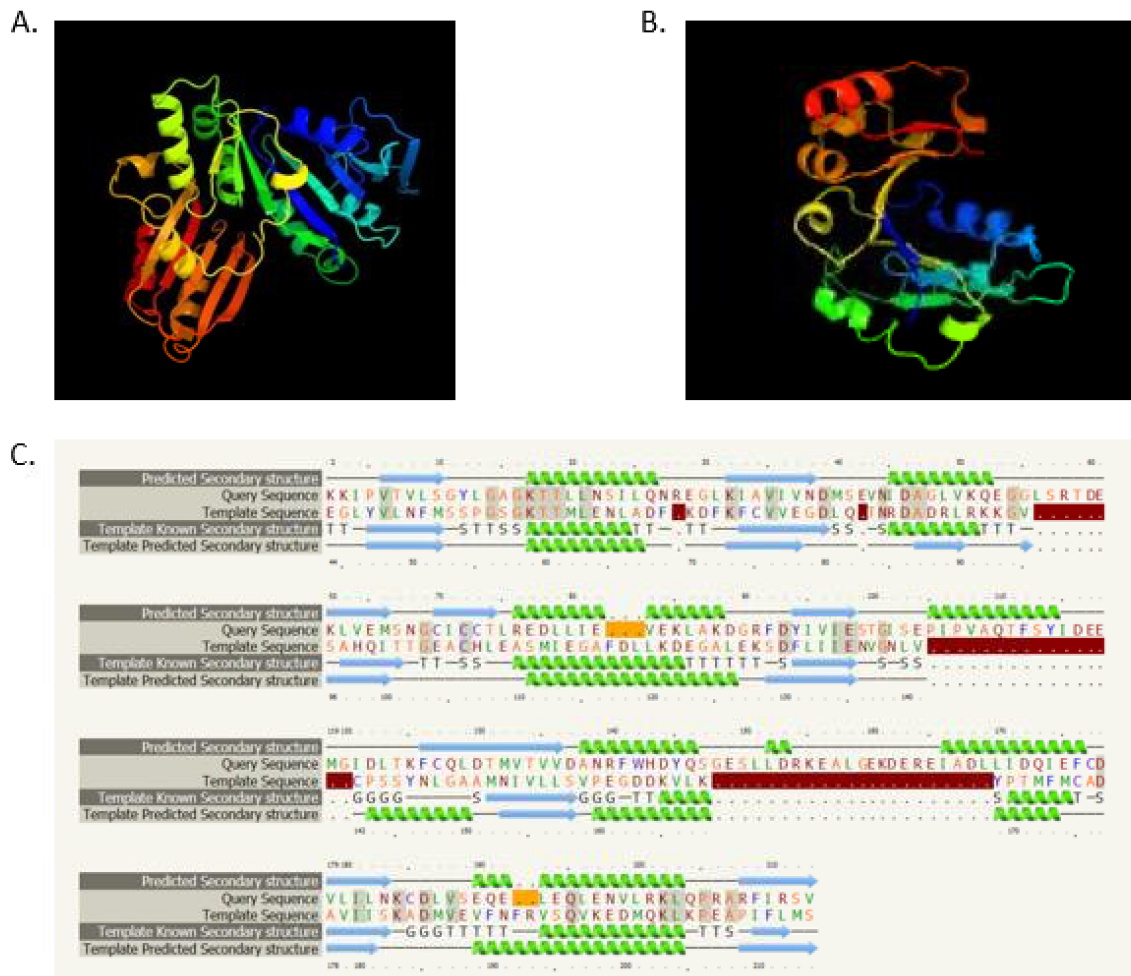


Figure 5-23. Structural and folding analysis of *B. subtilis* YciC using PHYRE2.

A. Protein structure of YciC produced by PHYRE2. B. PHYRE2 image of hydrogenase/urease nickel incorporation protein HypB; showing 99.7% confidence. C. Alignment of YciC *B. subtilis* and HypB *H. pylori*.

5.2.6.2 Growth Analysis of $\Delta yciC$

This information gives us confidence that *yciC* (*zagA*) may play a role in urease activation in *B. subtilis* as UreG. This hypothesis led us to identify the *yciC* knockout should be investigated further for the urease activity.

Growth analysis was carried out on $\Delta yciC$ to determine late exponential urease activity. As shown in Figure 5-24, the growth of $\Delta yciC$ was similar to that of strain 168 until cells enter the end of the exponential stage. The end exponential of $\Delta yciC$ was slightly later in the wild-type 168 at 50 hours and the growth had a very short stationary phase before cell death.

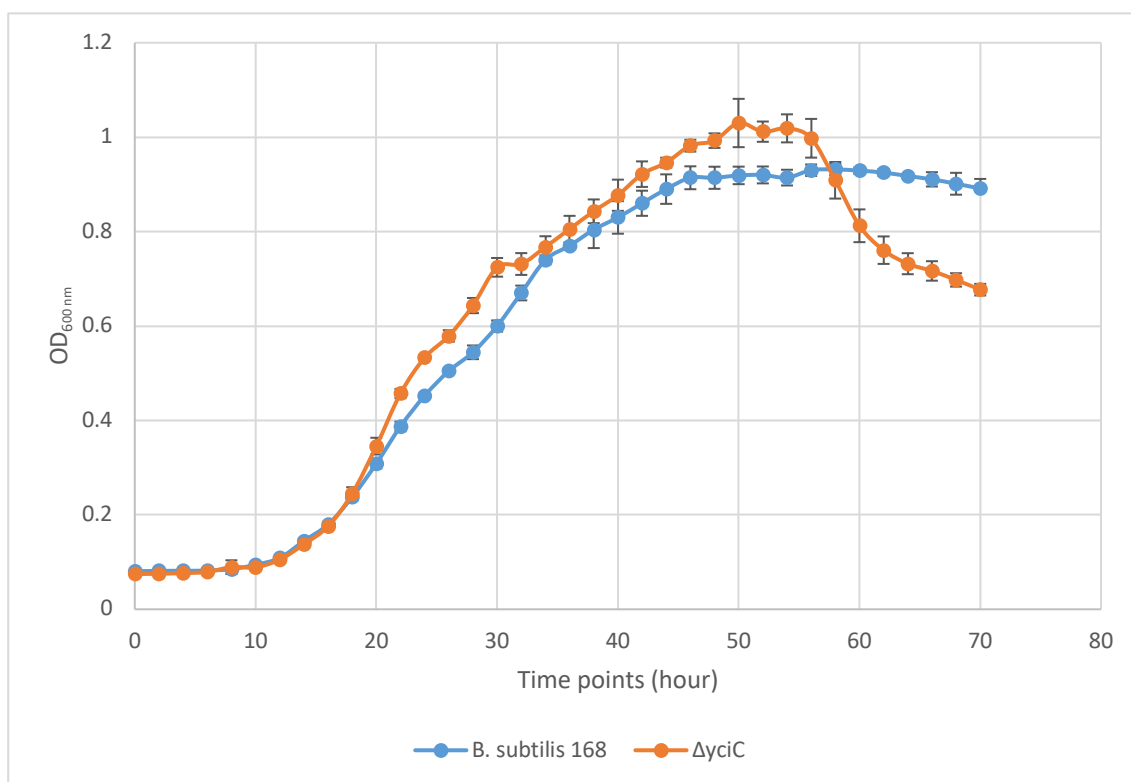


Figure 5-24. Growth analysis of *B. subtilis* 168 and $\Delta yciC$ in BSS (JW).

Growth analysis of *B. subtilis* 168 and $\Delta yciC$ in BSS (JW) using the biotek synergy plate reader at 30°C and medium shaking. Data is based on 4 biological and 2 technical replicates.

5.2.6.3 Urease enzyme assay and proteomics analysis of $\Delta yciC$

Urease activity was determined at late exponential phase in $\Delta yciC$ using both WC and CFE in the enzyme assays. As shown in Figure 5-25 and Figure 5-26, urease activity in both WC and CFE enzyme assays were comparable to wild-type 168. Although these results were unexpected, we carried on to analyse the urease express in $\Delta yciC$. The proteomic data has shown the urease subunits UreA and UreB to be downregulated 2.09 and 2.46 fold, respectively, in $\Delta yciC$.

Based on these results we have ruled out our initial hypothesis that YciC plays a role in urease activation, and we conclude that YciC does not act as UreG for *B. subtilis* urease activation.

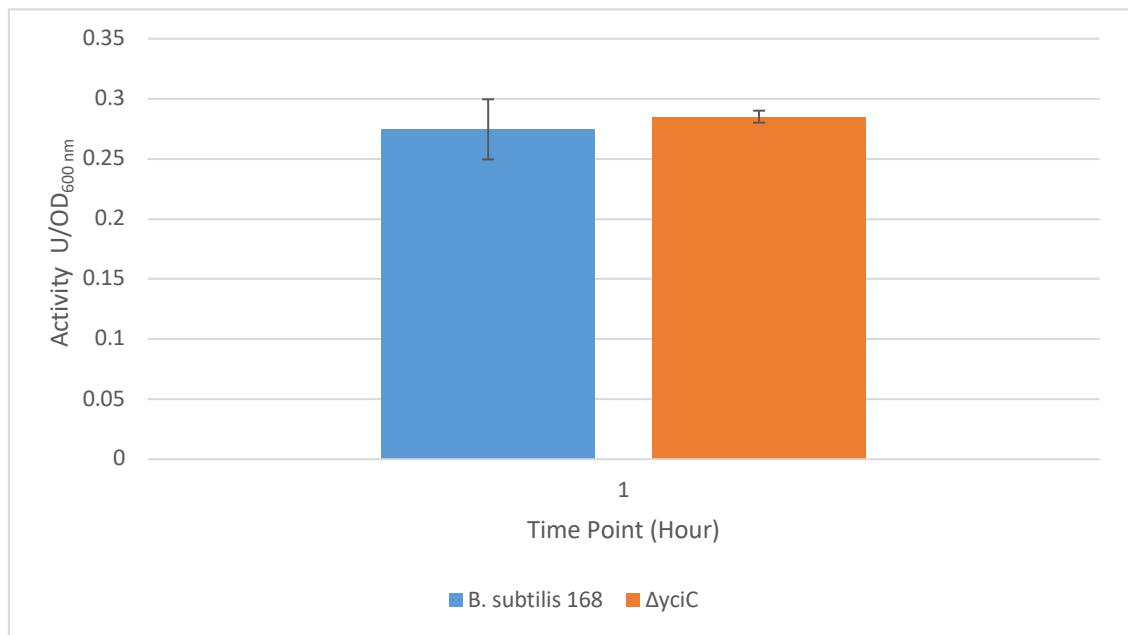


Figure 5-25. Urease activity of *B. subtilis* 168 and Δ yciC urease in whole cell.

Data points are based on 4 biological and 3 technical replicates.

Urease activity in both WC and CFE enzyme assays were comparable to wild-type 168. This confirmed the initial hypothesis is not true, i.e. YciC does not act as UreG for *B. subtilis* urease activation. Proteomic analysis was carried out to determine urease expression and as seen in Appendix Table 9-4, UreA and UreB were downregulated 2.09 and 2.46 fold, respectively, which is insignificant and reflects the comparable activity assays (figures 5 -25 and 5 -26).

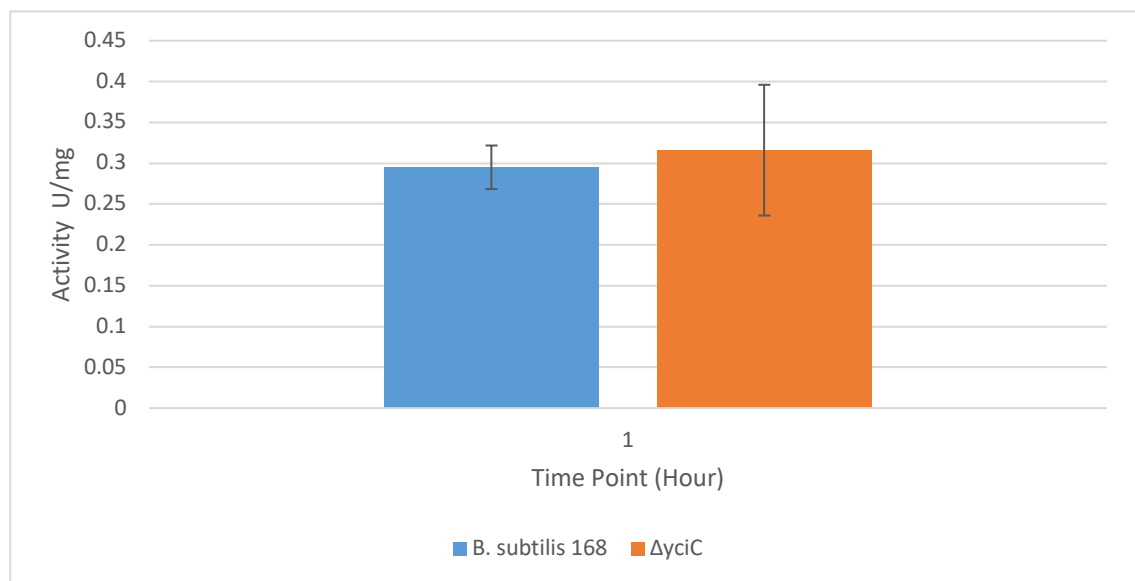


Figure 5-26. Urease activity of *B. subtilis* 168 and Δ yciC in CFE.

Data points are based on 4 biological and 3 technical replicates.

Further research has proved that YciC is a Zn²⁺ metallochaperone that supports *de novo* folate biosynthesis under conditions of zinc limitation (Chandrangsu *et al.*, 2019). Folates act as donors and acceptors in reactions that are involved in many major metabolic processes and are used in synthesis of nucleic acids and amino acids. The upregulation of the protein in this condition of peptide and nitrogen limitation is more relatable than that of urease activation.

5.2.1 Further Y genes of interest

A number of y genes identified were proposed to be involved in urease activation in *B. subtilis* based on the proteomics analysis of wild-type 168. Due to the time limitation, analysis of the y genes of interest (Table 5-5) was conducted in the lab by undergraduate project students. Growth curve analysis was carried out for each knockout used by the students to identify end exponential. Enzyme assays were carried out at end exponential and urease activity observed. In all y gene knockouts there was no compelling change in urease activity compared to the wild-type. Proteomic and bioinformatic analysis was also investigated by the students which determined that none of the y gene knockouts were candidate genes in urease activation in *B. subtilis*.

Table 5-5. Y genes chosen for knockout analysis identified via nitrogen limitation media

Y gene	Molecular Function (if known)
<i>ywpJ</i>	Hydrolase Metal ion binding
<i>yjoB</i>	ATPase (possibly involved in protein degradation) Metal ion binding
<i>yhfE</i>	Putative aminopeptidase Metal ion binding
<i>ykfD</i>	Putative oligopeptide transport ATP-binding protein ATPase
<i>yrdA</i>	Uncharacterized protein Metal ion binding
<i>yvdB</i>	Uncharacterized metallophosphoesterase-like protein
<i>yisK</i>	Metal ion binding Catalytic activity Induction: In response to ammonium, tryptophan, glucose, and phosphate starvation
<i>yufO</i>	Uncharacterized ABC transporter ATP-binding protein
<i>yfiT</i>	Possible metal-dependent hydrolase Metal ion binding
<i>yjbM</i>	ATP binding Metal ion binding Response to starvation
<i>yxeP</i>	Metal binding (Ni ²⁺) Hydrolase
<i>ytrE</i>	ATPase

5.3 Summary

The aim of this chapter was to investigate the potential role of proteins, which were identified using a proteomic study, involved in urease activity. Those proteins investigated had been previously identified in Chapter 3 from the comparative proteomic study using NLM and NPM. Further analysis of proteins upregulated in these knockouts were then investigated.

The growth of the knockout strains were analysed in BSS (JW) and end exponential growth stage for each knockout was attained. Urease enzyme assays were completed and those knockout strains, which demonstrated a change in urease activity, were further analysed using a proteomic approach. The knockout strains analysed in this chapter consisted mainly of transport systems (*oppABCDF* and *znuABC*) and so WC assays were included to give an understanding and comparison of the process in the cell, regarding urease activity. This is because in WC assays the transport of substrate in and out of the cell can be taken into account. Whereas in CFE assays this is not taken into account and so the reaction rate may differ, therefore CFE assays may be more realistic of urease activity involved.

The comparative proteomic and bioinformatic analysis using NLM and NPM, along with literature, enabled us to propose the hypothesis that was OppA may be a Ni²⁺ binding protein as well as peptide transporter. Therefore in $\Delta oppA$ we would expect to see abolishment or a decrease in urease activity. The $\Delta oppA$ analysis detailed a surprising increase in urease activity in both WC and CFE enzyme assays compared to 168. The proteomic analysis has shown this increase is due to the upregulation of urease structural genes. The remaining *opp* genes were also investigated for their role in urease activation in *B. subtilis*. WC and CFE enzyme assays of $\Delta oppB$, $\Delta oppC$, $\Delta oppD$ and $\Delta oppF$ confirmed urease activity to be comparable to strain 168. The proteomics analysis detailed no difference in urease expression. In $\Delta oppB$, UreC was upregulated 2.42 fold but this fold change was deemed relevant. The reason for the increased expression of UreC in $\Delta oppA$ and $\Delta oppB$ may also be linked to nitrogen transport. The knockouts may be more involved in transport of nitrogenous products into the cell, so without these transporter components an increase in urease is required to fill the limitation of nitrogenous sources. Although OppA has been demonstrated to be involved in urease activation in other organisms, we can confirm this is not true in *B. subtilis*.

The *dpp* transport system was also drawn to our attention, and the DppA knockout was analysed in this chapter. The Zn²⁺ binding DppA was hypothesised to be involved in urease activation in *B. subtilis*, due to the upregulation of the *dpp* operon in wild-type 168 and also literature detailed that it had been considered to be involved in urease activation in other species (Davis and Mobley,

2005). The enzyme assay demonstrated that urease activity was decreased in $\Delta dppA$, however, expression of *ureABC* was also downregulated in this knockout, therefore we conclude that urease activity was decreased due to the downregulation of urease in this knockout strain. Further work would include the analysis of the knockouts of the remaining *dpp* genes, such as; *dppE*, which shares 42% homology to *oppA*. However, the involvement of *dpp* in urease activation is unlikely due to the downregulation of the system in $\Delta oppA$ where an increase in urease activity was determined. The likely reason for the upregulation of *dpp* in $\Delta oppA$ is due to the NLM creating a NLC which is then exacerbated by the knockout of a main peptide transport SBP (OppA) and thus *dppA* is a proteome signature of ammonium and tryptophan starvation (Tam le *et al.*, 2006) which reflects this condition.

The proteomics analysis of $\Delta oppA$ further identified ZnuABC as an interesting transporter to consider in urease activation or perhaps regulation. We have observed a decrease in urease activity in both $\Delta znuA$ and $\Delta znuB$, however the decrease in urease expression demonstrated this transporter was not directly involved in urease activation, however the transport system may indirectly affect urease regulation via an unknown mechanism. The GTPase YciC was also investigated due to the high fold change (136.3) in $\Delta oppA$ and bioinformatics analysis which allowed us to speculate it may be the UreG (the GTPase during enzyme activation) of urease in *B. subtilis*. However, enzyme assays identified comparable urease activity in this knockout with strain 168 and recent literature identified its role in folate synthesis during Zn^{2+} limitation. The decrease in urease activity in both $\Delta znuA$ and Δznu and the downregulation of urease identifies that the transport system impacts urease activity but is not involved in urease activation.

There were 12 common proteins of interest from both the wild-type 168 and $\Delta oppA$ proteomic analysis. Once fold change > 3 was considered this number decreased to 8. Of these proteins we were identifying any that could have an association to urease activation in *B. subtilis*. The 2 proteins PucR and TnrA regulate *ureABC* expression in *B. subtilis*. UreC was also one of those 8 proteins which we know houses the active site of urease. The remaining proteins GapA, NasD and NasC were upregulated, we suspect, due to the growth limiting conditions and then there were two chemotactic proteins, CheA and YvzB, upregulated in both the wild-type 168 and $\Delta oppA$.

The two-component sensor kinase and chemotactic signal modulator CheA was upregulated in all conditions with increased UreC expression (wild-type 168, $\Delta oppA$ and $\Delta oppB$), which could cause us to hypothesise its involvement in urease activity in *B. subtilis*. However, under adverse growth conditions *B. subtilis* undergoes transitional responses that are designed to maintain or restore growth such as chemotaxis and motility (Wipat and Harwood, 1999). CheA is often upregulated in different (Nikodinovic-Runic *et al.*, 2009) NLCs in various bacteria and not just *B. subtilis* (Jürgen *et al.*, 2005). The conditions faced by *B. subtilis* in the NLM are adverse and so there is a great understanding why chemotactic proteins are upregulated and therefore more likely to be upregulated due to growth conditions than linked to urease activation. However, this argument of chemotaxis being the reason for upregulation needs to be confirmed and future work would include CheA knockout analysis to determine the role of this protein in urease activation in *B. subtilis*.

For a protein to be involved in urease activation, the knockout of the specific gene of that protein would incur a decrease in urease activity. Then, the proteomic analysis of the specific knockout would ideally reveal an increase in or same level of urease structural unit expression, so that the decrease is only due to no activation. This confirms the necessity for the combination of the enzyme assays and proteomic evaluations in determining urease activity. However, from all the knockout analysis carried out this scenario was never achieved (Table 5-6). Table 5-6 identifies particular knockouts tested and the urease activity and expression determined. An increase in urease activity is mirrored by an increase in urease expression, e.g. $\Delta oppA$. Comparable urease activity to 168 is reflected by no difference in urease expression. Decreased urease activity is reflected in the knockouts by decreased urease expression, e.g. $\Delta znuA$ and $\Delta znuB$.

There is the possibility that as, unlike transcriptome analysis, proteomic studies do not necessarily cover all possible gene products of the cell as it is difficult to identify the proteins that have low level expression (Otto *et al.*, 2010). Therefore, the proteins which may have potentially played a role in urease activation may have been missed in the analysis. However, this is unlikely due to the replicates and repeats of analysis in the conditions in which urease activity was increased.

Table 5-6. A simplistic reference to urease activity and expression in *B. subtilis* 168 knockouts used in this study compared to the wild-type 168 cultured in NLM.

Candidate gene	Data justifying inclusion			Urease Expression	
	Upregulated in	Fold Change	Urease Activity	Protein sources	Urease expression (UreABC)
<i>oppA</i>	168	3.72	Increased	$\Delta oppA$ vs 168	Increased
<i>oppB</i>	168	9.61	Comparable	$\Delta oppB$ vs 168	No Significant Difference
<i>oppC</i>	168	5.93	Comparable	$\Delta oppC$ vs 168	No Difference
<i>oppD</i>	168	4.56	Comparable	$\Delta oppD$ vs 168	No Difference
<i>oppF</i>	168	1.95	Comparable	$\Delta oppF$ vs 168	No Difference
<i>znuA</i>	$\Delta oppA$	18.05	Decreased	$\Delta znuA$ vs $\Delta oppA$	Decreased
<i>znuB</i>	$\Delta oppA$	10.04	Decreased	$\Delta znuB$ vs $\Delta oppA$	Decreased
<i>yciC</i>	$\Delta oppA$	136.3	Comparable	$\Delta yciC$ vs $\Delta oppA$	No difference
<i>dppA</i>	168	3.22	Decreased	$\Delta dppA$ vs 168	Decreased

This led us to consider the protein as a whole entity, instead of considering each associated subunit. The protein may function well in providing a baseline level of urease without the need for typical urease accessory proteins in order to utilise urea produced internally via purine degradation pathways and processes employed in order to sustain survival in NLCs. However, the level of urease expression may also be at baseline because the protein is unable to form the correct conformation in order to become fully catalytically active. Particular proteins that enable protein conformation may be absent in this 168 lab strain.

Chapter 6 Recombinant urease expression and activity

6.1 Introduction

The systematic sequencing of the *B. subtilis* genome identified the presence of the *ureABC* operon which consists of three structural genes *ureABC* in the operon (Figure 6-1). The genetic organisation including promoters, PucR and CodY, and GlnR binding sites, as discussed in 3.1.4, are detailed in Figure 6-1. The genes encoding the urease accessory proteins of *B. subtilis* 168 are tightly linked with the *ureABC* genes in *Bacillus* sp. strain TB-90 and most other ureolytic bacteria, yet unlike any other ureolytic bacteria, *B. subtilis* lacks any known urease accessory proteins in its genome.



Figure 6-1. *B. subtilis* *ureABC* operon including promoters and binding sites (CodY, PucR and GlnR) (Karp *et al.*, 2019).

The production of recombinant urease has been utilised by many groups to understand various features and applications of the enzyme. Hu *et al.* (1993) investigated recombinant *H. pylori* urease expression in *E. coli* however conditions needed to be optimised to achieve near clinical isolate levels of activity. It was discovered via radioactive assays that the low catalytic activity of the recombinant clones grown in Luria broth or M9 medium containing 0.5% Casamino Acids was due to chelation of Ni^{2+} by the medium components. They concluded recombinant *H. pylori* urease is optimally expressed when Ni^{2+} transport is not inhibited and when there is sufficient synthesis of the urease subunits UreA and UreB (Hu and Mobley, 1993).

In order to understand the urease operon of *Campylobacter Sputorum* biovar *Paraureolyticus* Nakajima *et al.* (2016) synthesised a recombinant full length gene cluster of the 7 genes, *ureG*, *ureH*, *ureA*, *ureB*, *ureC*, *ureE* and *ureF*, and expressed them in *Escherichia coli* JM109 cells. The recombinant urease subunits UreA and UreC were immunologically identified via western blot analysis using polyclonal anti-urease α (A) and β (B), raised against *H. pylori* (Nakajima *et al.*, 2014). They identified that the recombinant full-length urease gene cluster, and all deletion recombinants of the *ureE* gene, demonstrated increased urease activities when cultured in a

medium containing NiCl₂, but no activity was increased in *C. sputorum* cultured in NiCl₂, identifying that elements of *E. coli* must be aiding the transport of Ni²⁺.

Ethylcarbamate is a carcinogenic compound formed from urea and ethanol in rice wine. So, the enzymatic degradation of urea is highly favoured. Liu *et al.* (2019) investigated recombinant urease expression of a *B. paralicheniformis* iron-containing urease in *B. subtilis* for a food-grade expression system (Liu *et al.*, 2019). They reassembled the urease gene cluster and inserted a ribosome binding site and increased production from 38 U/L to 187 U/L. To further improve activity, they then coexpressed the iron transporter encoding gene *ureH* and the activity was again increased creating a recombinant urease system for use in food grade applications.

6.1.1 *B. subtilis* Recombinant Urease Activity in Literature

The pURE91 plasmid was initially created by Fishers lab (Cruz-Ramos *et al.*, 1997) whilst studying the isolation and analysis of the *ureABC* operon. Cruz-Ramos *et al.* (1997) identified *ureABC* to be functional in *B. subtilis*, as they demonstrated *B. subtilis ureC* was necessary for the utilisation of urea as a nitrogen source by inactivating *ureC* with a spectinomycin resistance gene inserted at a unique *NsiI* site within *ureC*. This mutant strain was able to grow like the 168 strain in glucose MM containing glutamine, NH₄Cl, or glutamate as the nitrogen source. However the disruption to the gene produced a partial growth defect in MM that contained limited amounts of arginine or allantoin as the sole nitrogen source (Cruz-Ramos *et al.*, 1997). pURE91 is derived from pET23 (Appendix Fig. 9-1) and created by inserting the *ureABC* genes from *B. subtilis*.

Hausingers lab then utilised pURE91 to investigate the biosynthesis of active *B. subtilis* urease without any known accessory proteins (Kim, Mulrooney and Hausinger, 2005a). They successfully expressed the recombinant protein in *E. coli* C41 (DE3) at 37°C with 0.5 mM IPTG in terrific broth medium. Urease was highly expressed however activity was low at 0.14 U/mg. Various Ni²⁺ concentrations were added to the growth media and a maximum activity of 6.4 U/mg was achieved with 5-7 mM NiCl₂ which revealed that *B. subtilis* urease activity was Ni²⁺ dependent. To understand the low level of urease activity in *E. coli* C41 (DE3) cells containing pURE91, even when cultured with high Ni²⁺ and despite the increased expression of urease subunits they attempted to purify recombinant urease. This was pursued via ion exchange,

hydrophobic interaction chromatography resins. However, all purified urease produced was inactive.

Their work also investigated the overexpression of *B. subtilis ureABC* in *B. subtilis* RB247. The *B. subtilis ureABC* sequence was cloned into pDR111 to create the pDR-BsABC plasmid. This plasmid was expressed in *B. subtilis* RB247 and activity was compared to that of *B. subtilis* SF10 cells. SF10 cells contained no visible expression whereas RB247 expression was greater but activity was lower (0.081 U/mg). *B. subtilis* RB247 cells containing pDR-BsABC were cultured with increasing Ni^{2+} concentrations (Kim, Mulrooney and Hausinger, 2005a) and produced approximately 3.5 fold more activity (0.281U/mg) than SF10 cells. They also tested the influence of Ni^{2+} and Mn^{2+} in growth media on urease activities. The addition of Ni^{2+} to the recombinant *B. subtilis* did not alter urease activity and in the nonrecombinant, activity was decreased by 50%. Kim *et al.* (2005) confirmed *B. subtilis* urease was Ni^{2+} containing via investigations using inductivity coupled plasma emission analysis which identified 0.13-0.29 mol Ni^{2+} which correlates to the observed level of activity and 0.063-0.070 mol of Zn^{2+} per mol of *B. subtilis ureABC*. They proposed from the results that *B. subtilis* urease is activated, but with low efficiency (Kim, Mulrooney and Hausinger, 2005a).

These studies conclude that the *B. subtilis* genome includes an active urease that is Ni^{2+} containing, however the urease is activated with low efficiency. The production of recombinant *B. subtilis* urease in *E. coli* demonstrated increased expression but with comparable urease activity to *B. subtilis*. This suggests an increased efficiency of activation in *B. subtilis* that could arise from an increased intracellular Ni^{2+} or bicarbonate concentration, recombinant protein folding issues in *E. coli*, or novel accessory gene(s) (Kim, Mulrooney and Hausinger, 2005a). To further investigate this we considered novel accessory genes focused on recombinant protein folding. The trimer of trimer is the active conformational state of urease, if the protein is not folding as the correct conformational state and synthesising say more dimer of trimer or single trimer then activity will be reduced in the recombinant. The expression system in *E. coli* needs investigating and may need optimised.

6.1.2 Aims of this Chapter

The aim of this chapter was to utilise heterologous expression to compare the activity between native *B. subtilis* urease and recombinant urease expressed in *E. coli* and explore the activation of urease in *E. coli*. Recombinant proteins would be transformed and expressed in the host, *E. coli* BL21 (DE3) and urease activity would be determined and compared to *B. subtilis* 168. The protein would be further analysed using size exclusion chromatography (SEC) techniques in combination with SDS-PAGE gel electrophoresis and protein ID analysis to explore the possible mechanism for activation.

6.2 Results and Discussion

The aim of this chapter was to utilise heterologous expression to compare the activity of native *B. subtilis* urease and recombinant urease expressed in *E.coli* and investigate the activation of urease in *E.coli*. Recombinant proteins were transformed and expressed in *E.coli* BL21 (DE3) and urease activity was determined and compared to *B. subtilis* 168. Urease was further analysed using SEC techniques in combination with SDS-PAGE gel electrophoresis and protein ID analysis to explore the possible mechanism for activation.

6.2.1 Urease expression in recombinant strain

The plasmid pURE91, which contained *B. subtilis ureABC* was transformed into *E.coli* BL21 (DE3) cells, the suspension was spread onto an LB + Amp (10 mg/ml) agar plate which produced 30 colonies. Whereas the control transformation of pET22b into *E.coli* BL21 (DE3) produced over 200 colonies confirming the *E.coli* cells were efficient.

The expression of recombinant urease was optimized initially. There are several parameters that could influence the expression of heterologous proteins, particularly regarding temperature. It is understood that high temperatures will create a negative impact upon protein folding due to hydrophobic interactions which include a temperature dependence and will aid conformational stresses. Ideally, it is important to produce proteins at lower temperatures to prevent mis-folding and improve the quality of the products (Gasser *et al.*, 2008).

Investigations into protein expression would identify the recombinant protein was expressed and soluble and the optimum condition for the expression. Initial investigations into the optimum temperature for recombinant *ureABC* expression in *E.coli* BL21 (DE3) were at 16°C, 30°C and 37°C (see Appendix Figure 9-3), inducing with 1 mM IPTG. Limited protein was recovered from *B. subtilis* at 16°C and 37°C was similar to 30°C, so protein expression at 20°C and 30°C were investigated further with 1 mM IPTG. The results, as shown in Figure 6-2 determined that recombinant expression was optimum at 30°C (lanes 1 & 2) induced with 1 mM IPTG at 100 rpm and these conditions would be used for further study in the recombinant strain.

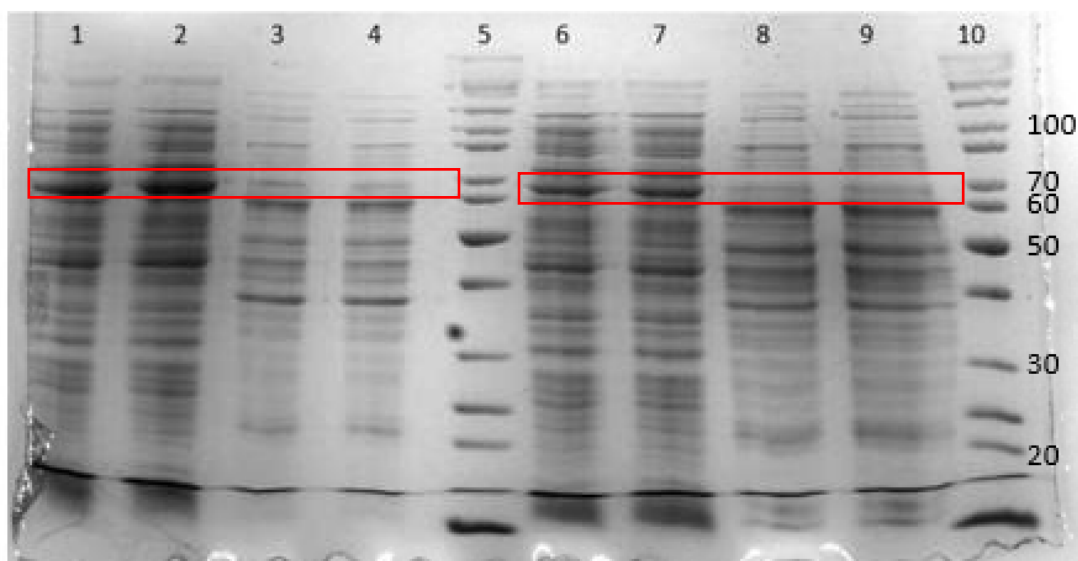


Figure 6-2. Urease expression in *B. subtilis* 168 and the recombinant strain *E. coli* BL21 (DE3) at 20°C and 30°C with additions of 1 mM IPTG.

Lane 1 & 2 CFE from BL21 (DE3) + pURE91 and Lane 3 & 4 CFE from *B. subtilis* at 30°C. Lane 5 Ladder. Lanes 6 & 7 CFE from BL21 (DE3) + pURE91 and lanes 8 & 9 CFE from *B. subtilis* at 20°C. Lane 10 ladder. Protein expression of UreC (highlighted in red) is greater in the recombinant at 30°C.

After the expression condition was investigated, a large quantity of recombinant urease was expressed at 30°C with 1 mM IPTG. The CFE was visualised on SDS-PAGE (Figure 6-3). The CFE detailed the presence of UreC, UreA and UreB.

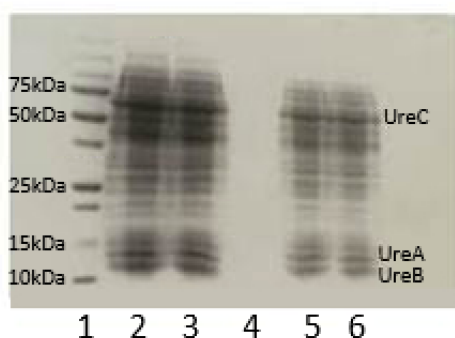


Figure 6-3. Recombinant urease expression visualised using 14% (w/v) SDS-PAGE.

Lane 1 ladder, lanes 2 & 3 CFE dilutions 1:4, lanes 5 & 6 1:10. UreC, UreA and UreB are highlighted.

6.2.1 Western blot analysis to confirm the expression of UreC

In order to determine the presence of the urease subunits in *B. subtilis* 168 and in recombinant urease produced by *E.coli* BL21 (DE3), a Western blot analysis was performed to identify the structural unit α (UreC) in the CFE samples from both cells.

Anti-*Helicobacter pylori* urease β antibody was selected as the primary antibody for this analysis. The catalytic β subunit of *H. pylori* is approximately 66 kDa and is known as the α subunit (UreC) in most other bacteria. This homology to the α subunit of *B. subtilis* (61 kDa) is 61.38% and is detailed in Figure 6-4. The synthetic antibody used contained a sequence corresponding to a region within amino acids 341 and 398 of *H.pylori* urease subunit β (underlined in Figure 6-4). The AA sequence comparison identifies how similar the 2 sequences are, the majority of AA are the same which concludes this is the correct antibody to use.

```

H.      MKKISRKEYVSMYGPTTGDKVRLGDTDLIAEVEHDYTIYGEELKFGGGKTLREGMSQSNN
B.      -MKMSREEYAEELFGPTTGDKIRLGDIDLWIEVEKDFTVYGEEMI FGGGKTIRDGMGQNGR
          *::**::**..::*****:***** **::*::**::**:: *****:*.*.*.
H.      PSKEE--LDLIITNALIVDYTGIIKADIGIKDKGIAGIGKGGNKMDQDGVKNNLSVGPAT
B.      ITGKDGALDLVITNVVLLDYTGIVKADVGVKDGRI VGVGKSGNPDIMDGVDPHVMVIGAGT
          : :: **::**::**..::***** **::*::**::**..*::**::** * : **.. : :*.
H.      EALAGEGLIVTAGGIDTHIHFI SPQQIPTAFASGVTTMIGGGTGPADGTNATTITPGRRN
B.      EVISGEGKILTAGGVDTHIHFI CPQQMEVALSSGVTTLLGGGTGPATGSKATTCTSGAWY
          *::** *::**::**..*::**::**..*::**::**..*::**::** *::** *.*
H.      LKWMLRAAEEYSMNLGFLAKGNASNDASLADQIEAGAIGFKIHEDWGTTPSAINHALDVA
B.      MARMLEAAEEFPINVGFLGKGNASDKAPLIEQVEAGAIGLKLHEDWGTTPSAIKTCMEVV
          : .* **::**..*::**::**..*::** *::**::**::**..*::**.. : :*.
H.      DKYDVQVAIHTDTLNEAGCVEDTMAAIAGRTMHTFHTEGAGGGHAPDI IKVAGEHNILPA
B.      DEADIQVAIHTDTINEAGFLENTLDAIGDRVIHTYHIEGAGGGHAPDIMKLASYANILPS
          * : *::**::**..*::** *::**::**..*::** * **::**..*::** * **::**..*::** :
H.      STNPTIPFTVNTAEHMDMLMVCHHLDKSIKEDVQFADSRIRPQTIAAEDTLHDMGIFSI
B.      STTPTIPYTVNTMDEHLDMMVCHHLDKVPEDVAFSHSRIRAAATIAAEDILHDIGAIMS
          **.*::**::**..*::**::**..*::** *::** *::**..*::**..*::** *::** :
H.      TSSDSQAMGRVGEVITRTWQTADKNKKEFGRLKEEKGDNDNFRIKRYLSKYTINPAIAHG
B.      TSSDSQAMGRVGEVIRTWQVADKMKKQRGALAGENG-NDNVRAKRYIAKYTINPAITHG
          *****:***** **::**..*::** *::** *::**..*::**..*::**..*::** :
H.      ISEYVGSVEVGKQVADLVLWSPAFFGVKPNMI IKGGFIALSQMGDANASIPTPQPVYIREM
B.      LSHEVGSVEKGLADLVLWDPVFFGVKPELVKGMIAARAQMGPDPNASIPTPEPVFMRQM
          :* ***** **::**..*::**..*::**..*::**..*::**..*::**..*::** *::**
H.      FAHHGKAKYDANITFVSQAAYDKGIKEELGLERQVLPVKNCRNITKKDMQFNDTTHAIEV
B.      YASYGKANRSTSI TFMSQASIERGVAESLGLEKRISPVKNIRKLSKLDMKNLSALPKIEI
          :* :***: ..*::**::**..*::** *::**..*::**..*::**..*::**..*::** :
H.      NPETYHVFVDGKEVTSKPAKVSLSLAQLFSIF
B.      DPKTYQVFADGEELSCQPVVDYVPLGQRYFLF
          *::**::**..*::**..*::**..*::**..*::**..*::**..*::**..*::**

```

1 : *H. pylori* 100.00 61.38
2 : *B. subtilis* 61.38 100.00

Figure 6-4. Sequence comparison of *B. subtilis* UreC and *H. pylori* UreB.

The amino acid sequence from 341 and 398 of *H.pylori* (H.) urease (subunit β) and *B. subtilis* 168 (B.) urease (UreC α subunit) are underlined. The Muscle alignment tool identifies the whole sequence homology between *H. pylori* and *B. subtilis* 168 as 61.38%.

CFE and total protein (TP) of *E.coli* BL21(DE3) + pURE91 and *B. subtilis* CFE produced as in method 2.1.7.2 was ran on SDS-PAGE and the proteins were transferred to 0.45 μM nitrocellulose membrane using Western blot method (2.1.10) and then detected with ECL and visualised on the G-Box as shown in Figure 6-5. Figure 6-5 indicated *B. subtilis* 168 urease (α subunit) was highly expressed (Figure 6-5 lanes 2&3) in the recombinant strain in both Total Protein (TP) lane 2 and CFE lane 3 samples compared to *B. subtilis* 168 CFE lane 6. There is no expression present in

BL21 (DE3) control lane 4 (CFE) and lane 5 (TP) and lane 6 demonstrates UreC expression of UreC in *B. subtilis* 168 in CFE.

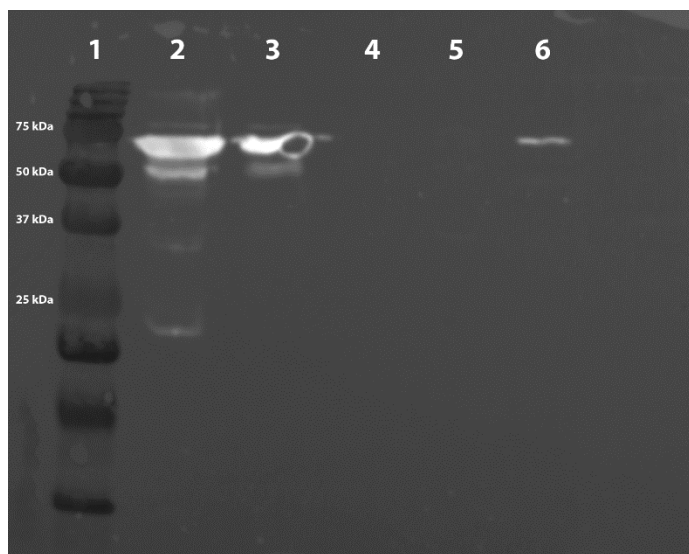


Figure 6-5. Western blot overlay of recombinant *E. coli* BL21+pURE91 total protein (TP), CFE and *B. subtilis* 168 CFE.

Lane 1 ladder, Lane 2 TP *E. coli* BL21 (DE3) + pURE91, Lane 3 CFE *E. coli* BL21 (DE3) + pURE91, Lane 4 BL21 control CFE, Lane 5 BL21 control TP and lane 6 168 CFE.

Western blot analysis demonstrated the correct proteins were being expressed in the recombinant strain and confirmed the presence in *B. subtilis* 168 CFE.

6.2.2 Urease activity comparison between *B. subtilis* 168 and recombinant *E. coli*

To understand and compare urease activity in the recombinant strain (BL21 (DE3) + pURE91) and native strain (*B. subtilis* 168) enzyme assays were carried out using both WC and CFE. WC urease activity was compared between native, recombinant and the control strain BL21 (DE3) (Figure 6-6). Activity in the control was negligible compared to the recombinant and the native. Urease activity is slightly increased by 0.06 U/OD in the native strain compared to the recombinant strain which, considering the expression in the recombinant, was not expected. The activity in the recombinant however confirms the transformation was a success as it was evident that the difference in urease expression was visible in the recombinant strain compared to no expression in BL21 (DE3) (Appendix Figure 9-4), as activity in the recombinant was present compared to the control BL21 (DE3).

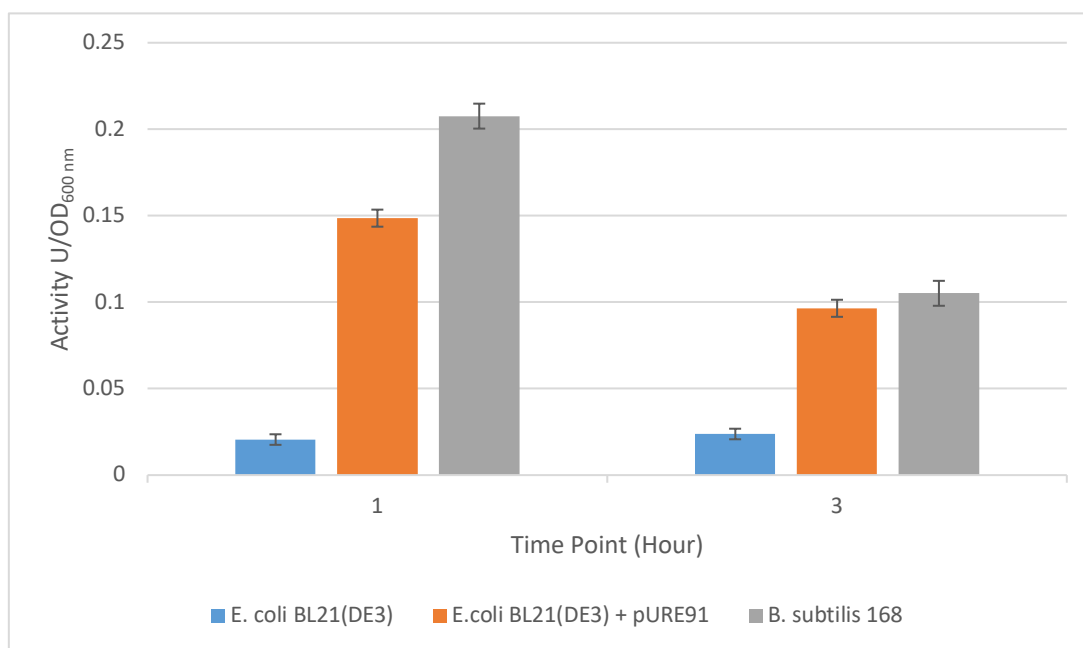


Figure 6-6. Urease activity of *B. subtilis* 168, the recombinant strain *E. coli* BL21 (DE3) + pURE91 and BL21 (DE3) control in whole cells.

Urease activity in whole cell *B. subtilis* 168, *E. coli* BL21 (DE3) + pURE91 and BL21(DE3). Data is based on 3 biological and 2 technical replicates.

The results from whole cell assays were useful in understanding urease activity, but the results may not truly reflect the urease activity, as there are many factors which can influence these results. For example the urea transportation system is different between *E. coli* and *B. subtilis*, as in *E. coli* non-selective uptake of urea occurs through the GlpF ‘glycerol facilitator’, a membrane channel (Sebbane *et al.*, 2002), whereas *B. subtilis* has no known urea transport system and works via diffusion across the membrane driven by a concentration gradient. Both bacteria include different mechanisms to cope with nitrogen limitation which could have a significant impact on the results we see. As NH_4^+ is detected via the enzyme assay, it is important to note that both species include NH_4^+ transporters in the form of AmtB (NrgA), which belong to the ammonia transporter channel family which is discussed in section 3.2.3 (Zheng *et al.*, 2004; Detsch and Stulke, 2003). However, a more accurate method, via CFE, was needed to determine urease activity which would be independent of the transport systems.

Ideally, purified urease would have been used in the assay, however, there are challenges to purify urease (Kim, Mulrooney and Hausinger, 2005a; Hu *et al.*, 1992; Sujoy and Aparna, 2012; Hu and Mobley, 1990; Lee *et al.*, 1993; Kim, Mulrooney and Hausinger, 2006). Regarding *B. subtilis*

urease, significant cell density is needed to upscale the amount of urease produced. Kim *et al.* (2005) described how their efforts to purify recombinant urease by various techniques such as ion exchange and hydrophobic interaction chromatography resulted in the loss of activity (Kim, Mulrooney and Hausinger, 2005a). UreD and UreF of *K. aerogenes* are also insoluble when overexpressed in *E.coli* (Kim, Mulrooney and Hausinger, 2006) and due to the enzyme cofactor being Ni²⁺, using his tag Ni²⁺ columns to purify was not an option. Regarding plant urease, purification is via three steps: acetone precipitation, DEAE-cellulose ion-exchange chromatography, and gel filtration chromatography (EL-Hefnawy *et al.*, 2014). The speed and simplicity of a purification method would be a distinct advantage as bacterial urease is inactivated rapidly during the purification procedure (Larson and Kallio, 1954). Therefore, CFE was chosen to be analysed for urease activity.

Urease activity of CFE was investigated in *B. subtilis* 168, BL21 (DE3)+ pURE91 and BL21(DE3), as seen in Figure 6-7. The trend in activity is similar to the WC assay, again there is negligible activity in the control BL21(DE3) which is expected and activity in the wild-type is again greater than in the recombinant strain. The difference is approximately 0.07 U/mg. This again contradicts the expression of urease seen in the SDS-PAGE gels, as more urease was present in the recombinant but less activity is seen.

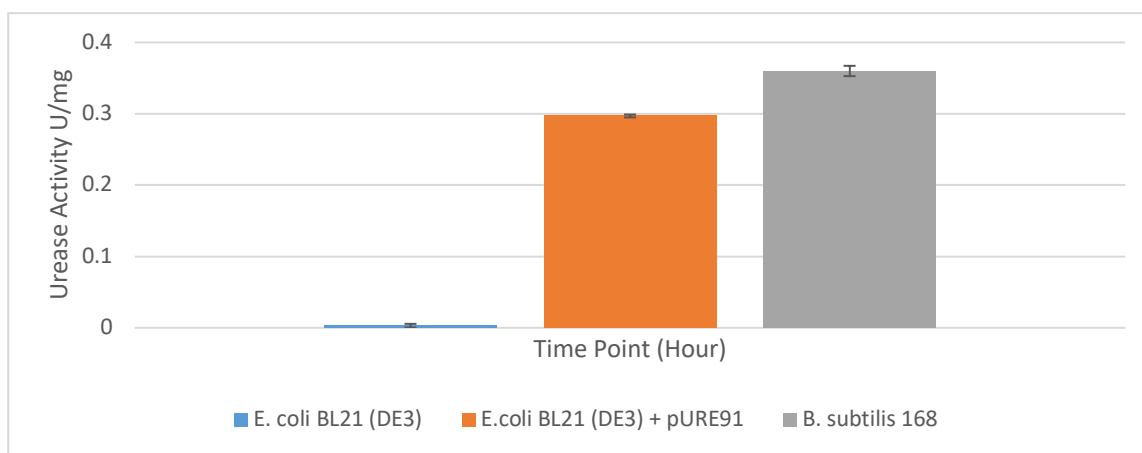


Figure 6-7. Urease activity of *B. subtilis* 168, *E. coli* BL21 (DE3) + pURE91 and BL21(DE3) (control) in CFE.

Data points are based on 3 biological and 2 technical replicates.

The combined data from the urease enzyme assays along with Western blot analysis and SDS-PAGE gel electrophoresis results indicate that although urease is being substantially expressed in the recombinant *E. coli*, the activity is lower than the native urease. This observation is consistent with the results of Kim *et al.* (2005). However, there are two possible reasons that could lead to this observation: 1) there are unknown accessory or associated proteins in *B. subtilis*, as proposed by Kim *et al.* (2005) and 2) the low level active enzyme could be due to incorrect protein conformation. This could be a result of the misfolding of the recombinant protein. Unknown accessory proteins have not been cloned into the recombinant strain but would be present in the native strain and would enable the activation of the enzyme. However, coexpression studies of *B. subtilis* with known urease accessory proteins from *K. aerogenes* and *S. pasteurii* failed to enhance activation in the native UreABC (Kim, Mulrooney and Hausinger, 2005a). So unidentified accessory proteins may be involved in *in vivo* urease activation. If the protein is misfolding then the conformation would not be optimum for full urease activity.

Ureases display a quaternary structure made of a functionally minimal trimer (Fig. 2-4) with each unit of the trimer hosting one enzyme active site (Urabe, Katagiri and Katsuki, 2020). The quaternary structure is the result from folded amino-acid chains in tertiary structures interacting further with each other to produce the functional protein. Urease is produced as a recombinant protein in *E. coli* BL21 (DE3) and many recombinant proteins misfold (Palombo *et al.*, 2017; Musiani *et al.*, 2004). Often, the misfolding of proteins in *E. coli* are associated with limitations in cell concentration of folding assistant elements which struggle to process newly synthesised aggregation prone polypeptides (Gasser *et al.*, 2008). Often coproduction of GroEL and DnaK, the main HSP chaperones helps correct folding of the protein of interest (Lesley *et al.*, 2002).

The work of Kim *et al.* (2005) identified urease activity of the recombinant to be greater (0.14 U/mg) than their native urease from SF10 cell (0.113 U/mg) which is low when compared to that of CFE of *K. aerogenes* urease 2 U/mg. The activity of the recombinant in this research is approximately double at 0.29 U/mg and in the native approximately 0.35U/mg. Their conditions for recombinant urease expression were carried out at 37°C which will affect protein conformation and hence activity, which may explain their lower urease activity value. The media they cultured

B. subtilis SF10 cells in is also less nitrogen limited than that used in this research, as the media contains 0.2% glutamate and 10mM (NH₄)₂SO₄, which is similar to the NPM used in this research which produces a lower urease activity in *B. subtilis*.

The results from SDS-PAGE and enzyme assays provide conflicting information with regards to the recombinant urease produced. With knowledge of urease structure and conformation and the effects upon activity, the conformation of urease needs to be investigated further.

6.2.3 Protein Conformation Analysis Using Native Tris-Glycine Gels

First investigations of protein conformation were carried out utilising native Tris-Glycine gels. The native Tris-Glycine gels were used to analyse urease in CFE from cells of both 168 and the recombinant strain. The active urease should be a triangle structure (Figure 2-4) which is formed by the trimer of the trimers. Each trimer contains all 3 structural units *ureABC* ($\alpha\beta\gamma$) and there are 9 units in total ($\alpha\beta\gamma$)₃. However, if the trimer of trimers does not fold properly, urease could be present in the form of a dimer of the trimer Ure(ABC)₂, a single trimer UreABC and even the single subunits as UreA, UreB and UreC respectively. Table 6-1 details all the possible molecular weights for each form of the urease structure proteins, i.e. the dimer of trimers' molecular weight will be 170 kDa and the single trimer would be 85 kDa.

Initially a 14% (w/v) Tris-Glycine gel was employed for the analysis with a precision plus dual colour protein ladder and gel filtration standards were used for comparison. The gel image (Appendix Figure 9-6) revealed a significant protein band between sizes 125 to 203 kDa. However, the majority of the proteins from both *B. subtilis* and *E.coli* CFE remained in the top half the gel which indicated that the 14% concentration was too high to analyse the CFEs from both cells. Therefore a 6% native gel was used for further analysis loaded with 20 μ l CFE per well. The result, as shown in Figure 6-8, shows that there is a significant band located between two markers which are size 125 and 203 kDa. This band is present from all the *B. subtilis* samples and *E.coli* samples, although the band from *B. subtilis* is higher and fainter than the one from *E.coli*. This indicates the proteins from *B. subtilis* are bigger than the proteins from *E.coli*. In section 6.2.1 we have shown that the recombinant *E.coli* can produce a significant amount of urease and also based on the denatured SDS-PAGE gel (Figure 6-3) and Western blot (Figure

6-5), we have confirmed that the recombinant proteins include UreC. We can therefore be fairly confident that the band presented in lanes 3 and 4 (R) in Figure 6-4, is the urease dimer of trimers Ure(ABC)₂, which is approximately 170 kDa.

There is also a band, although less intense in both the recombinant and 168 above the standard 203,926 kDa (Appendix Figure 9-6) and this could be the trimer of trimers Ure(ABC)₃ at 256 kDa.

The standards as used in Table 2-20 were utilised in the native tris glycine gels for comparison of molecular weights, however due to low protein concentration this did not work accurately and so the protein ladder was used as standard.

Table 6-1. Approximate molecular weights (kDa) of the urease structural subunits and their corresponding folding protein structures. Molecular weights (Consortium, 2018)

Urease Subunit/s	Approx. Molecular Weight kDa
UreA	13
UreB	11
UreC	61
Trimer UreABC	85
Dimer of trimers Ure(ABC) ₂	170
Trimer of trimers Ure(ABC) ₃	256

Although the results from the native gels were of great interest, it was proven that running the native gel correctly was challenging as the protein was so large and made up of various proteins which would have an isoelectric point (pI) and so different buffers may need to be used. In native Tris-glycine, the proteins are separated according to the net charge, size, and shape of their native structure. As each sub unit of urease (protein) would include a charge, which will depend on the primary amino acid sequence of the protein (isoelectric point) and the pH during electrophoresis, which influences the mobility of the protein during electrophoresis (Arndt *et al.*, 2012).

Based on the results from the native tris-glycine gels, it is reasonable to think that the low urease activity observed in recombinant samples may also be due to the incorrect protein conformation rather than a lack of accessory proteins as the sole reason. To prove this argument SEC was employed for the further analysis.

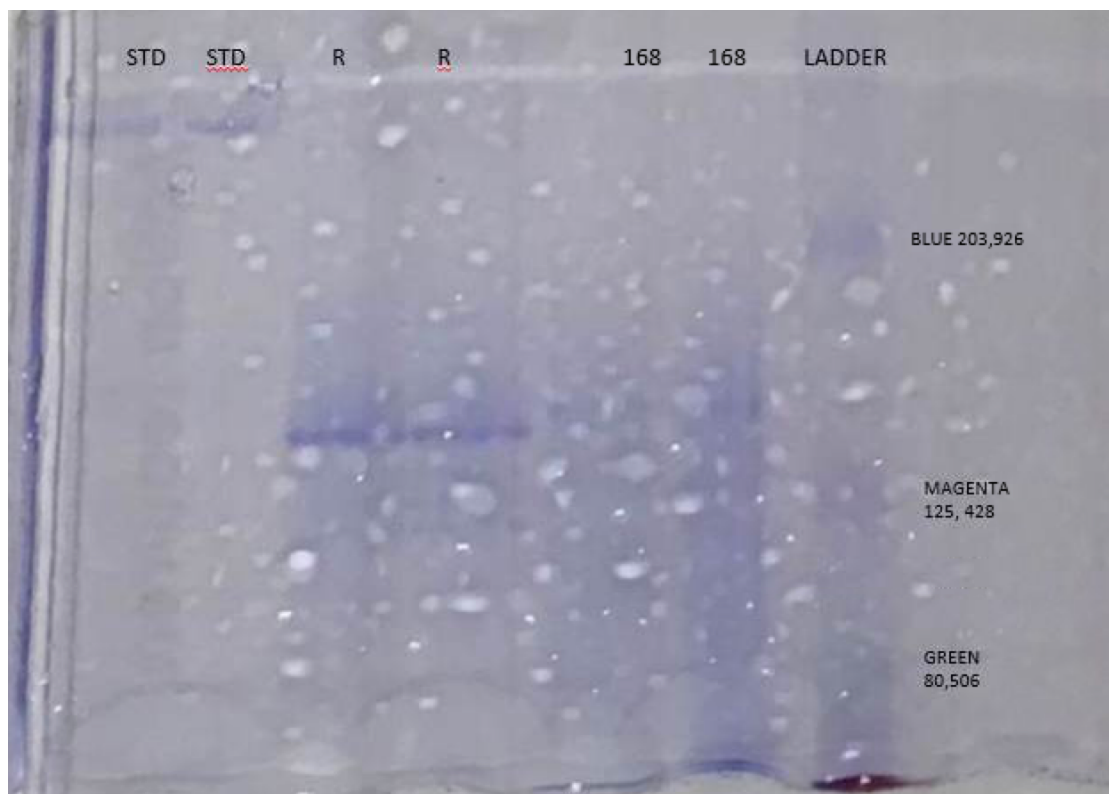


Figure 6-8. Native gel 6% analysis of urease in CFE from recombinant *E. coli* and 168 strain.

STD - Gel filtration standard, R = Recombinant *E. coli* CFE. 168 - 168 CFE. There is a large band present in both the recombinant (R) lanes between the protein marker of 125,438 and 203, 926 which would correspond to the dimer of trimers at 170 kDa.

6.2.4 Size Exclusion Chromatography (SEC) for Protein Conformation Analysis of Recombinant Urease.

We have confirmed that the expression of the 3 structural subunits of urease (UreABC) was greater in the recombinant urease than in the native urease. However, the enzyme assay results indicated that the enzyme activity was slightly lower as shown in Figure 6-6 and Figure 6-7. The preliminary analysis through native gels has shown that the majority of recombinant urease was forming as a dimer of trimers rather than a trimer of trimers which would be required for the active enzyme. This observation indicated that recombinant urease conformation was not correct

and so was not as active as indicated by the protein expression level. This needed to be further investigated through SEC.

SEC, also known as gel filtration, is a separation method of proteins, peptides, and oligonucleotides on the basis of size as they pass through a resin packed column. Unlike other chromatography techniques such as ion exchange chromatography (IEX) or affinity chromatography (AC), the molecules do not bind to the resin, and so the buffer composition does not directly affect the resolution. The molecules travel through the column of porous spherical particles (beads). The smaller the molecule the further they diffuse into the pores of the beads. Larger molecules diffuse quicker or not at all and so, leave the column first. The method of SEC separation occurs in less than one column volume.

If *B. subtilis* urease included the correct protein conformation the molecular weights of the trimer of trimers (Ure(ABC)₃) would be approximately 256 kDa (Table 6-1) and this weight would only include the structural proteins and not any accessories. If accessory proteins were bound the molecular weight would be greater than 256 kDa. Any proteins identified below this would indicate the protein was not folding as a trimer which it should do to create a fully active urease, expected by current theories.

In order to estimate the molecular size for the intact enzyme, from *B. subtilis* and *E.coli* BL21 (DE3) + pURE91, standards were processed on the gel filtration column first. The standards would be vital in the analysis of urease by providing elution volume profiles of standard proteins but it also contained two visible markers myoglobin (17 kDa) and vitamin B12 (13 kDa) (Table 2-20) to establish the column was correctly packed and also the sample is eluted from the column evenly.

6.2.4.1 Analysis using HiPrep Sephacryl S-200 column

Initially SEC for this research utilised the AKTA, with the HiPrep Sephacryl S-200 column with a 100 μ l loop. This column has a broad protein fraction range 5 kDa – 250 kDa for analysing mid-size proteins. Once primed it was used as in the size exclusion method 2.1.12.1. Unfortunately, although the separation on this column was efficient (chromatogram of standards

seen in Appendix Figure 9-7 and recombinant S-200 sample in Appendix Figure 9-8) the concentration of protein in the fractions eluted (1ml) was not sufficient enough to be visualised using SDS-PAGE. The protein fraction ranges for this column for what we were analysing (256 kDa) were also at the upper limit of this column. Therefore, the future analysis used the HiPrep Sephacryl S-300 column.

6.2.4.1 Analysis Using S-300 column with a 100 µl loop

The S-300 column (10 kDa - 1,500 kDa) initially enabled effective separation of the proteins. The remaining SEC standards (Table 2-20) were used on the S-300 and later a manual standard was also produced in order to form a calibration of the column to determine retention times of the proteins. Initially the 100 µl loop was used with the S-300 column.

The AKTA chromatogram (SEC standards Appendix Figure 9-9) enabled an approximate elution volume (EV) to be identified for each protein standard Table 6-2, so that the recombinant CFE and native CFE could be compared.

CFE produced from recombinant urease expressed in 4 x 50 ml LB of culture and then resuspended in 5 ml of 50 mM HEPES buffer was analysed. Of this CFE, 100 µl was loaded on the S-300 column through a 100 µl loop using the AKTA.

The SEC chromatogram from the S-300 and 100 µl loop as shown in Figure 6-9 produced effective separation of the recombinant urease and details three peaks present at EVs of approximately 40 ml, 60-65 ml and 100 ml. The first peak P1 (40 ml EV) is dominant and the following two are relatively small. Using the standards as detailed in Table 6-2, the molecular sizes of the proteins in each peak can be assumed. The peaks from this recombinant urease detail proteins of various sizes including proteins present of molecular size greater than 158 kDa (Peak 1 at EV 30 - 40 ml) which could be interpreted to include the trimer of trimers (256 kDa) or the dimer of trimers (170 kDa). A further peak P2 include proteins with a molecular weight of approximately 158 kDa – 44 kDa (peak present at EV 60 ml) which could be interpreted as the close to the trimer (85 kDa) or UreC (61 kDa); and the third peak P3 which included a molecular weight of approx. 17 kDa (EV 100 ml) which may be UreA (13 kDa) and UreB (11 kDa). However, the EV cannot confirm what type of trimer of urease is formed in the recombinant

proteins, as the first peak could be the trimer of trimers or the dimer of trimers. This chromatogram is of interest as the first peak possibly identifies the trimer of trimers as it would be a protein of size greater than 158 kDa but could also be interpreted as the dimer of trimers with consideration to the tris-glycine gel analysis.

The second peak at EV 60 ml approximately 44 – 158 kDa links to the trimer UreABC with a molecular weight of 85 kDa. The third peak at approximately 17 kDa could be UreA (13 kDa).

The data was interesting, but needed more validation and further analysis, which would include the use of different standards to identify the difference between the trimer and the dimer. Therefore, BSA was selected as an extra standard for further analysis.

Table 6-2. Approximate protein sizes identified from SEC standards on S-300 column using 100 µl loop.

Protein	Protein Size (kDa)	Approx. Elution Volume
		Range (ml)
Thyroglobulin	670	<10
γ-globulin	158	55-60
Ovalalbumin	44	75-80
Myoglobin	17	95-100
Vitamin B12	1	>130

In order to identify specific proteins present in SEC peak fractions further methods of analysis were required. Confirmation of the proteins present in the individual fractions of the peaks (S-300 100 µl) were separated and Bradford's performed which produced negligible results (low if any protein present). We then attempted to visualise the proteins on SDS-PAGE gel but this confirmed like the Bradford's low protein concentration as there was no visible proteins seen on the gel. The visualisation of proteins on SDS-PAGE after gel filtration was very difficult even though TCA precipitation was employed to concentrate the fractions due to the small amount of the standards (100 µl) used in the column. A 2 ml loop was then used with the S-300 column for the proceeding experiments.

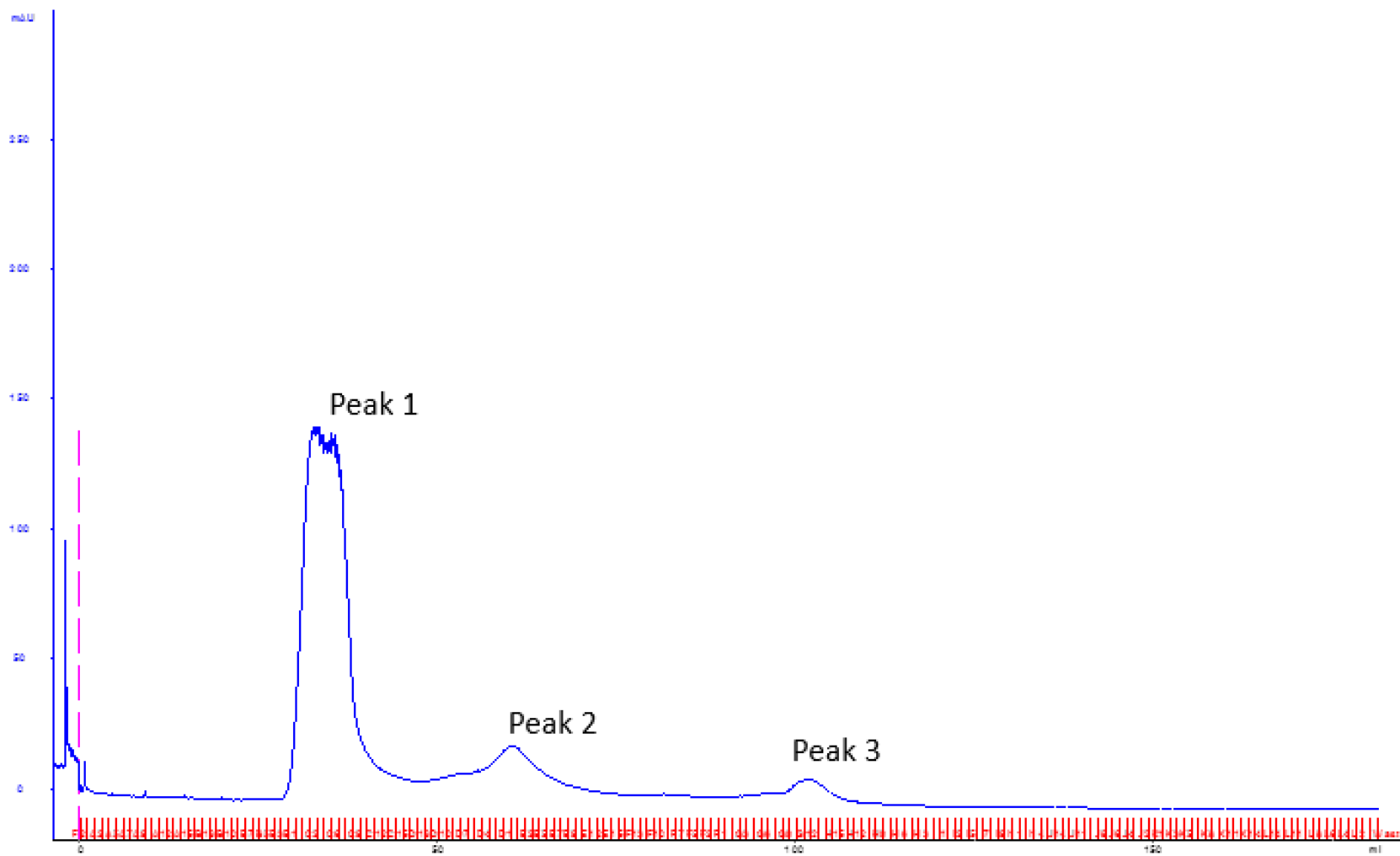


Figure 6-9. The SEC chromatogram of recombinant urease CFE utilising S-300 column and 100 μ l loop

6.2.4.2 Analysis Using S-300 column with a 2 ml loop

The column required frequent calibration to confirm approximate EVs. Bovine Serum Albumin (BSA) was also prepared as a standard (2.1.12.2) in order to determine a molecular weight of approximately 66 kDa and 132 kDa as at room temperature monomeric (66 kDa) and dimeric BSA (132 kDa) fractions are present in solution. The manually produced BSA standard 5 mg/ml was separated using the S-300 column with a 2 ml loop (see chromatogram in Appendix 9-10). Table 6-3 details the EVs and respective protein sizes of proteins separated.

Table 6-3. Approximate protein sizes identified from SEC standards on S-300-column using 100µl and BSA on 2 ml loop.

Protein	Protein Size (kDa)	Approx. Elution Volume
		Range (ml)
γ-globulin	158	55 - 60
BSA dimer	132	60 - 65
BSA monomer	66	70 - 75
Ovalalbumin	44	75 - 80
Myoglobin	17	95 - 100
Vitamin B12	1	>135

Recombinant urease CFE was then processed on the S-300 column with the 2 ml loop producing the chromatogram as shown in Figure 6-10. Separation was evident but not as efficient as using the 100 µl loop. This was confirmed by a technical replicate of the separation (Appendix Figure 9-11). However, now there was visualisation of approximately 5 peaks from those dominant proteins expressed in the recombinant cells. The EVs of the peaks were approximately: P1 45 ml, P2 50 – 65 ml, P3 70 ml and small peaks P4 100 ml and P5 150 ml. Utilising the standards (Table 6-3) facilitates the identification of the molecular weight of the proteins present. The proteins in P1 are greater than 158 kDa (EV 45 ml) which could contain the trimer of trimers or the dimer of trimers. The proteins in P2 EV 50 – 65 ml would include proteins of size 132 kDa

up to those proteins in Peak 1 which would correspond to the dimer of trimers at 170 kDa and confirm Peak 1 as the trimer of trimers. The third peak, P3 at EV 70 ml would include proteins of size 66 – 132 kDa which would correspond to the trimer which is 85 kDa. There are small peaks at EV 100 ml and 150 ml would correspond to UreA (13 kDa), UreB (11 kDa).

The difference in separation between the two loops could be explained as too much protein loaded on the column, but both chromatograms (Figure 6-10 and Appendix Figure 9-11) produced the same trend and the chromatograms of separation using S-300 chromatograms are complemented with that of the separation using the S-200 column.

The *B. subtilis* CFE was also separated on the S-300 column with 2 ml loop and a similar trend in peaks at particular EVs range were visible when compared to the recombinant (Figure 6-11). Understandably, *B. subtilis* CFE created more peaks on the chromatogram compared to the recombinant strain, as all proteins would be expressed in *B. subtilis*. Whereas the recombinant proteins, which are dominant in *E.coli*, will be expressed greater than native proteins which would be present as small peaks or even baseline in comparison. The peaks of interest in the *B. subtilis* CFE are at EVs 45 – 50 ml, 55 – 60 ml and 70 ml (Figure 6-11). We suspected that these EVs relate to the trimer of trimers, the dimer of trimers and the trimer respectively.

Table 5-13 summarised all the chromatogram results from standards, recombinant urease CFE, and native urease CFE, which were analysed through SEC using S-300 with 2 ml loop.

The combined analysis of recombinant urease using the native tris glycine gels and chromatograms produced via SEC indicate that the recombinant protein is present as the trimer of trimers, dimer of trimers, and the trimer with subunits also present. If this is the case, it would reflect the loss in activity compared to the visible amount of protein over expressed as shown on the SDS-PAGE gels Figure 6-2 and Figure 6-3). This needed to be confirmed using SDS-PAGE and protein ID analysis.

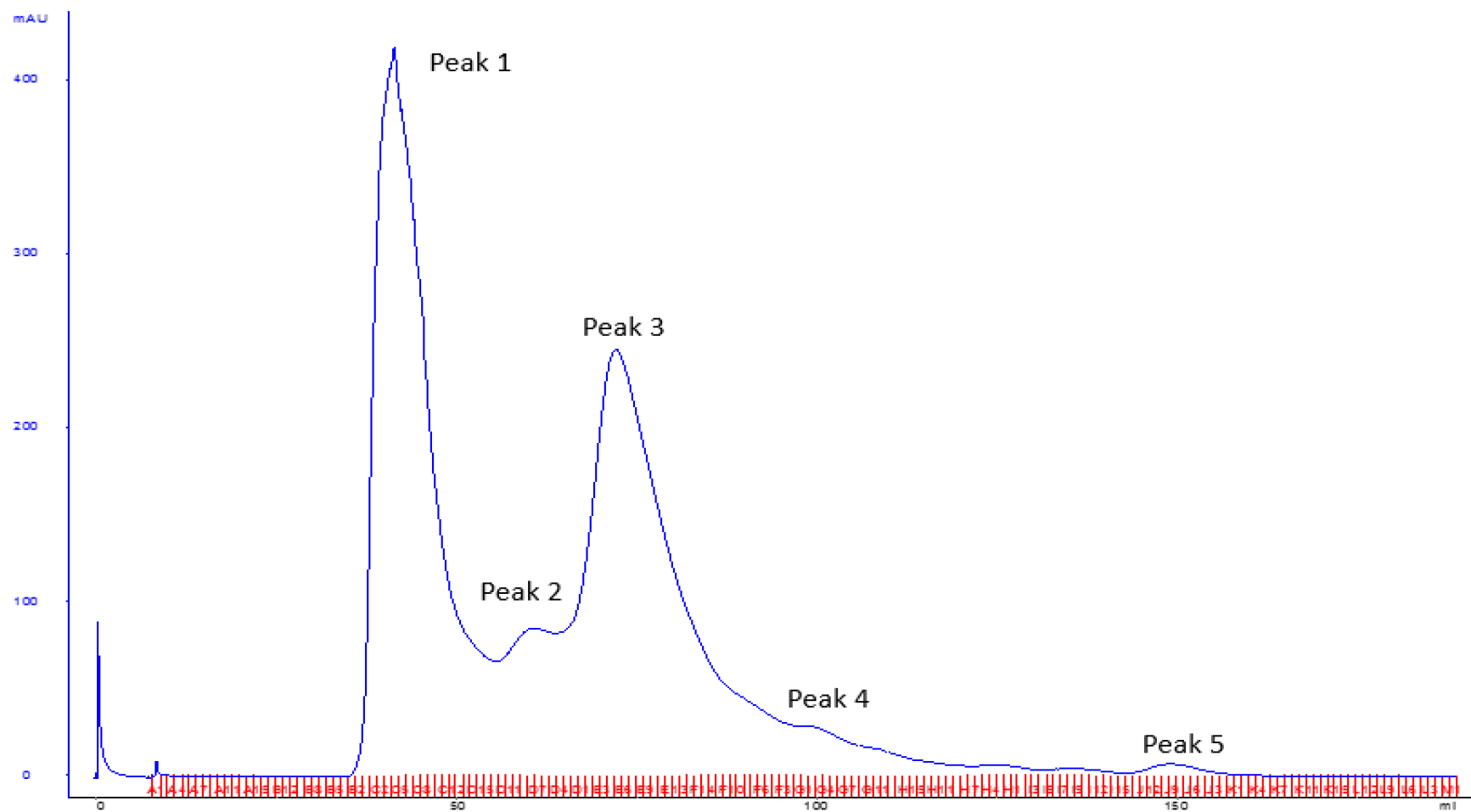


Figure 6-10. SEC Chromatogram of recombinant urease CFE separated using S-300 column with 2 ml loop. Chromatogram of recombinant CFE 2 ml detailing 5 peaks

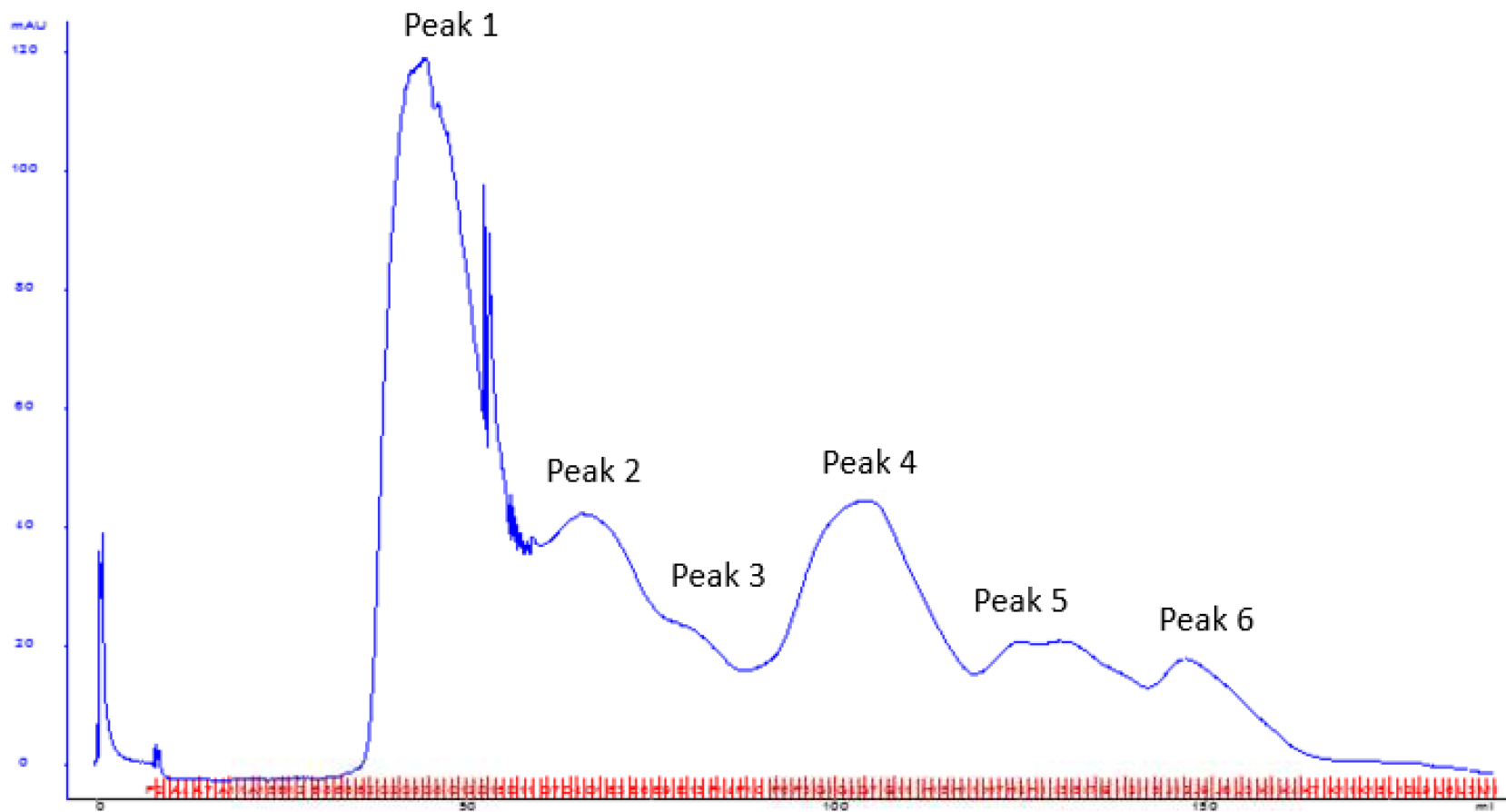


Figure 6-11. SEC Chromatogram of *B. subtilis* 168 urease CFE separated using S-300 column with 2 ml loop. *B. subtilis* 168 CFE chromatogram using S-300 2 ml loop identifying 6 prominent peaks.

Table 6-4. SEC Combined chromatogram results S-300 2ml loop

Recombinant/Native/Std	Peak	Approx. EV Range (ml)	Approx. Mol.wt (kDa)	Possible Description (mol. wt)	Figure (for ref.)
SEC Standard	1	< 5	670	Thyroglobulin	Appendix fig. 9-9
	2	55 - 60	158	γ -globulin	Appendix fig. 9-9
	3	75 - 85	44	Ovalalbumin	Appendix fig. 9-9
	4	95 - 100	17	Myoglobin	Appendix fig. 599
	5	> 135	1	Vitamin B12	Appendix fig. 9-9
BSA Standard dimer	1	60 - 65	132	BSA Standard	Appendix fig. 9-12
BSA Standard monomer	2	70 - 75	66	BSA Standard	Appendix fig. 9-12
Recombinant BL21(DE3) + pURE91	1	40 - 55	>158	Trimer of trimers (256 kDa)	Figure 6-14 and Appendix Figure 9-13
	2	50 - 65	>132<P1	Dimer of Trimers (170 kDa)	
	3	65 - 70	66 - 132	Trimer (85 kDa)	
	4	100 - 105	17 - 1	UreA (13 kDa)	
	5	145 - 150	\approx 1	UreB (11 kDa)	
Native <i>B. subtilis</i> (5 peaks of interest)	1	45 - 50	>158	Trimer of trimers (256 kDa)	Figure 6-11
	2	55 - 60	>132<P1	Dimer of Trimers (170 kDa)	
	3	70 - 80	66 - 132	Trimer (85 kDa)	
	4	95 - 110	17 - 1	UreA (13 kDa)	
	5	115 - 135	17 - 1	UreB (11 kDa)	

6.2.4.1 Further Analysis of SEC Fractions via SDS-PAGE and Protein ID Analysis

To identify the urease polymers formed by structural protein subunits in the SEC fractions, SDS-PAGE was utilised to visualize the proteins in all fractions within the identified peaks. Based on the chromatograms shown in Figure 6-14 and Appendix Figure 9-11, we have identified peak 1 contains fraction numbers B2 to C12, peak 2 contains fraction numbers C14 to D4 and peak 3 contains fraction numbers E3 to F11. 20 µl of each identified fraction was analysed by 14 % SDS-PAGE. As the volume of the loop was increased it enabled the protein/s in the fractions to be visualised on an SDS-PAGE gel.

The initial SDS-PAGE images detailed in Figure 6-12 demonstrated that the band corresponding to the size of UreC is peak 1 (Figure 6-12 A), which is highlighted in red. Same bands present in peak two (Figure 6-12 B) (highlighted in red) along with visible amounts of bands corresponding to the sizes of UreA and UreB (highlighted in blue). Peak 3 is also present for comparison (Figure 6-12 C), again, highlighted in red is the potential UreC, however protein concentration is again reduced in fractions of peak 3 when compared to fractions of peak 2. Based on these images, it appears that the potential UreC are more concentrated in the fractions of peak 2 as a far greater proportion of this band are evident in peak 2 compared to peak 1 and peak 3.

To compare the amount of potential urease in each peak, the fractions of each peak were then pooled, a TCA precipitation was carried out and the concentrated fractions were analysed on SDS-PAGE. The result confirmed that there was more potential urease present in peak 2 than in peaks 1 and 3 as shown in Figure 6-13. To confirm the ID of the potential UreC, GELC-MS/MS proteomics analysis was employed to analyse the bands that appear on the gel which correspond to the size of UreA, UreB and UreC. A MASCOT search utilising the *B. subtilis* protein database confirmed the bands as UreA, UreB and UreC.

The protein ID data (Appendix Table 9-6) and the results from Figure 6-13, confirmed that although some of the recombinant urease is folding (peak 1) as the trimer of trimers, the majority is folding incorrectly as the dimer of trimers. As within the recombinant CFE most of the protein

exists as the dimer of trimers (peak 2) and then the trimer of trimers (peak 1) which provides limited enzyme activity.

This knowledge confirms the enzyme is not fully functional as both Kim *et al.* (2005) and this study observed, due to the fact it is not forming correctly as an active enzyme, i.e. the trimer of trimers. The proteins are not all forming the correct functional unit and much is present as the dimer of trimer producing a less active urease enzyme in the recombinant urease. This would explain the protein being present in a high concentration, e.g. Western blot and SDS PAGE yet still only producing low level urease activity.

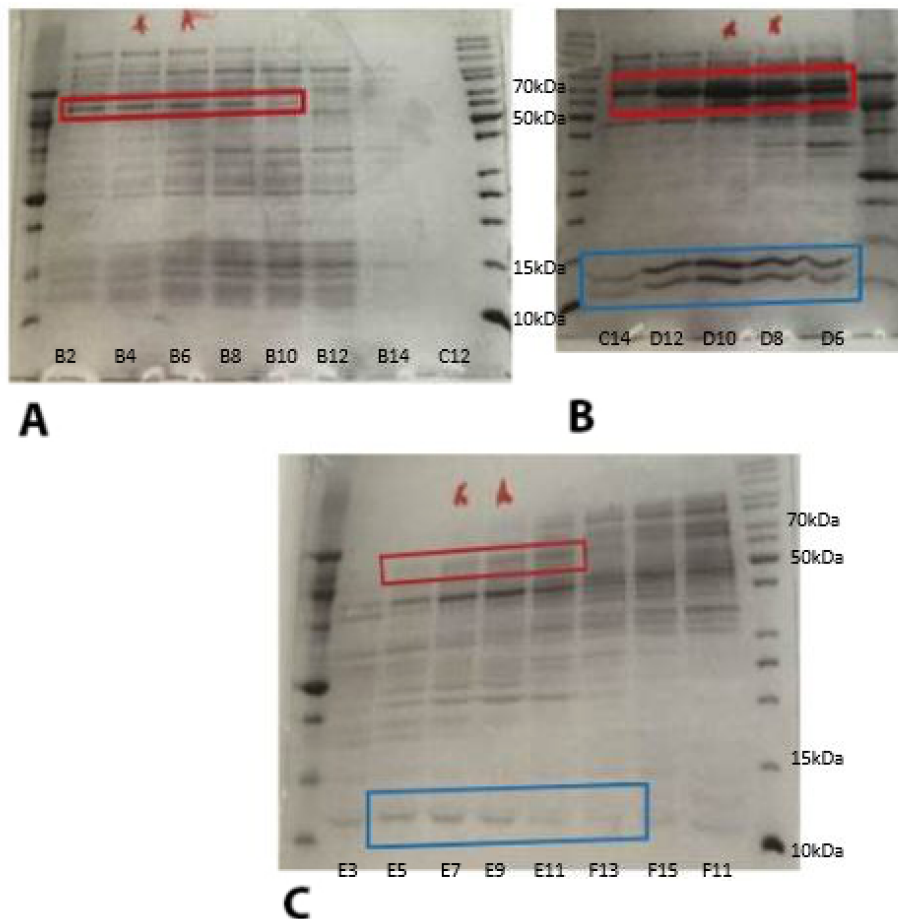


Figure 6-12. Recombinant CFE Peak fractions from AKTA S-300 2 ml loop.

A. Peak 1 fractions UreC visible (highlighted in red). B Peak 2 fractions UreC (highlighted in red), UreA and UreB visible (highlighted in blue), plus pooled Peaks 1,2 and 3. C. Peak 3 fractions UreC (highlighted in red), UreA and UreB (highlighted in blue) visible. A far greater proportion of urease subunits are evident in peak 2 compared to peak 1 and peak 3. *Samples used for in gel digestion.

Many proteins can have problems achieving their native configuration, however they are helped by chaperones to fold properly, using energy from ATP (Reynaud, 2010). Recent work by Zhao (2019) demonstrated the function of Hsp60 as a chaperone in urease stabilization and assembly in *H. pylori* urease (Zhao *et al.*, 2019a). Oligomeric proteins like urease are more advantageous than monomers as it is easier for multi-subunit proteins to repair their defects by replacing the flawed subunit. It is apparent that *in vivo* protein conformation is complicated and includes many physiological responses and cellular proteins. Recombinant protein production can produce conformational stress conditions which can greatly change the physiology of the host cell. The process can then generate in cell processes which attempt to manage misfolding and recover cell folding homeostasis (Gasser *et al.*, 2008).

If such a chaperone exists in *B. subtilis*, then the chaperone that enables UreABC to form the trimer of trimers in *B. subtilis* has not been cloned into BL21 (DE3)+pURE91 and so this may explain the inability to form the correct conformation of urease in the recombinant strain and also highlight that specific proteins in *B. subtilis* may still serve to enable a functioning urease. Recombinant proteins are also best expressed at low temperatures. In this research, we express at 30°C, which is lower than that of Kim *et al.* (2005), but still high for protein expression. We could hypothesise that the recombinant cells are producing vast amounts of the single unit of urease due to the efficient promoter but too fast to be able to form the correct protein conformation to produce the fully active urease. A lower temperature over a longer time may see a more optimised method whereby an active protein structure is achieved compared to the amount expressed.

Baneyx *et al.* (2004) discuss expression in *E. coli* and if the heterologous proteins do not require complex post-translational modifications and are expressed in a soluble form *E. coli* is best to pursue recombinant expression. However, it is not uncommon that overexpressed recombinant proteins fail to reach the correct conformation due to premature termination of translation, failure of the newly synthesised chain to reach the correct conformation and environmental stress (Baneyx and Mujacic, 2004).

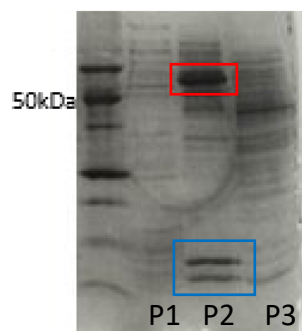


Figure 6-13. SDS-PAGE gel of each pooled peak from S-300 column with 2 ml loop of recombinant urease CFE.

It was necessary to understand the native urease with regard to the recombinant folding. The same specific 5 peaks of interest regarding urease present in the recombinant chromatograms can be visualised on the chromatogram for the *B. subtilis* CFE (Table 6-4) at the corresponding EVs. The conformation of native urease needed to be confirmed. So, the *B. subtilis* urease SEC fractions were investigated via SDS-PAGE gel electrophoresis (see Appendix Figure 9-12). However, due to a lower level of protein expression, the proteins from the fractions of each peak are not visible even after numerous optimisations including TCA precipitation and increasing culture volume for higher concentration of CFE. Nevertheless, the confirmation of the similarity of the recombinant and the native urease can be deduced from the chromatograms. Although it is hard to confirm the folding of the urease from *B. subtilis* cells without confirmation from SDS-PAGE gels.

6.3 Summary

This chapter of research focussed on recombinant urease produced in *E. coli* BL21(DE3) with the aim of comparing the findings to that of native *B. subtilis* urease to understand urease activation. The plasmid pURE91 contained *B. subtilis ureABC* which was transformed using *E. coli* BL21(DE3). Conditions for recombinant urease expression were optimised to 30°C and induced using 1 M IPTG. Protein expression of the recombinant urease was confirmed via SDS-PAGE see Figure 6-3 and Western blot analysis see Figure 6-5.

The expression of urease was far greater in the recombinant than in the native strain (Figure 6-2).

However, this was not echoed via enzyme activity assays (see Figure 6-6 and Figure 6-7). Unexpectedly, given the expression, urease activity was lower in the recombinant than in the native. Analysis through native gels highlighted that the recombinant urease may not be folding correctly and that the majority of the protein was forming as the dimer of trimers and not the trimer of trimers. The use of SEC combined with SDS-PAGE enabled further analysis of the protein and confirmed that urease is not folding correctly in the recombinant strain. The incorrect conformation of the protein could be connected to the requirement of energy in the cell to synthesise this quaternary protein. To assemble the correct protein conformation would require energy from e.g. ATPase so incorrect assembling may be due to the loss of a particular protein that is required. Ideally the protein conformations of each urease polymer would be investigated for urease activity and compared. But this was not possible due to the amount of protein present.

This work can hypothesise that there is no activation mechanism in *B. subtilis* based on the results from Chapter 4 and Chapter 5. We can however speculate that there may be proteins involved in post-translational modifications or acting allosterically such as chaperones due to the low but greater activity in the native compared to the recombinant. There are peaks in the native chromatogram Figure 6-11 that correlate to those in the recombinant chromatograms (see Figure 6-10 and Appendix Figure 9-11), however the low urease expression in the native meant the proteins from those peaks could not be investigated. So, we could not distinguish the proteins correctly in those peaks.

There are of course limitations in SEC and with regard to this study the main limitations were the need for a correct standard size that equated to the size of the trimer of trimers, dimer of trimers and trimer to enable correct identification. There was also the possibility the sample dilution before or during the SEC analysis may incur a dissociation of concentration dependent aggregate protein (Hughes *et al.*, 2009).

The results also indicated that the columns when connected to the 2 ml loop as opposed to the 100 µl loop were not separating the proteins as effectively. This could be due to various reasons: in theory SEC separations are based on the molecular size of the peptide or protein in a specific solution, however non ideal interactions can be experienced between the molecules and the

packing material within the column. These improper interactions can have great implications upon the retention time, the peak shape and the end recovery of the protein (Hong, Koza and Bouvier, 2012). The chromatograms also identify that using the 2ml loop may load too much protein on the column, however, this was necessary for visualisation of the eluted sample.

This work could be further investigated if time had permitted. Repeats of CFE harvesting especially for *B. subtilis* urease and SEC repeats utilising S-300 2 ml loop would further confirm the results along with confirmation via SDS-PAGE gel electrophoresis. The ability to achieve frequent running of the 5-standard mixture on the S-300 (2 ml loop) column would indicate how effective the column separation was (especially over time) and indicate definitive EVs for specific protein sizes.

This research enables us to state that the conclusion from Kim *et al.* (2005) was not comprehensive enough regarding recombinant urease. Their results which we mirrored identified urease expression in the recombinant to be greater than in the native, but in comparison to the amount of urease expressed, urease activity did not correlate. However, their study did not determine that the recombinant urease was not being synthesised in its fully active form and we describe how various forms of the enzyme exist *in vivo*: the trimer of trimers, the dimer of trimers and the trimer itself. We optimised their method and reduced the temperature of expression to 30°C and induced with 1 M IPTG, however further optimisation is needed. To prove our hypothesis, we need to optimise the *E. coli* expression system to understand the overall activation process. This optimisation could include temperature, a lower temperature over a longer period of time to encourage the slow formation of recombinant protein. The use of the highly efficient T7 could also be optimised in using a less efficient promoter to enable the slower production of the clone and enable the study of the enzyme interactions on the recombinant protein. Therefore, to optimise the recombinant expression would be essential for future work. If a protein in *B. subtilis* is discovered which is associated to urease activation or as we hypothesise conformation, then this too along with *ureABC* can be cloned successfully into BL21 (DE3) and the interactions explored fully via the optimised process.

Chapter 7 Conclusions and Future Work

This research was one work package of the EPSRC funded ‘Thinking Soils’ project. The ‘Thinking Soils’ project aims to develop a bacterial system using *B. subtilis* where urease expression is increased under pressure leading to CaCO₃ production for use in soil improvement and wider civil engineering applications. To achieve this, we need to understand the regulation and activation of urease in *B. subtilis*. The research carried out in this thesis aims to understand the absent knowledge in the activation of urease in *B. subtilis*. Based on previous findings, this project utilises various experiments performed in order to understand and identify urease activation in *B. subtilis* 168, involving altering growth conditions such as pH, nitrogen availability and metal ion concentrations; utilising a comparative proteomics approach to investigate the differentially expressed proteins and assessing their role in the activation of urease *in vivo*.

7.1 Summary and Conclusion

The regulation of *B. subtilis ureABC* is complex and it is regulated by PucR, TnrA, CodY, and GlnR, and expression is also dependent on SigA and SigH (Ter Beek *et al.*, 2008). As these regulons are connected to nitrogen availability and *B. subtilis* urease has been demonstrated to be greater in NLCs this would feature in the growth media. Therefore, initial investigations into *B. subtilis* urease activation and regulation involved defining a MM that would enable the growth of *B. subtilis* whilst also increasing urease activity. In Chapter 3, growth media conditions were investigated including nitrogen levels, pH and additions of metal ions (Figure 3-16). By defining two media (NPM and NLM) we could confirm urease activity in *B. subtilis* 168 was greater in the NLM. The MM BSS (JW) was defined which created a NLM to promote urease activity. The optimum growth phase of urease activity in this media was confirmed at end exponential. The production of 2 different media not only enabled a comparison for urease activity but could also be used in the comparative proteomics study investigating differentially expressed proteins potentially involved in the activation of urease. An optimised Nessler assay was developed as the suitable enzyme assay to detect urease activity for the future of this study.

To investigate the different proteins expressed in the different nitrogen conditions, a GELC-MS/MS comparative proteomics study was employed in Chapter 4. Initially three buffers were compared to achieve the maximum protein identification with good urease activity, HEPES +

PMSF was determined as the optimum buffer with a working pH of 7.4-8. Proteins differentially expressed in the NLM and NPM were investigated and initially 20 proteins were considered for their role in urease activation in *B. subtilis* based on their fold change, molecular function and literature searches. Those considered are detailed in Table 4-6 and knockouts of each were considered for further investigation.

In Chapter 5, initial investigations utilising knockouts purchased from Addgene were of the peptide transport system *opp*. This peptide transport system was chosen for a number of reasons: 1) the *opp* system was upregulated in wild-type 168 cultured in the NLM and it is regulated by TnrA under NLCs; 2) OppA belongs to the SBP family 5 which consists of peptide and nickel-binding proteins which includes the periplasmic nickel-binding protein NikA of *E. coli*; 3) literature identifies peptide transport systems originally annotated as *opp* are cobalt and nickel transporters that impact urease activity in *S. aureus* (Hiron *et al.*, 2010); and 4) OppA was of significance for urease activity and may be involved in urease activation in *B. subtilis* (Hausinger, unpublished work). Enzyme assay results demonstrated urease activity was greater in $\Delta oppA$ and UreC expression was also upregulated. Also investigated for their role in urease activation included the knockouts of the remaining *opp* system components OppB, OppC, OppD and OppF. The knockouts of these all included comparable urease activity to strain 168. The proteomics data then revealed urease expression was similar in $\Delta oppC$, $\Delta oppD$ and $\Delta oppF$ and in $\Delta oppB$ UreC was upregulated by a fold change of 2.42 which is not of a marked difference. This combination of results led us to acknowledge the *opp* system is not involved in urease activation.

DppA was also studied as it was differentially expressed in the wild-type 168 cultured in NLM and DppA proteins share similar conservations in their protein folding when compared to the Ni²⁺ binding protein NikA of *E. coli*. DppA had also been investigated in *H. pylori* for its contribution to urease activation (Davis and Mobley, 2005). The knockout demonstrated a decrease in urease activity however proteomic analysis detailed urease was downregulated corresponding to the activity, so it is unlikely DppA is involved in urease activation in *B. subtilis*.

The increase in urease activity in $\Delta oppA$ was not expected and so proteomic and bioinformatics analysis was carried out on this knockout. The increase in urease activity in $\Delta oppA$ is due to the

increased expression of urease which may be due to knockout strain creating further nitrogen limitation for the cells. Interestingly a GTPase was differentially expressed YciC 136-fold in $\Delta oppA$ along with 2 components (ZnuA and ZnuB) of the Zn^{2+} transporter ZnuABC. YciC was eagerly investigated as we hypothesised this protein may play a role similar to UreG in *B. subtilis*, as UreG is classified as a GTPase and provides energy for Ni^{2+} insertion during urease activation in other bacteria. Unfortunately, enzyme assay results identified the knockout of *yciC* in *B. subtilis* had little impact on urease activity. Which indicated that this protein is not involved in urease activation. At the same time, we were investigating the Zn^{2+} transporter ZnuABC. Knockouts of *znuA* and *znuB* demonstrated a decrease in urease activity compared to the 168 strain but proteomic analysis revealed urease was downregulated in both these knockouts which explained the decrease in activity.

The results of Chapter 5 led us to investigate the *B. subtilis* enzyme as a whole and its structure. So, in Chapter 6, we investigated the heterologous expression of *B. subtilis* urease, and aimed to create a system that can be used to explore the possible mechanism for urease activation. Initially we compared the activity between native *B. subtilis* urease and recombinant urease. The plasmid pURE91, which is a pET23 with *B. subtilis ureABC* inserted, was transformed into *E. coli*. Recombinant expression of *ureABC* was confirmed via SDS-PAGE and Western blot analysis. Expression was visibly greater in the recombinant compared to native expression however, urease activity was lower. SEC techniques in combination with SDS-PAGE and protein ID analysis identified the recombinant urease was not forming the typical active conformational structure of a trimer of trimers Ure(ABC)₃, but was mostly producing a dimer of trimers Ure(ABC)₂. The greater expression of urease in the recombinant cells with a lower activity enables us to hypothesise that there is no urease activation mechanism in *B. subtilis*. There may not be the specific accessory proteins as we understand for other ureolytic bacteria (such as UreDFG) but in *B. subtilis* there may be a protein that acts as a chaperone providing energy as recently identified by Zhao *et al.* (2019) the function of Hsp60 as a chaperone in urease stabilization and assembly in *H. pylori* urease (Zhao *et al.*, 2019a). This hypothesis of no activation mechanism utilising accessory proteins would explain the baseline level of urease activity in *B. subtilis* (Cruz-Ramos

et al., 1997) as typical accessory proteins are known to greatly enhance the efficiency of urease activity (Kim, Mulrooney and Hausinger, 2005a). The cells do not need to produce a fully functional urease in order for survival, the baseline level they produce is sufficient for the needs of the cell. The strain of *B. subtilis* utilised in this research is 168, a lab strain which is a descendent of the Marburg strain, and the 168 lineage shows genetic evidence of early domestication (Zeigler *et al.*, 2008). As the lab strain evolved and became more domesticated, the necessity for optimum urease activity may have diminished.

This conclusion of the work identifies the necessity for the recombinant expression method to be optimised in order to achieve a full understanding of urease activation in *B. subtilis*. Once the expression method was optimised and if a specific protein was identified from knockout analysis which may create stabilisation of the protein structure, then this gene could then be cloned along with *B. subtilis ureABC* and the mechanism for activation could be explored.

To conclude, urease is activated in *B. subtilis* but with low efficiency and no potential accessory proteins have been confirmed in this study. We have identified two transport systems that are connected to urease activity in *B. subtilis* but are not associated directly with the activation of the enzyme. The first is the oligopeptide transporter *oppABCDF*. Whereby in $\Delta oppA$ urease activity and expression was increased and in $\Delta oppB-oppF$ urease activity was comparable to the 168 strain and expression was not changed. The second transport system was the high affinity Zn^{2+} transport system, *ZnuABC*. Knockout strains of *znuA* and *znuB* demonstrated a decrease in urease activity and urease expression was also downregulated in both, therefore the transport system is not directly involved in the activation of urease and instead, they have an influence on the regulation of urease but this mechanism is not currently understood.

It seems unlikely that the typical accessory proteins present in ureolytic organisms such as UreDEFG are present in *B. subtilis*. However, as chaperones such as Hsp60 in *H. pylori* play a role in urease stabilization and assembly in *H. pylori* urease, similar proteins could be investigated in *B. subtilis*. This echoes the hypothesis of Kim *et al.* (2005) that there still may be an unidentified accessory protein acting stoichiometrically that activates urease in *B. subtilis* or as

we hypothesise a protein that acts allosterically. To confirm this we need to first optimise the urease expression system in *E.coli*.

It is obvious therefore that a greater understanding is still required of this important historical enzyme and that further investigations utilising the knowledge accomplished from this research are required to further understand urease activation in *B. subtilis*.

7.2 Future Work

Urease regulation and activation is complex. There has been extensive research into ureolytic pathogens such as *K. aerogenes* and *H. pylori* and yet those urease systems are still not fully understood. Throughout the 3 years of my PhD I investigated urease activation and regulation in *B. subtilis* 168. I have established under which conditions and also which individual genes impact urease activity. The activity is increased and decreased in certain conditions and specific gene knockouts, following proteomic techniques, have established urease expression in these conditions. To fully understand urease activity in *B. subtilis*, a recombinant urease expression system needs to be optimised. Due to time limitations there is further research I would like to undertake to optimise the *E.coli* expression system and fully establish urease activation in *B. subtilis*.

There were 2 media conditions where urease activity in *B. subtilis* was compared, NLM and NPM. *B. subtilis* 168 cultured in NLM saw an increase in urease activation as did the knockout of OppA. There were common proteins associated with both conditions detailed in Table 5-3 that were expressed in the 2 conditions (168 and $\Delta oppA$) when urease activity was increased. Of those common proteins the majority had clear biological roles, e.g. PucR and TnrA were associated with urease regulation, NasD and NasC are involved in nitrate assimilation. However, although CheA was not investigated due to time limitations of the research and the argument the protein was upregulated simply due to a chemotactic response, it would still be interesting to consider the knockout analysis of this gene. This sensor kinase was upregulated in both the wild-type 168 and $\Delta oppA$ and there is also a link being investigated in *H.pylori* in which chemotaxis and flagella are being considered to be involved in urease activation (McGee *et al.*, 1999; Gu, 2017). Knockout analysis of CheA would determine its role in urease activation in *B. subtilis*.

The expression of recombinant urease in *E. coli* also needs to be optimised. Using a recombinant system to study the role of a particular protein in a biological process is common practice. There are a few studies that have utilised this system to understand urease activation (Kim, Mulrooney and Hausinger, 2005a; Cruz-Ramos *et al.*, 1997). However, we have proved our expression system produces proteins that are unable to form the correct structure to be fully active. To be able to truly assess any potential accessory proteins for urease activation, we need to optimise the expression system. There are several steps we could adapt to reduce the urease expression rate and help to achieve the correct configuration: 1) produce the proteins in lower temperature, this was done but expression was low, however, the time at the lower temperature could be increased and expression could be visualised via SDS-PAGE and utilising SEC would determine if the conformation was correct; 2) protein chaperones and folding catalysts could be used as they prevent or correct the damage caused by misfolding; Hsp60 in *H. pylori* has been demonstrated to play a role in urease stabilization and assembly in *H. pylori* urease (Zhao *et al.*, 2019a); 3) using a less efficient expression system because T7 is such an efficient promoter, a promoter that expresses the clone at a reduced rate such as pBAD in BL21-AI host cells may encourage the correct folding. Optimising urease recombinant expression would enable a process whereby large amounts of active urease could be synthesised and therefore investigated. Once this process is achieved if a protein in *B. subtilis* is discovered which is associated to urease activation, then this too, along with *ureABC*, can be cloned successfully into BL21(DE3) and the interactions explored fully via the optimised system.

The optimisation of the expression of recombinant urease also links to the necessity to test different urease purification techniques. The testing and implementation of a reliable purification technique would enable us to purify large amounts of urease using e.g. DEAE cellulose columns to purify the enzyme to characterise the structure and in turn understand the activation process should one be present. Knockout strains could also be analysed for specific metal binding. We could utilise gel electrophoresis with X-ray Fluorescence (XRF) imaging which would determine the elemental composition of e.g. CFE. This would highlight if knockout strains bound different

metals during urease maturation causing a difference in activity and could also be combined with radioactive $^{63}\text{Ni}^{2+}$ studies understanding where Ni^{2+} is utilised and how much.

It would also be interesting to use specific bioinformatic programmes to compare the genome of *B. subtilis* to its parent strain and those related to ascertain if urease accessory genes have been 'lost' in mutational strain improvements. *B. subtilis* 168 is a lab strain which is a descendent of the Marburg strain, and the 168 lineage shows genetic evidence of early domestication (Zeigler *et al.*, 2008). As the lab strain evolved and became more domesticated, the necessity for optimum urease activity may have diminished. The comparison of the Marburg genome and 168 may demonstrate the loss of particular genes associated with urease activation in *B. subtilis*.

Chapter 8 **References**

Achal, V., Kumari, D. and Pan, X. (2011) 'Bioremediation of chromium contaminated soil by a brown-rot fungus, *Gloeophyllum sepiarium*', *Research Journal of Microbiology*, 6(2), pp. 166.

Achal, V., Mukherjee, A., Basu, P. and Reddy, M. S. (2009) 'Strain improvement of *Sporosarcina pasteurii* for enhanced urease and calcite production', *Journal of industrial microbiology & biotechnology*, 36(7), pp. 981-988.

Achal, V. and Pan, X. (2014a) 'Influence of calcium sources on microbially induced calcium carbonate precipitation by *Bacillus* sp. CR2', *Applied biochemistry and biotechnology*, 173(1), pp. 307-317.

Achal, V. and Pan, X. (2014b) 'Influence of calcium sources on microbially induced calcium carbonate precipitation by *Bacillus* sp. CR2', *Appl Biochem Biotechnol*, 173(1), pp. 307-17.

Amidi, S. and Wang, J. (2015) 'Surface treatment of concrete bricks using calcium carbonate precipitation', *Construction and Building Materials*, 80, pp. 273-278.

Arjes, H. A., Vo, L., Dunn, C. M., Willis, L., DeRosa, C. A., Fraser, C. L., Kearns, D. B. and Huang, K. C. (2020) 'Biosurfactant-Mediated Membrane Depolarization Maintains Viability during Oxygen Depletion in *Bacillus subtilis*', *Current Biology*.

Arndt, C., Koristka, S., Bartsch, H. and Bachmann, M. (2012) 'Native polyacrylamide gels', *Methods Mol Biol*, 869, pp. 49-53.

Ashraf, M. S., Azahar, S. B. and Yusof, N. Z. (2017) 'Soil improvement using MICP and biopolymers: A review', *Mater. Sci. and Eng*, 226, pp. 012058.

Atkinson, M. R. and Fisher, S. H. (1991) 'Identification of genes and gene products whose expression is activated during nitrogen-limited growth in *Bacillus subtilis*', *J Bacteriol*, 173(1), pp. 23-7.

Bachmeier, K. L., Williams, A. E., Warmington, J. R. and Bang, S. S. (2002) 'Urease activity in microbiologically-induced calcite precipitation', *Journal of biotechnology*, 93(2), pp. 171-181.

Balasubramanian, A. and Ponnuraj, K. (2010) 'Crystal structure of the first plant urease from jack bean: 83 years of journey from its first crystal to molecular structure', *J Mol Biol*, 400(3), pp. 274-83.

Bandow, J. E., Brötz, H., Leichert, L. I. O., Labischinski, H. and Hecker, M. (2003) 'Proteomic approach to understanding antibiotic action', *Antimicrobial agents and chemotherapy*, 47(3), pp. 948-955.

Baneyx, F. and Mujacic, M. (2004) 'Recombinant protein folding and misfolding in *Escherichia coli*', *Nature biotechnology*, 22(11), pp. 1399-1408.

Bauerfeind, P., Garner, R., Dunn, B. and Mobley, H. (1997) 'Synthesis and activity of *Helicobacter pylori* urease and catalase at low pH', *Gut*, 40(1), pp. 25-30.

Bauerfeind, P., Garner, R. M. and Mobley, L. (1996) 'Allelic exchange mutagenesis of *nixA* in *Helicobacter pylori* results in reduced nickel transport and urease activity', *Infection and immunity*, 64(7), pp. 2877-2880.

Baysal, Ö., Lai, D., Xu, H.-H., Siragusa, M., Çalışkan, M., Carimi, F., Da Silva, J. A. T. and Tör, M. (2013) 'A proteomic approach provides new insights into the control of soil-borne plant pathogens by *Bacillus* species', *PLoS One*, 8(1).

Beier, L., Nygaard, P., Jarmer, H. and Saxild, H. H. (2002) 'Transcription analysis of the *Bacillus subtilis* PucR regulon and identification of a cis-acting sequence required for PucR-regulated expression of genes involved in purine catabolism', *Journal of bacteriology*, 184(12), pp. 3232-3241.

Belitsky, B. R., Barbieri, G., Albertini, A. M., Ferrari, E., Strauch, M. A. and Sonenshein, A. L. (2015) 'Interactive regulation by the *Bacillus subtilis* global regulators CodY and ScoC', *Molecular microbiology*, 97(4), pp. 698-716.

Belitsky, B. R. and Sonenshein, A. L. (1998) 'Role and regulation of *Bacillus subtilis* glutamate dehydrogenase genes', *J Bacteriol*, 180(23), pp. 6298-305.

Belitsky, B. R. and Sonenshein, A. L. (2011) 'CodY-mediated regulation of guanosine uptake in *Bacillus subtilis*', *J Bacteriol*, 193(22), pp. 6276-87.

Bellucci, M., Zambelli, B., Musiani, F., Turano, P. and Ciurli, S. (2009) '*Helicobacter pylori* UreE, a urease accessory protein: specific Ni(2+)- and Zn(2+)-binding properties and interaction with its cognate UreG', *Biochem J*, 422(1), pp. 91-100.

Benoit, S. L. and Maier, R. J. (2011) 'Mua (HP0868) is a nickel-binding protein that modulates urease activity in *Helicobacter pylori*', *MBio*, 2(2), pp. e00039-11.

Benoit, S. L., Mehta, N., Weinberg, M. V., Maier, C. and Maier, R. J. (2007) 'Interaction between the *Helicobacter pylori* accessory proteins HypA and UreE is needed for urease maturation', *Microbiology (Reading, England)*, 153(Pt 5), pp. 1474.

Bernhardt, J., Weibezahn, J., Scharf, C. and Hecker, M. (2003) '*Bacillus subtilis* during feast and famine: visualization of the overall regulation of protein synthesis during glucose starvation by proteome analysis', *Genome research*, 13(2), pp. 224-237.

Berntsson, R. P., Smits, S. H., Schmitt, L., Slotboom, D. J. and Poolman, B. (2010) 'A structural classification of substrate-binding proteins', *FEBS Lett*, 584(12), pp. 2606-17.

Biochemicals, R. M. (2006) 'The complete guide for protease inhibition', *Roche Molecular Biochemicals*.

Blindauer, C. A. (2015) 'Advances in the molecular understanding of biological zinc transport', *Chemical Communications*, 51(22), pp. 4544-4563.

Boer, J. L., Quiroz-Valenzuela, S., Anderson, K. L. and Hausinger, R. P. (2010) 'Mutagenesis of *Klebsiella aerogenes* UreG to probe nickel binding and interactions with other urease-related proteins', *Biochemistry*, 49(28), pp. 5859-5869.

Bolhuis, A., Broekhuizen, C. P., Sorokin, A., van Roosmalen, M. L., Venema, G., Bron, S., Quax, W. J. and van Dijk, J. M. (1998) 'SecDF of *Bacillus subtilis*, a molecular Siamese twin required for the efficient secretion of proteins', *J Biol Chem*, 273(33), pp. 21217-24.

Bose, H. and Satyanarayana, T. (2017) 'Microbial Carbonic Anhydrases in Biomimetic Carbon Sequestration for Mitigating Global Warming: Prospects and Perspectives', *Front Microbiol*, 8, pp. 1615.

Bossé, J. T., Gilmour, H. D. and MacInnes, J. I. (2001) 'Novel Genes Affecting Urease Activity in *Actinobacillus pleuropneumoniae*', *Journal of bacteriology*, 183(4), pp. 1242-1247.

Brandenburg, J. L., Wray, J. L. V., Beier, L., Jarmer, H., Saxild, H. H. and Fisher, S. H. (2002a) 'Roles of PucR, GlnR, and TnrA in Regulating Expression of the *Bacillus subtilis* ure P3 Promoter', *Journal of Bacteriology*, 184(21), pp. 6060-6064.

Brandenburg, J. L., Wray Jr, L. V., Beier, L., Jarmer, H., Saxild, H. H. and Fisher, S. H. (2002b) 'Roles of PucR, GlnR, and TnrA in regulating expression of the *Bacillus subtilis* ure P3 promoter', *Journal of bacteriology*, 184(21), pp. 6060-6064.

Brandenburg, J. L., Wray, L. V., Jr., Beier, L., Jarmer, H., Saxild, H. H. and Fisher, S. H. (2002c) 'Roles of PucR, GlnR, and TnrA in regulating expression of the *Bacillus subtilis* ure P3 promoter', *J Bacteriol*, 184(21), pp. 6060-4.

Brauer, A. L., Learman, B. S. and Armbruster, C. E. (2020) 'Ynt is the primary nickel import system used by *Proteus mirabilis* and specifically contributes to fitness by supplying nickel for urease activity', *Molecular Microbiology*.

Brayman, T. G. and Hausinger, R. P. (1996) 'Purification, characterization, and functional analysis of a truncated *Klebsiella aerogenes* UreE urease accessory protein lacking the histidine-rich carboxyl terminus', *Journal of bacteriology*, 178(18), pp. 5410-5416.

Breydo, L. and Uversky, V. N. (2011) 'Role of metal ions in aggregation of intrinsically disordered proteins in neurodegenerative diseases', *Metallomics*, 3(11), pp. 1163-1180.

Buono, F., Testa, R. and Lundgren, D. G. (1966) 'Physiology of growth and sporulation in *Bacillus cereus*. I. Effect of glutamic and other amino acids', *J Bacteriol*, 91(6), pp. 2291-9.

Carter, E. L., Flugga, N., Boer, J. L., Mulrooney, S. B. and Hausinger, R. P. (2009) 'Interplay of metal ions and urease', *Metallomics*, 1(3), pp. 207-221.

Carter, E. L. and Hausinger, R. P. (2010) 'Characterization of the *Klebsiella aerogenes* urease accessory protein UreD in fusion with the maltose binding protein', *Journal of bacteriology*, 192(9), pp. 2294-2304.

Carter, E. L., Tronrud, D. E., Taber, S. R., Karplus, P. A. and Hausinger, R. P. (2011) 'Iron-containing urease in a pathogenic bacterium', *Proc Natl Acad Sci USA*, 108(32), pp. 13095-9.

Castro Alonso, M. J., Montañez Hernández, L. E., Sanchez Muñoz, M. A., Franco, M., Rubi, M., Narayanasamy, R. and Balagurusamy, N. (2019) 'Microbially Induced Calcium carbonate Precipitation (MICP) and its potential in Bioconcrete: Microbiological and molecular concepts', *Frontiers in Materials*, 6, pp. 126.

Chandrangsu, P., Huang, X., Gaballa, A. and Helmann, J. D. (2019) 'Bacillus subtilis FOLE is sustained by the ZagA zinc metallochaperone and the alarmone ZTP under conditions of zinc deficiency', *Molecular microbiology*, 112(3), pp. 751-765.

Charpentier, B., Bardey, V., Robas, N. and Branlant, C. (1998) 'The EIIGlc Protein Is Involved in Glucose-Mediated Activation of *Escherichia coli* gapA and gapB-pgk Transcription', *Journal of bacteriology*, 180(24), pp. 6476-6483.

Chasin, L. A. and Magasanik, B. (1968) 'Induction and repression of the histidine-degrading enzymes of *Bacillus subtilis*', *J Biol Chem*, 243(19), pp. 5165-78.

Cheggour, A., Fanuel, L., Duez, C., Joris, B., Bouillenne, F., Devreese, B., Van Driessche, G., Van Beeumen, J., Frère, J. M. and Goffin, C. (2000) 'The dppA gene of *Bacillus subtilis* encodes a new d-aminopeptidase', *Molecular microbiology*, 38(3), pp. 504-513.

Chen, H.-J., Huang, Y.-H., Chen, C.-C., Maity, J. P. and Chen, C.-Y. (2019a) 'Microbial induced calcium carbonate precipitation (MICP) using pig urine as an alternative to industrial urea', *Waste and Biomass Valorization*, 10(10), pp. 2887-2895.

Chen, Y., Barat, B., Ray, W. K., Helm, R. F., Melville, S. B. and Popham, D. L. (2019b) 'Membrane proteomes and ion transporters in *Bacillus anthracis* and *Bacillus subtilis* dormant and germinating spores', *Journal of bacteriology*, 201(6), pp. e00662-18.

Chen, Y., Feng, Y., Deveaux, J. G., Masoud, M. A., Chandra, F. S., Chen, H., Zhang, D. and Feng, L. (2019c) 'Biom mineralization Forming Process and Bio-inspired Nanomaterials for Biomedical Application: A Review', *Minerals*, 9(2), pp. 68.

Chen, Y. Y. and Burne, R. A. (2003) 'Identification and characterization of the nickel uptake system for urease biogenesis in *Streptococcus salivarius* 57.I', *J Bacteriol*, 185(23), pp. 6773-9.

Cheng, L., Cord-Ruwisch, R. and Shahin, M. A. (2013) 'Cementation of sand soil by microbially induced calcite precipitation at various degrees of saturation', *Canadian Geotechnical Journal*, 50(1), pp. 81-90.

Ciurli, S., Safarov, N., Miletti, S., Dikiy, A., Christensen, S. K., Kornetzky, K., Bryant, D. A., Vandenberghe, I., Devreese, B., Samyn, B., Remaut, H. and van Beeumen, J. (2002) 'Molecular characterization of *Bacillus pasteurii* UreE, a metal-binding chaperone for the assembly of the urease active site', *J Biol Inorg Chem*, 7(6), pp. 623-31.

Clemens, D. L., Lee, B.-Y. and Horwitz, M. A. (1995) 'Purification, characterization, and genetic analysis of *Mycobacterium tuberculosis* urease, a potentially critical determinant of host-pathogen interaction', *Journal of bacteriology*, 177(19), pp. 5644-5652.

Collins, C. M. and Falkow, S. (1988) 'Genetic analysis of an *Escherichia coli* urease locus: evidence of DNA rearrangement', *Journal of bacteriology*, 170(3), pp. 1041-1045.

Consortium, T. U. (2018) 'UniProt: a worldwide hub of protein knowledge', *Nucleic Acids Research*, 47(D1), pp. D506-D515.

Costa, O. Y., Raaijmakers, J. M. and Kuramae, E. E. (2018) 'Microbial extracellular polymeric substances: ecological function and impact on soil aggregation', *Frontiers in microbiology*, 9, pp. 1636.

Cox, E. H. and McLendon, G. L. (2000) 'Zinc-dependent protein folding', *Current opinion in chemical biology*, 4(2), pp. 162-165.

Cruz-Ramos, H., Glaser, P., Wray, L. V., Jr. and Fisher, S. H. (1997) 'The *Bacillus subtilis* ureABC operon', *J Bacteriol*, 179(10), pp. 3371-3.

Culotta, V. and Scott, R. A. (2016) *Metals in cells*. John Wiley & Sons.

D'Urzo, A., Santambrogio, C., Grandori, R., Ciurli, S. and Zambelli, B. (2014) 'The conformational response to Zn (II) and Ni (II) binding of *Sporosarcina pasteurii* UreG, an intrinsically disordered GTPase', *JBIC Journal of Biological Inorganic Chemistry*, 19(8), pp. 1341-1354.

Dattelbaum, J. D., Lockett, C. V., Johnson, D. E. and Mobley, H. L. (2003) 'UreR, the transcriptional activator of the *Proteus mirabilis* urease gene cluster, is required for urease activity and virulence in experimental urinary tract infections', *Infection and immunity*, 71(2), pp. 1026-1030.

Davis, D., Lynch, H. and Varley, J. (1999) 'The production of surfactin in batch culture by *Bacillus subtilis* ATCC 21332 is strongly influenced by the conditions of nitrogen metabolism', *Enzyme and Microbial Technology*, 25(3-5), pp. 322-329.

Davis, G. S. and Mobley, H. L. (2005) 'Contribution of dppA to urease activity in *Helicobacter pylori* 26695', *Helicobacter*, 10(5), pp. 416-423.

Dawes, I. and Mandelstam, J. (1970) 'Sporulation of *Bacillus subtilis* in continuous culture', *Journal of bacteriology*, 103(3), pp. 529-535.

de Koning-Ward, T. F. and Robins-Browne, R. M. (1997) 'A novel mechanism of urease regulation in *Yersinia enterocolitica*', *FEMS microbiology letters*, 147(2), pp. 221-226.

De Muynck, W., De Belie, N. and Verstraete, W. (2010) 'Microbial carbonate precipitation in construction materials: a review', *Ecological Engineering*, 36(2), pp. 118-136.

DeJong, J., Soga, K., Kavazanjian, E., Burns, S., Van Paassen, L., Al Qabany, A., Aydilek, A., Bang, S., Burbank, M. and Caslake, L. F. 'Biogeochemical processes and geotechnical applications: progress, opportunities and challenges'. *Bio-and Chemo-Mechanical Processes in Geotechnical Engineering: Géotechnique Symposium in Print 2013*: Ice Publishing, 143-157.

Della Scala, G., Volontè, F., Ricci, G., Pedersen, M. B., Arioli, S. and Mora, D. (2019) 'Development of a milk-based medium for the selection of urease-defective mutants of *Streptococcus thermophilus*', *International journal of food microbiology*, 308, pp. 108304.

Demain, A. L. (1958) 'Minimal media for quantitative studies with *Bacillus subtilis*', *Journal of bacteriology*, 75(5), pp. 517.

Detsch, C. and Stülke, J. (2003) 'Ammonium utilization in *Bacillus subtilis*: transport and regulatory functions of NrgA and NrgB', *Microbiology*, 149(Pt 11), pp. 3289-97.

Detsch, C. and Stülke, J. (2003) 'Ammonium utilization in *Bacillus subtilis*: transport and regulatory functions of NrgA and NrgB', *Microbiology*, 149(11), pp. 3289-3297.

Deutscher, M. P. (1990) *Guide to protein purification*. Gulf Professional Publishing.

Dhami, N. K., Alsubhi, W. R., Watkin, E. and Mukherjee, A. (2017) 'Bacterial Community Dynamics and Biocement Formation during Stimulation and Augmentation: Implications for Soil Consolidation', *Front Microbiol*, 8, pp. 1267.

Dhami, N. K., Reddy, M. S. and Mukherjee, A. (2014) 'Application of calcifying bacteria for remediation of stones and cultural heritages', *Frontiers in microbiology*, 5, pp. 304.

Dharmakeerthi, R. and Thenabadu, M. (2013) 'Urease activity in soils: a review', *Journal of the National Science Foundation of Sri Lanka*, 24(3).

Doroshchuk, N. A., Gel'fand, M. S. and Rodionov, D. A. (2006) '[Regulation of nitrogen metabolism in gram-positive bacteria]', *Mol Biol (Mosk)*, 40(5), pp. 919-26.

Dreisbach, A., Otto, A., Becher, D., Hammer, E., Teumer, A., Gouw, J. W., Hecker, M. and Völker, U. (2008) 'Monitoring of changes in the membrane proteome during stationary phase adaptation of *Bacillus subtilis* using in vivo labeling techniques', *Proteomics*, 8(10), pp. 2062-2076.

Eitinger, T., Suhr, J., Moore, L. and Smith, J. A. (2005) 'Secondary transporters for nickel and cobalt ions: theme and variations', *Biometals*, 18(4), pp. 399-405.

EL-Hefnawy, M. E., Sakran, M., Ismail, A. I. and Aboelfetoh, E. F. (2014) 'Extraction, purification, kinetic and thermodynamic properties of urease from germinating *Pisum Sativum* L. seeds', *BMC biochemistry*, 15(1), pp. 15.

Ernst, F. D., Kuipers, E. J., Heijens, A., Sarwari, R., Stoof, J., Penn, C. W., Kusters, J. G. and van Vliet, A. H. (2005) 'The nickel-responsive regulator NikR controls activation and repression of gene transcription in *Helicobacter pylori*', *Infection and immunity*, 73(11), pp. 7252-7258.

Errington, J. and Aart, L. T. v. d. (2020) 'Microbe Profile: *Bacillus subtilis*: model organism for cellular development, and industrial workhorse', *Microbiology*, 166(5), pp. 425-427.

Eymann, C., Antelmann, H., Albrecht, D. and Hecker, M. (2007) 'Global gene expression profiling of *Bacillus subtilis* in response to ammonium and tryptophan starvation as revealed by transcriptome and proteome analysis', *Journal of molecular microbiology and biotechnology*, 12(1-2), pp. 121-130.

Eymann, C., Dreisbach, A., Albrecht, D., Bernhardt, J., Becher, D., Gentner, S., Tam, L. T., Büttner, K., Buurman, G. and Scharf, C. (2004) 'A comprehensive proteome map of growing *Bacillus subtilis* cells', *Proteomics*, 4(10), pp. 2849-2876.

Farazmand, A., Yakhchali, B., Shariati, P., Minuchehr, Z. and Ofoghi, H. (2012) 'In silico genome-wide screening for TnrA-regulated genes of *Bacillus clausii*', *Iranian Journal of Biotechnology*, 10(1), pp. 62-66.

Farrugia, M. A., Macomber, L. and Hausinger, R. P. (2013) 'Biosynthesis of the urease metallocenter', *J Biol Chem*, 288(19), pp. 13178-85.

Fedorova, K., Tarasov, N., Khalitova, A., Iljinskaya, O., Barabanshchikov, B. and Kayumov, A. (2013) 'The role of AmtB, GlnK and glutamine synthetase in regulation of transcription factor TnrA in *Bacillus subtilis*', *Cell and Tissue Biology*, 7(3), pp. 297-301.

Feist, P. and Hummon, A. B. (2015) 'Proteomic challenges: sample preparation techniques for microgram-quantity protein analysis from biological samples', *International journal of molecular sciences*, 16(2), pp. 3537-3563.

Fisher, S. H. (1999) 'Regulation of nitrogen metabolism in *Bacillus subtilis*: vive la difference!', *Molecular microbiology*, 32(2), pp. 223-232.

Fisher, S. H. and Wray, L. V. (2002) '*Bacillus subtilis* 168 contains two differentially regulated genes encoding L-asparaginase', *Journal of bacteriology*, 184(8), pp. 2148-2154.

Flores, M. E. (1996) 'Nitrogen regulation of urease synthesis in *Saccharopolyspora erythraea* ATCC 11365', *FEMS microbiology letters*, 139(1), pp. 57-62.

Follmer, C. (2008) 'Insights into the role and structure of plant ureases' *Phytochemistry*, 69(1), pp. 18-28.

Follmer, C. (2010) 'Ureases as a target for the treatment of gastric and urinary infections', *Journal of Clinical Pathology*, 63(5), pp. 424-430.

Follmer, C., Carlini, C., Yoneama, M.-L. and Dias, J. (2002) 'PIXE analysis of urease isoenzymes isolated from *Canavalia ensiformis* (jack bean) seeds', *Nuclear Instruments and Methods in Physics Research Section B: Beam Interactions with Materials and Atoms*, 189(1-4), pp. 482-486.

Fong, Y. H., Wong, H. C., Chuck, C. P., Chen, Y. W., Sun, H. and Wong, K.-B. (2011) 'Assembly of preactivation complex for urease maturation in *Helicobacter pylori* CRYSTAL STRUCTURE OF UreF-UreH PROTEIN COMPLEX', *Journal of Biological Chemistry*, 286(50), pp. 43241-43249.

Fong, Y. H., Wong, H. C., Yuen, M. H., Lau, P. H., Chen, Y. W. and Wong, K.-B. (2013a) 'Structure of UreG/UreF/UreH complex reveals how urease accessory proteins facilitate maturation of *Helicobacter pylori* urease', *PLoS biology*, 11(10).

Fong, Y. H., Wong, H. C., Yuen, M. H., Lau, P. H., Chen, Y. W. and Wong, K. B. (2013b) 'Structure of UreG/UreF/UreH complex reveals how urease accessory proteins facilitate maturation of *Helicobacter pylori* urease', *PLoS Biol*, 11(10), pp. e1001678.

Foster, A. W., Osman, D. and Robinson, N. J. (2014) 'Metal preferences and metallation', *J Biol Chem*, 289(41), pp. 28095-103.

Franceschini, A., Szklarczyk, D., Frankild, S., Kuhn, M., Simonovic, M., Roth, A., Lin, J., Minguez, P., Bork, P. and Von Mering, C. (2012) 'STRING v9. 1: protein-protein interaction networks, with increased coverage and integration', *Nucleic acids research*, 41(D1), pp. D808-D815.

Frankel, R. B. and Bazylnski, D. A. (2003) 'Biologically induced mineralization by bacteria', *Reviews in mineralogy and geochemistry*, 54(1), pp. 95-114.

Fu, M. S., Coelho, C., De Leon-Rodriguez, C. M., Rossi, D. C., Camacho, E., Jung, E. H., Kulkarni, M. and Casadevall, A. (2018) 'Cryptococcus neoformans urease affects the outcome of intracellular pathogenesis by modulating phagolysosomal pH', *PLoS pathogens*, 14(6), pp. e1007144.

Fujishiro, T. (2019) 'A route for metal acquisition for chelatase reaction catalyzed by SirB from *Bacillus subtilis*', *Unpublished*.

Fujita, Y., Taylor, J. L., Gresham, T. L., Delwiche, M. E., Colwell, F. S., McLing, T. L., Petzke, L. M. and Smith, R. W. (2008) 'Stimulation of microbial urea hydrolysis in groundwater to enhance calcite precipitation', *Environmental science & technology*, 42(8), pp. 3025-3032.

Gabriel, S. E., Miyagi, F., Gaballa, A. and Helmann, J. D. (2008) 'Regulation of the *Bacillus subtilis* yciC gene and insights into the DNA-binding specificity of the zinc-sensing metalloregulator Zur', *J Bacteriol*, 190(10), pp. 3482-8.

Galperin, M. Y., Kristensen, D. M., Makarova, K. S., Wolf, Y. I. and Koonin, E. V. (2019) 'Microbial genome analysis: the COG approach', *Briefings in bioinformatics*, 20(4), pp. 1063-1070.

Gasser, B., Saloheimo, M., Rinas, U., Dragosits, M., Rodríguez-Carmona, E., Baumann, K., Giuliani, M., Parrilli, E., Branduardi, P. and Lang, C. (2008) 'Protein folding and conformational stress in microbial cells producing recombinant proteins: a host comparative overview', *Microbial cell factories*, 7(1), pp. 11.

Ge, R.-G., Wang, D.-X., Hao, M.-C. and Sun, X.-S. (2013) 'Nickel trafficking system responsible for urease maturation in *Helicobacter pylori*', *World journal of gastroenterology: WJG*, 19(45), pp. 8211.

Geisel, N. (2011) 'Constitutive versus responsive gene expression strategies for growth in changing environments', *PLoS One*, 6(11), pp. e27033.

Gendlina, I., Gutman, D. M., Thomas, V. and Collins, C. M. (2002) 'Urea-dependent signal transduction by the virulence regulator UreR', *J Biol Chem*, 277(40), pp. 37349-58.

Gimpel, M. and Brantl, S. (2016) 'Dual-function sRNA encoded peptide SR1P modulates moonlighting activity of B. subtilis GapA', *RNA biology*, 13(9), pp. 916-926.

Gomez, M. G., Martinez, B. C., DeJong, J. T., Hunt, C. E., deVlaming, L. A., Major, D. W. and Dworatzek, S. M. (2015) 'Field-scale bio-cementation tests to improve sands', *Proceedings of the Institution of Civil Engineers-Ground Improvement*, 168(3), pp. 206-216.

Gorospe, C. M., Han, S.-H., Kim, S.-G., Park, J.-Y., Kang, C.-H., Jeong, J.-H. and So, J.-S. (2013) 'Effects of different calcium salts on calcium carbonate crystal formation by *Sporosarcina pasteurii* KCTC 3558', *Biotechnology and bioprocess engineering*, 18(5), pp. 903-908.

Gu, H. (2017) 'Role of Flagella in the Pathogenesis of *Helicobacter pylori*', *Current microbiology*, 74(7), pp. 863-869.

Gunka, K. and Commichau, F. M. (2012) 'Control of glutamate homeostasis in *Bacillus subtilis*: a complex interplay between ammonium assimilation, glutamate biosynthesis and degradation', *Molecular microbiology*, 85(2), pp. 213-224.

Hahne, H., Mäder, U., Otto, A., Bonn, F., Steil, L., Bremer, E., Hecker, M. and Becher, D. (2010) 'A comprehensive proteomics and transcriptomics analysis of *Bacillus subtilis* salt stress adaptation', *Journal of bacteriology*, 192(3), pp. 870-882.

Hausinger, R. P. (2011) 'Urease Activation', *Encyclopedia of Inorganic and Bioinorganic Chemistry*, pp. 1-10.

He, L., Diedrich, J., Chu, Y.-Y. and Yates III, J. R. (2015) 'Extracting accurate precursor information for tandem mass spectra by RawConverter', *Analytical chemistry*, 87(22), pp. 11361-11367.

Hecker, M., Schumann, W. and Völker, U. (1996) 'Heat - shock and general stress response in *Bacillus subtilis*', *Molecular microbiology*, 19(3), pp. 417-428.

Hiron, A., Posteraro, B., Carriere, M., Remy, L., Delporte, C., La Sorda, M., Sanguinetti, M., Juillard, V. and Borezee-Durant, E. (2010) 'A nickel ABC-transporter of *Staphylococcus aureus* is involved in urinary tract infection', *Mol Microbiol*, 77(5), pp. 1246-60.

Hoffmann, A., Bukau, B. and Kramer, G. (2010) 'Structure and function of the molecular chaperone Trigger Factor', *Biochimica et Biophysica Acta (BBA)-Molecular Cell Research*, 1803(6), pp. 650-661.

Hong, P., Koza, S. and Bouvier, E. S. (2012) 'A review size-exclusion chromatography for the analysis of protein biotherapeutics and their aggregates', *Journal of liquid chromatography & related technologies*, 35(20), pp. 2923-2950.

- Howitt, S. M. and Udvardi, M. K. (2000) 'Structure, function and regulation of ammonium transporters in plants', *Biochimica et Biophysica Acta (BBA)-Biomembranes*, 1465(1-2), pp. 152-170.
- Hu, L. and Mobley, H. (1993) 'Expression of catalytically active recombinant *Helicobacter pylori* urease at wild-type levels in *Escherichia coli*', *Infection and immunity*, 61(6), pp. 2563-2569.
- Hu, L. T., Foxall, P. A., Russell, R. and Mobley, H. (1992) 'Purification of recombinant *Helicobacter pylori* urease apoenzyme encoded by ureA and ureB', *Infection and immunity*, 60(7), pp. 2657-2666.
- Hu, L. T. and Mobley, H. (1990) 'Purification and N-terminal analysis of urease from *Helicobacter pylori*', *Infection and immunity*, 58(4), pp. 992-998.
- Hu, P., Leighton, T., Ishkhanova, G. and Kustu, S. (1999) 'Sensing of nitrogen limitation by *Bacillus subtilis*: comparison to enteric bacteria', *J Bacteriol*, 181(16), pp. 5042-50.
- Huang, S.-C., Burne, R. A. and Chen, Y.-Y. M. (2014) 'The pH-dependent expression of the urease operon in *Streptococcus salivarius* is mediated by CodY', *Appl. Environ. Microbiol.*, 80(17), pp. 5386-5393.
- Huergo, L. F., Chandra, G. and Merrick, M. (2013) 'PII signal transduction proteins: nitrogen regulation and beyond', *FEMS microbiology reviews*, 37(2), pp. 251-283.
- Hughes, A., Wilson, S., Dodson, E. J., Turkenburg, J. P. and Wilkinson, A. J. (2019) 'Crystal structure of the putative peptide-binding protein AppA from *Clostridium difficile*', *Acta Crystallographica Section F: Structural Biology Communications*, 75(4).
- Hughes, H., Morgan, C., Brunyak, E., Barranco, K., Cohen, E., Edmunds, T. and Lee, K. (2009) 'A multi-tiered analytical approach for the analysis and quantitation of high-molecular-weight aggregates in a recombinant therapeutic glycoprotein', *The AAPS journal*, 11(2), pp. 335-341.
- Islam, M. N., Zhang, M. and Adhikari, B. (2014) 'The inactivation of enzymes by ultrasound—a review of potential mechanisms', *Food Reviews International*, 30(1), pp. 1-21.
- Jabri, E., Carr, M. B., Hausinger, R. P. and Karplus, P. A. (1995) 'The crystal structure of urease from *Klebsiella aerogenes*', *Science*, 268(5213), pp. 998-1004.
- Jia, M., Xu, M., He, B. and Rao, Z. (2013) 'Cloning, expression, and characterization of L-asparaginase from a newly isolated *Bacillus subtilis* B11-06', *Journal of agricultural and food chemistry*, 61(39), pp. 9428-9434.

Jones, M. D., Li, Y. and Zamble, D. B. (2018) 'Acid-responsive activity of the *Helicobacter pylori* metalloregulator NikR', *Proc Natl Acad Sci U S A*.

Jürgen, B., Tobisch, S., Wümpelmann, M., Gördes, D., Koch, A., Thurow, K., Albrecht, D., Hecker, M. and Schweder, T. (2005) 'Global expression profiling of *Bacillus subtilis* cells during industrial-close fed-batch fermentations with different nitrogen sources', *Biotechnology and bioengineering*, 92(3), pp. 277-298.

Kappaun, K., Piovesan, A. R., Carlini, C. R. and Ligabue-Braun, R. (2018) 'Ureases: Historical aspects, catalytic, and non-catalytic properties - A review', *J Adv Res*, 13, pp. 3-17.

Karp, P. D., Billington, R., Caspi, R., Fulcher, C. A., Latendresse, M., Kothari, A., Keseler, I. M., Krummenacker, M., Midford, P. E. and Ong, Q. (2019) 'The BioCyc collection of microbial genomes and metabolic pathways', *Briefings in bioinformatics*, 20(4), pp. 1085-1093.

Kelley, L. A., Mezulis, S., Yates, C. M., Wass, M. N. and Sternberg, M. J. (2015) 'The Phyre2 web portal for protein modeling, prediction and analysis', *Nature protocols*, 10(6), pp. 845.

Kim, J. K., Mulrooney, S. B. and Hausinger, R. P. (2005a) 'Biosynthesis of active *Bacillus subtilis* urease in the absence of known urease accessory proteins', *J Bacteriol*, 187(20), pp. 7150-4.

Kim, J. K., Mulrooney, S. B. and Hausinger, R. P. (2005b) 'Biosynthesis of Active *Bacillus subtilis* Urease in the Absence of Known Urease Accessory Proteins', *Journal of Bacteriology*, 187(20), pp. 7150-7154.

Kim, J. K., Mulrooney, S. B. and Hausinger, R. P. (2006) 'The UreEF fusion protein provides a soluble and functional form of the UreF urease accessory protein', *Journal of bacteriology*, 188(24), pp. 8413-8420.

Koide, A. and Hoch, J. A. (1994a) 'Identification of a second oligopeptide transport system in *Bacillus subtilis* and determination of its role in sporulation', *Molecular microbiology*, 13(3), pp. 417-426.

Koide, A. and Hoch, J. A. (1994b) 'Identification of a second oligopeptide transport system in *Bacillus subtilis* and determination of its role in sporulation', *Mol Microbiol*, 13(3), pp. 417-26.

Koide, A., Perego, M. and Hoch, J. A. (1999) 'ScoC regulates peptide transport and sporulation initiation in *Bacillus subtilis*', *J Bacteriol*, 181(13), pp. 4114-7.

Konieczna, I., Zarnowiec, P., Kwinkowski, M., Kolesinska, B., Fraczyk, J., Kaminski, Z. and Kaca, W. (2012) 'Bacterial urease and its role in long-lasting human diseases', *Curr Protein Pept Sci*, 13(8), pp. 789-806.

Koo, B. M., Kritikos, G., Farelli, J. D., Todor, H., Tong, K., Kimsey, H., Wapinski, I., Galardini, M., Cabal, A., Peters, J. M., Hachmann, A. B., Rudner, D. Z., Allen, K. N., Typas, A. and Gross, C. A. (2017) 'Construction and Analysis of Two Genome-Scale Deletion Libraries for *Bacillus subtilis*', *Cell Syst*, 4(3), pp. 291-305.e7.

Kovacs, A. T. (2019) '*Bacillus subtilis*', *Trends Microbiol.*

Krajewska, B. (2009) 'Ureases I. Functional, catalytic and kinetic properties: A review', *Journal of Molecular Catalysis B: Enzymatic*, 59(1-3), pp. 9-21.

Krasny, L., Bland, P., Kogata, N., Wai, P., Howard, B. A., Natrajan, R. C. and Huang, P. H. (2018) 'SWATH mass spectrometry as a tool for quantitative profiling of the matrisome', *Journal of proteomics*, 189, pp. 11-22.

Kuenzl, T., Li-Blatter, X., Srivastava, P., Herdewijn, P., Sharpe, T. and Panke, S. (2018) 'Mutant variants of the substrate-binding protein DppA from *Escherichia coli* enhance growth on nonstandard γ -glutamyl amide-containing peptides', *Applied and environmental microbiology*, 84(13).

Larson, A. D. and Kallio, R. (1954) 'Purification and properties of bacterial urease', *Journal of bacteriology*, 68(1), pp. 67.

Latip, W., Knight, V. F., Abdul Halim, N., Ong, K. K., Mohd Kassim, N. A., Yunus, W., Zin, W. M., Noor, M., Aminah, S. and Ali, M. (2019) 'Microbial Phosphotriesterase: Structure, Function, and Biotechnological Applications', *Catalysts*, 9(8), pp. 671.

LeDeaux, J. R., Solomon, J. M. and Grossman, A. D. (1997) 'Analysis of non-polar deletion mutations in the genes of the spo0K (opp) operon of *Bacillus subtilis*', *FEMS Microbiol Lett*, 153(1), pp. 63-9.

Lee, M. H., Mulrooney, S. B., Renner, M. J., Markowicz, Y. and Hausinger, R. P. (1992) 'Klebsiella aerogenes urease gene cluster: sequence of ureD and demonstration that four accessory genes (ureD, ureE, ureF, and ureG) are involved in nickel metallocenter biosynthesis', *Journal of bacteriology*, 174(13), pp. 4324-4330.

Lee, M. H., Pankratz, H. S., Wang, S., Scott, R. A., Finnegan, M. G., Johnson, M. K., Ippolito, J. A., Christianson, D. W. and Hausinger, R. P. (1993) 'Purification and characterization of *Klebsiella aerogenes* UreE protein: a nickel - binding protein that functions in urease metallocenter assembly', *Protein Science*, 2(6), pp. 1042-1052.

Lee, Y. S. and Park, W. (2018) 'Current challenges and future directions for bacterial self-healing concrete', *Appl Microbiol Biotechnol*, 102(7), pp. 3059-3070.

Lerm, B., Kenyon, C., Schwartz, I. S., Kroukamp, H., de Witt, R., Govender, N. P., de Hoog, G. S. and Botha, A. (2017) 'First report of urease activity in the novel systemic fungal pathogen *Emergomyces africanus*: a comparison with the neurotrope *Cryptococcus neoformans*', *FEMS yeast research*, 17(7), pp. fox069.

Lesley, S. A., Graziano, J., Cho, C. Y., Knuth, M. W. and Klock, H. E. (2002) 'Gene expression response to misfolded protein as a screen for soluble recombinant protein', *Protein Eng*, 15(2), pp. 153-60.

Levdikov, V. M., Blagova, E. V., Brannigan, J. A., Wright, L., Vagin, A. A. and Wilkinson, A. J. (2005) 'The structure of the oligopeptide-binding protein, AppA, from *Bacillus subtilis* in complex with a nonapeptide', *Journal of molecular biology*, 345(4), pp. 879-892.

Li, Q., Csetenyi, L. and Gadd, G. M. (2014) 'Biomining of metal carbonates by *Neurospora crassa*', *Environmental science & technology*, 48(24), pp. 14409-14416.

Li, Y., Zou, A.-H., Ye, R.-Q. and Mu, B.-Z. (2009) 'Counterion-induced changes to the micellization of surfactin-C16 aqueous solution', *The Journal of Physical Chemistry B*, 113(46), pp. 15272-15277.

Lin, W., Mathys, V., Ang, E. L. Y., Koh, V. H. Q., Gómez, J. M. M., Ang, M. L. T., Rahim, S. Z. Z., Tan, M. P., Pethe, K. and Alonso, S. (2012) 'Urease activity represents an alternative pathway for *Mycobacterium tuberculosis* nitrogen metabolism', *Infection and immunity*, 80(8), pp. 2771-2779.

Liu, Q., Chen, Y., Yuan, M., Du, G., Chen, J. and Kang, Z. (2017) 'A *Bacillus paralicheniformis* Iron-Containing Urease Reduces Urea Concentrations in Rice Wine', *Appl Environ Microbiol*, 83(17).

Liu, Q., Jin, X., Fang, F., Li, J., Du, G. and Kang, Z. (2019) 'Food-grade expression of an iron-containing acid urease in *Bacillus subtilis*', *Journal of biotechnology*, 293, pp. 66-71.

Lopez, J. (2007) 'Two-dimensional electrophoresis in proteome expression analysis', *Journal of chromatography B*, 849(1-2), pp. 190-202.

Luzzatto-Knaan, T., Melnik, A. V. and Dorrestein, P. C. (2019) 'Mass Spectrometry Uncovers the Role of Surfactin as an Interspecies Recruitment Factor', *ACS chemical biology*, 14(3), pp. 459-467.

Mäder, U., Antelmann, H., Buder, T., Dahl, M., Hecker, M. and Homuth, G. (2002) 'Bacillus subtilis functional genomics: genome-wide analysis of the DegS-DegU regulon by transcriptomics and proteomics', *Molecular Genetics and Genomics*, 268(4), pp. 455-467.

Maroney, M. J. and Ciurli, S. (2013) 'Nonredox nickel enzymes', *Chemical reviews*, 114(8), pp. 4206-4228.

Marty-Mazars, D., Horiuchi, S., Tai, P. C. and Davis, B. D. (1983) 'Proteins of ribosome-bearing and free-membrane domains in Bacillus subtilis', *J Bacteriol*, 154(3), pp. 1381-8.

McGee, D. J., May, C. A., Garner, R. M., Himpsl, J. M. and Mobley, H. L. (1999) 'Isolation of Helicobacter pylori genes that modulate urease activity', *Journal of bacteriology*, 181(8), pp. 2477-2484.

Merloni, A., Dobrovolska, O., Zambelli, B., Agostini, F., Bazzani, M., Musiani, F. and Ciurli, S. (2014) 'Molecular landscape of the interaction between the urease accessory proteins UreE and UreG', *Biochimica et Biophysica Acta (BBA)-Proteins and Proteomics*, 1844(9), pp. 1662-1674.

Mitchell, J. K. and Santamarina, J. C. (2005) 'Biological considerations in geotechnical engineering', *Journal of geotechnical and geoenvironmental engineering*, 131(10), pp. 1222-1233.

Mobley, H. and Hausinger, R. (1989) 'Microbial ureases: significance, regulation, and molecular characterization', *Microbiology and Molecular Biology Reviews*, 53(1), pp. 85-108.

Mobley, H., Island, M. D. and Hausinger, R. P. (1995) 'Molecular biology of microbial ureases', *Microbiol. Mol. Biol. Rev.*, 59(3), pp. 451-480.

Moncrief, M. B. and Hausinger, R. P. (1997) 'Characterization of UreG, identification of a UreD-UreF-UreG complex, and evidence suggesting that a nucleotide-binding site in UreG is required for in vivo metallocenter assembly of Klebsiella aerogenes urease', *J Bacteriol*, 179(13), pp. 4081-6.

Mondal, S. and Ghosh, A. D. (2018) 'Investigation into the optimal bacterial concentration for compressive strength enhancement of microbial concrete', *Construction and Building Materials*, 183, pp. 202-214.

Montoya, B., DeJong, J. and Boulanger, R. (2013) 'Dynamic response of liquefiable sand improved by microbial-induced calcite precipitation', *Géotechnique*, 63(4), pp. 302.

Moraes, P. M., Seyffert, N., Silva, W. M., Castro, T. L., Silva, R. F., Lima, D. D., Hirata, R., Jr., Silva, A., Miyoshi, A. and Azevedo, V. (2014) 'Characterization of the Opp peptide

transporter of *Corynebacterium pseudotuberculosis* and its role in virulence and pathogenicity', *Biomed Res Int*, 2014, pp. 489782.

Mortensen, B. and DeJong, J. (2011) 'Strength and stiffness of MICP treated sand subjected to various stress paths', *Geo-Frontiers 2011: Advances in Geotechnical Engineering*, pp. 4012-4020.

Mujah, D., Shahin, M. A. and Cheng, L. (2017) 'State-of-the-art review of biocementation by microbially induced calcite precipitation (MICP) for soil stabilization', *Geomicrobiology Journal*, 34(6), pp. 524-537.

Mukherjee, S. and Kearns, D. B. (2014) 'The structure and regulation of flagella in *Bacillus subtilis*', *Annual review of genetics*, 48, pp. 319-340.

Mulrooney, S. B. and Hausinger, R. P. (2003) 'Nickel uptake and utilization by microorganisms', *FEMS Microbiol Rev*, 27(2-3), pp. 239-61.

Mulrooney, S. B., Pankratz, H. S. and Hausinger, R. P. (1989) 'Regulation of gene expression and cellular localization of cloned *Klebsiella aerogenes* (*K. pneumoniae*) urease', *J Gen Microbiol*, 135(6), pp. 1769-76.

Mulrooney, S. B., Ward, S. K. and Hausinger, R. P. (2005) 'Purification and properties of the *Klebsiella aerogenes* UreE metal-binding domain, a functional metallochaperone of urease', *Journal of bacteriology*, 187(10), pp. 3581-3585.

Murphy, T. F. and Brauer, A. L. (2011) 'Expression of urease by *Haemophilus influenzae* during human respiratory tract infection and role in survival in an acid environment', *BMC microbiology*, 11(1), pp. 183.

Musiani, F., Zambelli, B., Stola, M. and Ciurli, S. (2004) 'Nickel trafficking: insights into the fold and function of UreE, a urease metallochaperone', *Journal of inorganic biochemistry*, 98(5), pp. 803-813.

Nakajima, T., Kuribayashi, T., Yamamoto, S., Moore, J. E., Millar, B. C. and Matsuda, M. (2014) 'Construction and expression of a recombinant urease gene cluster from *Campylobacter sputorum* biovar paraureolyticus', *Br J Biomed Sci*, 71(2), pp. 58-65.

Nakano, M. M., Hoffmann, T., Zhu, Y. and Jahn, D. (1998) 'Nitrogen and oxygen regulation of *Bacillus subtilis* nasDEF encoding NADH-dependent nitrite reductase by TnrA and ResDE', *Journal of bacteriology*, 180(20), pp. 5344-5350.

Nakano, M. M. and Hulett, F. M. (1997) 'Adaptation of *Bacillus subtilis* to oxygen limitation', *FEMS microbiology letters*, 157(1), pp. 1-7.

Nakano, M. M. and Zuber, P. (1998) 'Anaerobic growth of a "strict aerobe"(Bacillus subtilis)', *Annual review of microbiology*, 52(1), pp. 165-190.

Nakayama, T., Munoz, L. E., Sadaie, Y. and Doi, R. H. (1978) 'Spore coat protein synthesis in cell-free systems from sporulating cells of Bacillus subtilis', *J Bacteriol*, 135(3), pp. 952-60.

Ngo, T., Phan, A., Yam, C. and Lenhoff, H. (1982) 'Interference in determination of ammonia with the hypochlorite-alkaline phenol method of Berthelot', *Analytical Chemistry*, 54(1), pp. 46-49.

Nikodinovic-Runic, J., Flanagan, M., Hume, A. R., Cagney, G. and O'Connor, K. E. (2009) 'Analysis of the Pseudomonas putida CA-3 proteome during growth on styrene under nitrogen-limiting and non-limiting conditions', *Microbiology*, 155(10), pp. 3348-3361.

Nim, Y. S. and Wong, K.-B. (2019) 'The Maturation Pathway of Nickel Urease', *Inorganics*, 7(7), pp. 85.

Ninfa, A. J. and Magasanik, B. (1986) 'Covalent modification of the glnG product, NRI, by the glnL product, NRII, regulates the transcription of the glnALG operon in Escherichia coli', *Proceedings of the National Academy of Sciences*, 83(16), pp. 5909-5913.

Nygaard, P., Bested, S. M., Andersen, K. A. and Saxild, H. H. (2000) 'Bacillus subtilis guanine deaminase is encoded by the yknA gene and is induced during growth with purines as the nitrogen source', *Microbiology*, 146(12), pp. 3061-3069.

Ogawa, K., Akagawa, E., Yamane, K., Sun, Z. W., LaCelle, M., Zuber, P. and Nakano, M. M. (1995) 'The nasB operon and nasA gene are required for nitrate/nitrite assimilation in Bacillus subtilis', *J Bacteriol*, 177(5), pp. 1409-13.

Okwadha, G. D. and Li, J. (2010) 'Optimum conditions for microbial carbonate precipitation', *Chemosphere*, 81(9), pp. 1143-1148.

Okyay, T. O. and Rodrigues, D. F. (2013) 'High throughput colorimetric assay for rapid urease activity quantification', *Journal of microbiological methods*, 95(3), pp. 324-326.

Otto, A., Bernhardt, J., Meyer, H., Schaffer, M., Herbst, F.-A., Siebourg, J., Mäder, U., Lalk, M., Hecker, M. and Becher, D. (2010) 'Systems-wide temporal proteomic profiling in glucose-starved Bacillus subtilis', *Nature communications*, 1, pp. 137.

Özbek, B. and Ülgen, K. Ö. (2000) 'The stability of enzymes after sonication', *Process Biochemistry*, 35(9), pp. 1037-1043.

Palombo, M., Bonucci, A., Etienne, E., Ciurli, S., Uversky, V. N., Guigliarelli, B., Belle, V., Mileo, E. and Zambelli, B. (2017) 'The relationship between folding and activity in UreG, an intrinsically disordered enzyme', *Scientific reports*, 7(1), pp. 1-10.

Park, I. S. and Hausinger, R. P. (1996) 'Metal ion interaction with urease and UreD-urease apoproteins', *Biochemistry*, 35(16), pp. 5345-52.

Patra, A., Dutta, A., Jatav, S. S., Choudhary, S. and Chattopadhyay, A. (2019) 'Horizon of nickel as essential to toxic element', *IJCS*, 7(2), pp. 1185-1191.

Perego, M., Higgins, C. F., Pearce, S. R., Gallagher, M. P. and Hoch, J. A. (1991) 'The oligopeptide transport system of *Bacillus subtilis* plays a role in the initiation of sporulation', *Mol Microbiol*, 5(1), pp. 173-85.

Perkins, D. N., Pappin, D. J., Creasy, D. M. and Cottrell, J. S. (1999) 'Probability-based protein identification by searching sequence databases using mass spectrometry data', *ELECTROPHORESIS: An International Journal*, 20(18), pp. 3551-3567.

Pervez, H., Iqbal, M. S., Tahir, M. Y., Nasim, F.-u.-H., Choudhary, M. I. and Khan, K. M. (2008) 'In vitro cytotoxic, antibacterial, antifungal and urease inhibitory activities of some N 4-substituted isatin-3-thiosemicarbazones', *Journal of Enzyme Inhibition and Medicinal Chemistry*, 23(6), pp. 848-854.

Petrackova, D., Vecer, J., Svobodova, J. and Herman, P. (2010) 'Long-term adaptation of *Bacillus subtilis* 168 to extreme pH affects chemical and physical properties of the cellular membrane', *Journal of Membrane Biology*, 233(1-3), pp. 73-83.

Pflock, M., Kennard, S., Delany, I., Scarlato, V. and Beier, D. (2005) 'Acid-induced activation of the urease promoters is mediated directly by the ArsRS two-component system of *Helicobacter pylori*', *Infection and immunity*, 73(10), pp. 6437-6445.

Pham, V. P., van Paassen, L. A., van der Star, W. R. and Heimovaara, T. J. (2018) 'Evaluating strategies to improve process efficiency of denitrification-based MICP', *Journal of Geotechnical and Geoenvironmental Engineering*, 144(8), pp. 04018049.

Phang, I. R. K., San Chan, Y., Wong, K. S. and Lau, S. Y. (2018) 'Isolation and characterization of urease-producing bacteria from tropical peat', *Biocatalysis and agricultural biotechnology*, 13, pp. 168-175.

Picon, A. and van Wely, K. H. (2001) 'Peptide binding to the *Bacillus subtilis* oligopeptide-binding proteins OppA and AppA', *Molecular Biology Today*, 2(2), pp. 21-25.

Qin, Y. and Cabral, J. M. (2002) 'Review properties and applications of urease', *Biocatalysis and biotransformation*, 20(1), pp. 1-14.

Rajasekar, A., Loo Chin Moy, C. and Wilkinson, S. 'MICP and advances towards eco-friendly and economical applications'. *IOP Conference Series: Earth and Environmental Science*.

Raut, S. H., Sarode, D. and Lele, S. (2014) 'Biocalcification using *B. pasteurii* for strengthening brick masonry civil engineering structures', *World Journal of Microbiology and Biotechnology*, 30(1), pp. 191-200.

Remaut, H. and Goffin, C. (2004) 'd-Aminopeptidase DppA', *Handbook of Proteolytic Enzymes*: Elsevier, pp. 992-994.

Remy, L., Carrière, M., Derré-Bobillot, A., Martini, C., Sanguinetti, M. and Borezée-Durant, E. (2013) 'The *S. taphylococcus aureus* Opp1 ABC transporter imports nickel and cobalt in zinc-depleted conditions and contributes to virulence', *Molecular microbiology*, 87(4), pp. 730-743.

Reynaud, E. (2010) 'Protein misfolding and degenerative diseases', *Nature Education*, 3(9), pp. 28.

Robert, E. L. (1988) *The Sigma-Aldrich library of chemical safety data*. Ed. 2. [Milwaukee, Wis., USA] : Sigma-Aldrich Corp., [1988] ©1988.

Robinson, P. K. (2015) 'Enzymes: principles and biotechnological applications', *Essays in biochemistry*, 59, pp. 1-41.

Rodionov, D. A., Hebbeln, P., Gelfand, M. S. and Eitinger, T. (2006) 'Comparative and functional genomic analysis of prokaryotic nickel and cobalt uptake transporters: evidence for a novel group of ATP-binding cassette transporters', *J Bacteriol*, 188(1), pp. 317-27.

Rosenstein, I., Hamilton-Miller, J. and Brumfitt, W. (1980) 'The effect of acetohydroxamic acid on the induction of bacterial ureases', *Investigative urology*, 18(2), pp. 112-114.

Rutherford, J. C. (2014) 'The emerging role of urease as a general microbial virulence factor', *PLoS pathogens*, 10(5).

Saggese, A., Culurciello, R., Casillo, A., Corsaro, M. M., Ricca, E. and Baccigalupi, L. (2018) 'A marine isolate of *Bacillus pumilus* secretes a pumilacidin active against *Staphylococcus aureus*', *Marine drugs*, 16(6), pp. 180.

Sanchez, L. 2001. TCA protein precipitation protocol. Caltech.

Santosh, K., Ramachandran, S., Ramakrishnan, V. and Bang, S. (2001) 'Remediation of concrete using microorganisms', *American Concrete Institute Journal*, 98, pp. 3-9.

Sarda, D., Choonia, H. S., Sarode, D. and Lele, S. (2009) 'Biocalcification by *Bacillus pasteurii* urease: a novel application', *Journal of industrial microbiology & biotechnology*, 36(8), pp. 1111-1115.

Schultz, A. C., Nygaard, P. and Saxild, H. H. (2001) 'Functional analysis of 14 genes that constitute the purine catabolic pathway in *Bacillus subtilis* and evidence for a novel regulon controlled by the PucR transcription activator', *Journal of Bacteriology*, 183(11), pp. 3293-3302.

Sebbane, F., Bury-Moné, S., Cailliau, K., Browaeys-Poly, E., De Reuse, H. and Simonet, M. (2002) 'The *Yersinia pseudotuberculosis* Yut protein, a new type of urea transporter homologous to eukaryotic channels and functionally interchangeable in vitro with the *Helicobacter pylori* UreI protein', *Molecular microbiology*, 45(4), pp. 1165-1174.

Sebbane, F., Mandrand-Berthelot, M. A. and Simonet, M. (2002) 'Genes encoding specific nickel transport systems flank the chromosomal urease locus of pathogenic yersiniae', *J Bacteriol*, 184(20), pp. 5706-13.

Seifan, M. and Berenjian, A. (2019) 'Microbially induced calcium carbonate precipitation: a widespread phenomenon in the biological world', *Applied microbiology and biotechnology*, 103(12), pp. 4693-4708.

Seifan, M., Samani, A. K. and Berenjian, A. (2016) 'Induced calcium carbonate precipitation using *Bacillus* species', *Appl Microbiol Biotechnol*, 100(23), pp. 9895-9906.

Serror, P. and Sonenshein, A. L. (1996) 'Interaction of Cody, a novel *Bacillus subtilis* DNA-binding protein, with the dpp promoter region', *Molecular microbiology*, 20(4), pp. 843-852.

Shan, S.-o. (2016) 'ATPase and GTPase tangos drive intracellular protein transport', *Trends in biochemical sciences*, 41(12), pp. 1050-1060.

Shi, R., Munger, C., Asinas, A., Benoit, S. L., Miller, E., Matte, A., Maier, R. J. and Cygler, M. (2010) 'Crystal structures of apo and metal-bound forms of the UreE protein from *Helicobacter pylori*: role of multiple metal binding sites', *Biochemistry*, 49(33), pp. 7080-7088.

Shin, J.-H. and Helmann, J. D. (2016) 'Molecular logic of the Zur-regulated zinc deprivation response in *Bacillus subtilis*', *Nature communications*, 7(1), pp. 1-9.

Shivers, R. P. and Sonenshein, A. L. (2005) '*Bacillus subtilis* ilvB operon: an intersection of global regulons', *Molecular microbiology*, 56(6), pp. 1549-1559.

Siegbahn, P. E., Chen, S.-L. and Liao, R.-Z. (2019) 'Theoretical Studies of Nickel-Dependent Enzymes', *Inorganics*, 7(8), pp. 95.

Singh, A., Panting, R. J., Varma, A., Saijo, T., Waldron, K. J., Jong, A., Ngamskulrungrroj, P., Chang, Y. C., Rutherford, J. C. and Kwon-Chung, K. J. (2013) 'Factors required for activation of urease as a virulence determinant in *Cryptococcus neoformans*', *MBio*, 4(3), pp. e00220-13.

Slack, F. J., Serror, P., Joyce, E. and Sonenshein, A. L. (1995) 'A gene required for nutritional repression of the *Bacillus subtilis* dipeptide permease operon', *Mol Microbiol*, 15(4), pp. 689-702.

Solomon, J., Su, L., Shyn, S. and Grossman, A. D. (2003) 'Isolation and characterization of mutants of the *Bacillus subtilis* oligopeptide permease with altered specificity of oligopeptide transport', *J Bacteriol*, 185(21), pp. 6425-33.

Sonenshein, A. L. (2007) 'Control of key metabolic intersections in *Bacillus subtilis*', *Nature Reviews Microbiology*, 5(12), pp. 917-927.

Song, B.-H. and Neuhard, J. (1989) 'Chromosomal location, cloning and nucleotide sequence of the *Bacillus subtilis* *cdd* gene encoding cytidine/deoxycytidine deaminase', *Molecular and General Genetics MGG*, 216(2-3), pp. 462-468.

Song, H. K., Mulrooney, S. B., Huber, R. and Hausinger, R. P. (2001) 'Crystal Structure of *Klebsiella aerogenes* UreE, a Nickel-binding Metallochaperone for Urease Activation', *Journal of Biological Chemistry*, 276(52), pp. 49359-49364.

Song, Y., Nikoloff, J. M., Fu, G., Chen, J., Li, Q., Xie, N., Zheng, P., Sun, J. and Zhang, D. (2016) 'Promoter Screening from *Bacillus subtilis* in Various Conditions Hunting for Synthetic Biology and Industrial Applications', *PloS one*, 11(7), pp. e0158447.

Soriano, A., Colpas, G. J. and Hausinger, R. P. (2000) 'UreE stimulation of GTP-dependent urease activation in the UreD-UreF-UreG-urease apoprotein complex', *Biochemistry*, 39(40), pp. 12435-12440.

Strugatsky, D., McNulty, R., Munson, K., Chen, C.-K., Soltis, S. M., Sachs, G. and Luecke, H. (2013) 'Structure of the proton-gated urea channel from the gastric pathogen *Helicobacter pylori*', *Nature*, 493(7431), pp. 255-258.

Sujoy, B. and Aparna, A. (2012) 'Isolation, partial purification, characterization and inhibition of urease (EC 3.5. 1.5) enzyme from the *Cajanus cajan* seeds', *Asian Journal of Bio Science*, 7(2), pp. 203-209.

Sumner, J. B. (1937) 'The story of urease', *Journal of Chemical Education*, 14(6), pp. 255.

Tam le, T., Antelmann, H., Eymann, C., Albrecht, D., Bernhardt, J. and Hecker, M. (2006) 'Proteome signatures for stress and starvation in *Bacillus subtilis* as revealed by a 2-D gel image color coding approach', *Proteomics*, 6(16), pp. 4565-85.

Tanaka, K. J., Song, S., Mason, K. and Pinkett, H. W. (2018) 'Selective substrate uptake: The role of ATP-binding cassette (ABC) importers in pathogenesis', *Biochim Biophys Acta Biomembr*, 1860(4), pp. 868-877.

Tang, C.-S., Yin, L.-y., Jiang, N.-j., Zhu, C., Zeng, H., Li, H. and Shi, B. (2020) 'Factors affecting the performance of microbial-induced carbonate precipitation (MICP) treated soil: a review', *Environmental Earth Sciences*, 79(5), pp. 1-23.

Tarun, E., Metelitsa, D. and Adzerikho, I. (2003) 'Inactivation of urease under the action of ultrasonically induced cavitation', *Russian Journal of Physical Chemistry A*, 77(3), pp. 468-476.

Tatusov, R. L., Galperin, M. Y., Natale, D. A. and Koonin, E. V. (2000) 'The COG database: a tool for genome-scale analysis of protein functions and evolution', *Nucleic acids research*, 28(1), pp. 33-36.

Tatusov, R. L., Natale, D. A., Garkavtsev, I. V., Tatusova, T. A., Shankavaram, U. T., Rao, B. S., Kiryutin, B., Galperin, M. Y., Fedorova, N. D. and Koonin, E. V. (2001) 'The COG database: new developments in phylogenetic classification of proteins from complete genomes', *Nucleic acids research*, 29(1), pp. 22-28.

Ter Beek, A., Keijser, B. J., Boorsma, A., Zakrzewska, A., Orij, R., Smits, G. J. and Brul, S. (2008) 'Transcriptome analysis of sorbic acid-stressed *Bacillus subtilis* reveals a nutrient limitation response and indicates plasma membrane remodeling', *Journal of bacteriology*, 190(5), pp. 1751-1761.

Thomas, V. J. and Collins, C. M. (1999) 'Identification of UreR binding sites in the Enterobacteriaceae plasmid-encoded and *Proteus mirabilis* urease gene operons', *Molecular microbiology*, 31(5), pp. 1417-1428.

Torres-Aravena, Á., Duarte-Nass, C., Azócar, L., Mella-Herrera, R., Rivas, M. and Jeison, D. (2018) 'Can microbially induced calcite precipitation (MICP) through a ureolytic pathway be successfully applied for removing heavy metals from wastewaters?', *Crystals*, 8(11), pp. 438.

Torzewska, A. and Różalski, A. (2015) 'Various intensity of *Proteus mirabilis*-induced crystallization resulting from the changes in the mineral composition of urine', *Acta Biochimica Polonica*, 62(1).

Uberti, A. F., Olivera-Severo, D., Wassermann, G. E., Scopel-Guerra, A., Moraes, J. A., Barcellos-de-Souza, P., Barja-Fidalgo, C. and Carlini, C. R. (2013) 'Pro-inflammatory properties and neutrophil activation by *Helicobacter pylori* urease', *Toxicon*, 69, pp. 240-249.

Ugwu, S. O. and Apte, S. P. (2004) 'The effect of buffers on protein conformational stability', *Pharmaceutical Technology*, 28(3), pp. 86-109.

Urabe, G., Katagiri, T. and Katsuki, S. (2020) 'Intense Pulsed Electric Fields Denature Urease Protein', *Bioelectricity*, 2(1), pp. 33-39.

van der Steen, J. (2013) *The general stress response of Bacillus subtilis*. 9789461919762.

van Dijl, J. M. and Hecker, M. (2013) 'Bacillus subtilis: from soil bacterium to super-secreting cell factory', *Microb Cell Fact*, 12.

Van Vliet, A. H., Ernst, F. D. and Kusters, J. G. (2004) 'NikR-mediated regulation of *Helicobacter pylori* acid adaptation', *Trends in microbiology*, 12(11), pp. 489-494.

Vasanth, N. and FREESE, E. (1979) 'The role of manganese in growth and sporulation of *Bacillus subtilis*', *Microbiology*, 112(2), pp. 329-336.

Voland, P., Weeks, D. L., Marcus, E. A., Prinz, C., Sachs, G. and Scott, D. (2003) 'Interactions among the seven *Helicobacter pylori* proteins encoded by the urease gene cluster', *American Journal of Physiology-Gastrointestinal and Liver Physiology*, 284(1), pp. G96-G106.

Wacker, I., Ludwig, H., Reif, I., Blencke, H. M., Detsch, C. and Stulke, J. (2003) 'The regulatory link between carbon and nitrogen metabolism in *Bacillus subtilis*: regulation of the *gltAB* operon by the catabolite control protein CcpA', *Microbiology*, 149(Pt 10), pp. 3001-3009.

Wacker, T., Garcia-Celma, J. J., Lewe, P. and Andrade, S. L. (2014) 'Direct observation of electrogenic NH₄⁺ transport in ammonium transport (Amt) proteins', *Proceedings of the National Academy of Sciences*, 111(27), pp. 9995-10000.

Wang, Z., Zhang, N., Cai, G., Jin, Y., Ding, N. and Shen, D. (2017) 'Review of ground improvement using microbial induced carbonate precipitation (MICP)', *Marine Georesources & Geotechnology*, 35(8), pp. 1135-1146.

Weaver, C. A., Chen, Y.-Y. M. and Burne, R. A. (2000) 'Inactivation of the *ptsI* gene encoding enzyme I of the sugar phosphotransferase system of *Streptococcus salivarius*: effects on growth and urease expression', *Microbiology*, 146(5), pp. 1179-1185.

Weeks, D. L., Eskandari, S., Scott, D. R. and Sachs, G. (2000) 'A H⁺-gated urea channel: the link between *Helicobacter pylori* urease and gastric colonization', *Science*, 287(5452), pp. 482-485.

Weeks, D. L. and Sachs, G. (2001) 'Sites of pH regulation of the urea channel of *Helicobacter pylori*', *Molecular microbiology*, 40(6), pp. 1249-1259.

Whiffin, V. S. (2004) *Microbial CaCO₃ precipitation for the production of biocement*. Murdoch University.

Whiffin, V. S., Van Paassen, L. A. and Harkes, M. P. (2007) 'Microbial carbonate precipitation as a soil improvement technique', *Geomicrobiology Journal*, 24(5), pp. 417-423.

Wiktor, V. and Jonkers, H. M. (2011) 'Quantification of crack-healing in novel bacteria-based self-healing concrete', *Cement and Concrete Composites*, 33(7), pp. 763-770.

Wipat, A. and Harwood, C. R. (1999) 'The *Bacillus subtilis* genome sequence: the molecular blueprint of a soil bacterium', *FEMS Microbiology Ecology*, 28(1), pp. 1-9.

Witte, C.-P., Rosso, M. G. and Romeis, T. (2005) 'Identification of three urease accessory proteins that are required for urease activation in *Arabidopsis*', *Plant physiology*, 139(3), pp. 1155-1162.

Won, H. S., Lee, Y. H., Kim, J. H., Shin, I. S., Lee, M. H. and Lee, B. J. (2004) 'Structural characterization of the nickel-binding properties of *Bacillus pasteurii* urease accessory protein (Ure)E in solution', *J Biol Chem*, 279(17), pp. 17466-72.

Wray, L., Ferson, A. E. and Fisher, S. H. (1997a) 'Expression of the *Bacillus subtilis* ureABC operon is controlled by multiple regulatory factors including CodY, GlnR, TnrA, and Spo0H', *Journal of bacteriology*, 179(17), pp. 5494-5501.

Wray, L. V., Jr., Ferson, A. E. and Fisher, S. H. (1997b) 'Expression of the *Bacillus subtilis* ureABC operon is controlled by multiple regulatory factors including CodY, GlnR, TnrA, and Spo0H', *J Bacteriol*, 179(17), pp. 5494-501.

Wray, L. V., Jr., Ferson, A. E., Rohrer, K. and Fisher, S. H. (1996) 'TnrA, a transcription factor required for global nitrogen regulation in *Bacillus subtilis*', *Proc Natl Acad Sci U S A*, 93(17), pp. 8841-5.

Yamauchi, R., Maguin, E., Horiuchi, H., Hosokawa, M. and Sasaki, Y. (2019) 'The critical role of urease in yogurt fermentation with various combinations of *Streptococcus thermophilus* and *Lactobacillus delbrueckii* ssp. *bulgaricus*', *Journal of dairy science*, 102(2), pp. 1033-1043.

Yang, X., Koohi-Moghadam, M., Wang, R., Chang, Y.-Y., Woo, P. C., Wang, J., Li, H. and Sun, H. (2018) 'Metallochaperone UreG serves as a new target for design of urease inhibitor: A novel strategy for development of antimicrobials', *PLoS biology*, 16(1), pp. e2003887.

Yang, Y., Kang, Z., Zhou, J., Chen, J. and Du, G. (2015) 'High-level expression and characterization of recombinant acid urease for enzymatic degradation of urea in rice wine', *Applied microbiology and biotechnology*, 99(1), pp. 301-308.

Yonekura, K., Maki-Yonekura, S. and Namba, K. (2003) 'Complete atomic model of the bacterial flagellar filament by electron cryomicroscopy', *Nature*, 424(6949), pp. 643-650.

Young, G. M., Amid, D. and Miller, V. L. (1996) 'A bifunctional urease enhances survival of pathogenic *Yersinia enterocolitica* and *Morganella morganii* at low pH', *J Bacteriol*, 178(22), pp. 6487-95.

Zalieckas, J. M., Wray, L. V., Jr. and Fisher, S. H. (2006) 'Cross-regulation of the *Bacillus subtilis* *glnRA* and *tnrA* genes provides evidence for DNA binding site discrimination by GlnR and TnrA', *J Bacteriol*, 188(7), pp. 2578-85.

Zambelli, B., Banaszak, K., Merloni, A., Kiliszek, A., Rypniewski, W. and Ciurli, S. (2013) 'Selectivity of Ni (II) and Zn (II) binding to *Sporosarcina pasteurii* UreE, a metallochaperone in the urease assembly: a calorimetric and crystallographic study', *JBIC Journal of Biological Inorganic Chemistry*, 18(8), pp. 1005-1017.

Zambelli, B., Musiani, F., Benini, S. and Ciurli, S. (2011) 'Chemistry of Ni²⁺ in urease: sensing, trafficking, and catalysis', *Accounts of chemical research*, 44(7), pp. 520-530.

Zambelli, B., Stola, M., Musiani, F., De Vriendt, K., Samyn, B., Devreese, B., Van Beeumen, J., Turano, P., Dikiy, A., Bryant, D. A. and Ciurli, S. (2005b) 'UreG, a chaperone in the urease assembly process, is an intrinsically unstructured GTPase that specifically binds Zn²⁺', *J Biol Chem*, 280(6), pp. 4684-95.

Zeigler, D. R., Prágai, Z., Rodriguez, S., Chevreux, B., Muffler, A., Albert, T., Bai, R., Wyss, M. and Perkins, J. B. (2008) 'The origins of 168, W23, and other *Bacillus subtilis* legacy strains', *Journal of bacteriology*, 190(21), pp. 6983-6995.

Zhang, J., Zhou, A., Liu, Y., Zhao, B., Luan, Y., Wang, S., Yue, X. and Li, Z. (2017) 'Microbial network of the carbonate precipitation process induced by microbial consortia and the potential application to crack healing in concrete', *Sci Rep*, 7(1), pp. 14600.

Zhang, M., Bao, Z., Zhao, Q., Guo, H., Xu, K., Wang, C. and Zhang, P. (2014) 'Structure of a pantothenate transporter and implications for ECF module sharing and energy coupling of group II ECF transporters', *Proceedings of the National Academy of Sciences*, 111(52), pp. 18560-18565.

Zhao, H., Wu, Y., Xu, Z., Ma, R., Ding, Y., Bai, X., Rong, Q., Zhang, Y., Li, B. and Ji, X. (2019a) 'Mechanistic insight into the interaction between *Helicobacter pylori* urease subunit α and its molecular chaperone Hsp60', *Frontiers in microbiology*, 10, pp. 153.

Zhao, Y., Shi, R., Bian, X., Zhou, C., Zhao, Y., Zhang, S., Wu, F., Waterhouse, G. I., Wu, L. Z. and Tung, C. H. (2019b) 'Ammonia detection methods in photocatalytic and electrocatalytic experiments: how to improve the reliability of NH₃ production rates?', *Advanced Science*, 6(8), pp. 1802109.

Zheng, L., Kostrewa, D., Bernèche, S., Winkler, F. K. and Li, X.-D. (2004) 'The mechanism of ammonia transport based on the crystal structure of AmtB of Escherichia coli', *Proceedings of the National Academy of Sciences*, 101(49), pp. 17090-17095.

Zhu, B. and Stulke, J. (2018) 'SubtiWiki in 2018: from genes and proteins to functional network annotation of the model organism Bacillus subtilis', *Nucleic Acids Res*, 46(D1), pp. D743-d748.

Zhu, T. and Dittrich, M. (2016) 'Carbonate Precipitation through Microbial Activities in Natural Environment, and Their Potential in Biotechnology: A Review', *Front Bioeng Biotechnol*, 4, pp. 4.

Chapter 9 Appendices

9.1 *B. subtilis ureABC* genetic sequence

ATGAACTGA CACCAGTTGA ACAAGAGAAA TGCTCATT TTGCAGCGGG GGAATTAGCC
AAACAGCGAA AGGCGCGGG CGTCTGCTG AACTATCCTG AGGCTGCTGC TTATATCACC
TGCTTTATTA TGGAAGGCG ACGTGATGG AAGGGAGTAG CAGAGCTGAT GGAAGCCGGC
CGCCATGTAT TAACGGAAAA AGATGTGATG GAGGGTGTGC CTGAGATGCT GGACAGCATT
CAGGTGGAGG CCACATTTCC GGATGGTGA AAGCTTGTTA CGGTACATCA GCCAATTTCT
GCGGAGGTGA AGTC**AtGA**AG CGGGGAGCAT TTCAAATTGC TGAGGGAACC ATTACGATTA
ATGAAGGCCG TGAGATACGG GAGGTAACGG TAAAAAACAC CGGATCACGC TCCATTCAAG
TCCGTTTCGCA TTTTCATTTT GCGGAGGCCA ACGGGGCTTT ATTATTTGAC CGTGAGCTGG
CGATCGGCAT GCGTCTTGAT GTTCCATCAG GCACGTCGGT CCGTTTTGAG CCGGGAGAGC
AGAAAACGGT CTCACTAGTG GAAATCAGAG GACGCAAGAC AATTAGAGGG CTGAACGGAA
TGGCCGACAC GTTTATCGAT GAACGCGGCA AAGAAAAAAC GTTGGCCAAC TTAAAAACAAG
CCGGTGGAT GGAGGGTGA ATCCG**atgAA** AATGTACCG GAGGAATATG CGGAAGCTGT
TGGCCCGACA ACGGGCGATA AAATCAGATT GGGCGACACG GATTTATGGA TCGAAGTCGA
AAAGGATTTT ACAGTATACG GTGAAGAAAT GATCTTTGGC GGCGGAAAAA CTATCCGAGA
CGGCATGGGC CAAAACGGCA GAATCACAGG GAAGGACGGC GCTTTGGATT TGGTTATCAC
CAACGTCGTG CTTTGGATT ACACAGGCAT TGTCAAAGCG GATGTCGGTG TGAAAGACGG
CCGATTGTC GGTGTGCGAA AAAGCGGAAA TCCTGATATC ATGGATGGAG TCGATCCGCA
CATGGTCAATC GGAGCGGGGA CAGAGGTGAT TTCCGGTGAA GGCAAAATTT TAACAGCCGG
GGGAGTGGAC ACGCACATTC ATTTTATTTG TCCTCAGCAG ATGGAAGTTG CGCTTTCTTC
AGGTGTGAGC ATGGAAAGTTC GAGGCGGAAC AGGACCCGCT ACAGGAAGCA AAGCGACAAC
ATGTACGTCC GGGCGTGGT ATATGGCGAG GATGCTGGAA GCGGCCGAGG AGTTTCCGAT
CAATGTCCGC TTCTTAGGAA AAGGGAATGC ATCCGATAAA GCGCCGCTGA TCGAGCAGGT
GGAAGCAGGC GCCATCGGTC TTAAGCTCCA TGAAGACTGG GGAACGACGC CAAGCGCCAT
TAAAACGTGT ATGGAAGTTC TGGACGAGGC TGATATTCAA GTTGCCATCC ATACCGATAC
GATTAACGAA GCGGGCTTTT TGAAAAACAC GCTCGACGCG ATCGGGGACC GGGTTATTCA
TACTTATCAC ATTGAAGGGG CAGGCGGCGG TCACGCTCCG GATATTATGA AGCTCGCCTC
TTACGCGAAC ATTCTGCCGT CATCTACAAC GCCAACCATT CCTTATACCG TTAATACGAT
GGATGAGCAT CTTGACATGA TGATGGTCTG CCACCAATTA GATGCGAAAAG TGCCTGAAGA
TGTGGCATT AGCCATTCCA GAATCAGGGC GGCGACGATT GCCGCGGAGG ATATTCTCCA
TGATATAGGT GCGATCAGCA TGACATCATC GGATTCCTCAA GCGATGGGGC GGGTCGGTGA
AGTGATCATC CGAACATGGC AGGTAGCCGA TAAAATGAAA AAACAGCGCG GCGCTCTTGC
CGGTGAAAAC GGGAATGACA ATGTGCCGCG AAAACGGTAC ATTGCCAAAT ACACGATTAA
TCCGGCAATT ACGCACGGGC TCAGCCATGA GGTCGGCTCG GTGAAAAAAG GGAAGCTTGC
TGATCTCGTT CTGTGGGACC CGGTATTTTT CGGCGTGAAA CCGGAAGTGG TCTTAAAGGG
CGGCATGATT GCACGTGCGC AAATGGGAGA TCCGAACGCG TCCATCCCGA CTCCTGAACC
GGTTTTCATG CGCCAAATGT ATGCGTCTTA CGGAAAAGCC AACCGCTCAA CCTCGATTAC
ATTTATGTCT CAGGCAAGCA TAGAGCGTGG TGTGGCGGAA AGCTTAGGGC TGGAAAAAAG
GATTTCTCCA GTCAAAAATA TCAGAAAAGCT GAGCAAGCTG GATATGAAGC TGAATTCGGC
TTTGCCGAAG ATTGAGATTG ATCCAAAAAC CTATCAGGTC TTTGCTGACG GGGAGGAATT
GTCTTGCCAG CCTGTCGATT ATGTCCCACT TGGACAAAGA TATTTCTTAT Tttga

Appendix Figure 9-1 *Bacillus subtilis* 168 *ureABC* gene sequence (Region: 376714 - 3769108 (reverse complement))

Specific genes are underlined *ureA* (blue), *ureB* (green) and *ureC* (red). Overlapping gene sequences are highlighted yellow and bold. Start and end codons are underlined for each gene.

The genetic organisation of *ureABC* is detailed in Appendix Figure 9-1, the *ureA* stop codon overlaps the first two nucleotides of the *ureB* start codon. This also occurs between the stop codon of *ureB* and the *ureC* start codon.

9.2 Chapter 2

Progenesis Guide:

Visualise and analyse complex LC-MS data to support your 'omics research

Stage Description

- 1. LC-MS Import Data:** Selection and review of data files for analysis.
- 2. Automatic Alignment:** Automatic Reference selection and alignment
- 3. Review Alignment:** automatic and manual run alignment
- 4. Filtering:** defining filters for peaks based on Retention Time, m/z, Charge and Number of Isotopes.
- 5. Review Normalisation:** explains LC-MS normalisation
- 6. Experiment Design Setup:** defining one or more group set ups for analysed aligned runs
- 7. Review Peak Picking:** review and validate results, edit peak detection, tag groups of peaks and select peaks for further analysis
- 8. Peptide Statistics:** performing multivariate statistical analysis on tagged and selected groups of peptides
- 9. Identify Peptides:** managing export of MS/MS spectra to, and import of peptide ids from Peptide Search engines
- 10. Refine Identifications:** manage peptide ids and filters
- 11. Resolve Conflicts:** validation and resolution of peptide id conflicts for data entered from Database Search engines
- 12. Review proteins:** review protein and peptide identity
- 13. Protein Statistics:** multivariate statistical analysis on proteins
- 14. Report:** generate a report for proteins and/or peptides

JWSOP:

- 1. LC-MS Import Data**
Import run data: Thermo Raw files
Pick files → Open (can take a while)
- 2. Automatic Alignment**
Start alignment process
Yes – Auto (automatically chooses the ref. run)
When scan is locked (Padlock appears)
- 3. Review Alignment:**
Section complete → start pick peaks → 'analysing' bar
- 4. Filtering:**
Click charges: 2-7 – Tick ALL
Delete NON MATCHING FEATURES
Section Complete
- 5. Review Normalisation**
Check → section complete
- 6. Experiment Design Setup**
Create Expt: Name
Condition 1 = Blank
Condition 2 = Specific Buffer
Section complete
- 7. Review Peak Picking**
Create tags – based on P value and fold change
Apply tags – create, move to show
Right click → quick tags → max fold → default
Create → include in show
Drag over → annova p value and max fold
Section complete

8. Peptide Statistics

PCA Plot – apply tags – should look like ears!

Section complete

At left of screen = Mascot → export → create new folder

It's now exporting 'peak lists' – this gives the mgf. File, identifies the difference between 'A' and 'B'.

OPEN MASCOT: <http://hls-mascot/mascot/>

MASCOT:

Access ms/ms ion search → perform search

Pick correct database (BS)40

Taxonomy: All entries

Fixed Modifications: Carbamidomethyl ©

Variable Modifications: Oxidation (M)

Peptide charge: 2, 3 and 4+

Peptide tol = 25 ppm

Ms/ms tol = 50ppm

C = 1

Data file = choose (as saved from progenesis)

Instrument: ESI-TRAP

Start search

EXPORT FILE as CSU → EXCEL

Then go back to Progenesis – in Mascot – Export as xml file – export – search results

Green bars appear

DOWNLOAD – exporting to be started

Save as W drive → raw file → new folder xml → view downloads

In progenesis → import search → open file → where it was saved

SECTION COMPLETE

9. Identify Peptides

Peptide search results

Section complete

Proteins – look for conflicts e.g. errors)

SCORE = less than 40

HITS less than 2

WILL BE REMOVED

10. DELETE MATCHING SEARCH RESULTS – once deleted can't get back!

Reduces the conflicts on the next stage

11. RESOLVE CONFLICTS:

Click on peptide, scroll along to conflict score, it needs to be ZERO → Delete from the right side until ZERO.

Create tags – quick tag

Tag upreg in condition one

NEXT

12. Review proteins

FINAL RESULTS

Click on left of screen to go through each protein

EDIT:

See if upregulated or down regulated

Start search as upreg in one condition therefore

Appendix Figure 9-2. SOP for Progenesis/MASCOT use.

9.3 Chapter 3

9.4 Proteomic Evaluation of NLM and NPM

Appendix Table 9-1. Upregulated proteins of NLM BSS 9JW) fold change <3.

Accession and description	Annova p	Fold Change
O34588 Uncharacterized protein YkuJ	1.66E-07	3.04
P24137 Oligopeptide transport ATP-binding protein	2.96E-06	2.95
P42297 Universal stress protein YxiE	5.52E-03	2.93
O31587 Alternate 30S ribosomal protein S14	4.37E-03	2.92
O31636 Uncharacterized protein YjcN	7.42E-05	2.89
P37812 ATP synthase epsilon chain	5.03E-04	2.86
P54513 Uncharacterized protein YqhO	1.50E-04	2.83
P94551 Electron transfer flavoprotein subunit alpha	1.10E-08	2.8
P13792 Alkaline phosphatase synthesis transcriptional regulatory protein PhoP	8.89E-05	2.79
P68569 SPBc2 prophage-derived disulphide bond formation protein	5.34E-05	2.74
P40406 Beta-hexosaminidase	7.53E-09	2.71
P94494 Alanine racemase 2 O	4.63E-05	2.68
P54422 Glutathione hydrolase proenzyme	1.65E-03	2.63
P54528 2-methylisocitrate lyase	3.49E-07	2.59
Q45596 Putative exported peptide YydF	0.04	2.58
P39062 Acetyl-coenzyme A synthetase	7.33E-09	2.57
P08064 Succinate dehydrogenase cytochrome b558 subunit	5.34E-04	2.57
O06746 UPF0234 protein yitk O	5.73E-06	2.55
O31638 Uncharacterized protein YjcP	5.84E-03	2.55

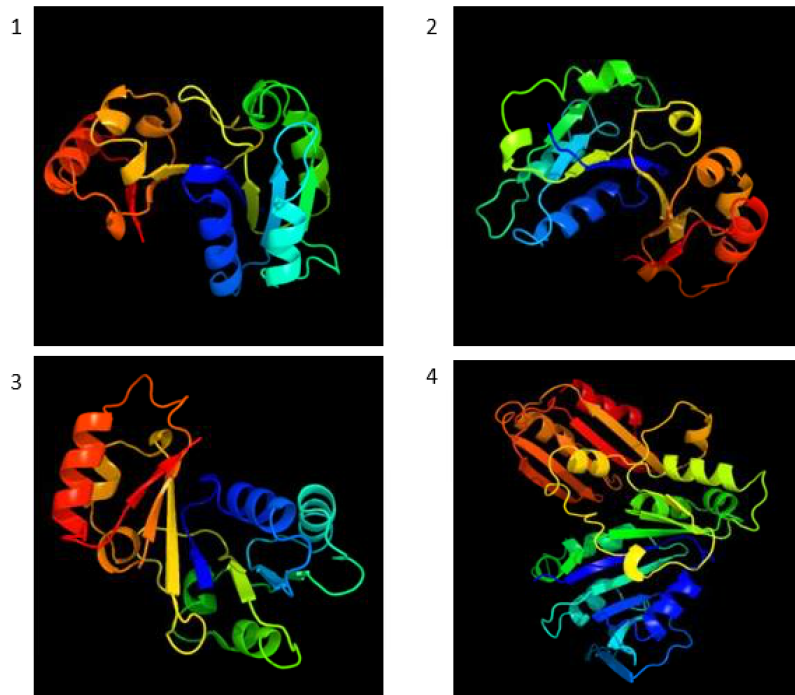
P40740 Aryl-phospho-beta-D-glucosidase BglH	3.43E-09	2.53
O34549 Uncharacterized protein YlbO	2.72E-07	2.49
P40397 Uncharacterized oxidoreductase YhxC	1.31E-08	2.49
Q04789 Acetolactate synthase	1.40E-04	2.47
P42412 Malonate-semialdehyde dehydrogenase	8.37E-06	2.47
P71012 PTS system fructose-specific EIIABC component	1.16E-05	2.45
P55874 ribosomal protein L35	0.02	2.44
P13800 Transcriptional regulatory protein DegU	0.04	2.43
Q7WY78 Polyisoprenyl-teichoic acid--peptidoglycan teichoic acid transferase TagT	2.96E-06	2.41
P12254 RNA polymerase sigma-K factor	2.65E-06	2.38
O34572 Putative HMP/thiamine permease protein YkoC	1.67E-05	2.38
P39790 Extracellular metalloprotease	1.05E-03	2.37
O31404 Acetoin:2,6-dichlorophenolindophenol oxidoreductase subunit alpha	8.01E-05	2.34
P35160 Thiol-disulfide oxidoreductase ResA	3.20E-04	2.34
P39158 Cold shock protein CspC	1.52E-03	2.33
P39812 Glutamate synthase [NADPH] large chain	2.79E-07	2.31
P39157 UPF0340 protein YwlG	1.09E-05	2.3
P12873 50S ribosomal protein L29	7.93E-03	2.29
O34645 Alpha-galactosidase	3.08E-04	2.28
P54423 Cell wall-associated protease	1.65E-03	2.27
O31649 Uncharacterized protein YjdH	5.94E-05	2.27
O31771 Uncharacterized membrane protein YmfM 3	2.30E-03	2.26
P39696 ComE operon protein 4	3.08E-07	2.25
P23545 Alkaline phosphatase synthesis sensor protein PhoR	1.91E-05	2.24

P94550 Electron transfer flavoprotein subunit beta	2.32E-07	2.23
P21468 30S ribosomal protein S6	9.15E-04	2.22
P38021 Ornithine aminotransferase	3.89E-06	2.21
O31589 Uncharacterized protein YhbB	1.43E-07	2.21
C0SP95 Copper transport protein YcnJ	1.68E-04	2.2
O05410 Probable metal-binding protein YrpE	1.25E-06	2.19
O32086 Putative transport protein YubA	5.94E-03	2.19
O31998 Probable ribonuclease YokI	6.69E-04	2.18
C0H3U9 Phenolic acid decarboxylase subunit D	3.21E-03	2.18
P39795 Trehalose-6-phosphate hydrolase	1.96E-05	2.17
P94523 L-arabinose isomerase	5.55E-05	2.17
P19946 50S ribosomal protein L15	3.43E-03	2.15
P39841 Putative mannose-6-phosphate isomerase YvyI	9.45E-05	2.14
O31796 RNA-binding protein Hfq	1.84E-03	2.13
P94447 Probable transcriptional regulatory protein YrbC	2.68E-05	2.11
P39645 Putative heme-dependent peroxidase YwfI	9.10E-05	2.07
O34844 HTH-type transcriptional regulator YodB	3.66E-03	2.07
P70976 Uncharacterized methyltransferase YbaJ	3.08E-06	2.07
Q45065 Uncharacterized protein YneT	1.32E-03	2.03
P32395 Uroporphyrinogen decarboxylase	2.11E-04	2.02
O31714 1-phosphofructokinase	1.05E-03	2.02
O31825 Uncharacterized carboxylase YngE	1.16E-05	2.01

9.5 *St. aureus opp* (Ni²⁺ transporter) and *B. subtilis opp* analysis

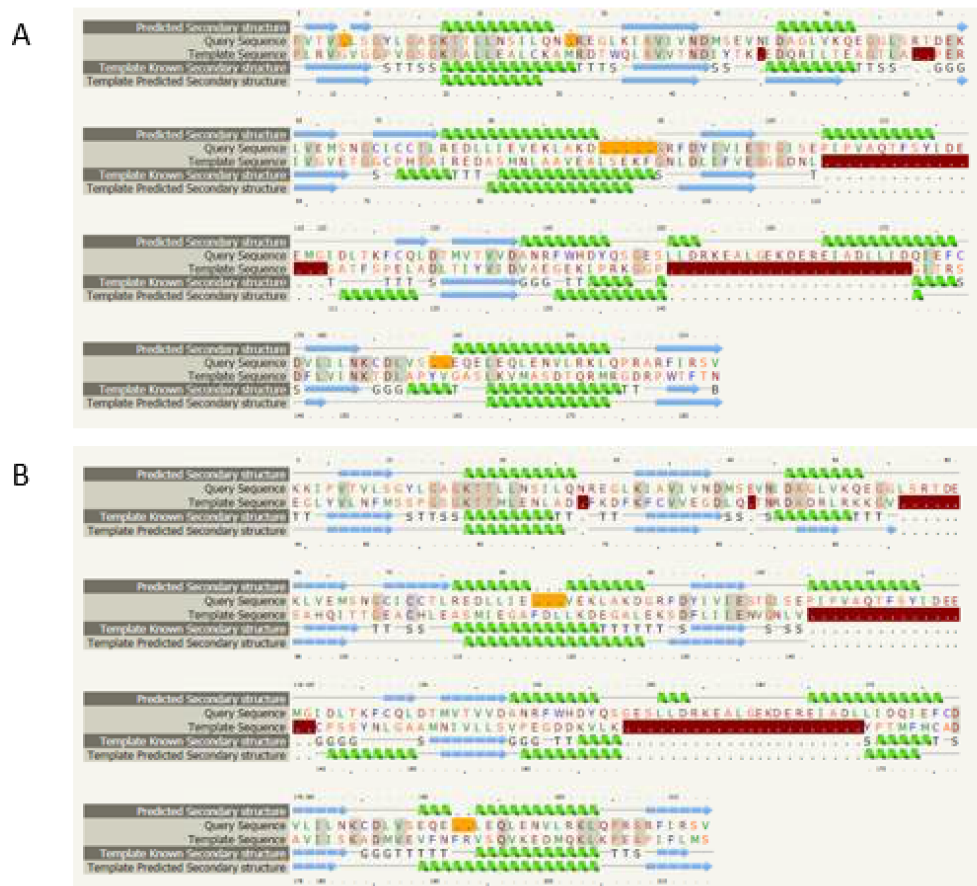
A.		
STOPPA BSOPPA	MRKLTKMSAMLLASGLILTGGC-----GNKGLEEKKENKQLTYTTVKDIGDMNPHVYGG MKKRWSIVTLMILFTLVLSACFGGTTGSENGEGKKDSKGGKTTLNINIKTEPFSLHPGLAND *.* .: :::* *:::*** ..:* :.:* :. * . . : : : * : . .	
STOPPA BSOPPA	SMSAESM--IYEPLVRNTKDG--IKPLLAKKWDVSEEDGKTYTFHLRDDVKFHDGTPFDAD- SVSGGVIRQTFEGLTRINADGPEEGMASKIETSKDGKTYTFTIRDGVKWSNGDPVTAQD *:* . : : * *.* . ** : : *.* :.*:***** :*.**: :* *.* :	
STOPPA BSOPPA	---AVKKNIDAVQENKKLHSLWKISTL-----IDNVKVK--DKYTVELNLKEAYQP FEYAWKWALDPNNEQYAYQLYYIKGAEAAANTGKGSLLDDVAVKAVNDKTLKVELNNP--TP * * . : * . : * . : . * . : : * * * * . . * : : : * : . . *	
STOPPA BSOPPA	ALAEELAMP RP YV FVSPK---DFKNGTTKDGVKKFDGTGPFKLGEHKKDESADFNKNDQYW YFTELTA FYTYMPINEKIAEKNNKWN TNAG--DDYVSN GPFKMTAWKHS GSITLEKNDQYW :***: .*: :. * . * : .*: * ..: ..****: .*: . * :*****	
STOPPA BSOPPA	G-EKSKLNKVQAKVMPAGETAFLSMKKGETNFAFTDDRGTDSLDKSLKQLKDTGDYQVK DKDKVKLKKIDMVMINNNNTELEKFKQAGELDWA---GMPLGQLPTESLPTLKKDGS LHV- . : * **:*: : : . : * : : : * * : * . . * . : * * * * . * : *	
STOPPA BSOPPA	RSQPMNTKMLVNSGKKDNAVSDKTVRQAIGHMVNRDKIAKEILDGQEKPATQLFAKNVT --EPI-AGVYWKFNTEAKPLDNVNI R KALTYSLDRQSI VKNVTQGEQMPAMA AV PPTMK :*: : : : : : : : : : : * : * : : : * : * : * : * : * : * : *	
STOPPA BSOPPA	DINFDMPT--RKYDLKKAESLLDEAGWKKG--KDSVQRQKDGKNLEMAMYDKGSSSQKE GFEDNKEGYFKDNDVKTAK EYLEKGLKEMGLSKASDLPK-----IKLSYNTDDAHAK- .: : : . . *:*.*. * : . . : * * * * : : : * : . . . : *	
STOPPA BSOPPA	QAEYLQAEFKK-MGIKLNINGETSDKIAERRTSGDYDLMFNQTWGLLYDPQSTIAAFKAK IAQAVQEMWKKNLGVDVELDNSEWNVYIDKLHSQDYQIGRMGWLGFNDPINFLELFRDK * : * * : * * : * : : : : . : . * * * : * : * * . : * . *	
STOPPA BSOPPA	NGYESATSGIENKDKIYNSIDDAFKIQNGKERSDAYKNILKQIDDEGIFI-----PISH NG-GNNDTGWENPE--FKLLNQSQTETDKTKRA---ELLKK--AEGIFIDEMPVAPIYF ** . : * * * : : : : : : : . . * . : : * * : * * * * * * * .	
STOPPA BSOPPA	GSMTVVAPKLEKVSFTQSQYELPFNEMQYK YTDTWVQDENLKGVI MPGTG-EVYFRNAYFK : * * : * : * : . : * : * : : *	
B.		
1: STOPPA	100.00	26.68
2: BSOPPA	26.68	100.00
C.		
STOPPB BSOPPB	MFKFIKRIALMFPLMIVVSFMTFLLLTYITNENPAVTILHAQGT PNVTPELIAETNEKYG MLKYIGRRLVYMIITL FVIVTVTFFLMQAAPGGP-----FSGEKKLPPEIEANLNAHYG *:*:* .*: . * : : : * : * : * : . * . * : : * * : * : * : *	
STOPPB BSOPPB	FNDPLLIQYKNWLEAMQFNFGTSY-ITGDPVAERIGP AFMNTLKLTI ISSVMVITSII LDKPLFVQYVSYLKSVMWDFGPSFKYKQSVNDLISSGFPVSFTLGAEAILLALALGVL : : * * : * * . * . : * * : * . * * : * . * * : * * : : : : . .	
STOPPB BSOPPB	LGVVSALKRKGFTDRAIRSVAFFL TALPSYWIASILIIYVSVKLNILPTSGLTGPESYIL FGVIAALYHNKWDYTVAILTIFGISVPSFIMA AVLQYVFSMKLGLFPVAGWDSWAYTFL : * : * * * . * : * : : : * : * * : * : * * . * : * : * : * : *	
STOPPB BSOPPB	PVIVITIA YAGIYFRNVRSMVEQLNEDYVLYLRASGV-KSITLMLHLVRNALQVAVSIF PSIALASMPMAFIARLSRSSMIEVLNSDYIRTA KAKGLSRPAVTVRHAIRNALLPVVTYM * * : : . : * * * * : * * * * : * . * : . . : * : * * * . * : :	
STOPPB BSOPPB	CMSIPMIMGGLVIEYIFAWPGLGQLSLKAILEHDFPVIQAYVLIVAVLFIVFNTLADII GMAAQVLTGFSFIIETIFGIPGLGAHFVNSITNRD YTVIMGVTVFFSVILLCLVIVDVL . : : * . : * * * . * * * : : * * : * : * * . . . : * : * : :	

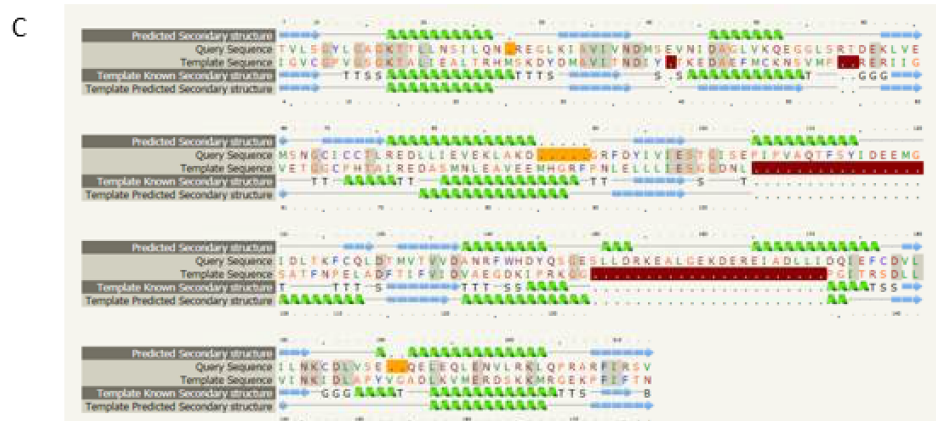
9.6 YciC (ZagA) and UreG sequence and structural comparison



Appendix Figure 9-2. PHYRE2 analysis of *B. subtilis* YciC sequence comparison.

Sequence comparison using PHYRE2 analysis to compare structural similarities between 1. UreG of *K. pneumoniae*, 2. HypB of *H. pylori*, 3. UreG of *H. pylori* and 4. YciC of *B. subtilis*.





Appendix Figure 9-3 Sequence alignment comparisons of *B. subtilis* YciC and UreG of *K. pneumonia*, HypB of *H. pylori* and UreG of *H. pylori*.

A. UreG of *K. pneumonia*, B. HypB of *H. pylori*, C. UreG of *H. pylori* and 4. YciC of *B. subtilis*.

Appendix Table 9-1 Genes activated by the PucR Regulon.

PucR Activation
<i>pucJ-pucK-pucL-pucM</i>
<i>guaD</i>
<i>ureA-ureB-ureC</i>
<i>pucI</i>
<i>pucH</i>
<i>pucF-pucG</i>
<i>pucA-pucB-pucC-pucD-pucE</i>

9.7 Proteomic data analysis

Appendix Table 9-2. Proteins upregulated < 3 fold in oppA

UniprotKB	Accession	COG	Anova (p)*	Fold	Description
P36430	Leucine--tRNA ligase LeuS	J	0.003	2.98	Leu-tRNA synthetase - translation
P13792	Alkaline phosphatase synthesis transcriptional regulatory protein PhoP	T	1.75E-07	2.94	Two-component response regulator, regulation of phosphate metabolism
O06974	Gluconeogenesis factor MgfK	S	3.94E-08	2.94	Required for morphogenesis under gluconeogenic growth conditions.
O34788	(R,R)-butanediol dehydrogenase O	E	0.00385	2.89	Dehydrogenase
P77837	Urease subunit alpha UreC	E	0.0000107	3.12	Urea amidohydrolase subunit alpha
P25994	Carbamoyl-phosphate synthase pyrimidine-specific large chain PyrAB	F N	3.64E-09	2.82	Composed of two chains; the small (or glutamine) chain promotes the hydrolysis of glutamine to ammonia, which is used by the large (or ammonia) chain to synthesize carbamoyl phosphate carbamoyl-phosphate synthetase ammonia chain
P37474	Transcription-repair-coupling factor mfd	L	3.54E-07	2.82	
P42297	Universal stress protein YxiE	T	0.000049	2.79	Universal stress protein
P13242	CTP synthase OS PyrG	F	0.00000463	2.75	Catalyzes the ATP-dependent amination of UTP to CTP with either L-glutamine or ammonia as the source of nitrogen. Regulates intracellular CTP levels through interactions with the four ribonucleotide triphosphates Catalyzes the ATP-dependent amination of UTP to CTP with either L-glutamine or ammonia as the source of nitrogen (By similarity)
Q45477	Isoleucine--tRNA ligase IleS	J	0.00395	2.73	isoleucyl-tRNA synthetase
O31875	Ribonucleoside-diphosphate reductase NrdEB subunit alpha	FL	0.03	2.73	Provides the precursors necessary for DNA synthesis. Catalyzes the biosynthesis of

					deoxyribonucleotides from the corresponding ribonucleotides
P39148	Serine hydroxymethyltransferase GlyA	E	0.00000685	2.71	Catalyzes the reversible interconversion of serine and glycine with tetrahydrofolate (THF) serving as the one-carbon carrier. This reaction serves as the major source of one-carbon groups required for the biosynthesis of purines, thymidylate, methionine, and other important biomolecules. A
P39773	2,3-bisphosphoglycerate-independent phosphoglycerate mutase GpmI	G	0.000645	2.7	Catalyzes the interconversion of 2-phosphoglycerate and 3-phosphoglycerate (By similarity)
P17922	Phenylalanine--tRNA ligase beta subunit PheT	J	0.00134	2.67	homoserine dehydrogenase Is required not only for elongation of protein synthesis but also for the initiation of all mRNA translation through initiator tRNA(fMet) aminoacylation (By
P19582	Homoserine dehydrogenase hom	E	0.000011	2.65	biosynthesis of methionine and threonine
P29726	Adenylosuccinate synthetase PurA	F	0.000424	2.62	Plays an important role in the de novo pathway of purine nucleotide biosynthesis. Catalyzes the first committed step in the biosynthesis of AMP from IMP Plays an important role in the de novo pathway of purine nucleotide biosynthesis
P54504	RsbT co-antagonist protein RsbRD	X	0.00021	2.62	One of 4 functionally non-identical RsbR paralogs, it functions in the environmental signaling branch of the general stress response.
P37571	Negative regulator of genetic competence ClpC/MecB	O	0.00157	2.56	ATP-dependent CLP protease ATP-binding subunit
P25995	Dihydroorotase PyrC	F	0.00187	2.55	Catalyzes the reversible cyclization of carbamoyl aspartate to dihydroorotate

P94545	Endonuclease MutS2	L	0.00117	2.53	Endonuclease that is involved in the suppression of homologous recombination and may therefore have a key role in the control of bacterial genetic diversity.
P28264	Cell division protein FtsA	D	0.00508	2.5	This protein may be involved in anomalous filament growth. May be a component of the septum
P45745	Dimodular nonribosomal peptide synthase DhbF	Q	0.000116	2.49	non-ribosomal peptide synthetase
P21880	Dihydrolipoyl dehydrogenase PdhD	C	0.000166	2.48	dihydrolipoyl dehydrogenase
P42433	Assimilatory nitrate reductase electron transfer subunit NasB	C	0.00114	2.48	nitrite reductase
P27876	Triosephosphate isomerase TpiA	G	0.00000666	2.47	Enzyme in glycolysis/ gluconeogenesis
P80877	5-methyltetrahydropteroyltriglutamate--homocysteine methyltransferase MetE	E	0.00212	2.47	Catalyzes the transfer of a methyl group from 5-methyltetrahydrofolate to homocysteine resulting in methionine formation
O34634	Putative pre-16S rRNA nuclease YrrK P	L	0.0017	2.46	
	O54408 GTP pyrophosphokinase RelA	KT	0.00352	2.45	This enzyme catalyzes the formation of pppGpp which is then hydrolyzed to form ppGpp, it is probably the hydrolysis activity that is required for optimal growth.
Q01465	Rod shape-determining protein MreB	D	0.0000213	2.42	Rod shape-determining protein, MreB
Q45666	HTH-type transcriptional regulator TnrA	K	0.00119	3.42	Transcription regulator that activates the transcription of genes required for nitrogen assimilation such as nrgAB (ammonium transport), nasABCDEF (nitrate/nitrite assimilation), ureABC (urea degradation) and gabP (GABA transport), during nitrogen limitation Also represses glnRA and gltAB in the absence of ammonium
P39914	Uncharacterized protein YtxJ	S Function unknown	0.0000155	2.34	UNCHARACTERISED

	P37870 DNA-directed RNA polymerase subunit beta RpoB	K Transcription	0.000212	2.33	RNA polymerase
P37877	Acetate kinase AckA	C	1.37E-08	2.31	acetate kinase - overflow metabolism
P37877	Uncharacterized protein YobJ	S	0.03	2.29	Uncharacterised
P37518	Ribosome-binding ATPase YchF	J	0.00416	2.28	gtp-binding protein
P80860	Glucose-6-phosphate isomerase pgi	G	0.04	2.28	enzyme in glycolysis / gluconeogenesis
P25993	Carbamoyl-phosphate synthase pyrimidine-specific small chain PyrAA	F	0.000602	2.27	2 ATP + H ₂ O + hydrogencarbonate + L-glutamine = 2 ADP + carbamoyl phosphate + 2 H ⁺ + L-glutamate + phosphate
P32396	Ferrochelatase HemH	H	0.00399	2.21	Biosynthesis of heme
	P39771 Formate-dependent phosphoribosylglycinamide formyltransferase PurT	F	0.00298	2.19	Purine biosynthesis
P37871	DNA-directed RNA polymerase subunit beta' RpoC	K	0.000896	2.18	RNA polymerase beta' subunit
P39812	Glutamate synthase [NADPH] large chain GltA	E	0.02	2.15	Catalytic activity: •2 L-glutamate + NADP ⁺ = 2-oxoglutarate + H ⁺ + L-glutamine + NADPH glutamate synthase
P40924	Phosphoglycerate kinase PgK	G	0.04	2.14	phosphoglycerate kinase

Appendix Table 9-3. Proteins downregulated in oppA with fold change >3

Accession	COG	Annova p	Fold Change
O06484 Uncharacterized protein YfnF	S	5.13E-06	43.49
O31542 Uncharacterized protein YfnD	S	5.16E-06	21.24
COSP84 Putative binding protein YtIA	P	1.4E-07	21.18
O06486 Probable glucose-1-phosphate cytidyltransferase	M	2.28E-07	16.18
O31449 Uncharacterized HTH-type transcriptional regulator Ybfl	K	3.86E-10	14.98

P5459 Lipoprotein YhcN	K	0.000781	14.46
	G		
P39123 Glycogen phosphorylase		2.73E-09	13.08
O0648 Putative sugar dehydratase/epimerase YfnG	S	1.58E-10	13.07
O34984 Uncharacterized metallohydrolase YodQ	E	3.2E-11	12.92
	P		
O08336 Bifunctional cytochrome P450/NADPH--P450 reductase 2		0.0000025	12.41
Q04809 Dipicolinate synthase subunit A	S	3.06E-12	11.75
O06997 Uncharacterized FAD-linked oxidoreductase YvdP	C	9.87E-08	10.87
Q08352 Alanine dehydrogenase	E	4.08E-09	10.29
O31429 Uncharacterized protein SkfG	S	4.43E-09	10.27
O34704 Uncharacterized protein YxnB	S	2.15E-08	10.14
P46328 Uncharacterized protein YxbD	S	8.11E-09	9.82
P39638 Prephenate decarboxylase	S	0.0000107	9.64
O08469 Cytochrome P450	Q	3.89E-09	9.49
O31663 Methylthioribose kinase	S	2.4E-14	9.38
O34677 Glutamine transport ATP-binding protein GlnQ	E	0.0000028	9.22
O34722 Uncharacterized protein YfmG	E	7.94E-07	9.15
P31847 Uncharacterized protein YpuA	S	1.78E-06	8.43
P96722 Putative ribonuclease YwqJ	S	8.45E-07	8.29
P39118 1,4-alpha-glucan branching enzyme GlgB	G	0.000762	8.13
O05242 Probable oligo-1,6-glucosidase	G	2.5E-08	8.1
P39152 Uncharacterized protein YwlB	E	0.0000019	8
P39640 Dihydroantcapsin 7-dehydrogenase	S	1.04E-09	7.86

P39643 Transaminase BacF	E	1.66E-11	7.82
P39630 dTDP-glucose 4,6-dehydratase 1	M	1.84E-11	7.77
Q08787 Surfactin synthase subunit 3	Q	3.05E-08	7.27
O32137 Allantoinase	F	7.81E-10	7.13
P12310 Glucose 1-dehydrogenase	S	8.78E-09	7.03
C0SPC3 Putative ADP-ribose pyrophosphatase YjhB	F	0.0000144	6.88
P45913 Uncharacterized protein YqaP	S	0.0000205	6.87
Q04810 Dipicolinate synthase subunit B	H	8.01E-10	6.84
O34538 Uncharacterized lipoprotein YcdA	S	3.22E-07	6.78
P71002 Response regulator aspartate phosphatase F	S	1.5E-07	6.75
O31782 Polyketide synthase PksN OS=Bacillus subtilis	Q	2.4E-07	6.74
P39779 GTP-sensing transcriptional pleiotropic repressor CodY	K	0.03	6.63
O35002 Carboxy-terminal processing protease CtpB	M	0.0000033	6.54
O31666 2,3-diketo-5-methylthiopentyl-1-phosphate enolase	G	1.96E-08	6.47
P39641 Alanine--anticapsin ligase	I	6.73E-11	6.38
P39639 H2HPP isomerase	S	4.71E-07	6.37
P0CI78 50S ribosomal protein L24	J	0.000218	6.32
P54477 Uncharacterized protein YqfT	S	8.28E-10	6.32
O34767 Oxalate decarboxylase OxdD	G	0.000541	6.28
O34932 Dephospho-CoA kinase	H	5.65E-07	6.25
O32201 Protein LiaH	KT	3.32E-08	6.2
O31455 Putative hydrolase YbfO	S	3.34E-06	6.16

P08838 Phosphoenolpyruvate-protein phosphotransferase	G	0.0000949	6.1
O31506 Putative ribonuclease YeeF	S	0.00199	6.08
P11018 Major intracellular serine protease 2	O	4.05E-07	6.04
P24809 Uncharacterized protein YqxJ	S	0.000857	5.94
C0SPB6 Single-stranded DNA-binding protein B	L	0.0000174	5.9
O34714 Oxalate decarboxylase OxdC	G	8.78E-08	5.89
O31784 Polyketide synthase PksR	Q	3.87E-10	5.78
P39134 Protein PrkA	T	2.74E-07	5.72
P27206 Surfactin synthase subunit 1	IQ	5.03E-06	5.66
P54586 Uncharacterized protein YhcB 1	S	0.00002	5.62
P94551 Electron transfer flavoprotein subunit alpha	C	0.0000193	5.61
P46327 Uncharacterized protein YxbC 1	S	2.53E-06	5.6
O05272 Asparagine synthetase [glutamine-hydrolyzing] 3	E	1.14E-07	5.51
P46911 Menaquinol-cytochrome c reductase iron-sulfur subunit 1	C	1.61E-07	5.47
C0SPB4 Uncharacterized ABC transporter ATP-binding protein YhaQ	S	5.68E-06	5.42
P54497 Uncharacterized protein YqgT	E	0.0000794	5.4
O32148 (S)-ureidoglycine--glyoxylate transaminase	E	8.84E-07	5.35
P08065 Succinate dehydrogenase flavoprotein subunit	C	0.04	5.28
P80865 Succinate--CoA ligase [ADP-forming] subunit alpha	C	0.00451	5.19
O34676 L-lysine 2,3-aminomutase	E	0.0000329	5.04
P42113 Asparagine synthetase [glutamine-hydrolyzing] 2	E	0.0000248	4.9
P96723 Putative antitoxin YwqK	S	0.0000297	4.86
O34508 L-Ala-D/L-Glu epimerase	M	1.97E-07	4.85
O34389 Probable NAD-dependent malic enzyme 3	C	0.000247	4.83
P39120 Citrate synthase 2	C	1.12E-06	4.77

P24141 Oligopeptide-binding protein OppA	E	8.33E-10	Infinity
O34482 L-asparaginase 2	E	0.00214	4.72
O07564 Glucose-6-phosphate 3-dehydrogenase	S	0.000171	4.66
O34725 Uncharacterized lipoprotein YjhA	S	0.0000152	4.63
O32141 Uric acid degradation bifunctional protein PuCL	S	2.27E-08	4.63
P45742 Stress response UPF0229 protein 2	S	0.0000911	4.58
Q45595 Putative peptide biosynthesis protein YydG	S	1.52E-06	4.58
O07566 3-oxo-glucose-6-phosphate:glutamate aminotransferase	E	0.0000574	4.51
P20429 DNA-directed RNA polymerase subunit alpha	K	8.76E-08	4.49
P26906 Dipeptide-binding protein DppE	E	8.18E-07	4.48
P49814 Malate dehydrogenase	C	0.00335	4.43
O31649 Uncharacterized protein YjdH	S	1.9E-07	4.42
O32178 Probable 3-hydroxyacyl-CoA dehydrogenase	I	0.0000416	4.37
Q05873 Valine--tRNA ligase	J	0.00158	4.29
O35010 Gamma-D-glutamyl-L-lysine dipeptidyl-peptidase	M	0.0000385	4.28
P23446 Flagellar basal-body rod protein FlgG	N	1.47E-10	4.26
P94391 1-pyrroline-5-carboxylate dehydrogenase 2	C	3.04E-08	4.25
O34544 Biotin carboxylase 2	I	0.00015	4.17
P54542 Uncharacterized protein YqjE	E	0.00582	3.97
P39124 Glycogen biosynthesis protein GlgD	G	4.3E-07	3.85
O34948 Uncharacterized oxidoreductase	I	0.00725	3.84
P45859 2-methylcitrate dehydratase	S	0.000175	3.84
P39629 Glucose-1-phosphate thymidyltransferase	M	0.000027	3.83
P96579 Putative ribosomal N-acetyltransferase YdaF	J	9.37E-08	3.81
O34851 Probable murein peptide carboxypeptidase	V	1.51E-06	3.8
P94544 DNA polymerase/3'-5' exonuclease PolX	E	2.06E-06	3.79

P37464 Serine--tRNA ligase	J	0.000966	3.78
P33166 Elongation factor Tu	J	0.02	3.75
P21466 30S ribosomal protein S4	J	0.000215	3.73
P94377 Catalase X	P	2.96E-06	3.73
P26905 Dipeptide transport ATP-binding protein DppD	EP	0.000188	3.69
Q04795 Aspartokinase 1	E	0.000163	3.69
P40397 Uncharacterized oxidoreductase YhxC 2	S	0.000018	3.67
P46326 Uncharacterized protein YxbB 1	S	0.000717	3.63
O34592 AB hydrolase superfamily protein YdjP	S	1.62E-07	3.62
O07635 Uncharacterized protein YlaK	S	0.000317	3.6
O32145 Probable xanthine dehydrogenase subunit C	S	0.00124	3.53
O34549 Uncharacterized protein YlbO 1	S	0.0000968	3.52
P45743 Isochorismatase	G	1.85E-06	3.51
P46353 Phosphopentomutase	G	0.0000897	3.5
P42407 Putative UTP--glucose-1-phosphate uridylyltransferase	M	0.0000027	3.46
Q45493 Ribonuclease J1	S	3.29E-07	3.46
O32176 Probable acyl-CoA dehydrogenase	I	1.97E-06	3.44
O31788 Serine protease AprX 1	O	0.0000476	3.43
P26902 D-aminopeptidase	E	0.0000118	3.43
P80700 Elongation factor Ts	J	0.000758	3.4
P40806 Polyketide synthase PksJ	IQ	5.59E-07	3.4
Q05470 Polyketide synthase PksL	Q	1.01E-07	3.4
Q45598 Uncharacterized protein YydD	S	0.000172	3.31
P32399 Uncharacterized protein YhgE 2	S	3.28E-06	3.3
Q00828 Response regulator aspartate phosphatase A	S	2.97E-06	3.28
O07597 D-alanine aminotransferase 1	E	0.01	3.24

O05267 NADH dehydrogenase-like protein YumB	C	3.07E-06	3.24
P24136 Oligopeptide transport ATP-binding protein OppD	EP	0.0000329	3.19
P29141 Minor extracellular protease vpr	O	0.00114	3.15
O31665 Transaminase MtnE	E	0.0000127	3.14
P50843 4-deoxy-L-threo-5-hexosulose-uronate ketol-isomerase	G	0.0000181	3.13
O34973 Putative hydrolase YtaP	S	0.000699	3.09
O31669 Acireductone dioxygenase	S	0.000357	3.09
P54423 Cell wall-associated protease	O	0.0000774	3.09

Appendix Table 9-4. *B. subtilis* 168 knockouts and expression of urease upregulated or downregulated

<i>B. subtilis</i> 168 Knockout	Urease subunits	Regulation	Fold Change
<i>ΔureC</i>	UreC UreB	Downregulated Downregulated	Infinity 61.78
<i>ΔoppB</i>	UreC	Upregulated	2.24
<i>ΔoppC</i>	Not Identified	No difference	N/A
<i>ΔoppD</i>	Not Identified	No difference	N/A
<i>ΔoppF</i>	Not Identified	No difference	N/A
<i>ΔdppA</i>	UreB UreC	Downregulated Downregulated	15.18 3.45
<i>ΔznuA</i>	UreC UreB UreA	Downregulated Downregulated Downregulated	4.71 4.24 2.96
<i>ΔznuB</i>	UreC UreB	Downregulated Downregulated	3.15 3.01
<i>ΔyciC</i>	UreB UreA	Downregulated Downregulated	2.16 2.09

9.8 NZY Miniprep Method

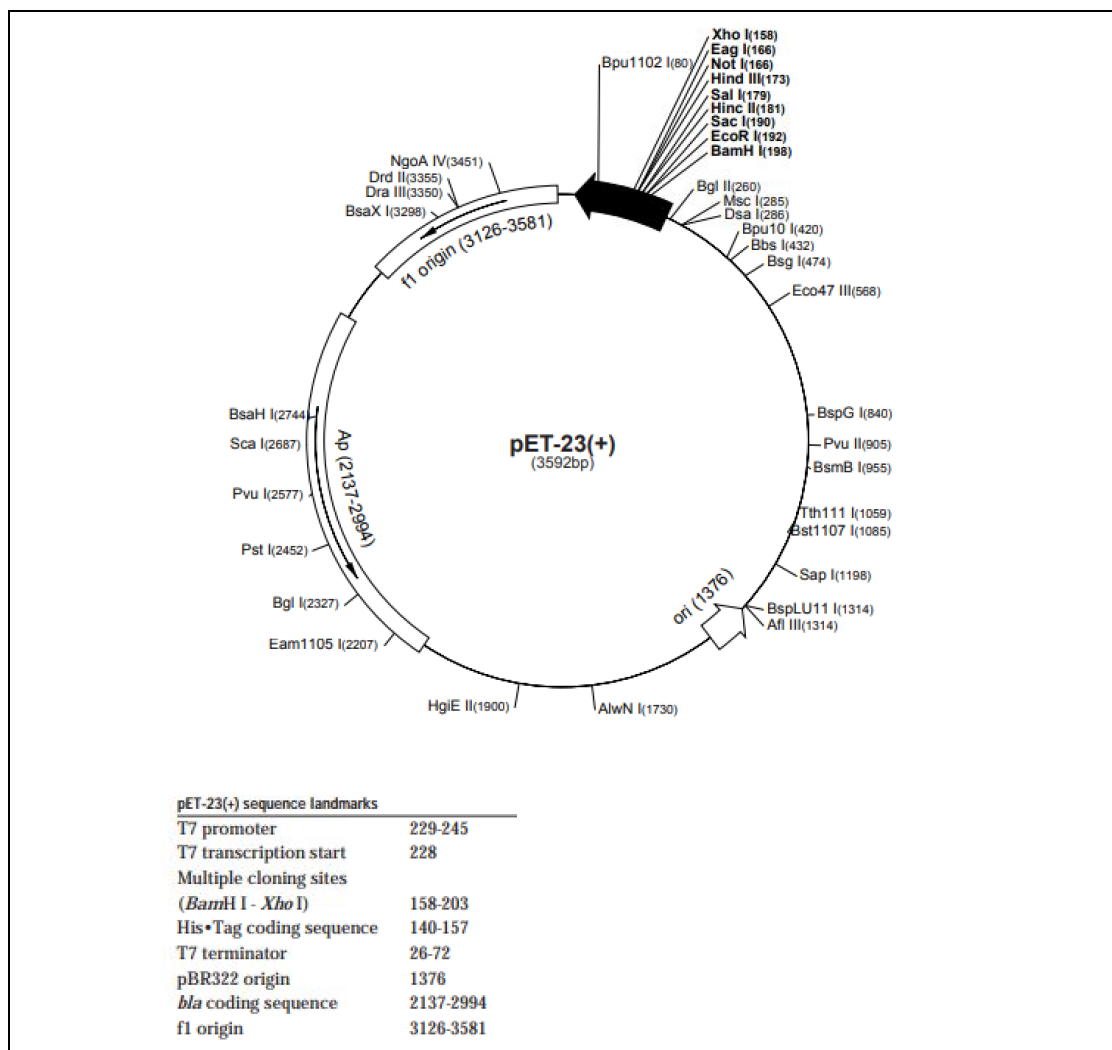
<https://www.nzytech.com/products-services/molecular-biology/dnarna-purification/plasmid-dna-purification/miniprep/mb010/>

Method: Growing of bacterial cultures

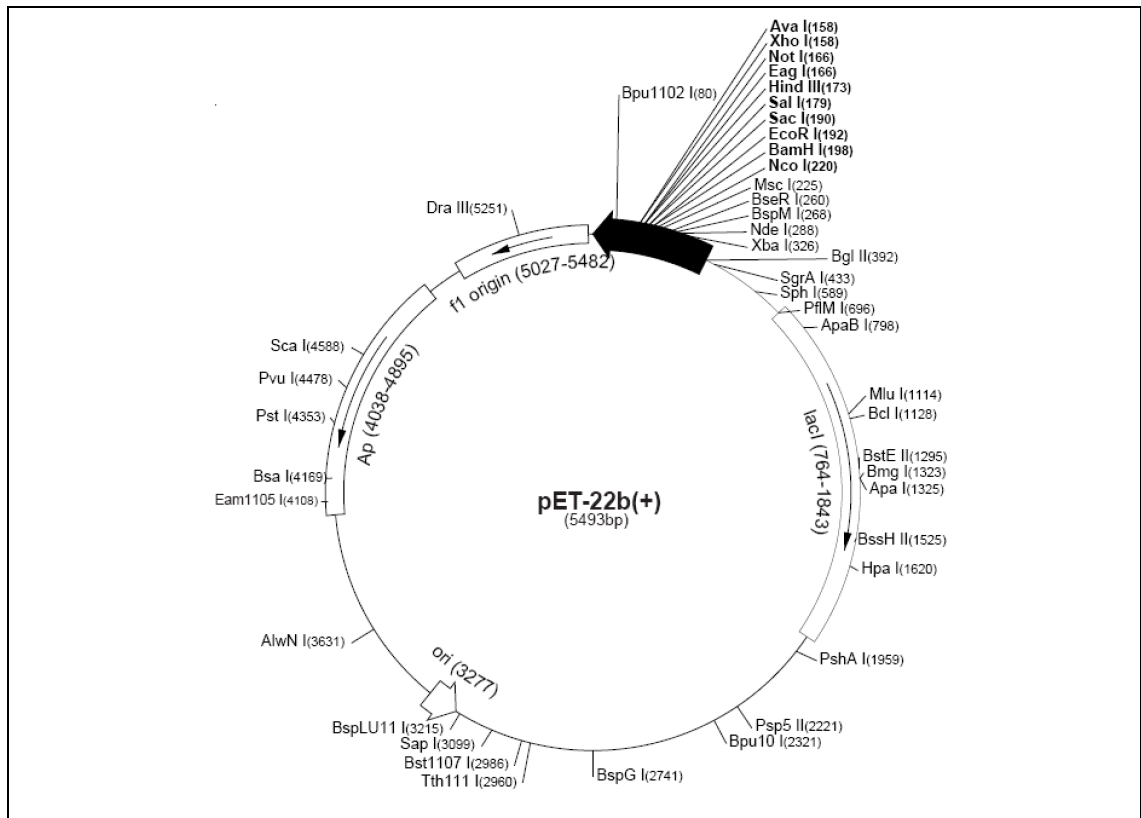
Pick a single colony from a freshly streaked selective plate and inoculate a culture of 1–5 mL LB medium containing the appropriate selective antibiotic. Incubate for 12–16 h at 37 °C with vigorous shaking. Protocol for plasmid DNA purification from *Escherichia coli* cells All centrifugations should be carried out at room temperature in a table-top microcentrifuge at >12000 xg (10000-15000 rpm depending on the rotor type).

1. Cultivate and harvest bacterial cells Pellet 1-5 mL of an *E. coli* LB culture for 30 s. Discard supernatant. Remove as much media as possible. For low copy number plasmids double the volume of cells and of lysis Buffers A1, A2 and A3.
2. Cell lysis Re-suspend cell pellet in 250 µL Buffer A1 by vigorous vortexing. Add 250 µL of Buffer A2 and mix gently by inverting the tube for 6-8 times. Incubate at room temperature for a maximum of 4 min. Do not vortex. Add 300 µL Buffer A3. Mix gently by inverting the tube for 6-8 times. Do not vortex.
3. Clarification of lysate Centrifuge for 5-10 min at room temperature, depending on initial culture volume.
4. Bind DNA Place NZYTech spin column in a 2 mL collecting tube and load the supernatant from step 3 onto the column. Centrifuge for 1 min at 11,000 xg. Discard flow-through.
5. Wash silica membrane Add 500 µL of Buffer AY onto the column. Centrifuge for 1 min. Discard flow-through. This step is crucial to increase the reading length of DNA sequencing reactions and to improve the performance of critical enzymatic reactions. When using endA+ strains, such as JM series, HB101 and its derivatives, or any wild-type strain, use pre-warmed Buffer AY (50 °C). Add 600 µL of Buffer A4 (make sure ethanol was previously added). Centrifuge for 1 min. Discard flow-through.
6. Dry silica membrane Re-insert the NZYTech spin column into the empty 2 mL collecting tube and centrifuge for 2 min.
7. Elute highly pure DNA Place the dried NZYTech spin column into a clean 1.5 mL microcentrifuge tube and add 50 µL of Buffer AE. Incubate 1 min at room temperature. Centrifuge for 1 min. By repeating this step the overall yield will increase by 15-20%. To obtain a highly concentrated miniprep (1.3 times higher) reduce the volume of elution buffer to 30 µL. Store the purified DNA at -20 °C. Note: It is extremely important to add the Elution Buffer into the centre part of the column. Incubating the column with the Elution Buffer at higher temperatures (37 to 50 °C) may slightly increase the yield especially of large (>10,000 bp) DNA Plasmids. Pre-warming the Elution Buffer at 55 to 80 °C may also slightly increase elution efficiency. If water is used for elution, make sure that its pH is between 7.0 and 8.5. Elution efficiency is dependent on pH and the maximum elution efficiency is achieved within this range. A pH <7 will decrease yield.

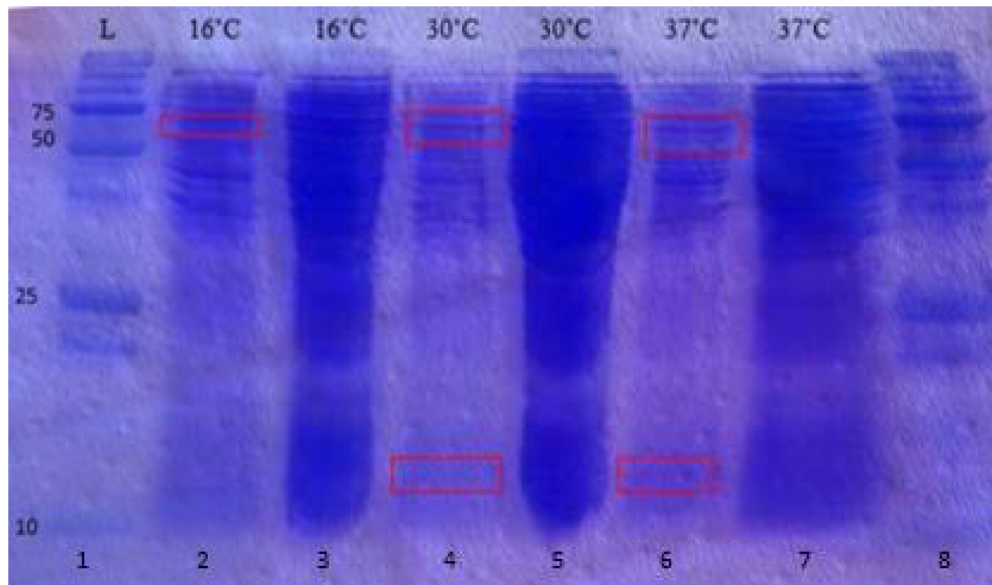
9.9 Vector Map pET22b



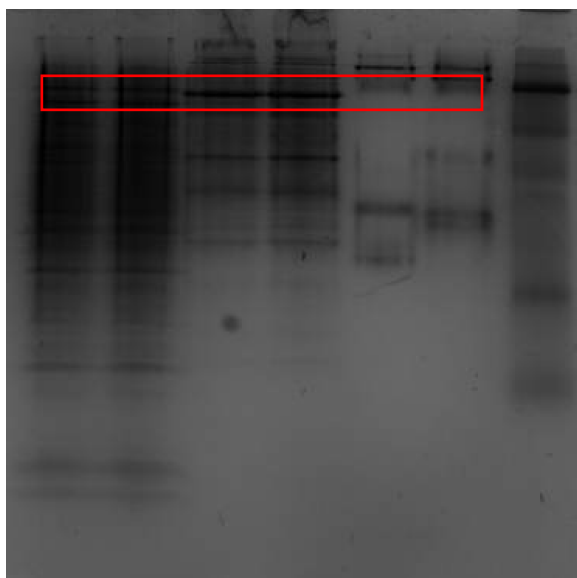
Appendix Figure 9-4. pET23 Vector Map and sequence landmarks (Robert, 1988)



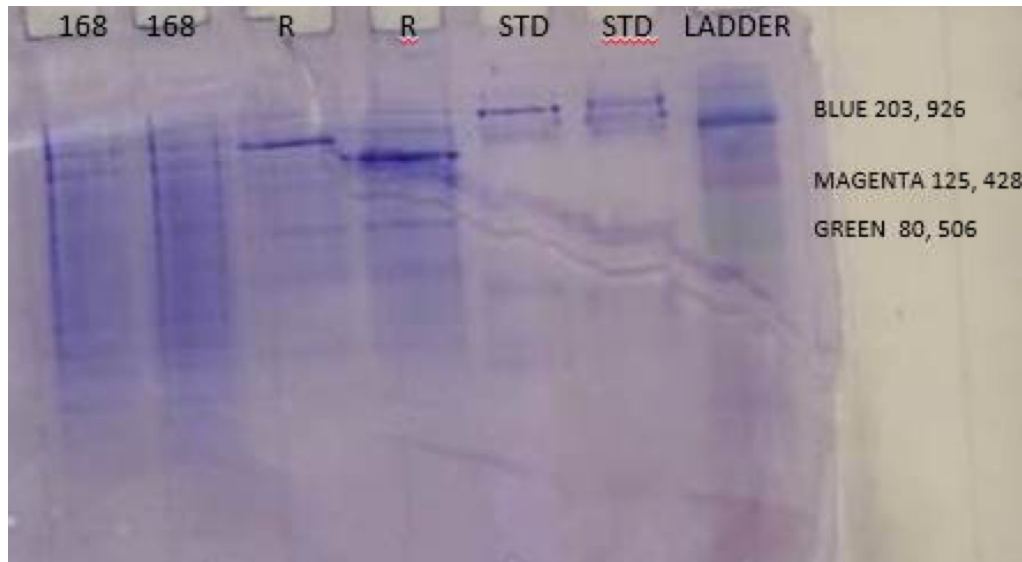
Appendix Figure 9-5. pET-22b Vector map



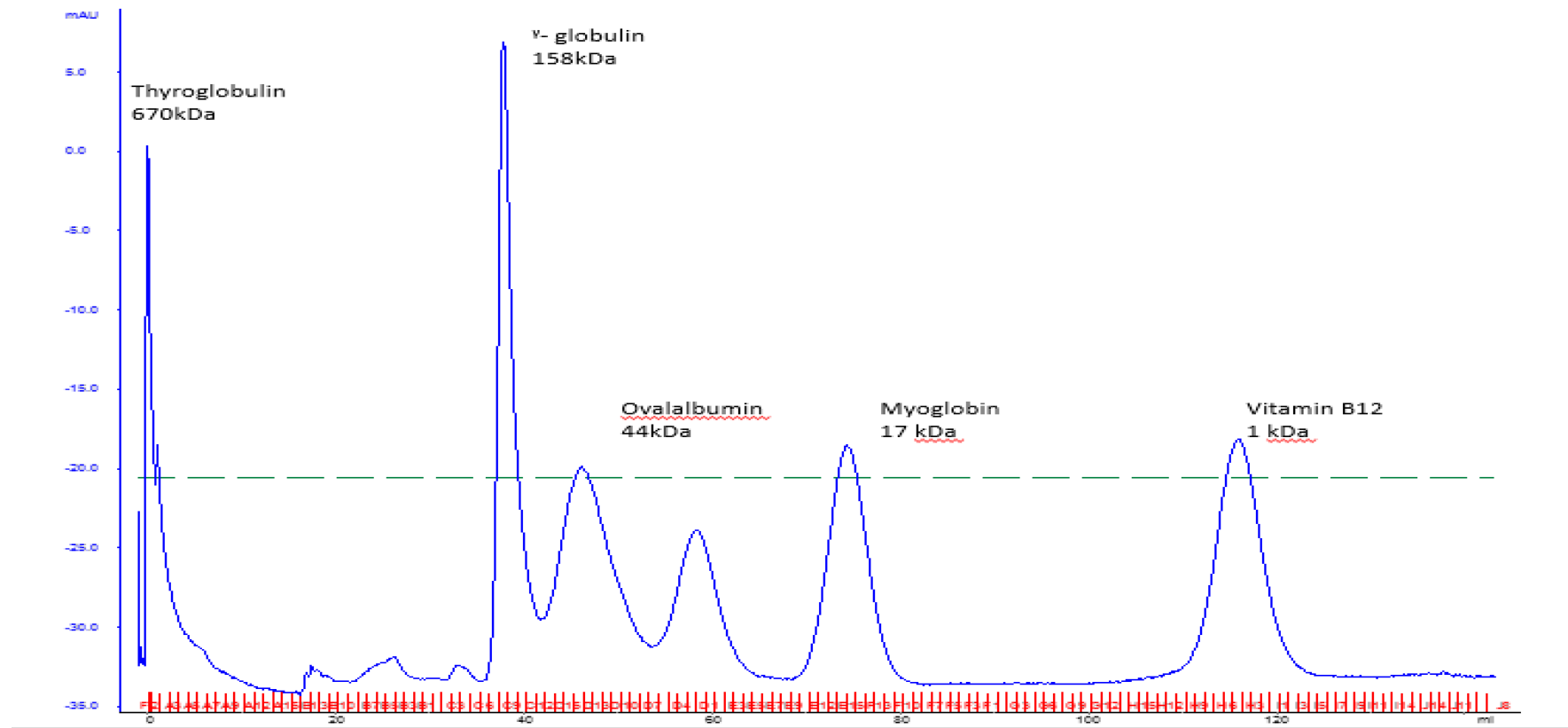
Appendix Figure 9-6. Recombinant urease expression at different temperatures with 1 mM IPTG. Lane 1 ladder, lane 2 CFE at 16°C, lane 3 TP at 16°C, lane 4 CFE at 30°C, lane 5 TP at 30°C, lane 6 CFE at 37°C and lane 7 TP at 37°C.



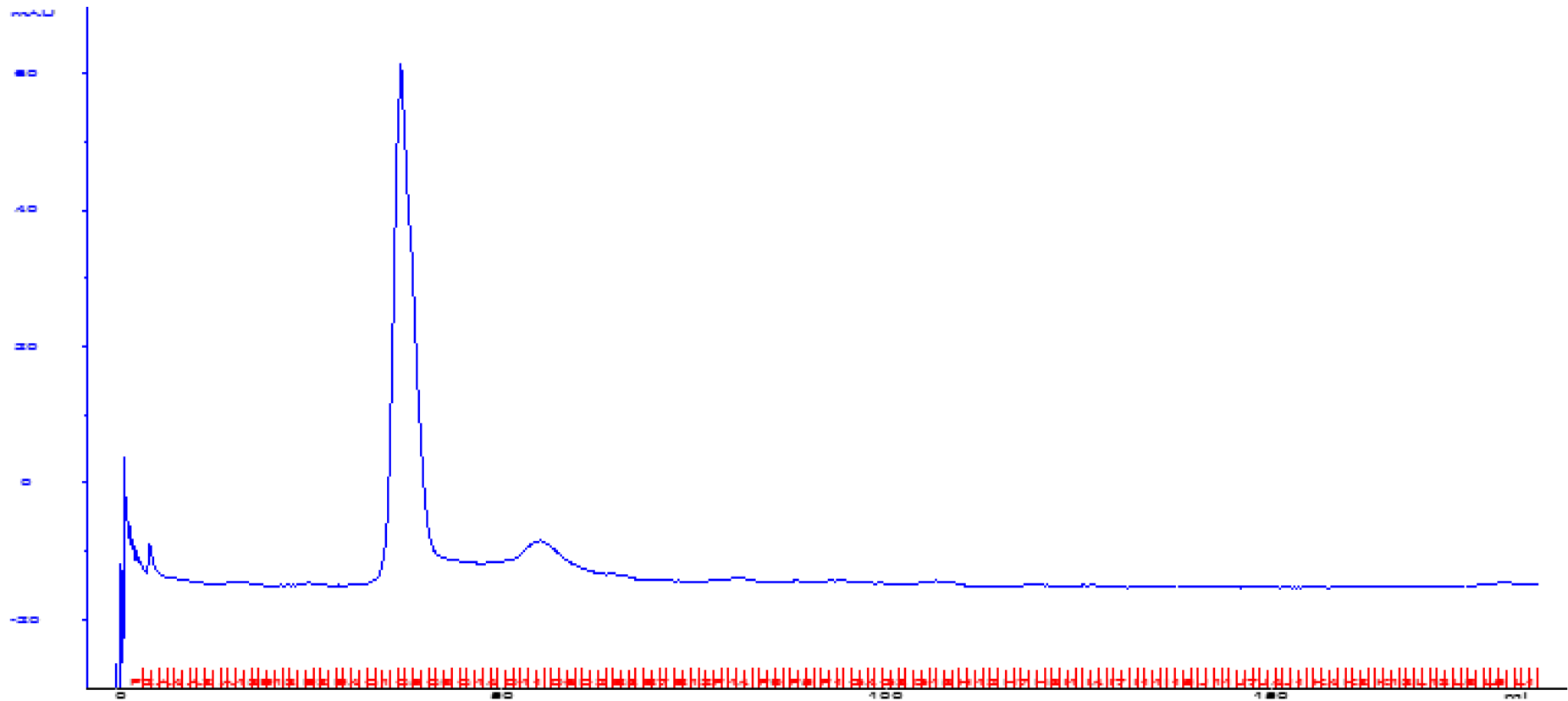
Appendix Figure 9-7. Urease expression in *B. subtilis* 168, *E. coli* BL21 (DE3) +pURE91 and *E. coli* BL21 (DE3) as a control. Lanes 1&2 *B. subtilis* 168 CFE, Lanes 3&4 Recombinant *E. coli* BL21 (DE3) +pURE91 and lanes 5&6 *E. coli* BL21 (DE3) control. Lane 7 Molecular marker. Highlighted in red is the active site of urease, UreC which is evident in the recombinant and not the control (*E. coli* cultured in different media)



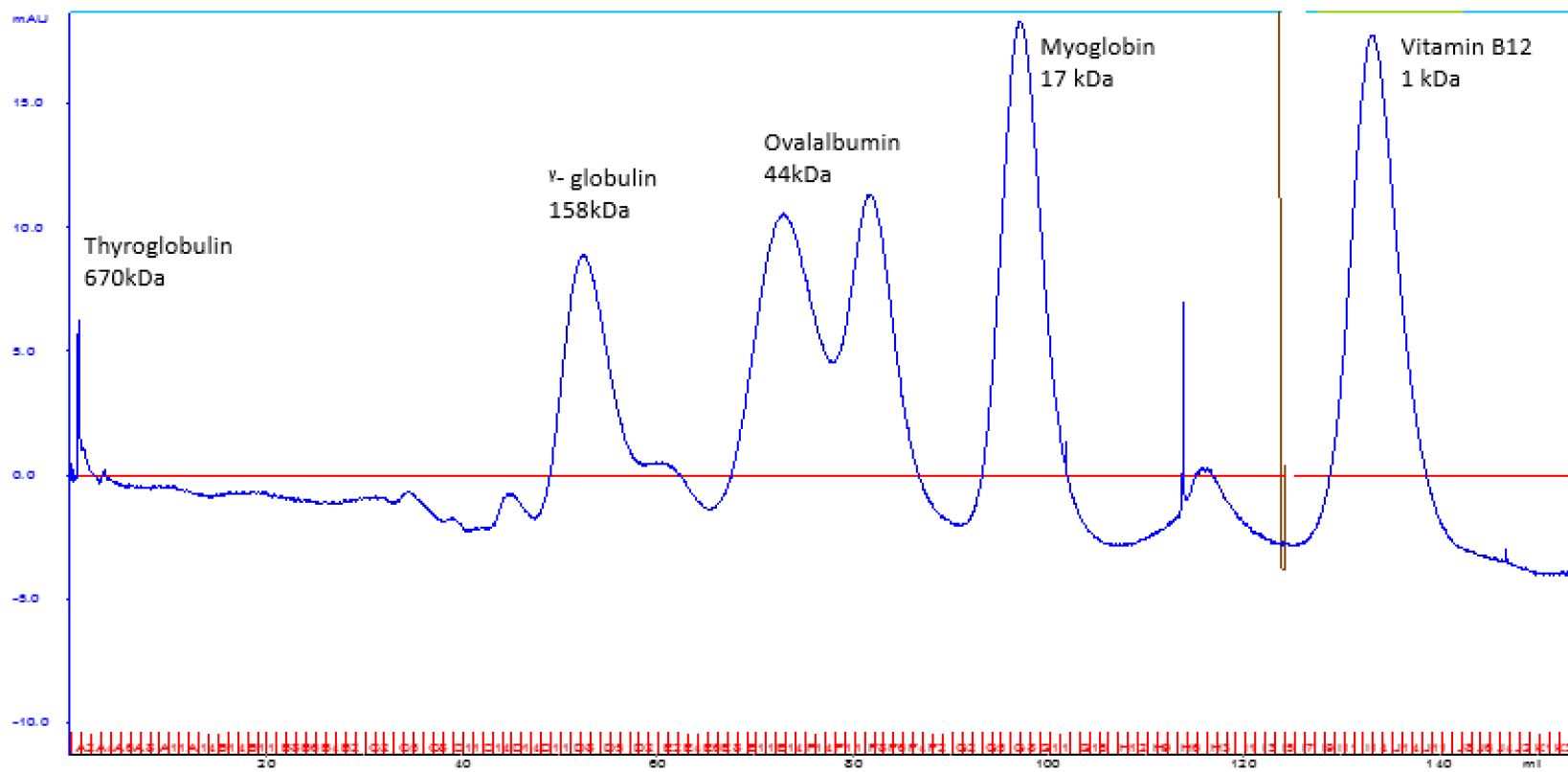
Appendix Figure 9-8. Native gel 14% including CFE from *B. subtilis* 168, Recombinant urease and the standards from size exclusion gel electrophoresis



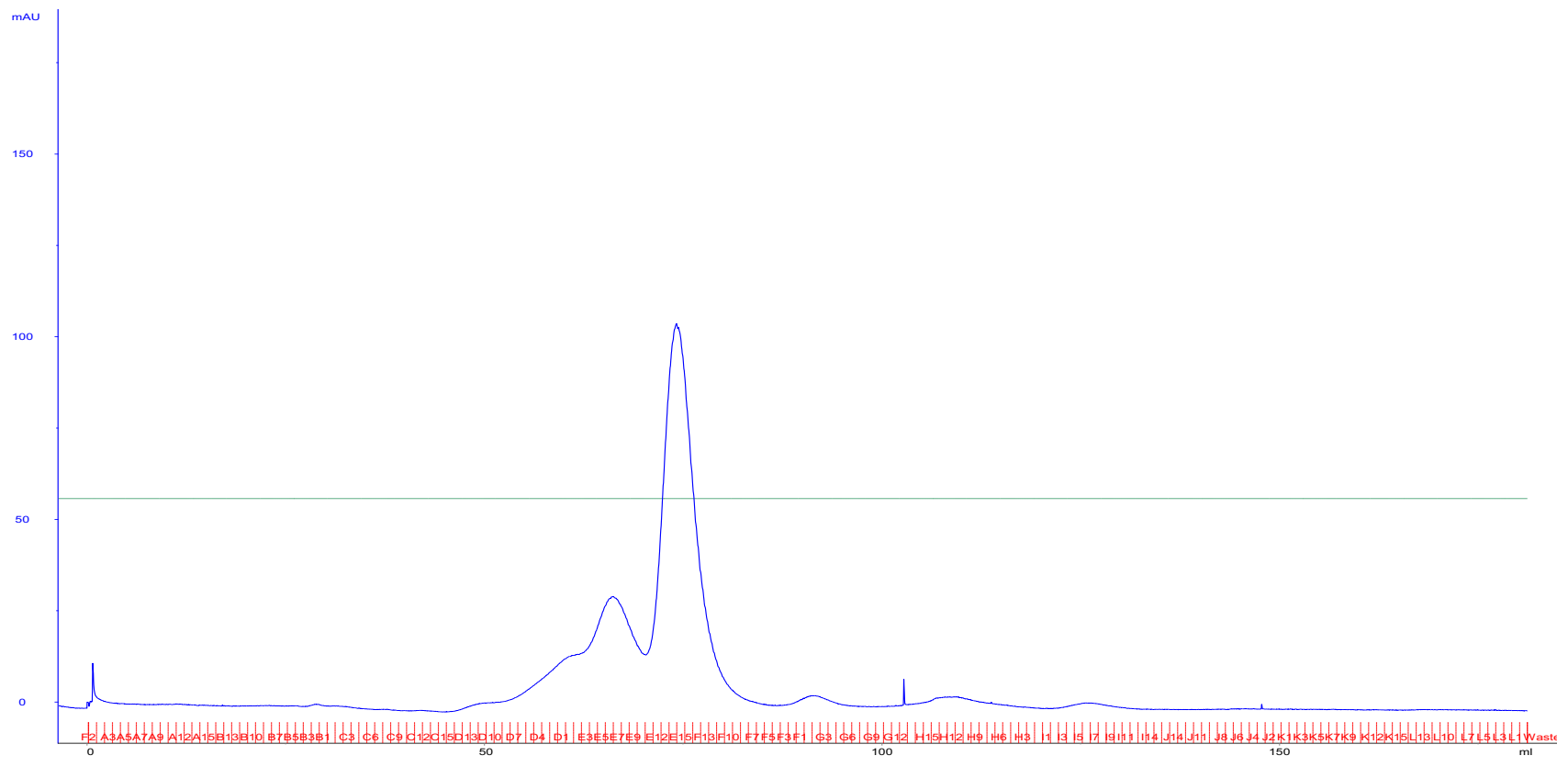
Appendix Figure 9-9. S-200 Chromatogram of HR Standards (5) using S-200 column with 100 μ l loop



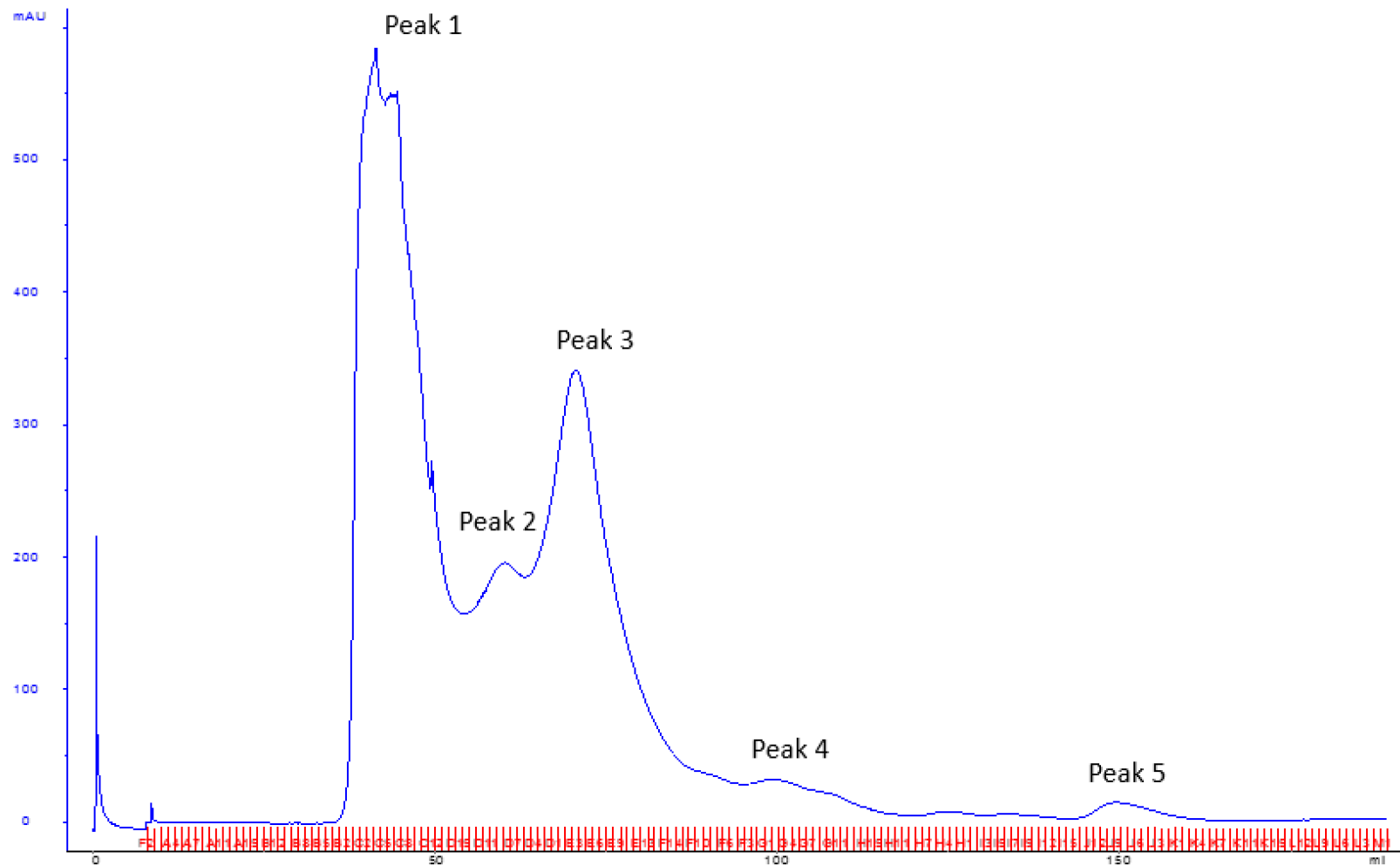
Appendix Figure 9-10. S-200 Chromatogram of Recombinant CFE using S-200 with 100 µl loop



Appendix Figure 9-11. S-300 Chromatogram of HR Standards (5) with 100 μ l loop



Appendix Figure 9-12. S-300 2 ml loop BSA Chromatogram. BSA chromatogram detailing two peaks. Peak 1 Dimer 132 kDa Peak 2 Monomer 66 kDa (Trimer EV 50)



Appendix Figure 9-13. Recombinant SEC Chromatogram of recombinant urease CFE separated using S-300 column with 2 ml loop. Repeated recombinant urease expression detailing 5 peaks

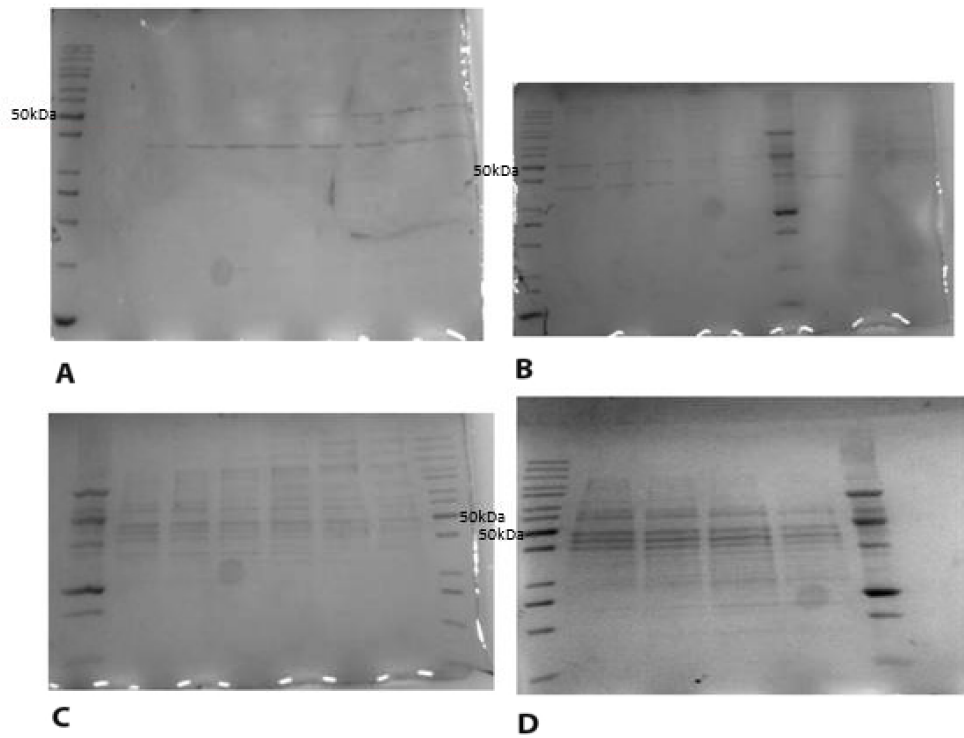


Figure 9-14 A. S-300 column fractions 168 CFE (peak 1). B. S-300 column fractions 168 CFE plus pooled P1, Peak 2. C. Gel 3 S-300 column fractions 168 CFE peaks 2 D. S-300 column fractions 168 CFE peak 3.

Expression of *B. subtilis* urease is too low to be visualised.

Appendix Table 9-5.

Majority protein IDs	Protein names	Gene names	Fasta headers	Peak 1 Average Protein Abundance	Standard Deviation	Peak 2 Average Protein Abundance	Standard Deviation	Peak 3 Average Protein Abundance	Standard deviation
P71035	Urease subunit beta	<i>ureB</i>	sp P71035 URE2_BACSU Urease subunit beta OS=Bacillus subtilis (strain 168)	4.04E+08	1.06E+08	4.57E+09	5E+09	5.63E+07	2E+07
P75030	Urease subunit gamma	<i>ureA</i>	sp P75030 URE3_BACSU Urease subunit gamma OS=Bacillus subtilis (strain 168)	1.96E+08	1.05E+08	3.26E+09	4E+09	6.22E+08	6E+08
P77837	Urease subunit alpha	<i>ureC</i>	sp P77837 URE1_BACSU Urease subunit alpha OS=Bacillus subtilis (strain 168)	7.76E+08	5.86E+08	3.42E+10	4E+10	5.50E+07	6E+07